CR 151,941

CHARACTERIZATION OF IRAS DOPED SILICON DETECTORS

INFRARED DEVICES GROUP
ELECTRONIC MATERIAL SCIENCES DIVISION
NAVAL ELECTRONICS LABORATORY CENTER
SAN DIEGO, CALIFORNIA 92152

DECEMBER 1976

THIS WORK PERFORMED FOR
NASA AMES RESEARCH CENTER
UNDER NASA P. R. No. A-31473-B

CHARACTERIZATION OF IRAS DOPED SILICON DETECTORS

INFRARED DEVICES GROUP
ELECTRONIC MATERIAL SCIENCES DIVISION
NAVAL ELECTRONICS LABORATORY CENTER
SAN DIEGO, CALIFORNIA 92152

DECEMBER 1976

THIS WORK PERFORMED FOR
NASA AMES RESEARCH CENTER
UNDER NASA P. R. No. A-31473-B

CHARACTERIZATION OF IRAS DOPED-SILICON DETECTORS

1.0 INTRODUCTION

The data presented in this report are the results of measurements performed in support of the IRAS program. This work was funded by NASA Purchase Request No. A-31473-B. NASA supplied to NELC, for test and evaluation, four types of doped-silicon detectors from three manufacturers. Data were obtained on one detector of each type supplied by each manufacturer over a range of operating conditions as specified by NASA. Ranges of operating conditions included:

background photon flux - 5×10^{7} to 2×10^{10} photons/sec/cm^{2};

operating temperature - 2.5K to 5.5K;

frequency - 0.01 Hz to 100 Hz.

Data are presented of detector signal, noise spectra, noise equivalent power, and spectral response.

2.0 DETECTOR DESCRIPTION

Detectors were supplied by Aerojet Electrosystems Co. (AESC), Rockwell International Corp., Missile Systems Division (RIC/MSD), and Santa Barbara Research Center (SBRC). All detectors were extrinsic doped-silicon. Table I gives the detector types supplied by each manufacturer and their nominal cutoff wavelengths. Each detector was equipped with a load resistor, a cryogenic field-effect transistor (FET) preamplifier, and a temperature sensor.

TABLE I. Detectors supplied.

Manufacturer	Detector Type	Cutoff Wavelength (μm)
AESC	Si:As	23.5
	Si:Bi	18.2
RIC/MSD	Si:As	24.0
	Si:Sb	25.5
	Si:P	29.0
SBRC	Si:As	24.0
	Si:P	28.0

2.1 AESC. The two detector types furnished by AESC were of a monolithic structure with five detector elements being delineated on a single silicon chip, one chip for each detector type. The electric field was impressed across the detector element by applying a bias voltage between a metallic contact located on the bottom of the detector element and a transparent electrode located on top of the chip. The electric field was thus parallel to the direction of the incident radiation. One detector of each 5-element array was chosen for evaluation.

2.2 RIC/MSD. RIC/MSD supplied detectors of three types, each detector was individually mounted on its own fixture. Two Si:As, three Si:Sb, and two Si:P detectors were supplied. These bulk detectors were

biased through electrodes located on opposite sides of the element such that the electric field was perpendicular to the direction of the incident radiation. Measurements were made on one detector of each type.

2.3 SBRC. Two detectors each of two types (Si:As, Si:P) were supplied by SBRC. All four detectors were mounted in a common package. The detectors were of the individual bulk type, but with transparent electrodes on the top surfaces. The electric field was thus parallel to the direction of the incident radiation. A single metallic mask with defining apertures was located immediately above the detector surfaces. One detector of each type was chosen for evaluation.

3.0 MEASUREMENT CONSIDERATIONS

3.1 Dewar. All measurements with the exception of the sensitivity contours were made with the detectors mounted in the NELC Spectral Dewar.[1] The background photon flux was reduced by:

(a) a narrow field of view (2.2×10^{-3} radians);

(b) a "neutral" density filter whose transmittance was about 5×10^{-4}; and

(c) a narrow band spectral filter whose center wavelength can be varied from 6.6 micrometers to 21.5 micrometers.

This cold spectral filter can also be removed from the optical path resulting in a higher (spectrally-broad) background condition. Data were obtained for each detector at a low background by using the spectral filter set to an appropriate wavelength, and at a higher, broad-band background.

3.2 Signal and Background Sources. The sources of signal irradiance and background photon flux were radiators outside of the Dewar. The source of background radiation was 300K room temperature radiation, and the source of signal irradiance was a 500K blackbody modulated by a 300K chopper. Background photon flux density and signal irradiance were calculated from the spectral characteristics of the blackbody radiators, transmittances of optical filters and windows, the detector field-of-view, and detector spectral response (for broadband measurements).

The blackbody had an aperture of 0.6" and a mechanical chopper could modulate the source at frequencies ranging from 0.012 Hz to 12 Hz. Since the detector field-of-view was so small, it was totally filled, alternately, by the blackbody and the chopper blade. Therefore when making signal measurements, the photon flux varies with time, being higher when the 500K blackbody fills the field-of-view. The background, during signal measurements, is considered to be the time average of the time varying photon flux.

3.3 Temperature Variation. Measurements were made on all detectors at a nominal temperature of 4.5K to 5.5K. This was the temperature achieved with liquid-helium in the Dewar (at ambient pressure) and with the FET of the detector turned on. Lower temperatures were achieved by pumping on the helium reservoir with a two-stage mechanical pump. A pressure of 9.5 mm of mercury over the liquid was reached, which corresponds to a liquid temperature of 1.73K. A nominal temperature of 2.5K

was measured by a calibrated temperature sensor located on the detector mounting plate. Some additional measurements were made on one detector (AESC Si:Bi) at elevated temperatures. These temperatures were obtained by electrically heating the detector mounting plate. Good agreement was observed between measurements made with NELC's temperature sensor and the sensors provided by the detector manufacturers.

3.4 Electronics. Figure 1 shows a block diagram of the electronics used for the detector measurements.

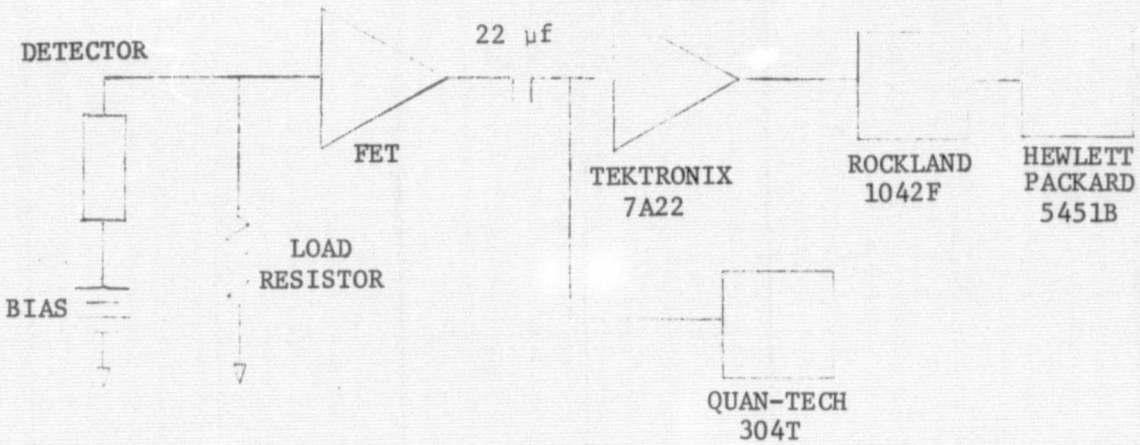

Figure 1. Measurement Electronics.

All detectors were supplied with a FET preamplifier and load resistor. Measurements were made with the FET connected in a source follower configuration so that the voltage gain of the FET was approximately 1. Some attempt was made in each case to achieve minimum FET noise by varying the currents and voltages to the source, substrate, and drain.

The output of the FETs was fed into a Tektronix 7A22 amplifier. This amplifier was used in the dc-coupled mode and had a flat frequency response down to the low frequencies (0.01 Hz) required for these measurements. Figure 2 is a plot of the noise spectrum of this amplifier with a 90Ω input resistance. However, since the output of the FETs were at a dc potential of 2 to 5 volts, a coupling capacitor was required between the FET and the amplifier. This 22μf capacitor together with the 1 MΩ input resistance of the 7A22, resulted in an input time constant of 22 seconds or a low frequency 3 dB point of 7.2×10^{-3} Hz. This low frequency roll-off required some minor corrections in the data at frequencies below 0.024 Hz.

The output of the 7A22 amplifier was fed through a Rockland 1042F filter and then into a Hewlett-Packard 5451B Fourier analyzer. The 5451B is a computer-based data acquisition system with an integral A/D converter. The input signal was digitized, stored, and the power spectrum calculated through the fast Fourier transform (FFT). This system was used for both frequency response and noise spectra measurements. The 1042F filter was used to remove noise components above one-half the sampling frequency to eliminate aliasing errors. The filter has an adjustable high frequency roll-off and a 48 dB/octave slope. A Quan-Tech model 304-T wave analyzer was also used to measure signal and noise as a function of detector bias voltage.

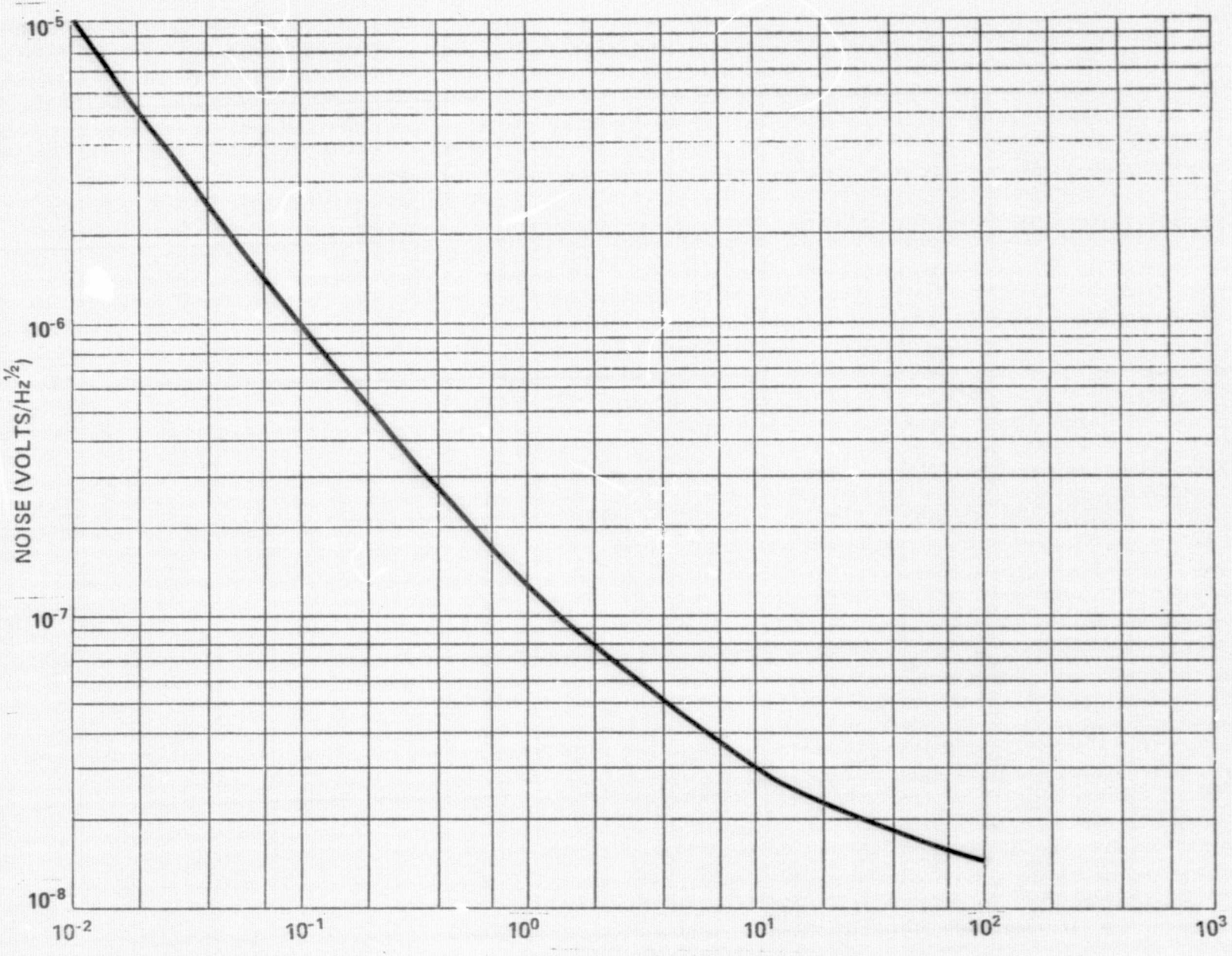

Figure 2. Noise spectrum of 7A22 amplifier

4.0 COMMENTS ON THE MEASURED PARAMETERS

Several different measurements were made on each detector element. Comments are made in this section about each measurement and these comments will generally apply to all detectors. Later, specific comments will be made about each detector. The order of these comments will follow the order in which the data graphs are presented.

4.1 Spectral Response. The relative response as a function of wavelength was measured for each detector. These data were obtained by comparing the detector signal to that of a calibrated thermocouple at wavelengths from 1 micrometer to the detector's cutoff wavelength. The background for these measurements was about 10^{13} photons/sec/cm^2 and the detector operating temperature was nominally 5K. Some concern existed[2] about a dependency of the relative spectral response on detector background and/or operating temperature. A number of measurements were made on the AESC Si:Bi detector at different backgrounds and operating temperatures. No change in relative response was observed. Due to the length of time required for these measurements, the relative spectral responses of the remaining detectors were obtained only at the nominal background and operating temperature.

4.2 Determination of "Optimum Bias." The "optimum bias" is defined as that bias which maximizes the signal-to-noise ratio. It is determined by observing signal and noise as functions of bias at a fixed background, temperature, and chopping frequency. The bias thus determined is then used for frequency response and noise spectra measurements for all other operating conditions. However, there is no assurance that this bias is

the optimum for these other operating conditions. In particular, the SBRC Si:As detector had different optimum biases at the different measurement backgrounds.

Most detectors exhibited some degree of spontaneous noise spiking.[3] The spiking rate was a function of bias, background, and operating temperature. In some cases these spikes contribute to the measured rms noise and thus effect the optimum bias measurement. If these spikes could be eliminated, the optimum bias could be somewhat different. On the other hand, perhaps the "optimum system" bias should be based on a maximum number of spikes per unit time. No attempt was made to quantify the spikes relative to their frequency of occurrence or their amplitude distribution.

4.3 Frequency Response. Detector signal was measured as a function of chopping frequency over a frequency range from 0.012 to 12 Hz. In some cases, additional measurements were made at higher frequencies, but in general, signals at higher frequencies were obtained by extrapolating the frequency response curve past 12 Hz.

The equivalent circuit for detector signal is shown in Fig. 3.

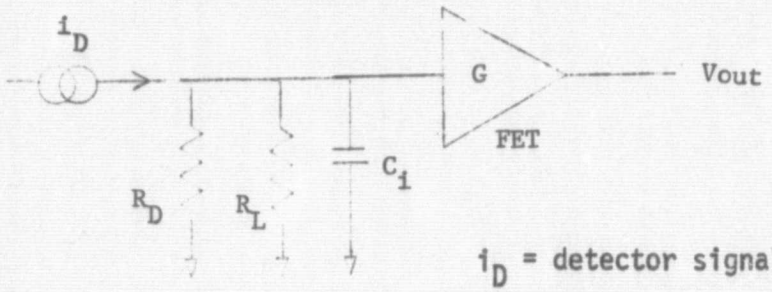

i_D = detector signal current (A)

R_L = load resistance (Ω)

C_i = input capacitance (f)

G = Gain of FET

V_{out} = output voltage (V)

Figure 3. Signal equivalent circuit.

The FET output voltage is thus

$$V_{out} = i_D \frac{R_L G}{(1 + \omega^2 R_L^2 C_i^2)^{1/2}}$$

If the detector signal current (i_D) is not a function of frequency, one would expect an output signal which was independent of frequency at low frequencies ($\omega R_L C_i << 1$), and proportional to the reciprocal of the chopping frequency at high frequencies ($\omega R_L C_i << 1$), i.e.:

Low Frequency: $V_{out} = i_D R_L G \ (\omega R_L C_i << 1)$

High Frequency: $V_{out} = i_D \left(\frac{1}{\omega C_i} \right) G \ (\omega R_L C_i >> 1)$.

This is the general shape observed in the data. However, in some cases i_D is not independent of frequency (due to dielectric relaxation) and an increase in signal is observed at low frequencies. The frequency at

which this increase occurs depends on the detector resistance (lower frequency for higher resistance). The detector resistance is, of course, a function of both background and operating temperature.

Three quantities in the above expression for output signal voltage may be functions of operating temperature, namely, detector current (i_D), the value of the load resistance and the gain of the FET. The resistance of the load resistor is known to increase as the operating temperature[4] is decreased. Gain measurements were made on one FET (RIC/MSD), and no change in gain was observed between temperature of 2.5 and 4.5K. If one assumes that all FET gains were independent of temperature, then all of the detectors reported here appeared to have a lower responsivity at lower temperatures. This conclusion is drawn from the temperature dependence of the output voltage at high frequencies ($V_{out} = i_D/\omega C_i$). At low frequencies and low temperatures the output signal voltage may increase or decrease depending on which quantity is more temperature dependent (i.e., the detector responsivity or the load resistance).

4.4 Noise Spectra. Noise spectra were obtained at frequencies from 0.01 Hz to 100 Hz. A spectrum was obtained at frequencies from 0.01 Hz to 10 Hz with a 0.01 Hz resolution, and another spectrum was obtained with 0.1 Hz resolution from 0.1 Hz to 100 Hz. Both sets of data were normalized to unit noise bandwidth and are presented as one curve with units of volts/$Hz^{1/2}$. Measurements were made at a minimum of two operating temperatures and two backgrounds using the optimum bias described above. In addition, some noise measurements were made with no

bias applied to the detector (V = 0), and also with bias applied but under a very low background condition ($Q_B < 10^6$ photons/sec.cm^2 or Q_B = ZILCH).

One experimental problem was encountered during the measurement of noise spectra. It was related to a long term dc drift in the output of the 7A22 amplifier caused by a drift in the leakage current of the coupling capacitor. This long term drift produced a noise spectrum which varied as the reciprocal of frequency ($\frac{1}{f}$), and gave rise to erroneously high values of noise at low frequencies. The problem was minimized by a software procedure called "Hanning," but the extremely low frequency points were still somewhat effected. The noise spectra reported here have been smoothed at low frequencies to further correct for the effect of this drift.

4.5 Noise Equivalent Power (NEP). Noise equivalent power was calculated at each frequency from the expression

$$NEP = \frac{N \cdot H \cdot A}{S} \quad \frac{watts}{Hz^{1/2}}$$

where N = Noise (volts/Hz$^{1/2}$)

S = Signal (volts)

H = Signal irradiance (watts/cm^2)

A = Detector Area (cm^2)

NEP is a function of wavelength and varies as the reciprocal of the relative spectral responsivity. NEPs are reported for a minimum of two backgrounds and two operating temperatures. Data for each detector are reported for a single wavelength for ease of comparison of the data.

4.6 Time Records. Detector outputs as functions of time are shown for each detector under each measurement condition. In general, detector outputs are shown with a 500K source, a 300K background source, and the output when varying between these two levels at a chopping frequency of 0.012 Hz. The electronic bandwith was 300 Hz for these records. These data were obtained using the system shown in Fig. 1. There are 4096 data points in each time record. The vertical scales are referred to the FET output terminal. Variations in biasing methods and bias polarity led to reversals in the sense of the output polarity (i.e., signal can be either up or down). The various plots are labeled to make this clear.

The input irradiance as a function of time was a square wave, but because of the capacitive coupling used, the detector outputs exhibit the expected droop in signal with time. The droop is not apparent for some detectors at low backgrounds. In fact, their output appears to be nearly a square wave. This is caused by the low frequency enhancement of detector signal due to the dielectric relaxation effect.

These time records at various backgrounds and temperatures, allow a rough determination of the frequency of occurence of spontaneous noise spikes.

4.7 Sensitivity Contours. Sensitivity contours were measured on the two AESC detectors and on the RIC/MSD Si:As detector. These data were obtained in a low background ($Q_B < 10^7$ photons/sec/cm^2), long wavelength (λ = 10 micrometer) spot-scanner. The nominal spot size for

these measurements was 2.5 mil. The spot was modulated at a frequency of 10 Hz and moved slowly over the detector surface while recording the detector output with a narrow band wave analyzer tuned to the modulation frequency. Measurements were not made on the SBRC detectors because of a failure in the electrical connector on the detector package.

5.0 DATA

Graphs of data obtained for each detector are given in this section. Detectors of the same type dopant are grouped together and the types are placed in order of increasing cutoff wavelength. Detectors of the same type are placed in alphabetical order by manufacturers. Since the comments made in the above section apply generally to each detector, the comments in this section will concern points which are unique to each detector.

Table II gives a summary of current responsivities of each detector as determined from measurements at the lowest background in each case. The temperature was that achieved at ambient pressure. Responsivity can be calculated from low frequency signal if the load resistor is known,

$$R(A/w) = \frac{V_{out}}{HA\ R_L} \text{ (low frequency)}$$

or from high frequency signal if the input capacitance is known,

$$R(A/w) = \frac{V_{out}\ \Omega\ C_i}{HA}$$

Neither R_L or C_i are known with any accuracy for any of the detectors measured here. However, the input capacitance for most FETs used at low temperatures is about 4 pf. Therefore, responsivities have been calculated for each detector from high frequency signals assuming an input

capacitance of 4 pf. Table II also gives the wavelength of maximum sensitivity (λ_{max}) and the responsivity at this wavelength. Responsivities are also given at an arbitrarily chosen comparison wavelength, λ_c.

TABLE II. Detector Current Responsivities

Manufacturer	Detector	λ_{max} (μm)	$R_{\lambda_{max}}$ (A/w)	λ_c (μm)	$R\lambda_c$ (A/w)
AESC	Si:Bi	17	3.7*	15	3.1*
AESC	Si:As	21	5.4	15	3.3
RIC/MSD	Si:As	22	7.5	15	4.6
SBRC	Si:As	20	4.0	15	3.0
RIC/MSD	Si:Sb	23.5	3.6	15	1.5
RIC/MSD	Si:P	27.5	1.6	25	1.6
SBRC	Si:P	26.5	0.87	25	0.87

*See text.

5.1 AESC Si:Bi. This detector (#2) was the first one evaluated on this program and it was used to test out various measurement techniques and the amount of time required for each measurement. As a result more data was acquired on this detector than on any other one. Based on the results from this detector, a number of planned measurements were deleted for other detectors due to time constraints.

A great deal of spontaneous spiking was observed in the output of this detector and the spiking rate was higher at the higher background.[5] The spikes can clearly be seen in the plots of detector output versus time. These spikes contributed significantly to the observed rms noise spectra.

The spatial sensitivity of this detector was quite nonuniform over its nominal sensitive area. The degree of nonuniformity can be seen to be a function of signal level (irradiance level) and detector bias. Signals were also observed when the spot was located in areas of the silicon chip presumably covered with an opaque metallic film. These two effects make the calculated current responsivity somewhat difficult to interpret since responsivity measurements were made with the entire silicon chip flooded with uniform illumination. Conversations with AESC have related these nonuniformities to a problem in the transparent electrode. This problem can and has been avoided in other detectors manufactured in a similar manner (see AESC Si:As below).

An examination of the detector chip upon completion of the evaluation revealed a number of cracks in the silicon chip. However, these

cracks were not located near detector #2 nor did they appear to effect the measurements in any way. The cause of these cracks could be the differential thermal expansion between the silicon chip and the metallic plate to which it was epoxied.

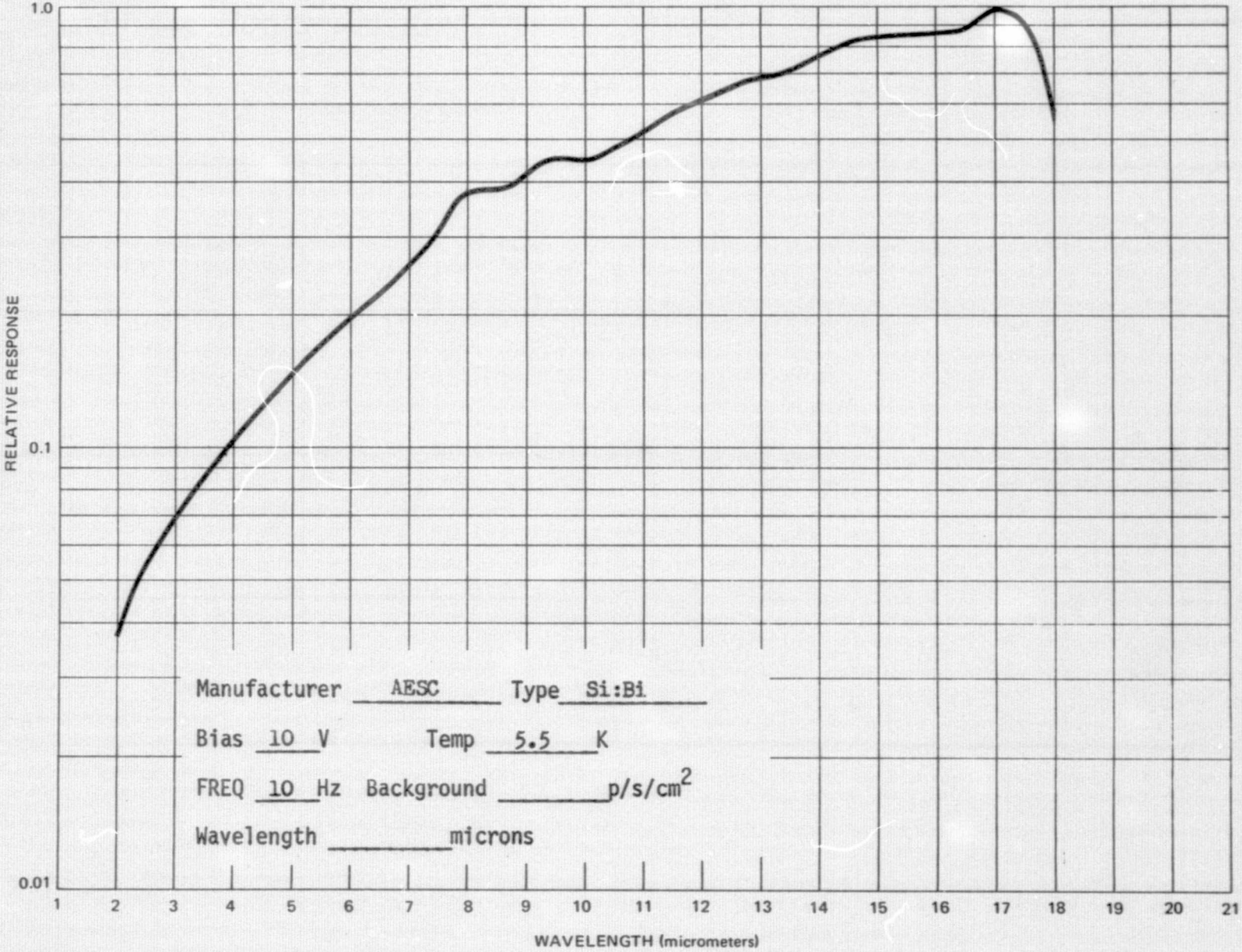
1.0
0.1
0.01
RELATIVE RESPONSE
1
2
3
4
5
6
7
8
9
10
11
12
13
14
15
16
17
18
19
20
21
WAVELENGTH (micrometers)
Manufacturer AESC Type Si:Bi
Bias 10 V Temp 5.5 K
FREQ 10 Hz Background _____ p/s/cm2
Wavelength _____ microns

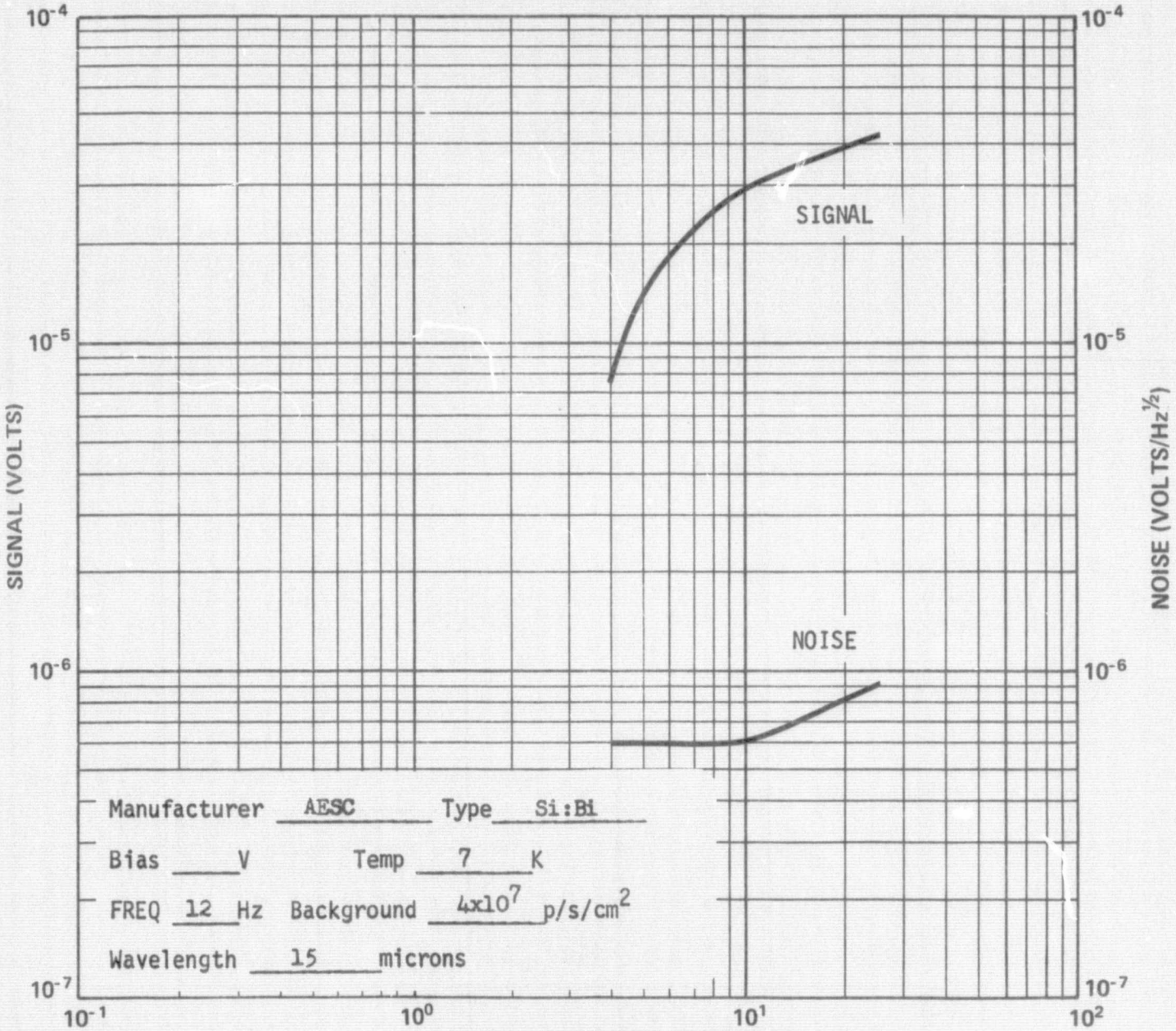

DETERMINATION OF OPTIMUM BIAS

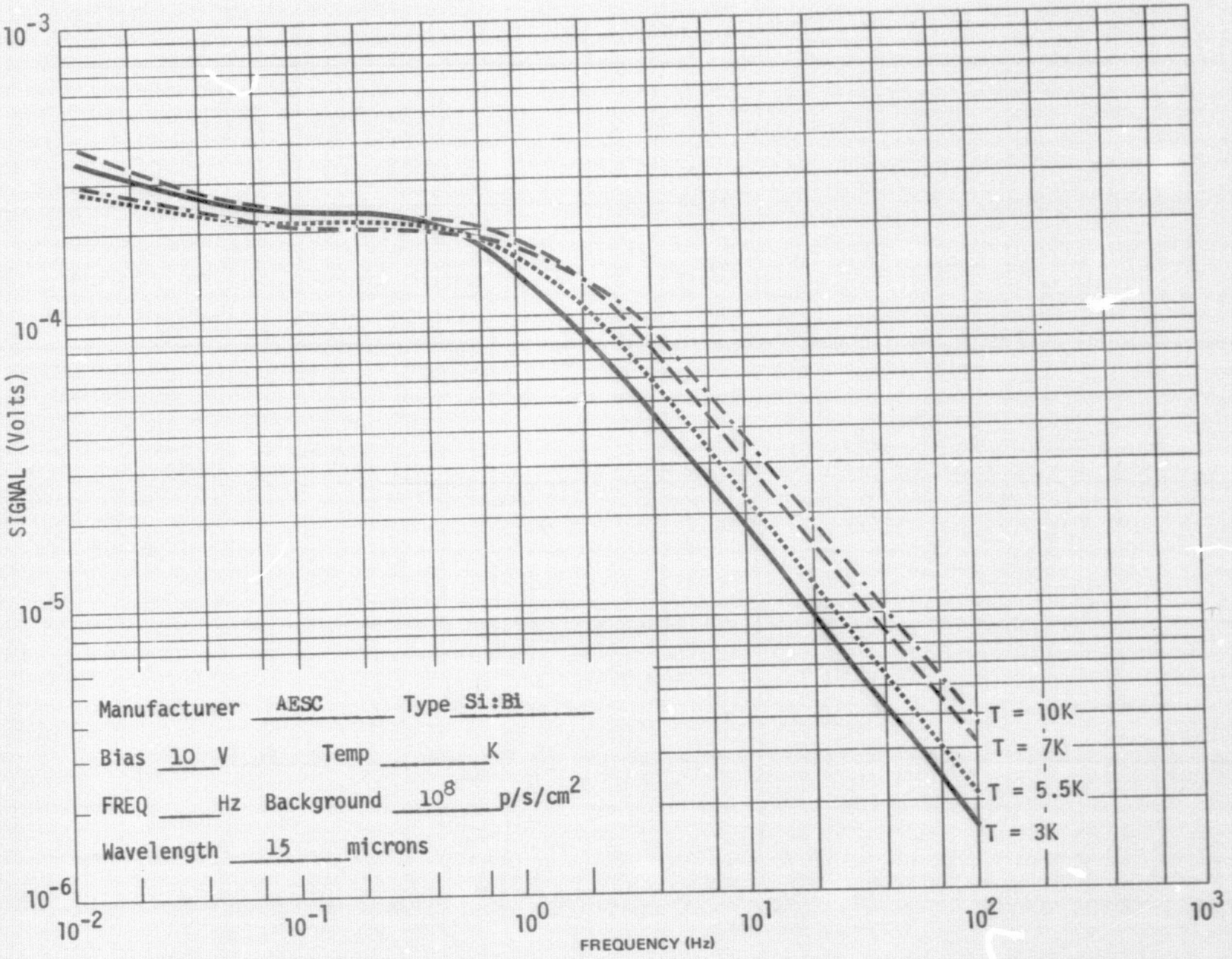
SIGNAL (Volts)
10^{-3}
10^{-4}
10^{-5}
10^{-6}
10^{-2}
10^{-1}
10^{0}
10^{1}
10^{2}
10^{3}
FREQUENCY (Hz)
Manufacturer AESC Type Si:Bi
Bias 10 V Temp ____K
FREQ ____Hz Background 10^{8} p/s/cm^2
Wavelength 15 microns
T = 10K
T = 7K
T = 5.5K
T = 3K

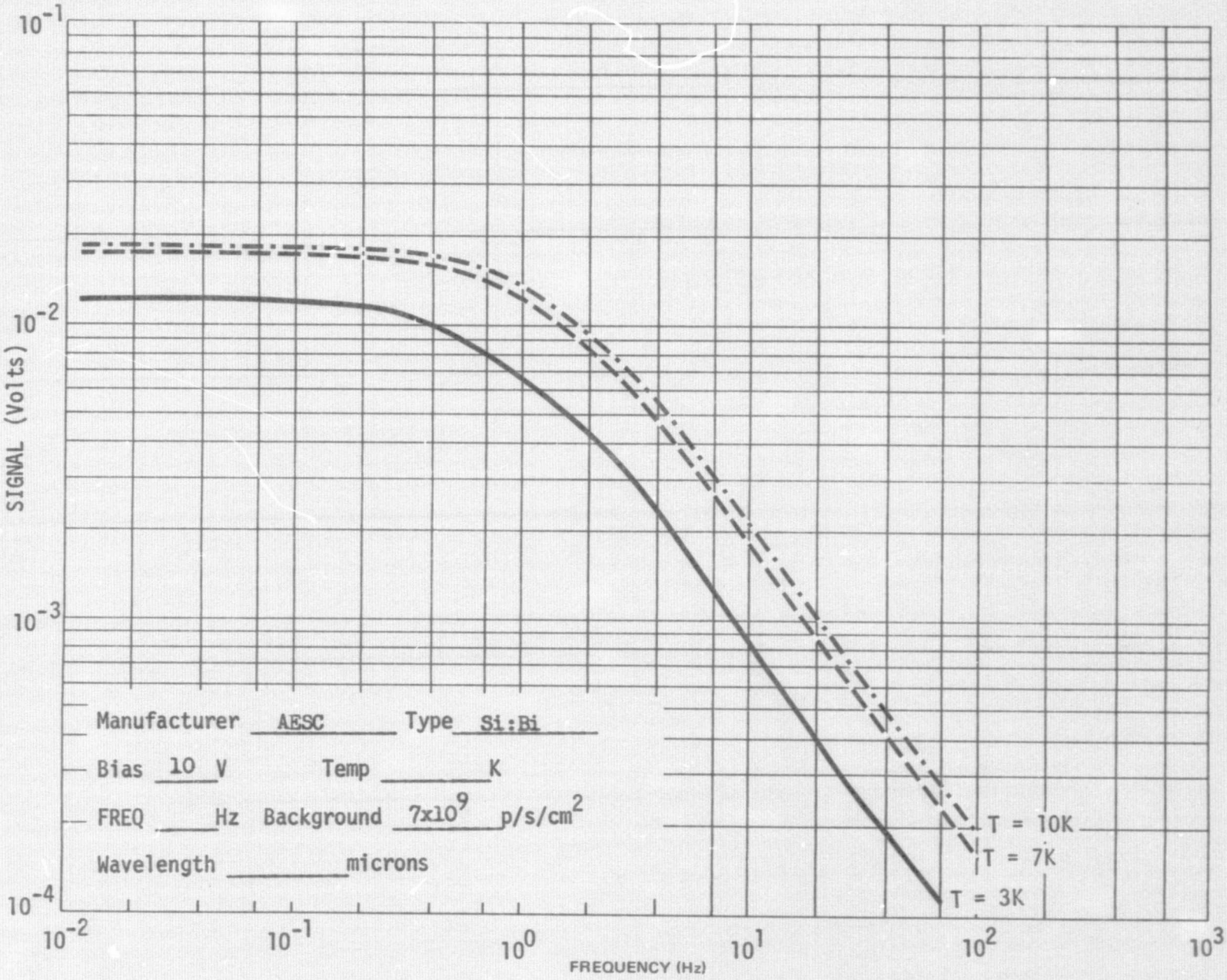
SIGNAL (Volts)
10^{-1}
10^{-2}
10^{-3}
10^{-4}
10^{-2}
10^{-1}
10^{0}
10^{1}
10^{2}
10^{3}
FREQUENCY (Hz)
Manufacturer AESC Type Si:Bi
Bias 10 V Temp ____ K
FREQ ____ Hz Background 7x10^9 p/s/cm^2
Wavelength ____ microns
T = 10K
T = 7K
T = 3K

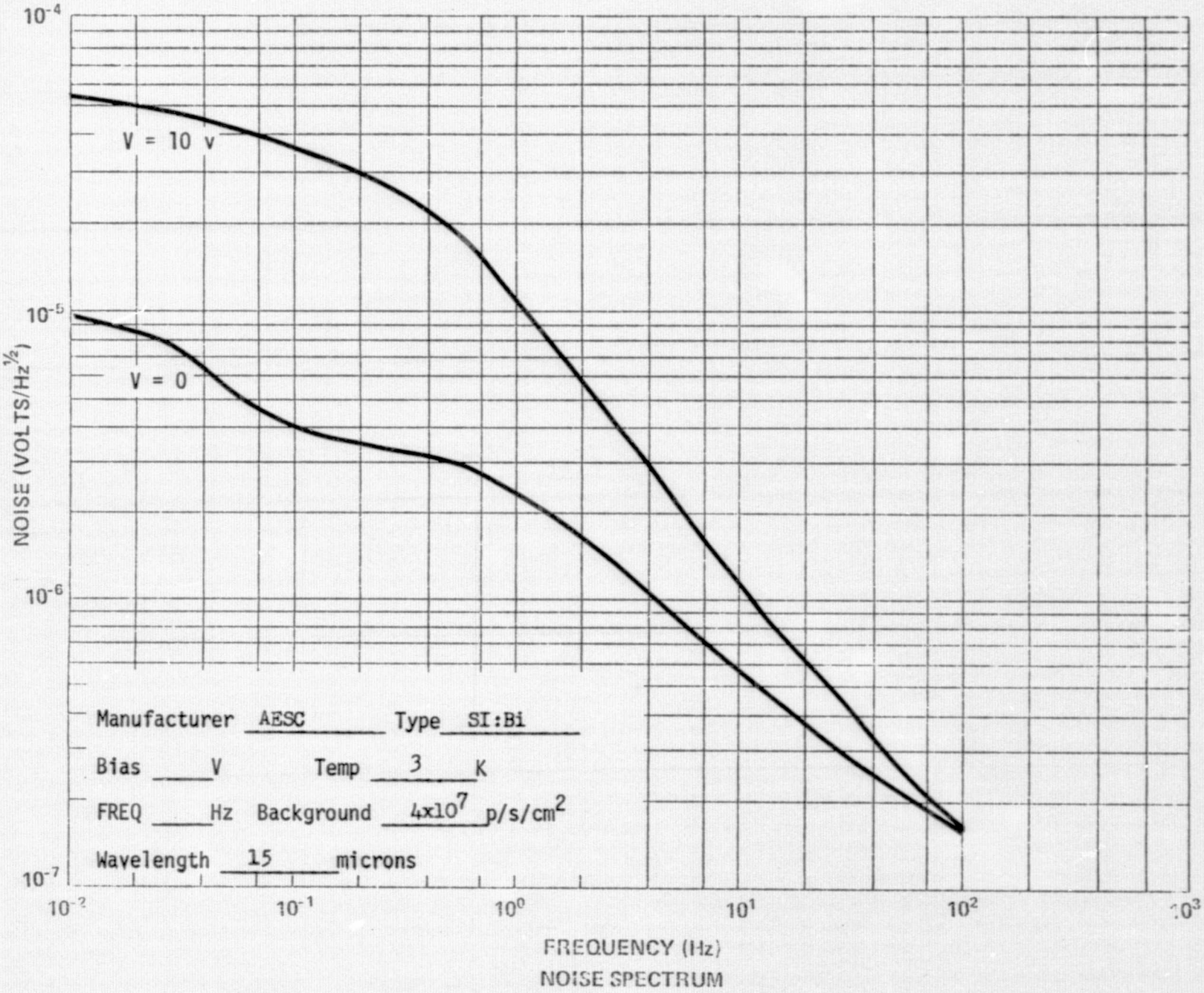

NOISE SPECTRUM

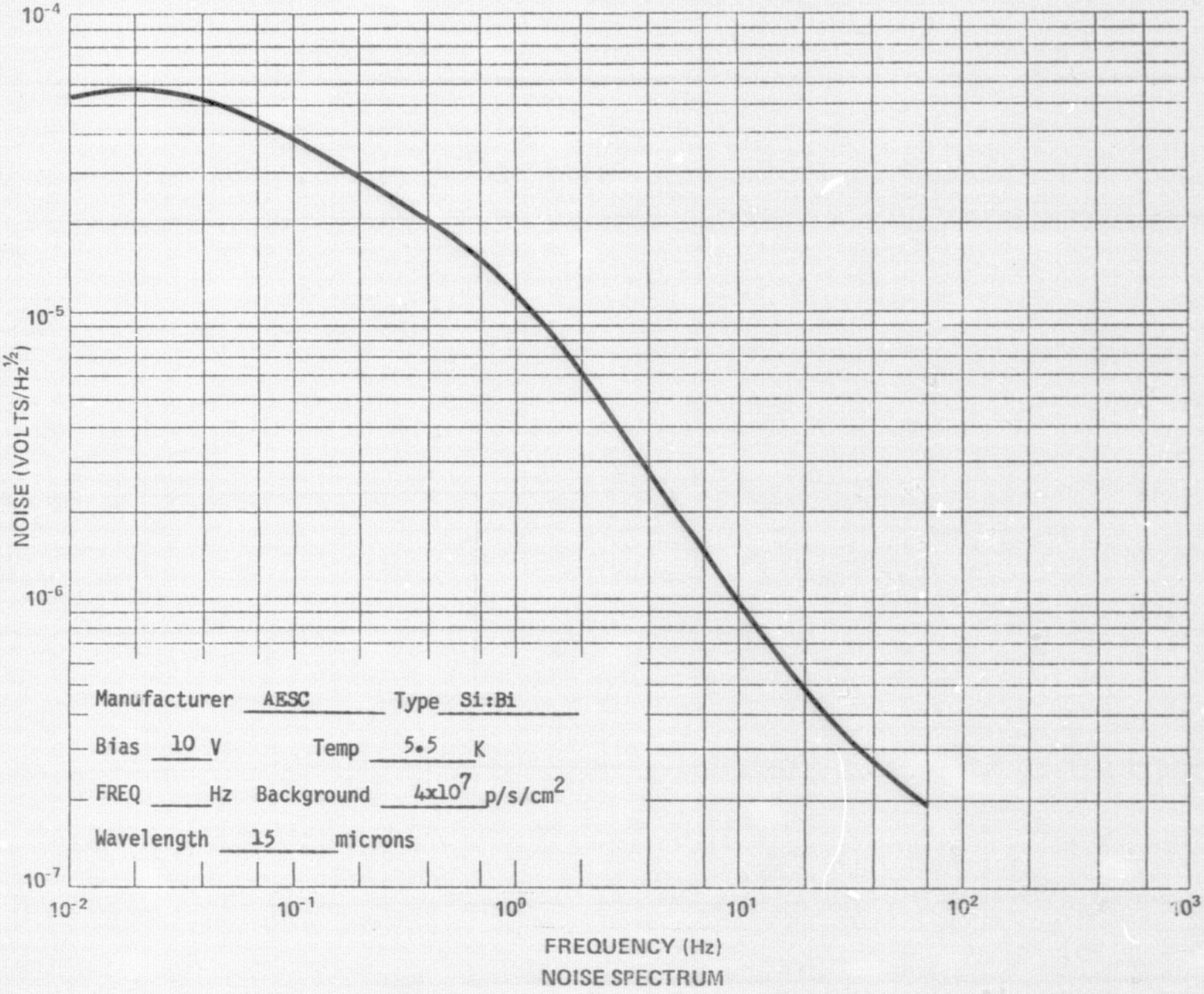

NOISE SPECTRUM

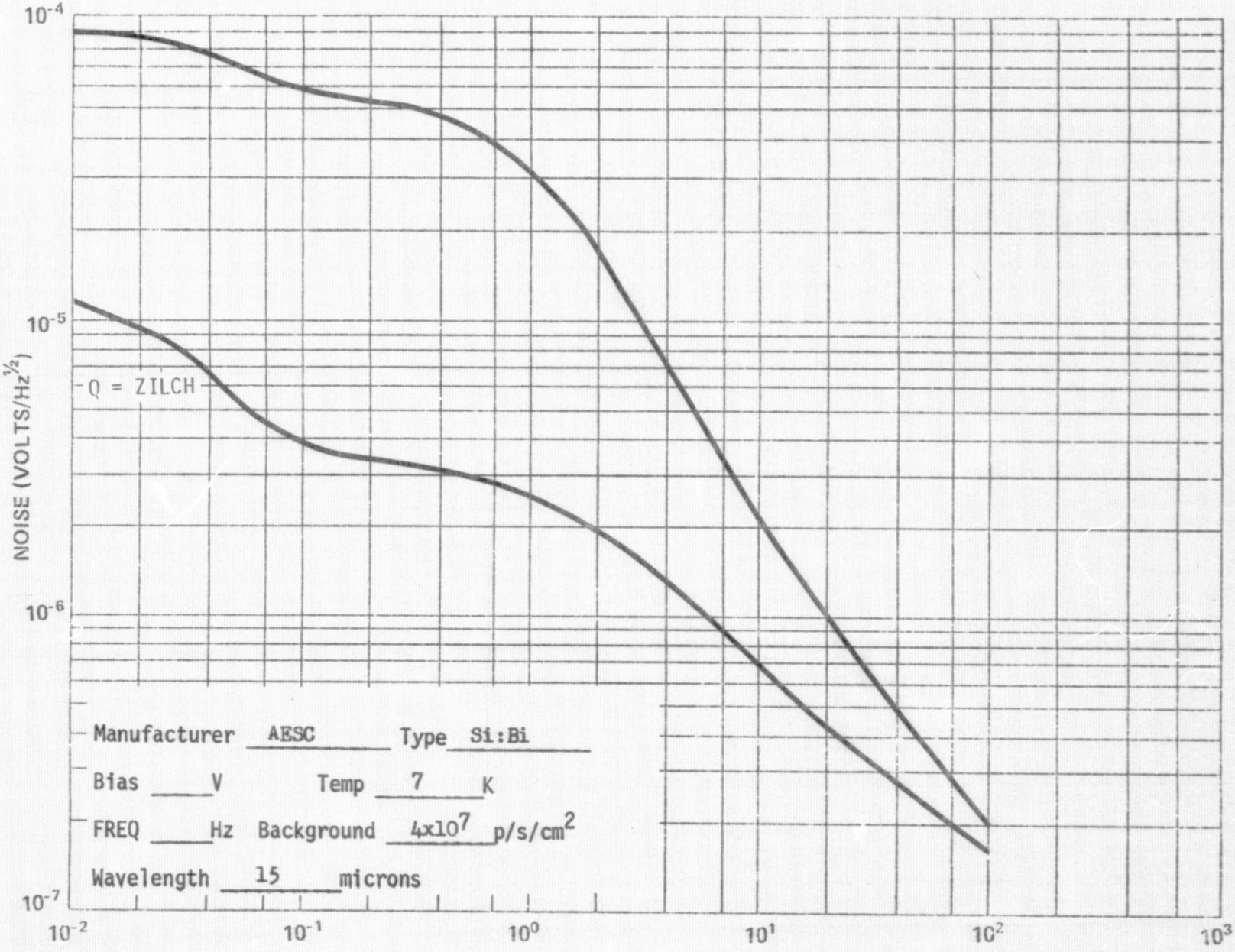

NOISE SPECTRUM

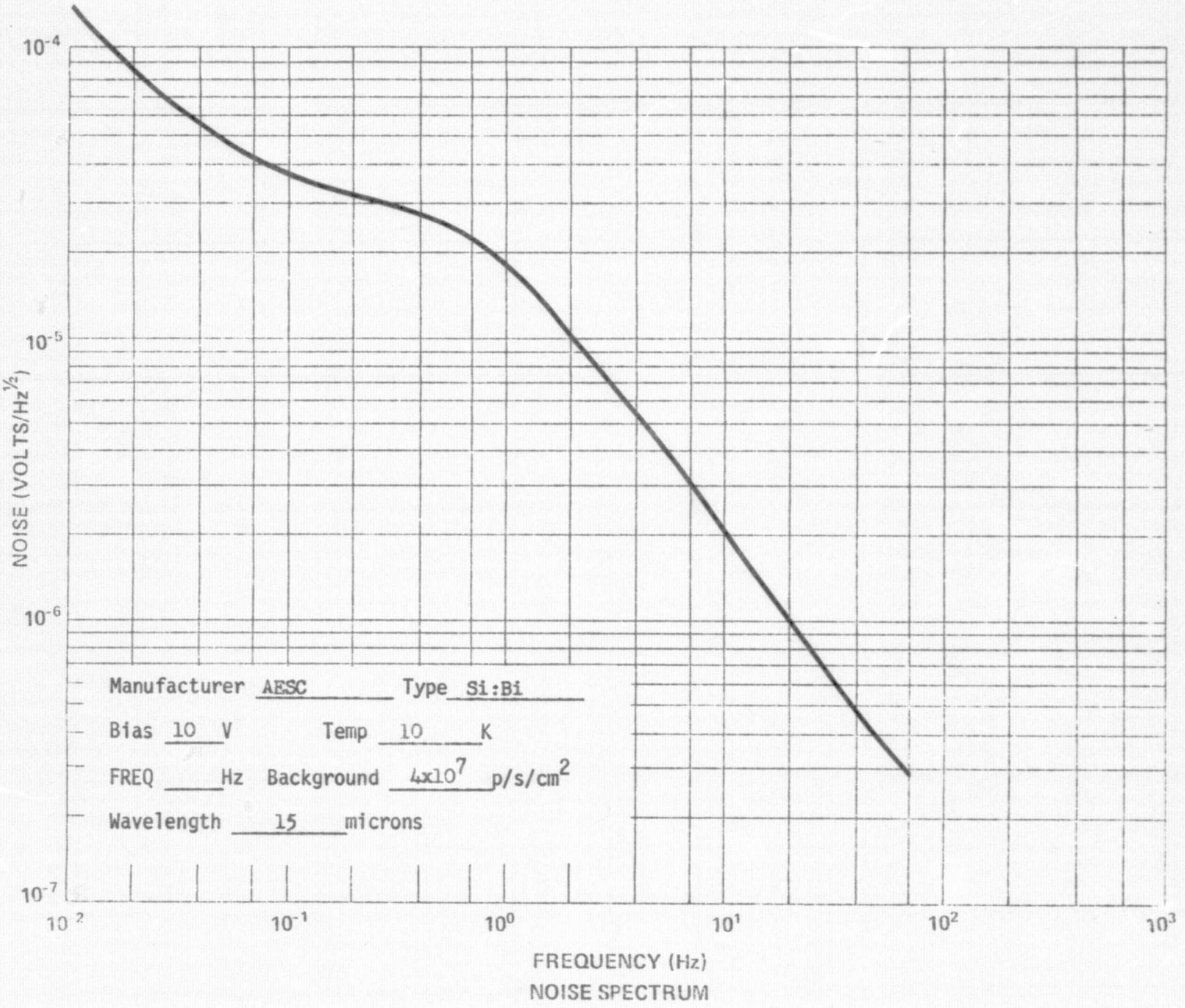

NOISE SPECTRUM

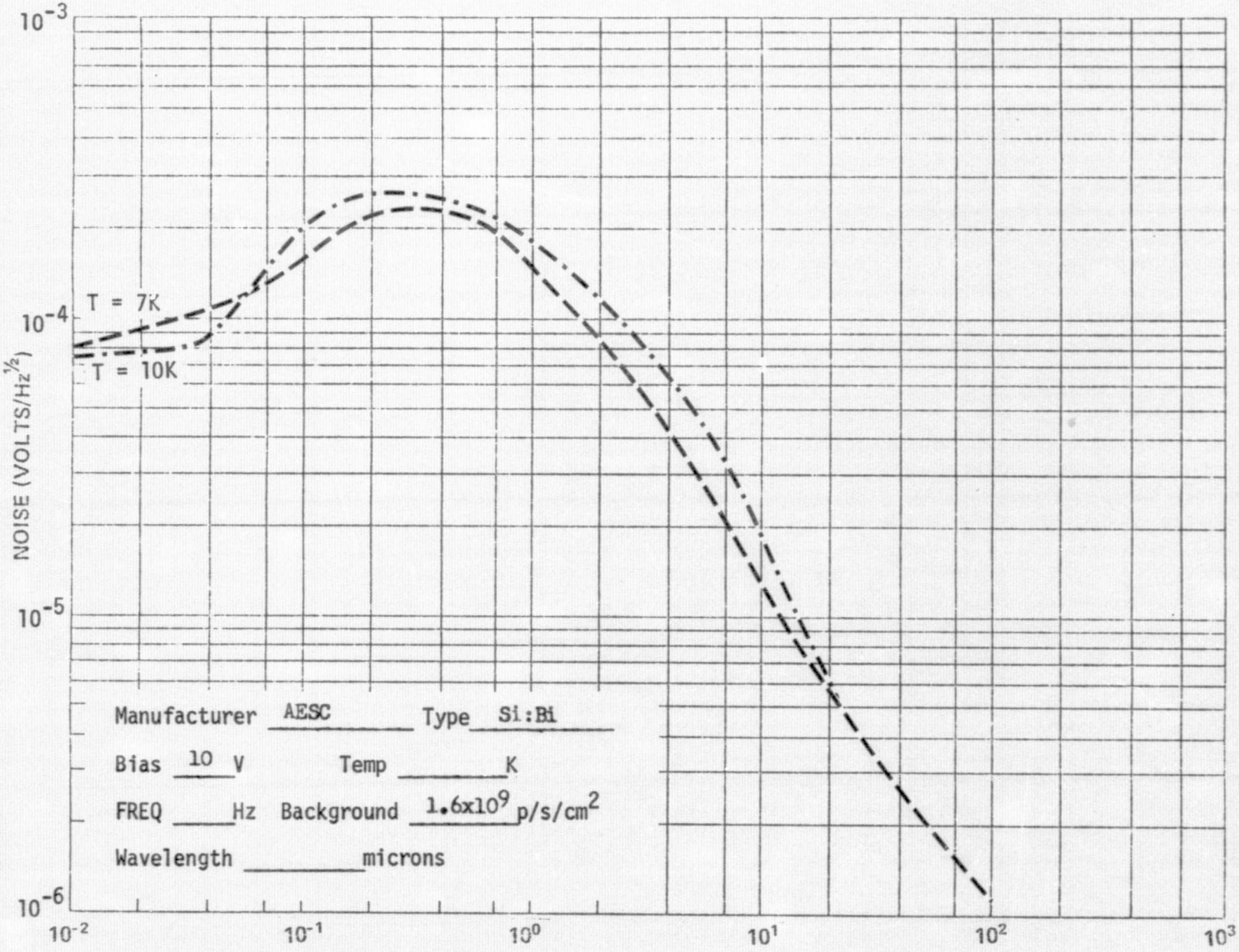

NOISE SPECTRUM

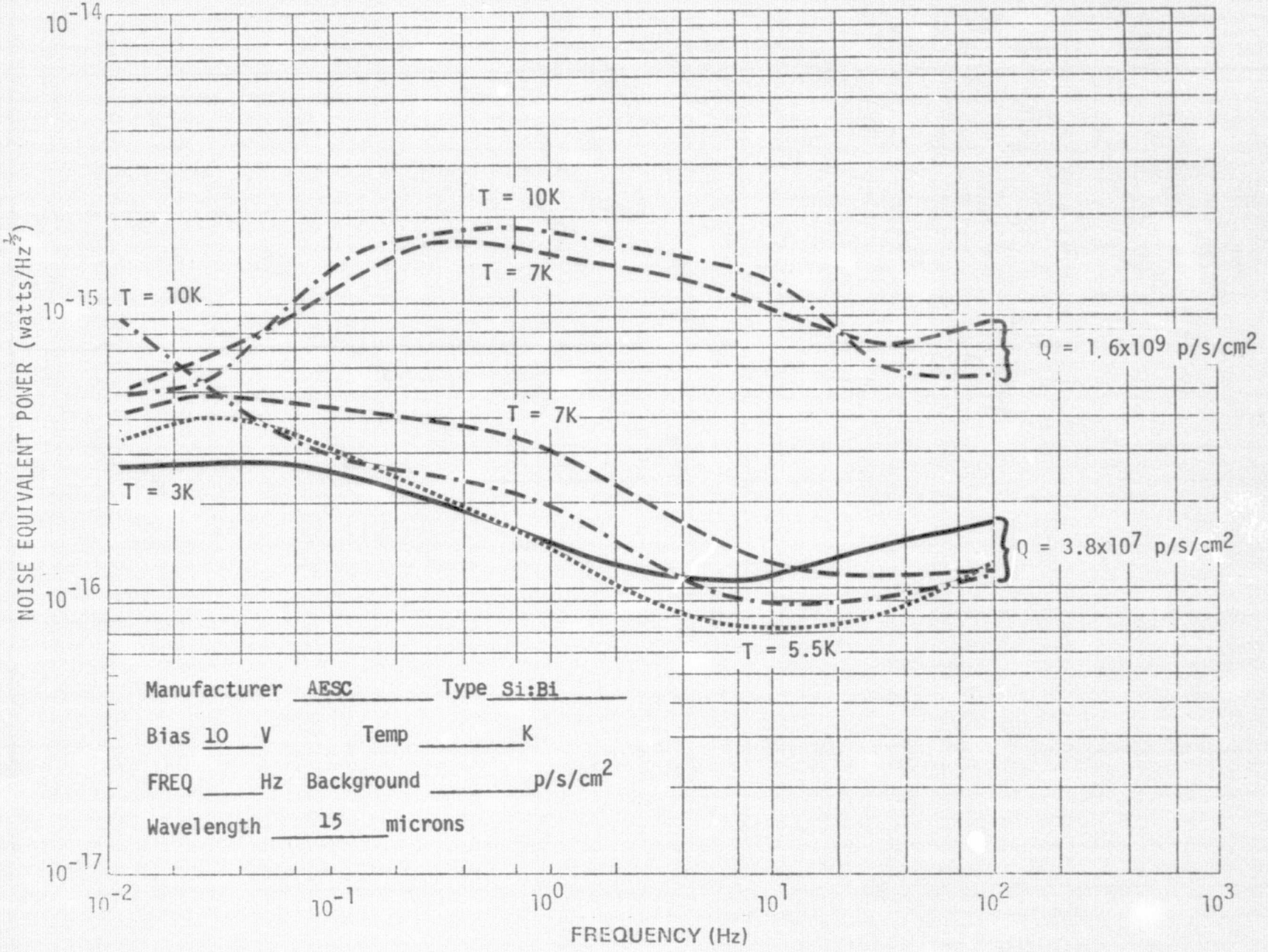
NOISE EQUIVALENT POWER (watts/Hz$^{\frac{1}{2}}$)
10^{-14}
10^{-15}
10^{-16}
10^{-17}
T = 10K
T = 7K
T = 10K
T = 7K
T = 3K
T = 5.5K
Q = 1.6x10^9 p/s/cm^2
Q = 3.8x10^7 p/s/cm^2
Manufacturer AESC Type Si:Bi
Bias 10 V Temp ____K
FREQ ____Hz Background ____p/s/cm^2
Wavelength 15 microns
10^{-2}
10^{-1}
10^{0}
10^{1}
10^{2}
10^{3}
FREQUENCY (Hz)

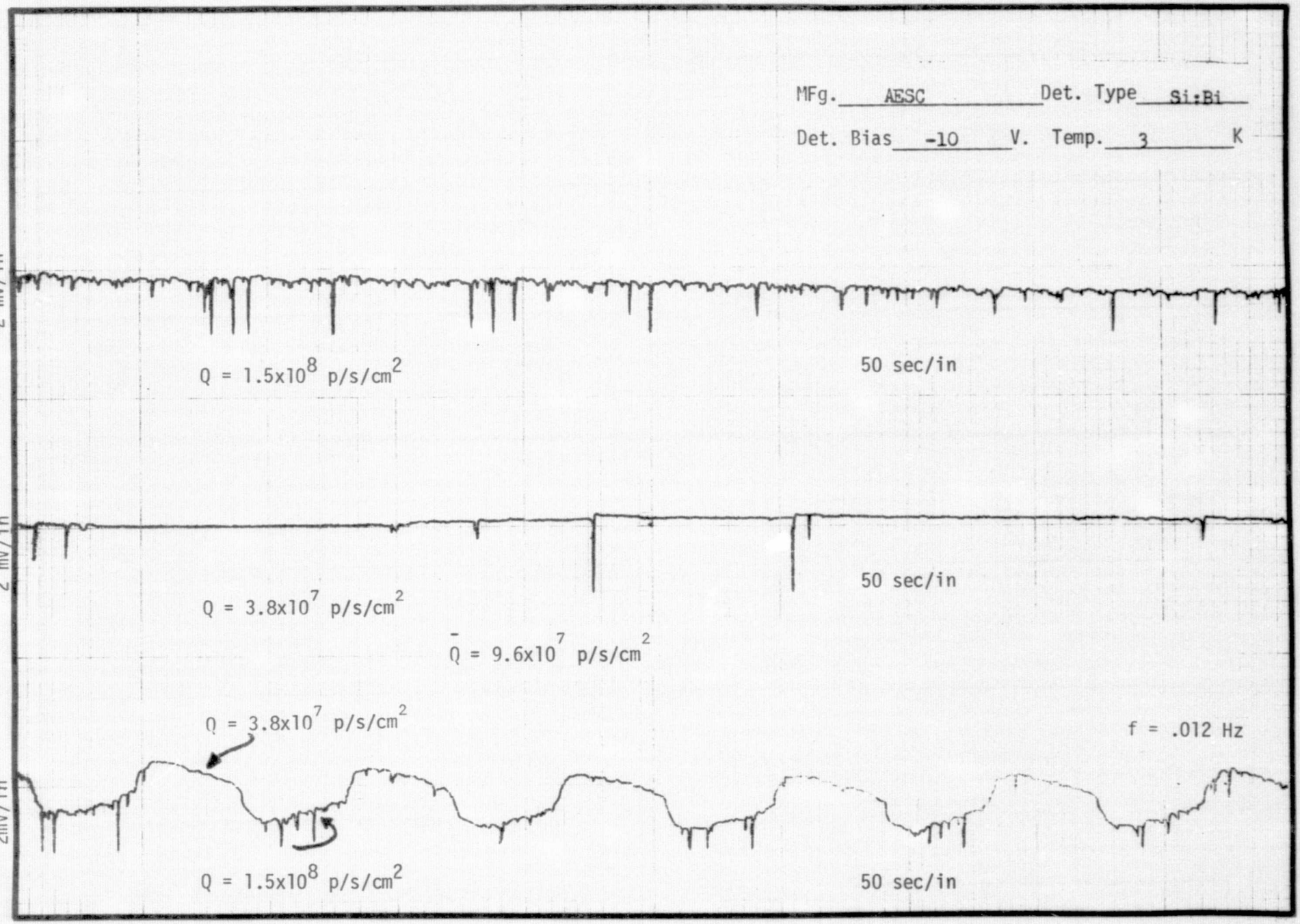
MFg. AESC Det. Type Si:Bi
Det. Bias -10 V. Temp. 3 K
2 mV/in
Q = 1.5x10^8 p/s/cm^2
50 sec/in
2 mV/in
Q = 3.8x10^7 p/s/cm^2
50 sec/in
Q = 9.6x10^7 p/s/cm^2
Q = 3.8x10^7 p/s/cm^2
f = .012 Hz
2mV/in
Q = 1.5x10^8 p/s/cm^2
50 sec/in
DETECTOR OUTPUT
TIME

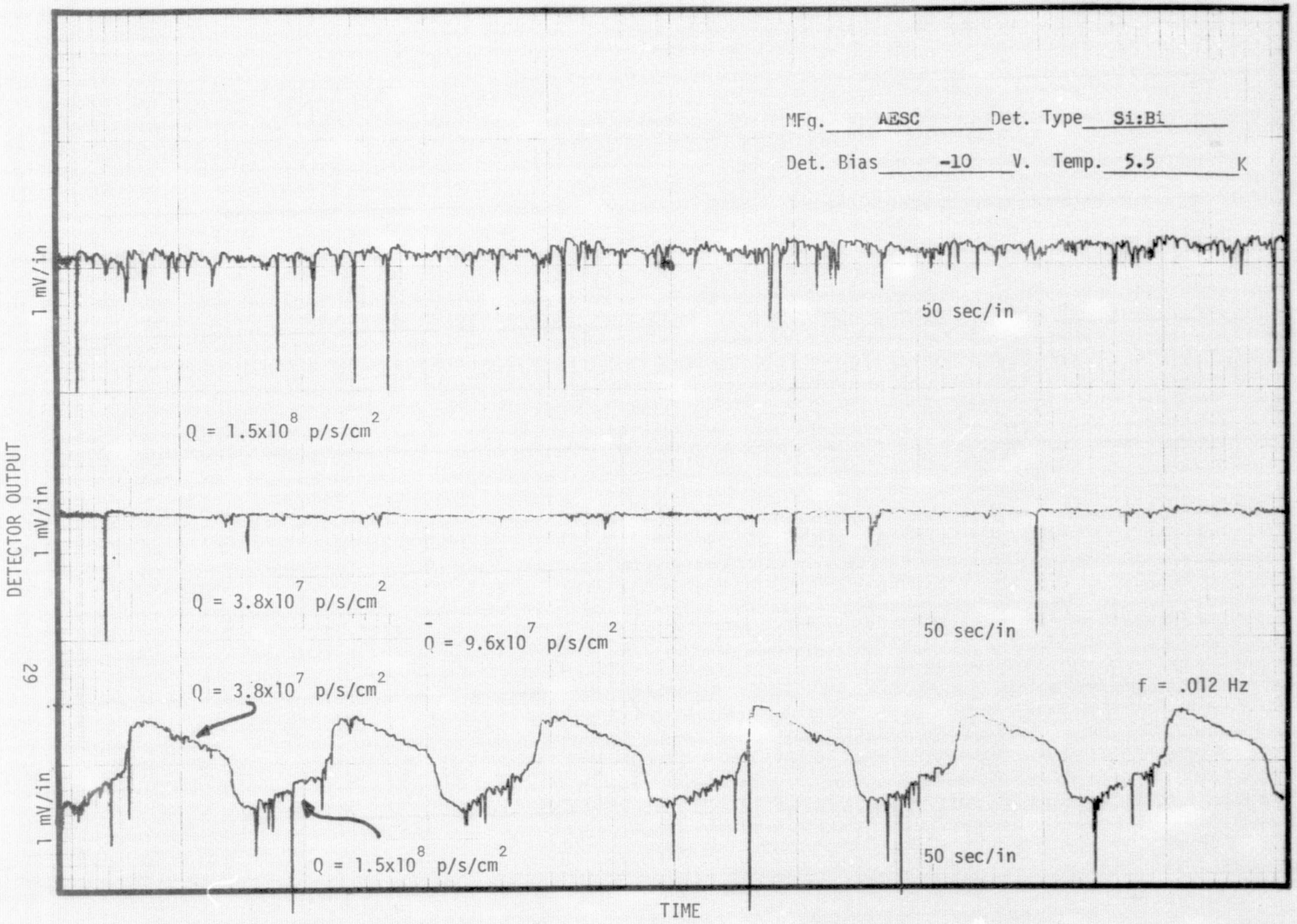
MFg. AESC Det. Type Si:Bi
Det. Bias -10 V. Temp. 5.5 K
1 mV/in
50 sec/in
Q = 1.5x10^8 p/s/cm^2
DETECTOR OUTPUT
1 mV/in
Q = 3.8x10^7 p/s/cm^2
Q = 9.6x10^7 p/s/cm^2
50 sec/in
62
Q = 3.8x10^7 p/s/cm^2
f = .012 Hz
1 mV/in
Q = 1.5x10^8 p/s/cm^2
50 sec/in
TIME

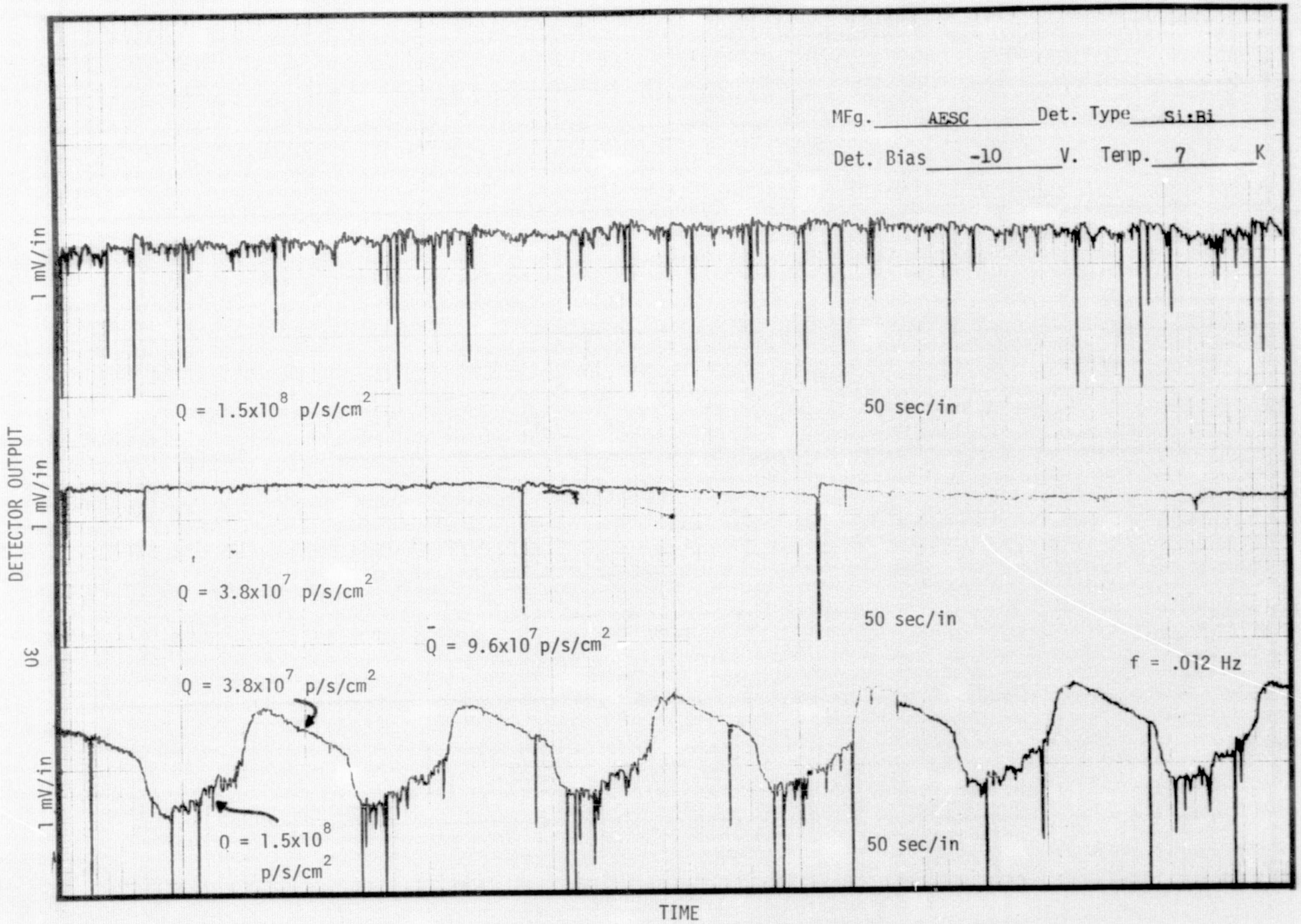
MFg. AESC Det. Type Si:Bi
Det. Bias -10 V. Temp. 7 K
1 mV/in
Q = 1.5x10^8 p/s/cm^2
50 sec/in
DETECTOR OUTPUT
1 mV/in
Q = 3.8x10^7 p/s/cm^2
50 sec/in
Q = 9.6x10^7 p/s/cm^2
Q = 3.8x10^7 p/s/cm^2
f = .012 Hz
1 mV/in
Q = 1.5x10^8 p/s/cm^2
50 sec/in
TIME

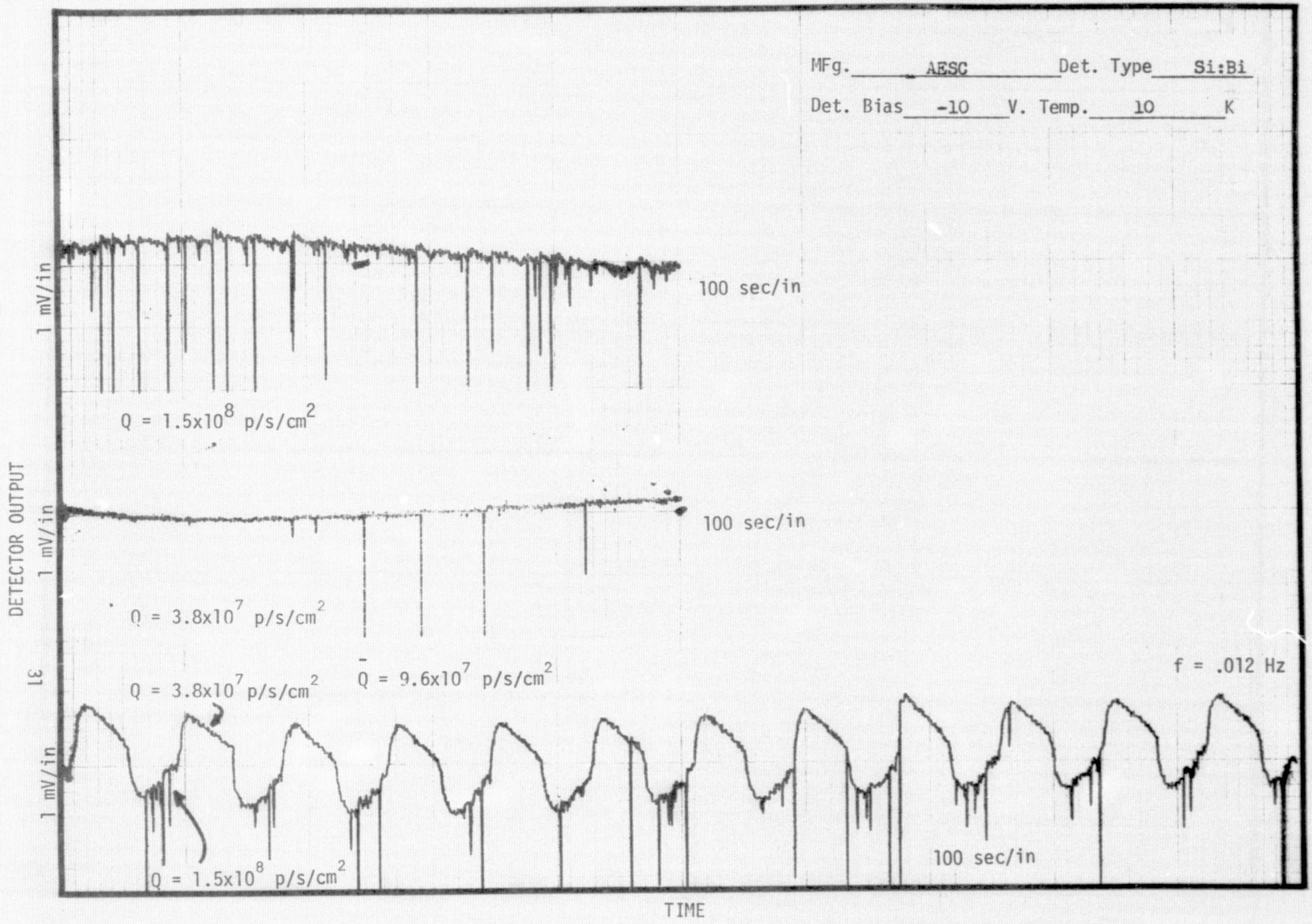
MFg. AESC Det. Type Si:Bi
Det. Bias -10 V. Temp. 10 K
DETECTOR OUTPUT
1 mV/in
100 sec/in
Q = 1.5x10^8 p/s/cm^2
1 mV/in
100 sec/in
Q = 3.8x10^7 p/s/cm^2
Q = 3.8x10^7 p/s/cm^2
Q = 9.6x10^7 p/s/cm^2
f = .012 Hz
1 mV/in
Q = 1.5x10^8 p/s/cm^2
100 sec/in
TIME

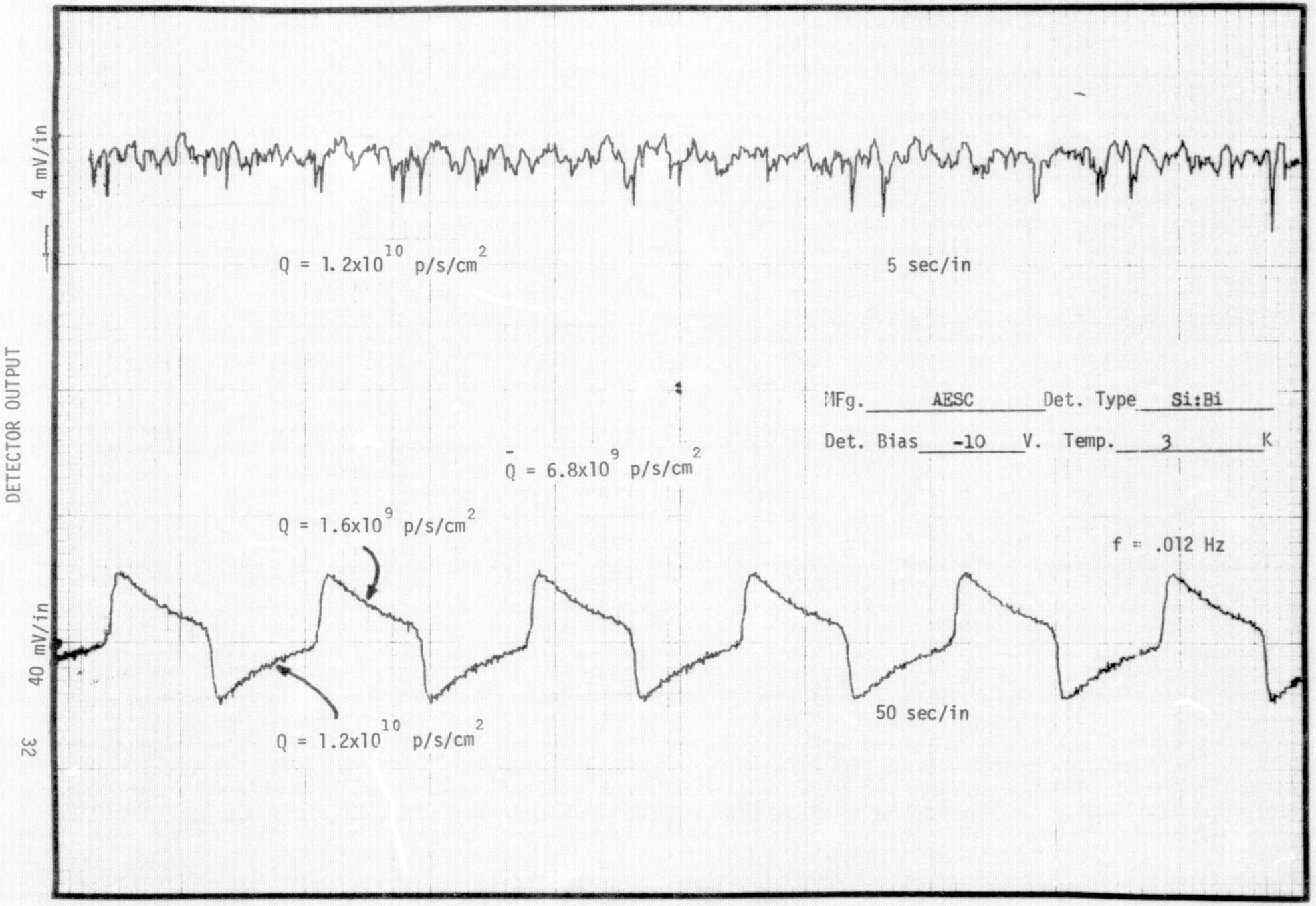
4 mV/in
Q = 1.2x10^10 p/s/cm^2
5 sec/in
MFg. AESC Det. Type Si:Bi
Det. Bias -10 V. Temp. 3 K
Q = 6.8x10^9 p/s/cm^2
Q = 1.6x10^9 p/s/cm^2
f = .012 Hz
40 mV/in
Q = 1.2x10^10 p/s/cm^2
50 sec/in
32
DETECTOR OUTPUT
TIME

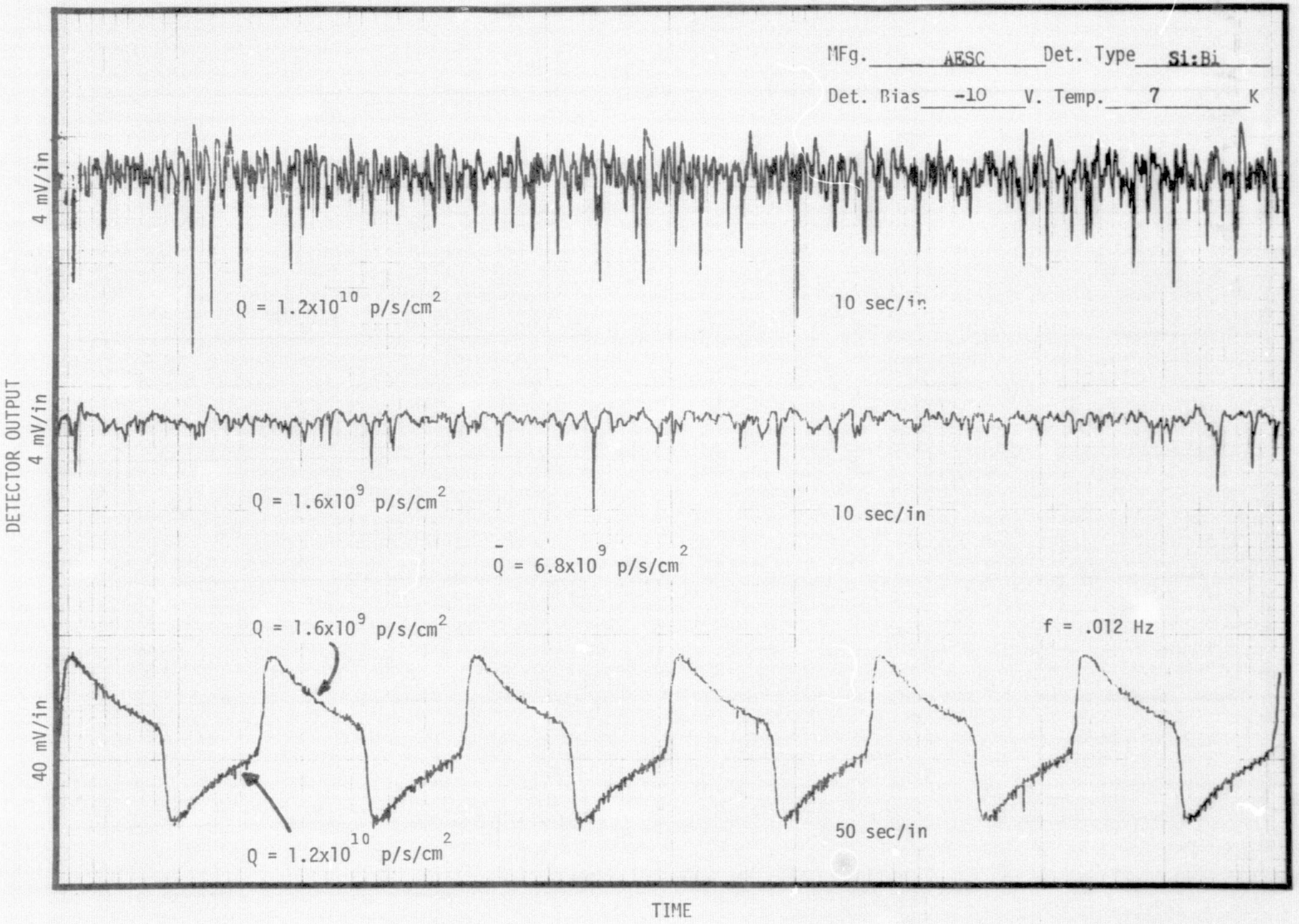
MFg. AESC Det. Type Si:Bi
Det. Bias -10 V. Temp. 7 K
DETECTOR OUTPUT
4 mV/in
Q = 1.2x10^10 p/s/cm^2
10 sec/in
4 mV/in
Q = 1.6x10^9 p/s/cm^2
10 sec/in
Q = 6.8x10^9 p/s/cm^2
Q = 1.6x10^9 p/s/cm^2
f = .012 Hz
40 mV/in
Q = 1.2x10^10 p/s/cm^2
50 sec/in
TIME

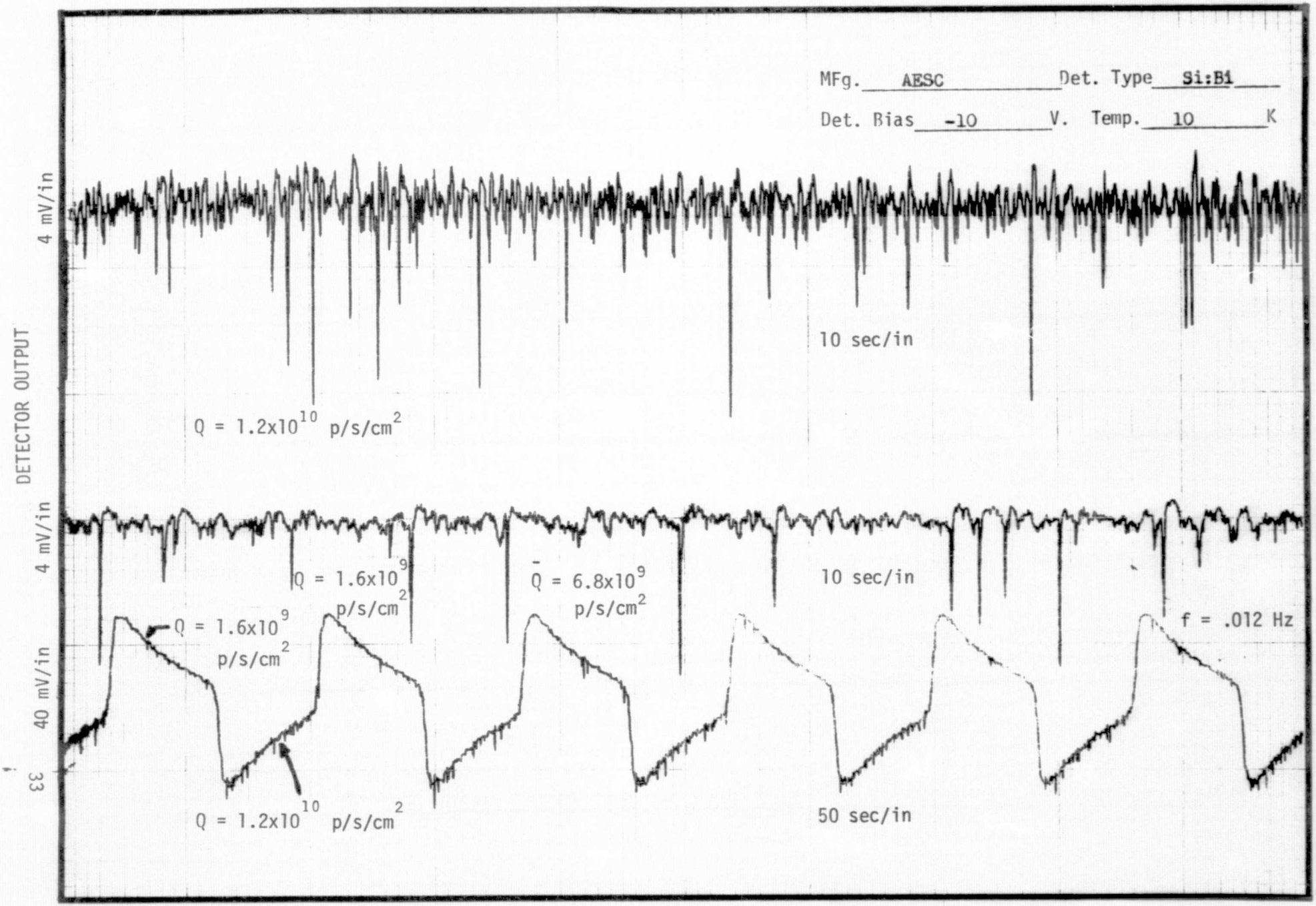
MFg. AESC
Det. Type Si:Bi
Det. Bias -10 V. Temp. 10 K
DETECTOR OUTPUT
4 mV/in
10 sec/in
Q = 1.2x10^10 p/s/cm^2
4 mV/in
Q = 1.6x10^9 p/s/cm^2
Q = 6.8x10^9 p/s/cm^2
10 sec/in
Q = 1.6x10^9 p/s/cm^2
f = .012 Hz
40 mV/in
Q = 1.2x10^10 p/s/cm^2
50 sec/in
TIME

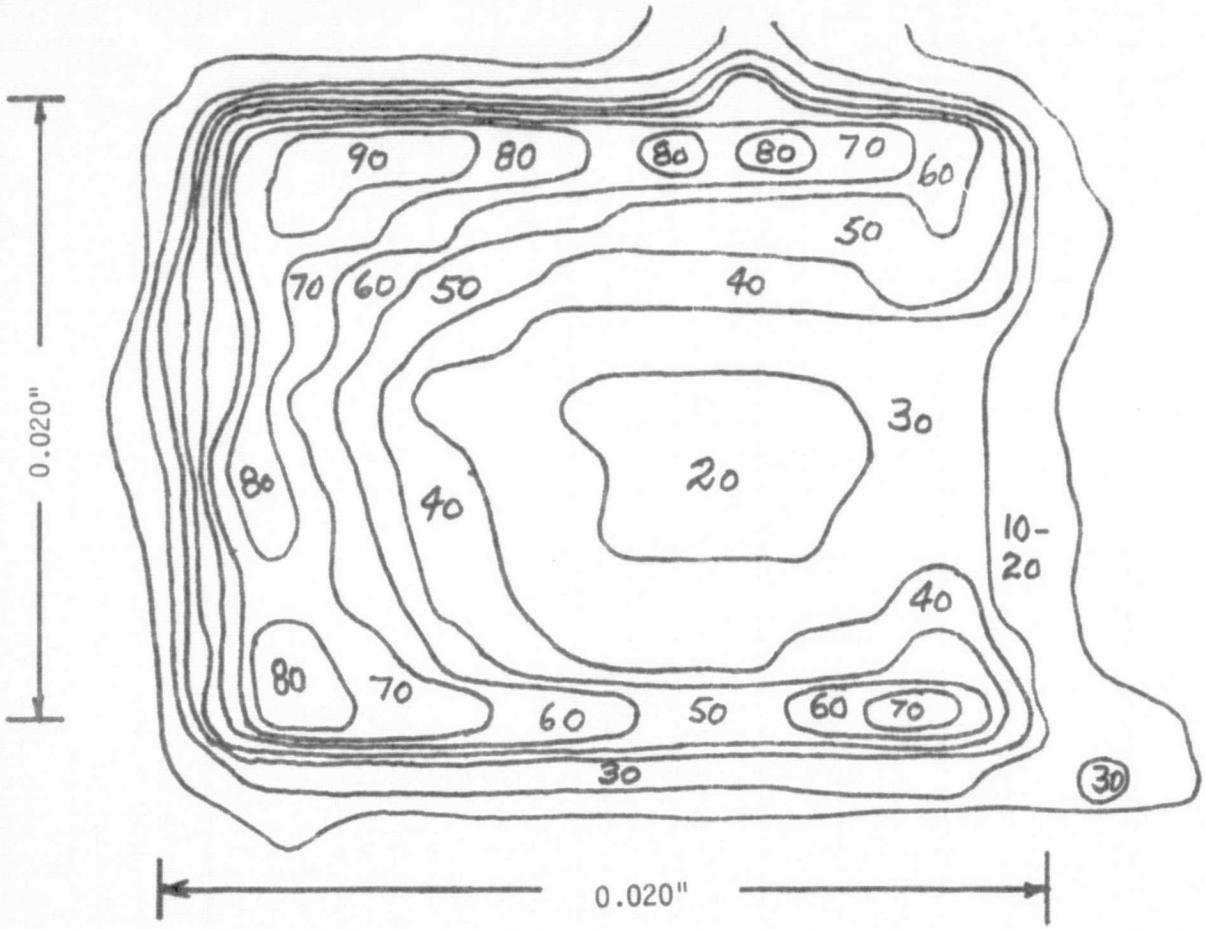

SENSIVITY CONTOUR

MAX. SIGNAL = 40μV

Manufacturer AESC Type Si:Bi

Bias 5 V Temp 5.5 K
FREQ 10 Hz Background 10^5 p/s/cm^2

Wavelength 10 microns

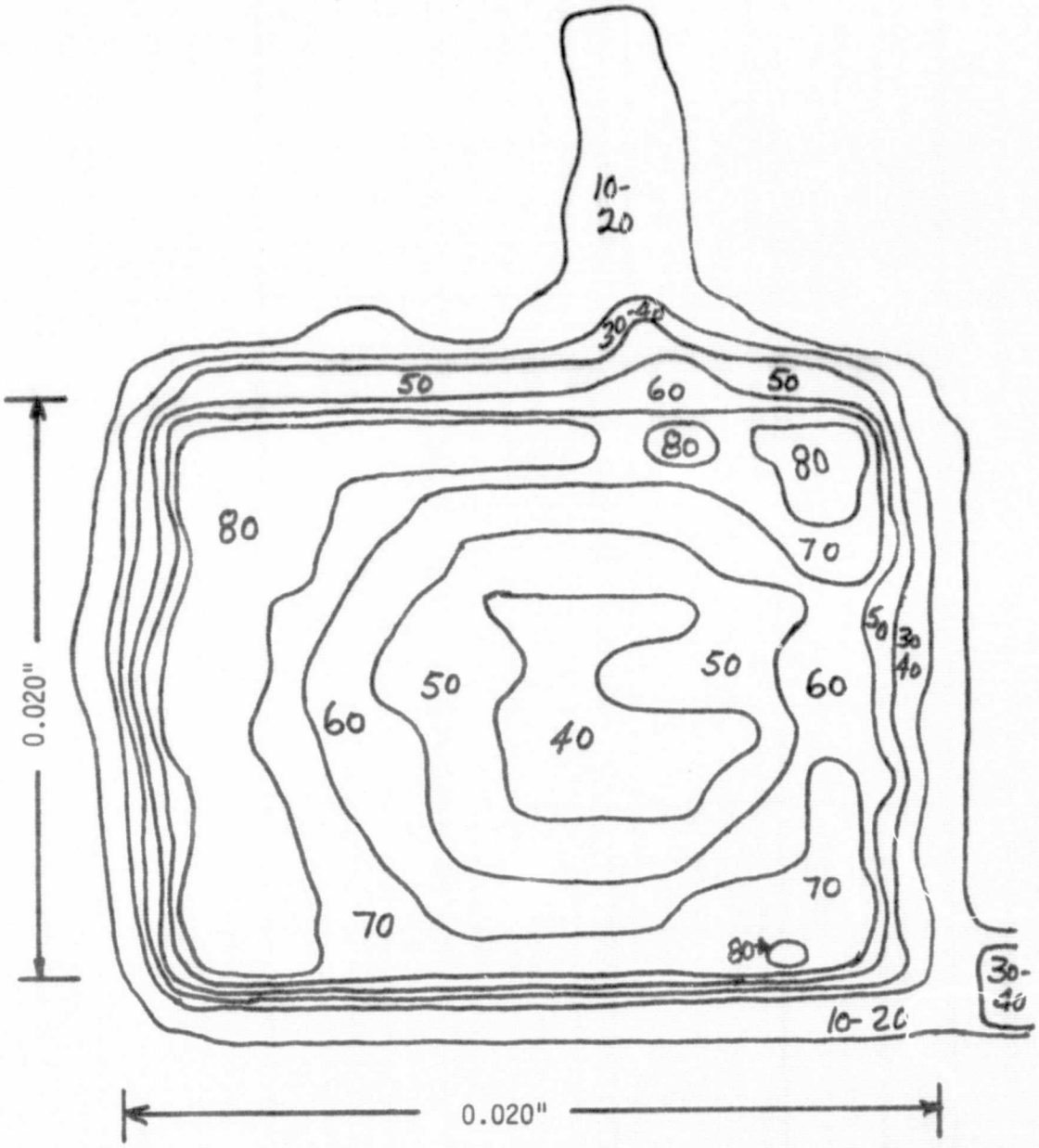

MAX. SIGNAL = 80μV

SENSIVITY CONTOUR

Manufacturer AESC Type Si:Bi

Bias 10 V Temp 5.5 K
FREQ 10 Hz Background 10^6 p/s/cm^2

Wavelength 10 microns

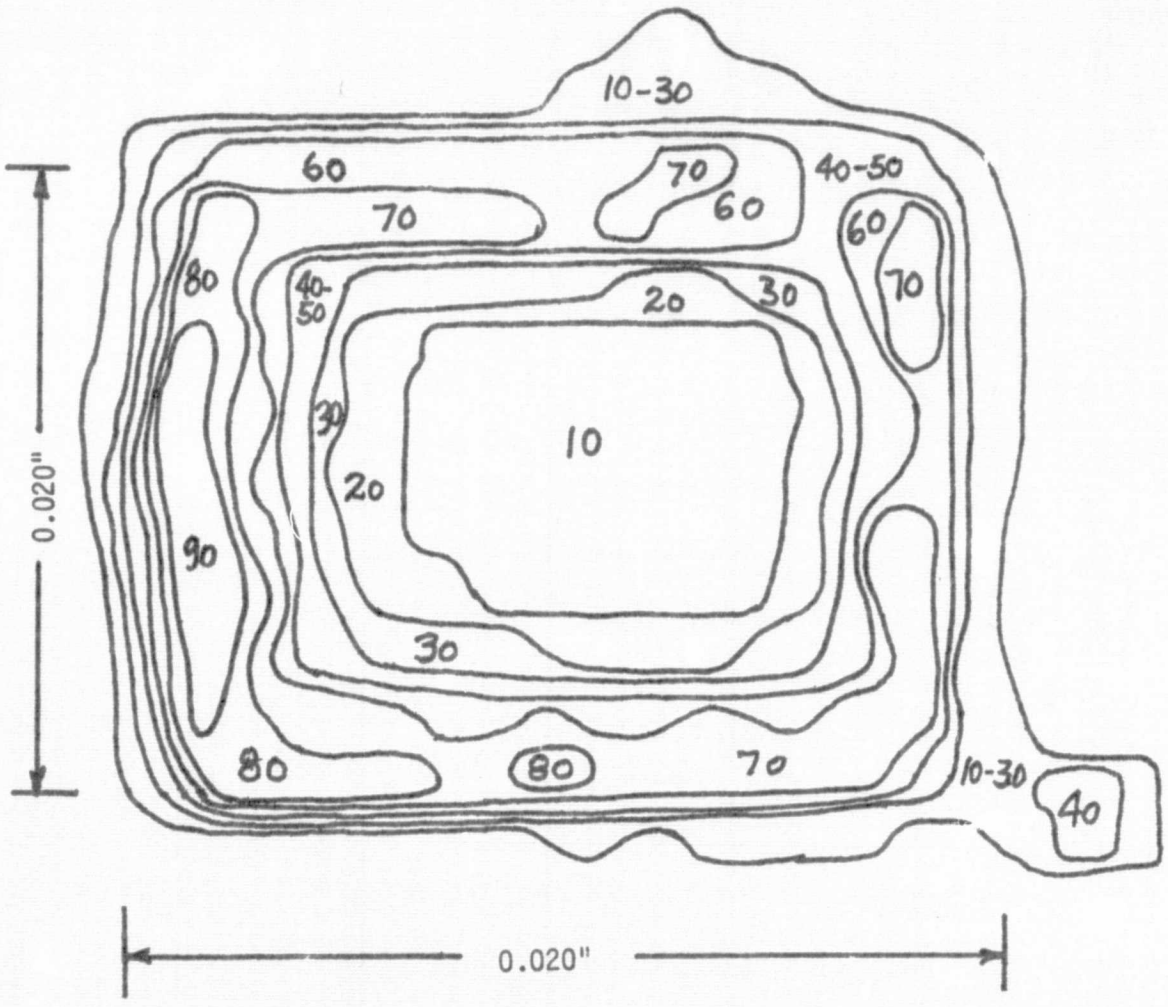

MAX. SIGNAL =8mV

SENSIVITY CONTOUR

Manufacturer AESC Type Si:Bi

Bias 10 V Temp 5.5 K

FREQ 10 Hz Background 10^6 p/s/cm^2

Wavelength 10 microns

5.2 AESC Si:As. When measurements were initiated on this detector (#4), a great deal of spontaneous spiking was observed and measurements were completed under the low background condition in the presence of these spikes. During the course of the high background measurements, the spiking rate decreased to zero. The low background noise spectra was remeasured, and these spectra are shown both with and without spikes. Detector outputs versus time are also shown both with and without spikes. The high background data are shown only in the absence of spikes. NEP data shown were calculated using the "no spike" noise spectra.

When the detector was removed from the measurement Dewar, a large crack was observed in the silicon chip near the measured detector. Although the crack did not appear to have effected signal measurements, it is possible that the appearance of the crack is related to the disappearance of the spikes. If the spikes were related to the mechanical stress set up in the silicon by differential thermal expansion between the silicon and the metallic mount, the crack may have relieved this stress and thus eliminated the spikes. The linear thermal contraction of silicon from 293K to 4K is 2.2×10^{-4} times the 293K length, whereas that of metals like aluminum and copper are about $3\text{-}4 \times 10^{-3}$ times the 293K length.

The spatial sensitivity of this detector was quite uniform with a variation of less than 10% over the entire active area.

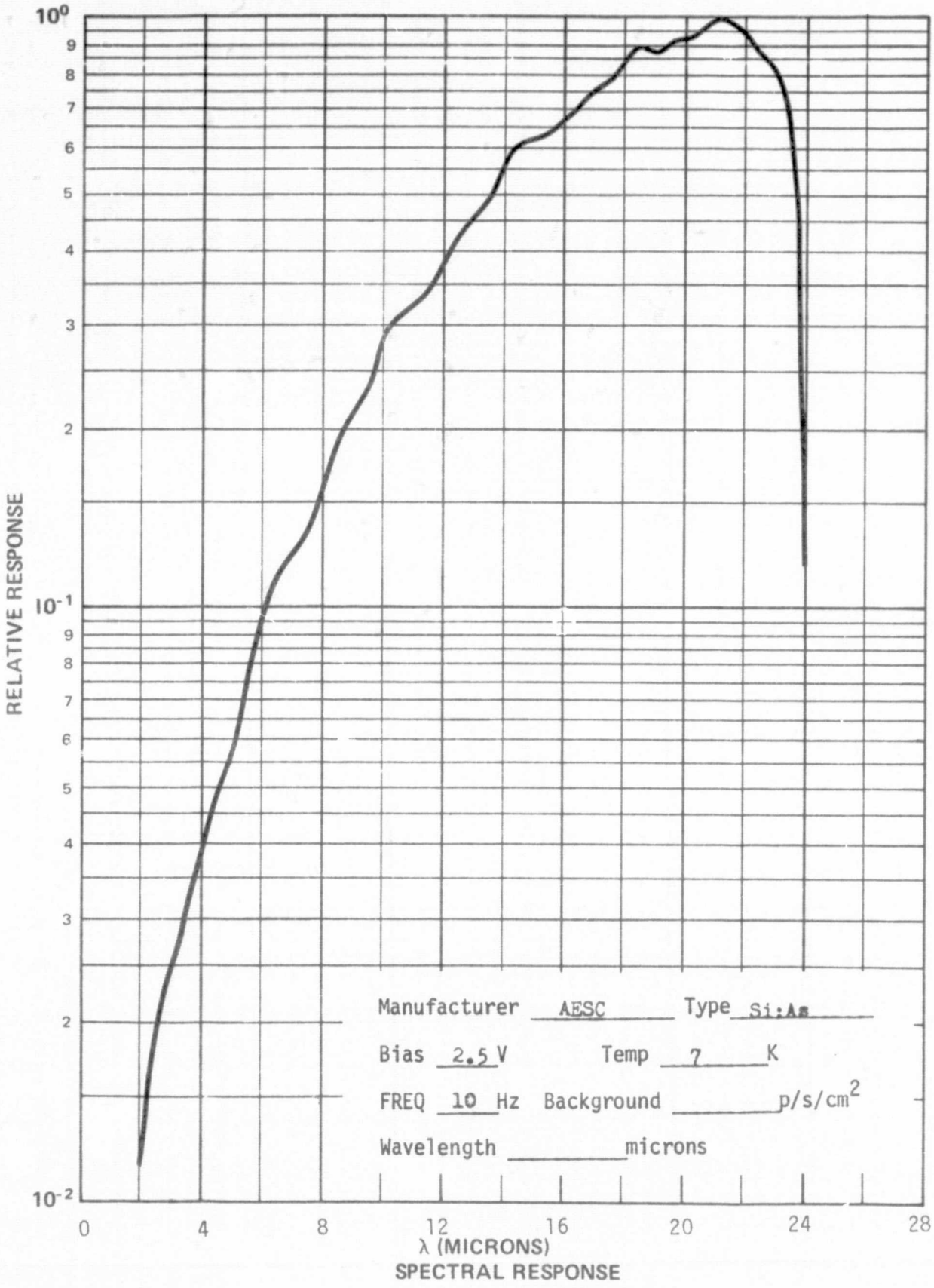

SPECTRAL RESPONSE

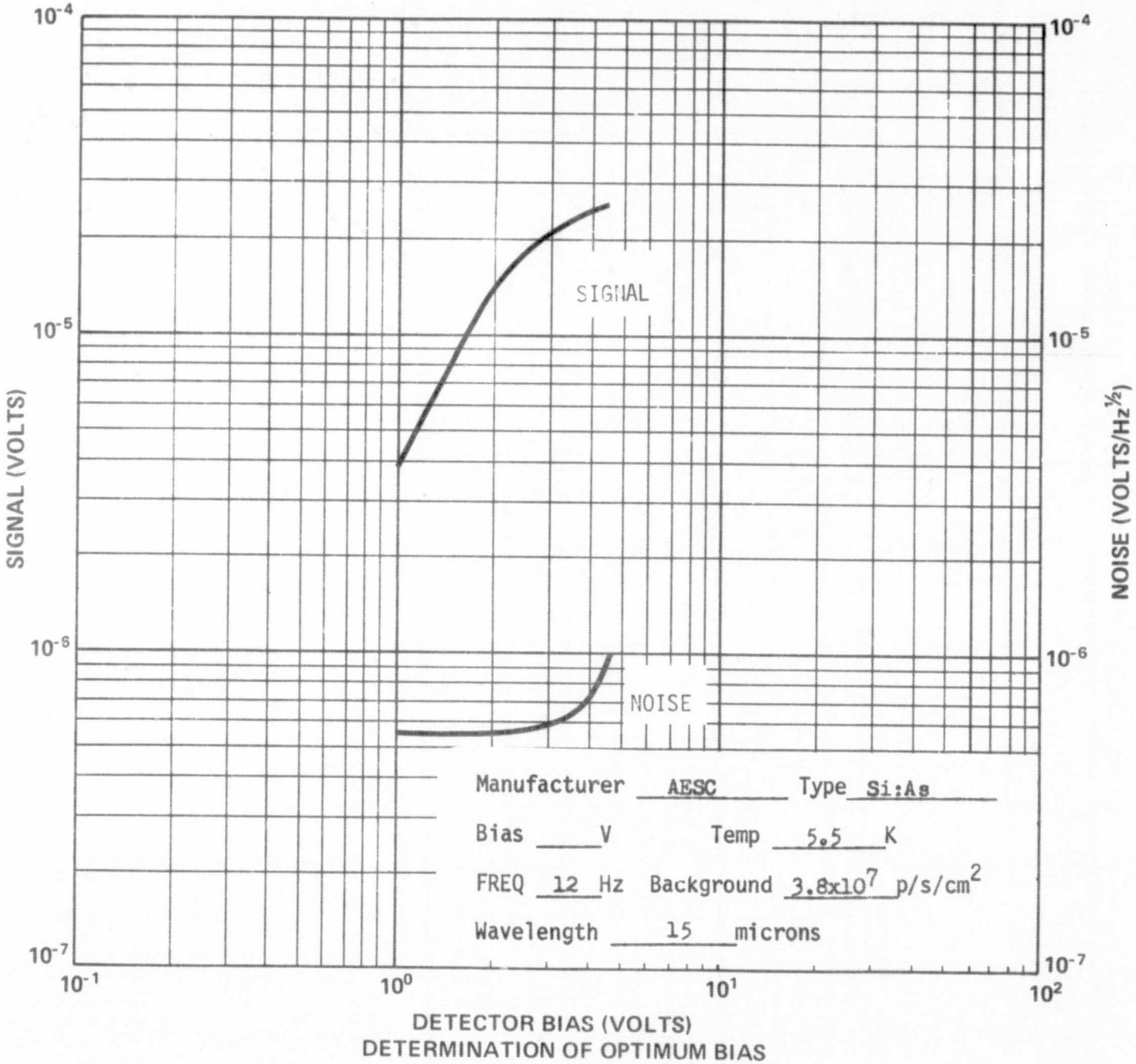

DETERMINATION OF OPTIMUM BIAS

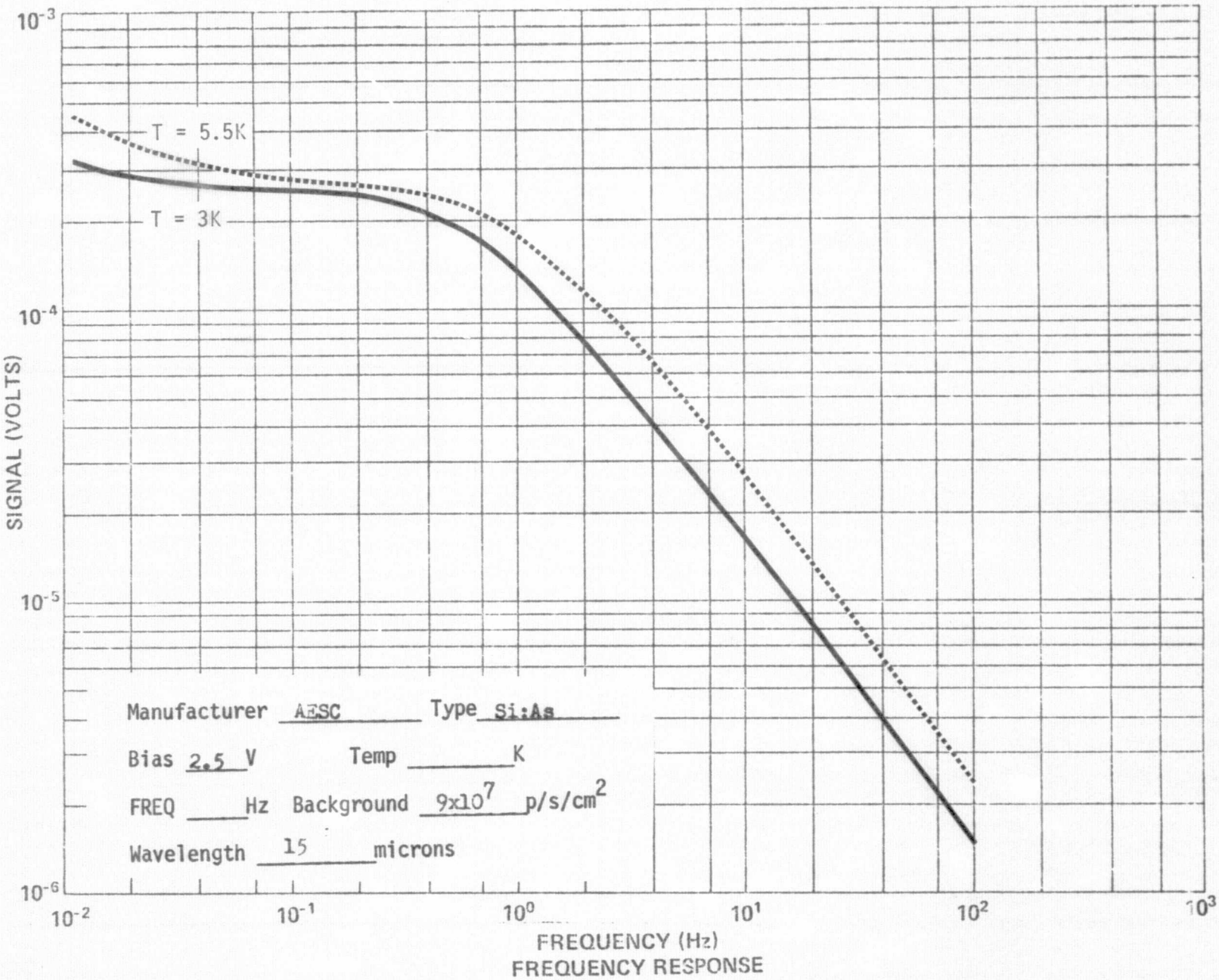

FREQUENCY RESPONSE

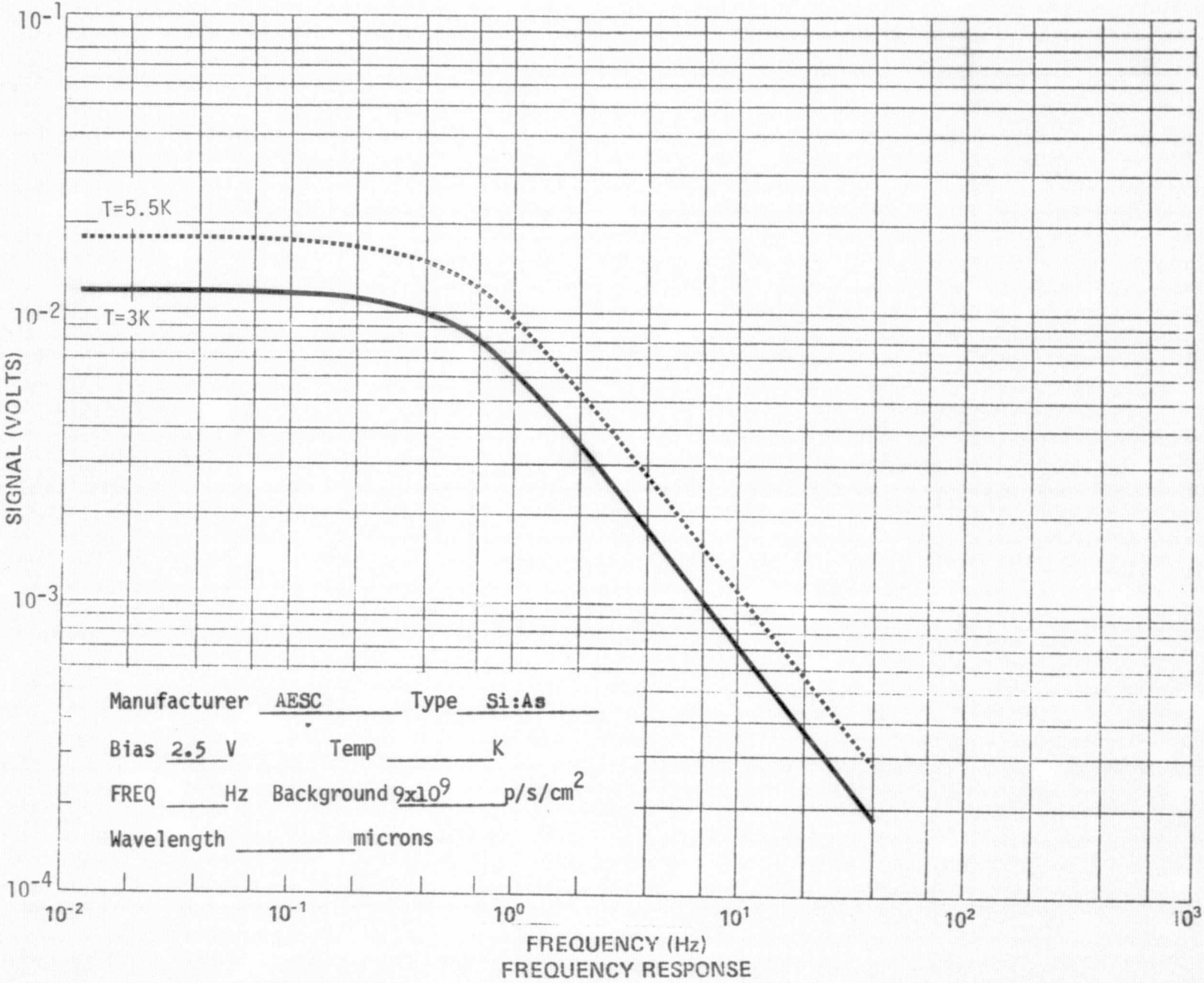

FREQUENCY RESPONSE

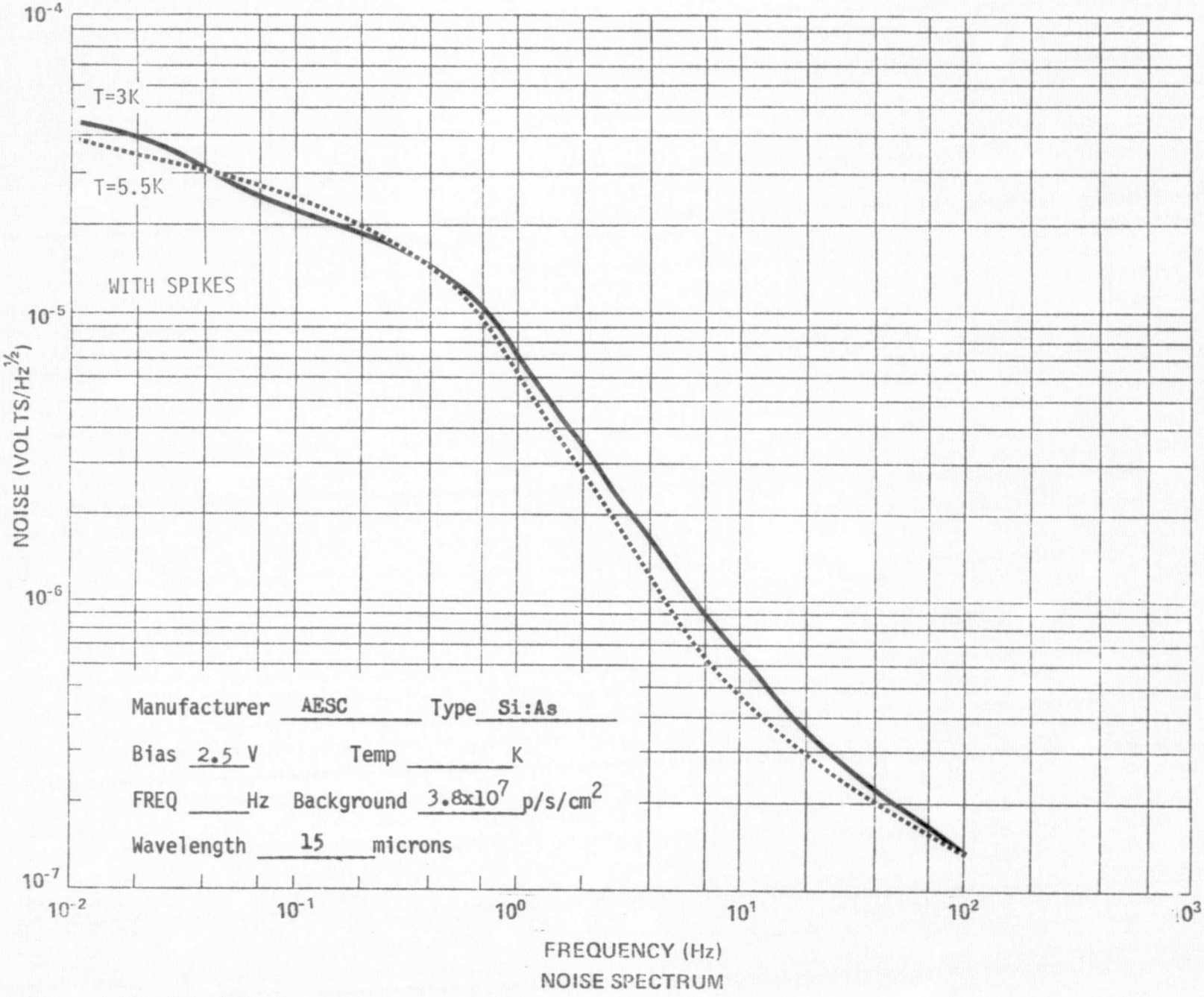

NOISE SPECTRUM

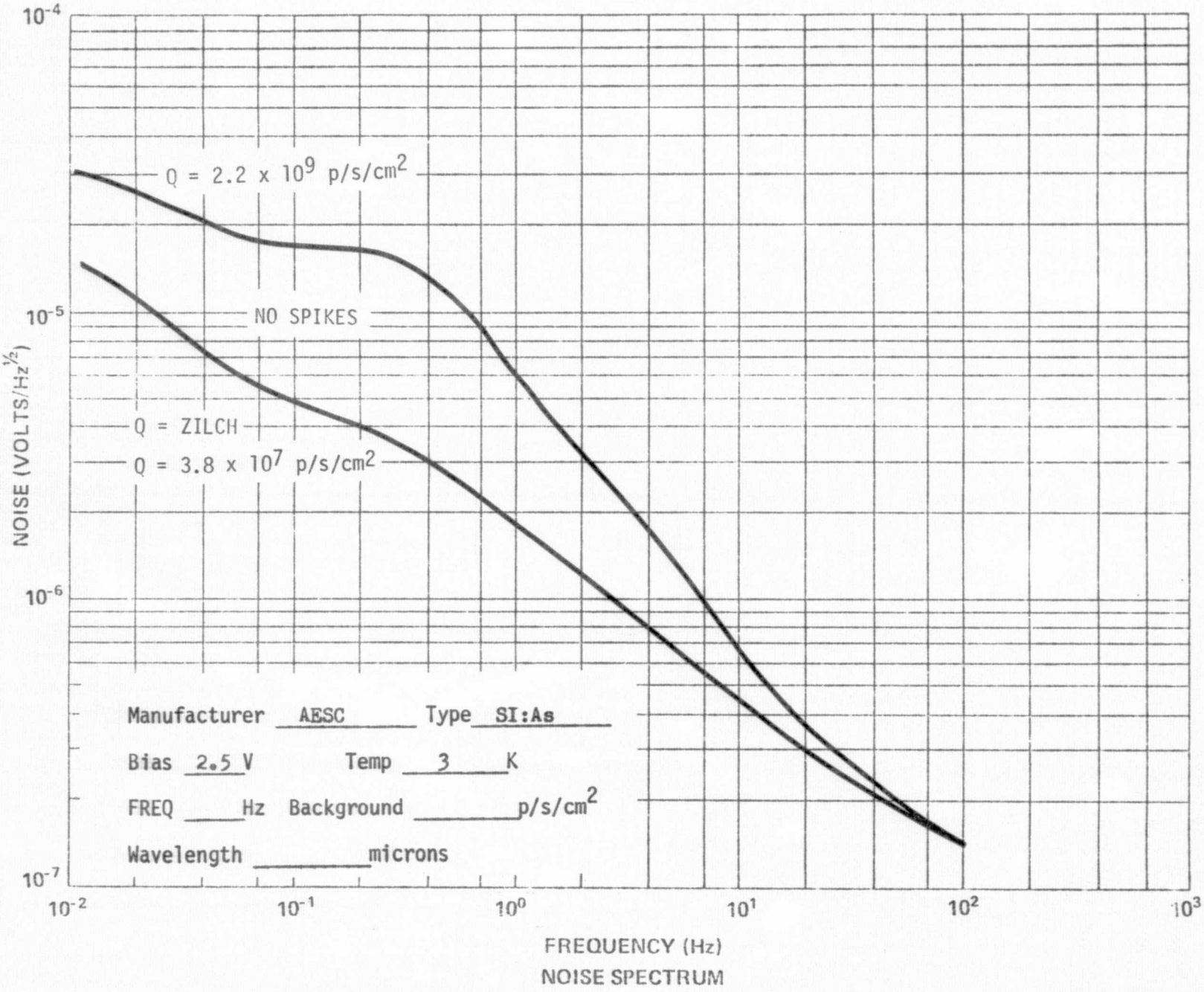

NOISE SPECTRUM

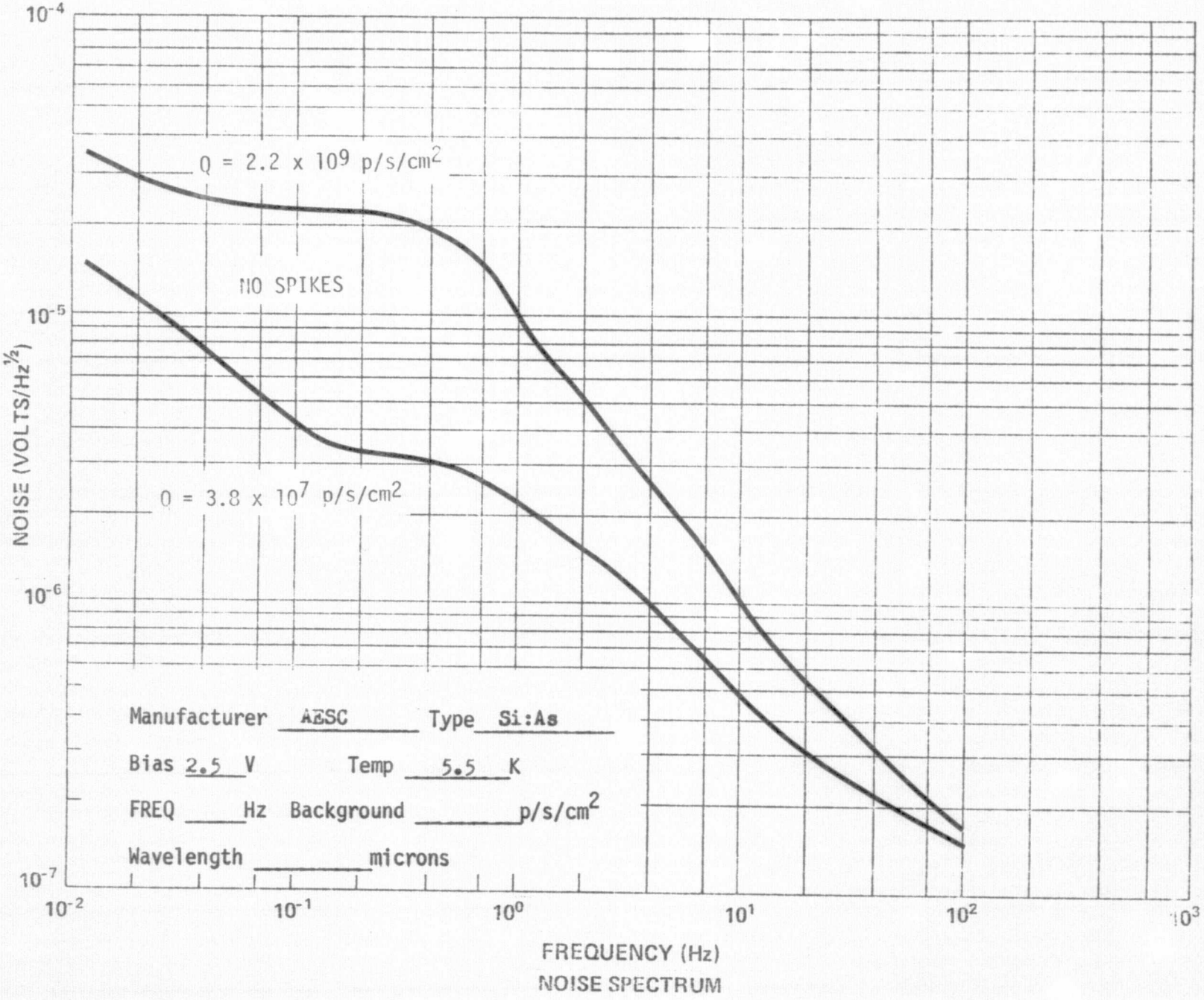

NOISE SPECTRUM

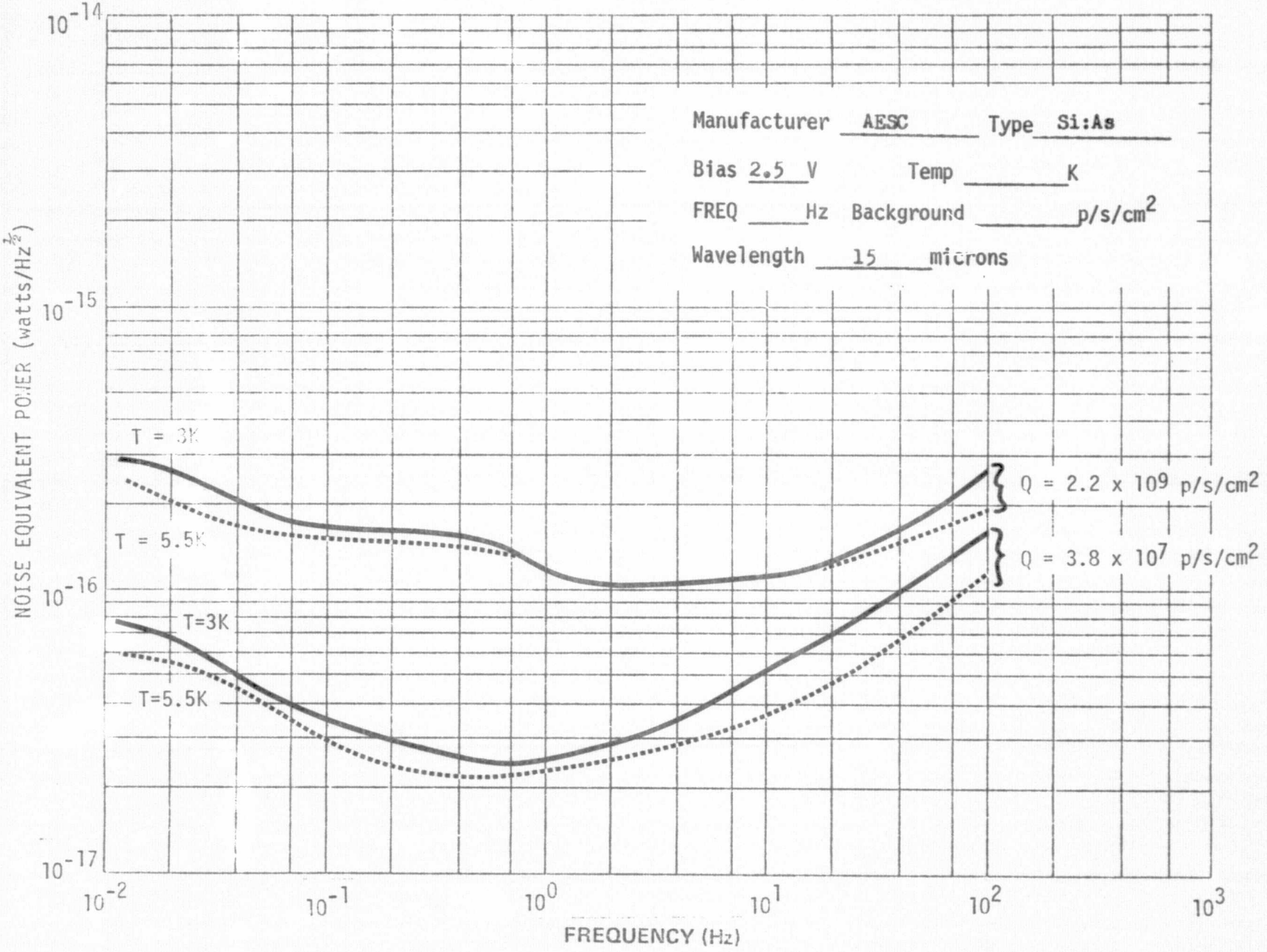
Manufacturer AESC Type Si:As
Bias 2.5 V Temp K
FREQ Hz Background p/s/cm2
Wavelength 15 microns
T = 3K
T = 5.5K
T=3K
T=5.5K
Q = 2.2 x 10^9 p/s/cm2
Q = 3.8 x 10^7 p/s/cm2
NOISE EQUIVALENT POWER (watts/Hz^½)
FREQUENCY (Hz)
10^-14
10^-15
10^-16
10^-17
10^-2
10^-1
10^0
10^1
10^2
10^3

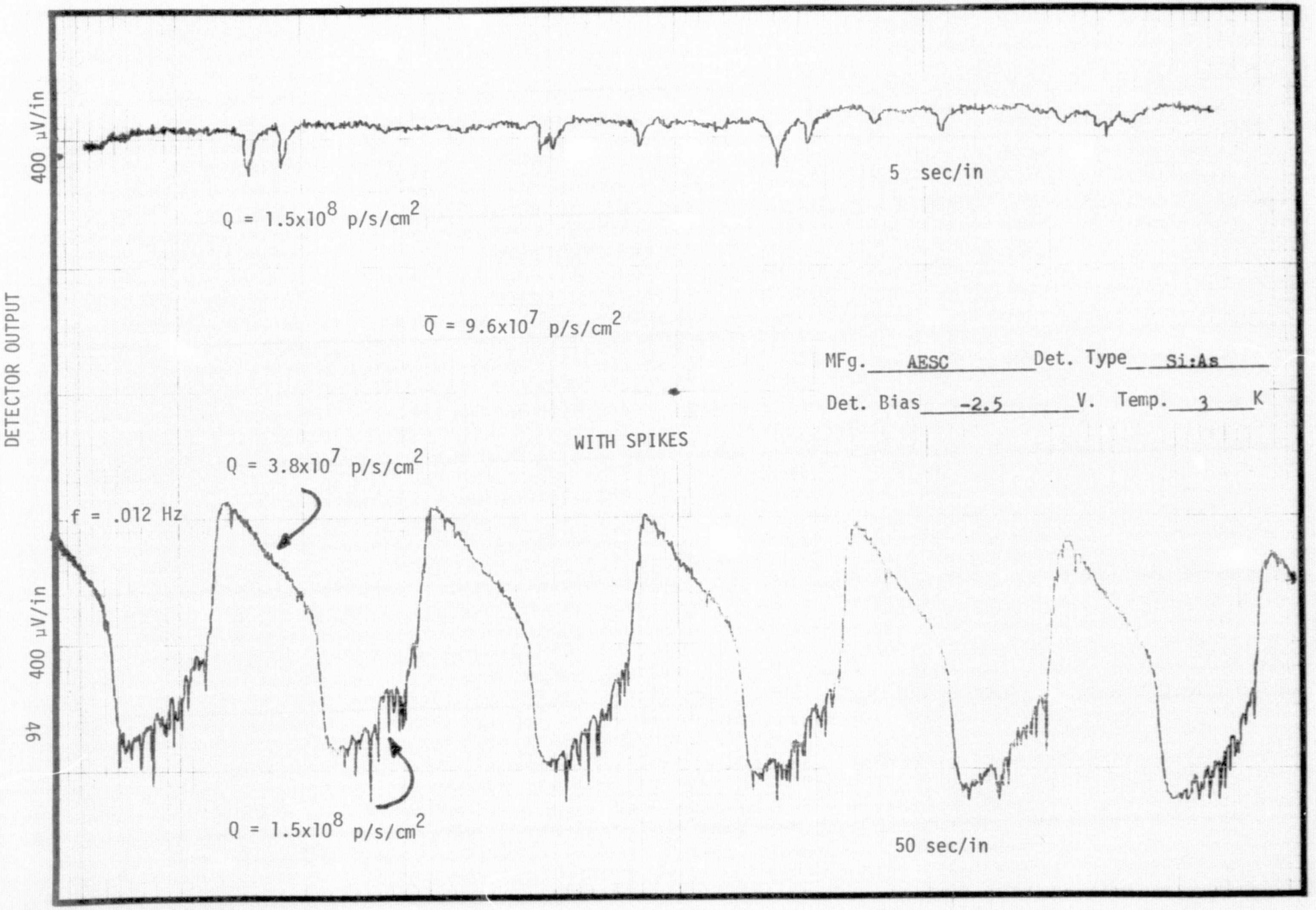
400 μV/in
5 sec/in
Q = 1.5x10^8 p/s/cm^2
Q̄ = 9.6x10^7 p/s/cm^2
MFg. AESC Det. Type Si:As
Det. Bias -2.5 V. Temp. 3 K
WITH SPIKES
Q = 3.8x10^7 p/s/cm^2
f = .012 Hz
400 μV/in
Q = 1.5x10^8 p/s/cm^2
50 sec/in
DETECTOR OUTPUT
TIME

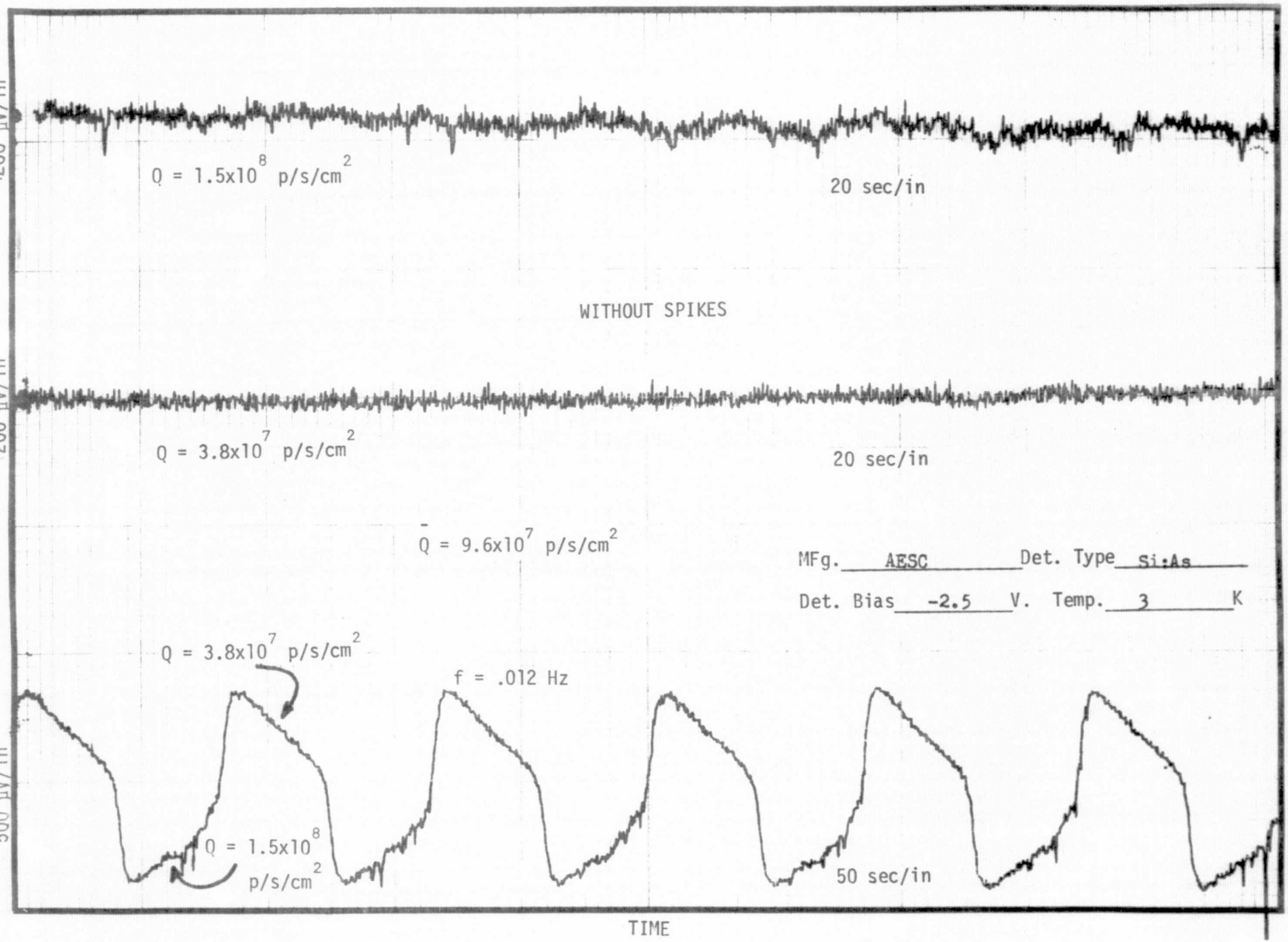
200 μV/in
Q = 1.5x10^8 p/s/cm^2
20 sec/in
WITHOUT SPIKES
200 μV/in
Q = 3.8x10^7 p/s/cm^2
20 sec/in
Q = 9.6x10^7 p/s/cm^2
MFg. AESC Det. Type Si:As
Det. Bias -2.5 V. Temp. 3 K
DETECTOR OUTPUT
47
Q = 3.8x10^7 p/s/cm^2
f = .012 Hz
500 μV/in
Q = 1.5x10^8 p/s/cm^2
50 sec/in
TIME

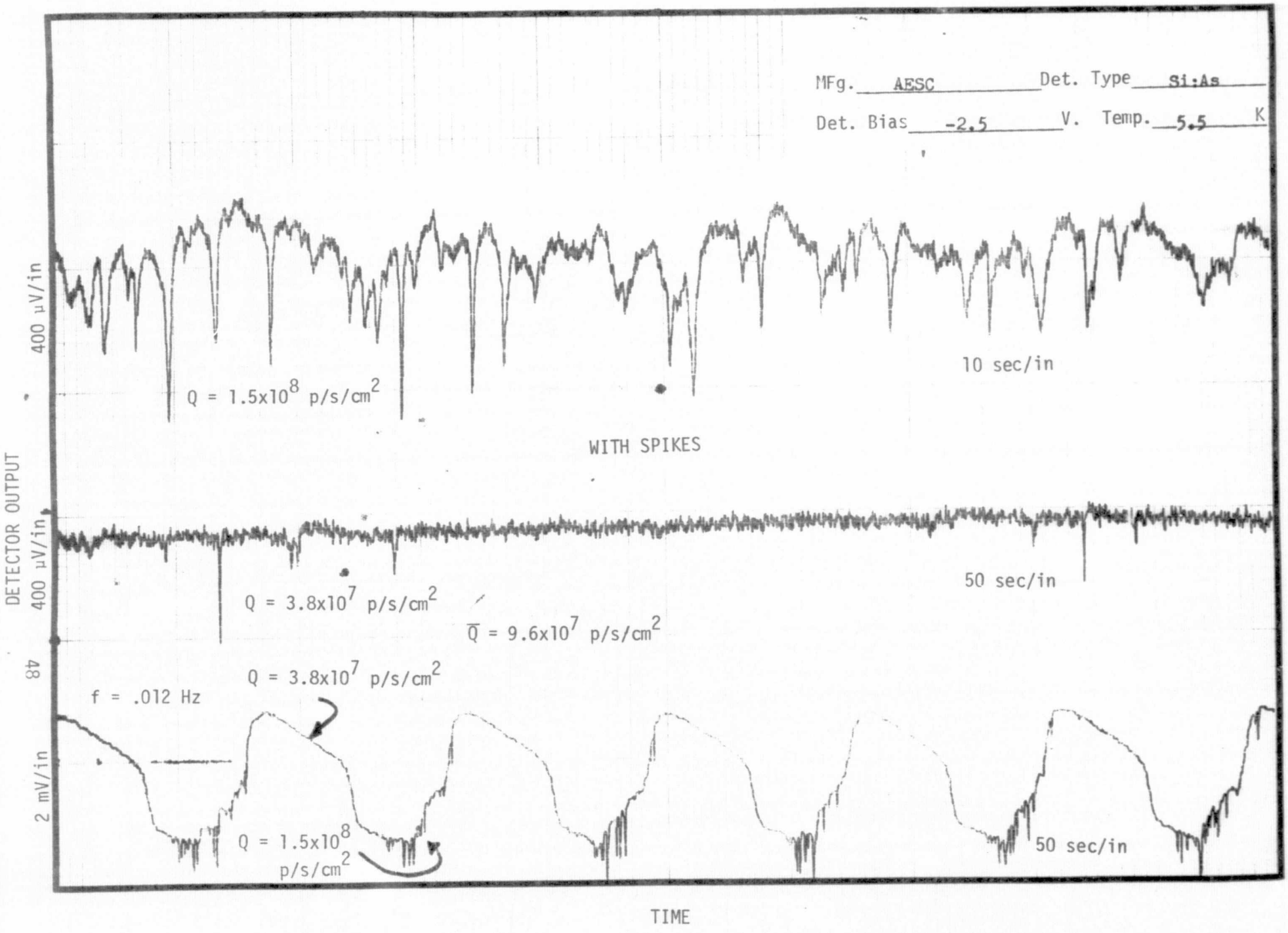
MFg. AESC
Det. Type Si:As
Det. Bias -2.5 V.
Temp. 5.5 K
400 μV/in
Q = 1.5x10^8 p/s/cm^2
10 sec/in
WITH SPIKES
DETECTOR OUTPUT
400 μV/in
Q = 3.8x10^7 p/s/cm^2
Q̄ = 9.6x10^7 p/s/cm^2
50 sec/in
48
Q = 3.8x10^7 p/s/cm^2
f = .012 Hz
2 mV/in
Q = 1.5x10^8 p/s/cm^2
50 sec/in
TIME

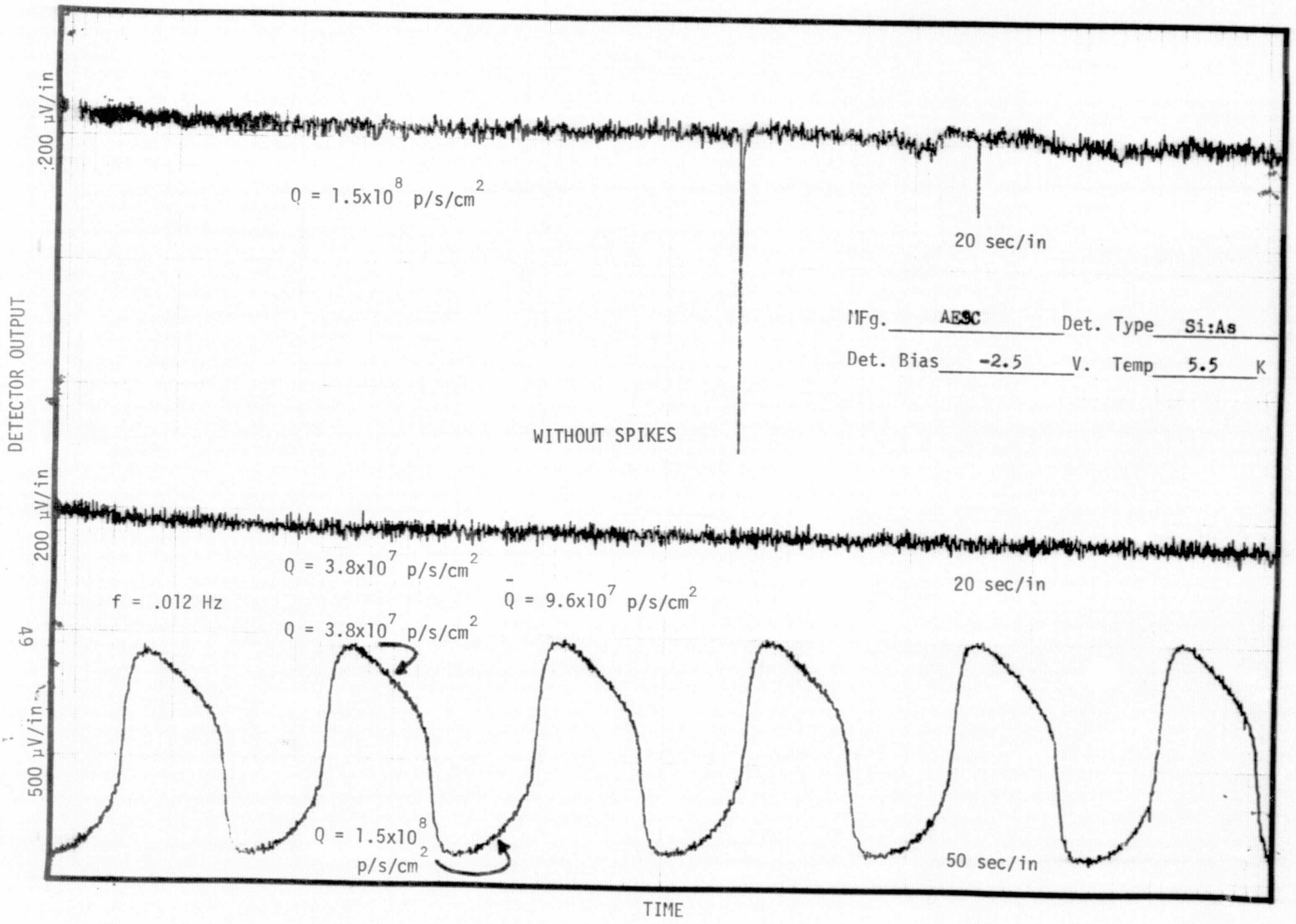
DETECTOR OUTPUT
200 μV/in
Q = 1.5x10^8 p/s/cm^2
20 sec/in
MFg. AESC
Det. Type Si:As
Det. Bias -2.5 V. Temp 5.5 K
WITHOUT SPIKES
200 μV/in
Q = 3.8x10^7 p/s/cm^2
Q = 9.6x10^7 p/s/cm^2
20 sec/in
f = .012 Hz
Q = 3.8x10^7 p/s/cm^2
49
500 μV/in
Q = 1.5x10^8 p/s/cm^2
50 sec/in
TIME

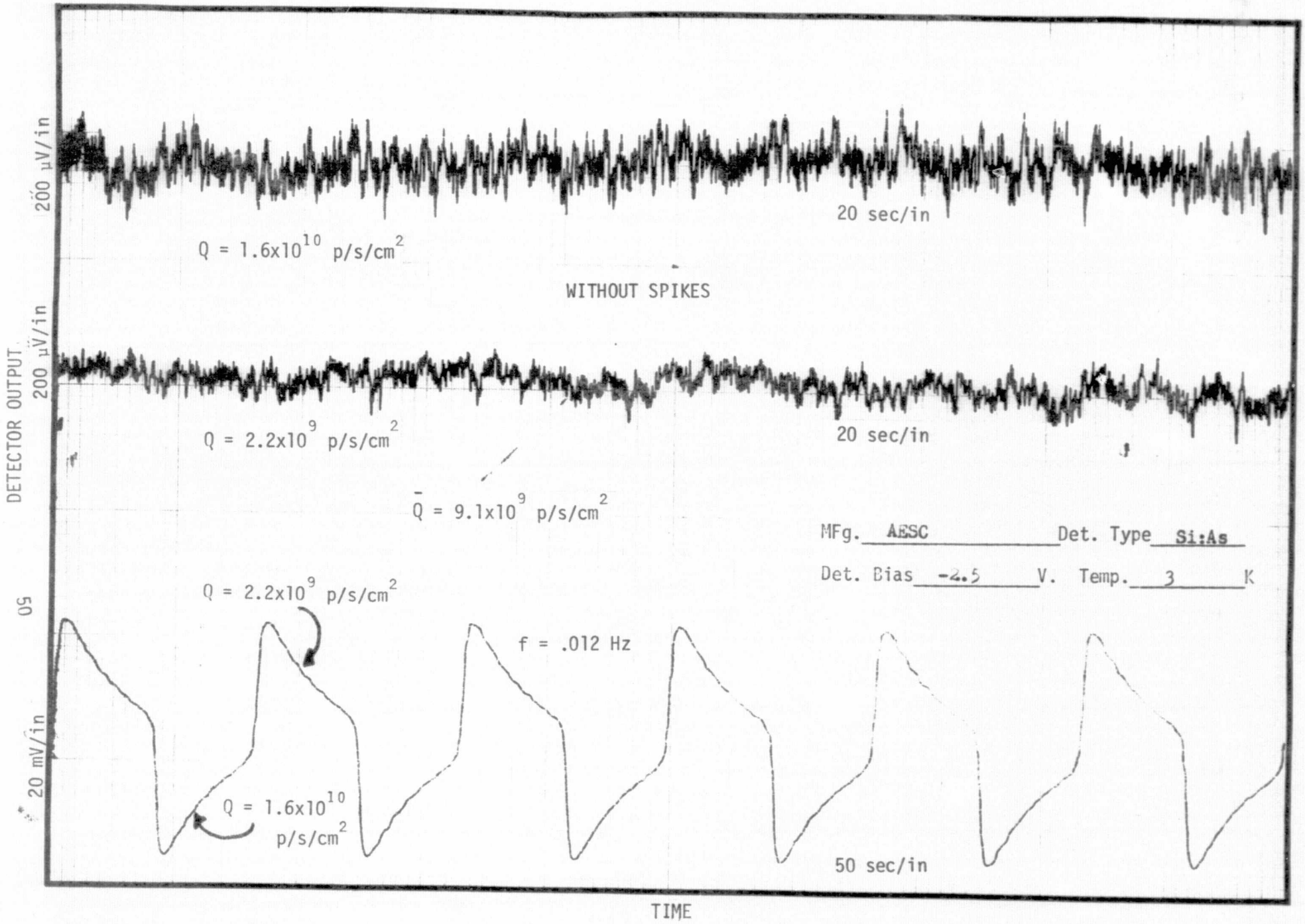
200 μV/in
20 sec/in
Q = 1.6x10^10 p/s/cm^2
WITHOUT SPIKES
DETECTOR OUTPUT
200 μV/in
Q = 2.2x10^9 p/s/cm^2
20 sec/in
Q̄ = 9.1x10^9 p/s/cm^2
MFg. AESC
Det. Type Si:As
Det. Bias -2.5 V. Temp. 3 K
Q = 2.2x10^9 p/s/cm^2
f = .012 Hz
20 mV/in
Q = 1.6x10^10 p/s/cm^2
50 sec/in
TIME

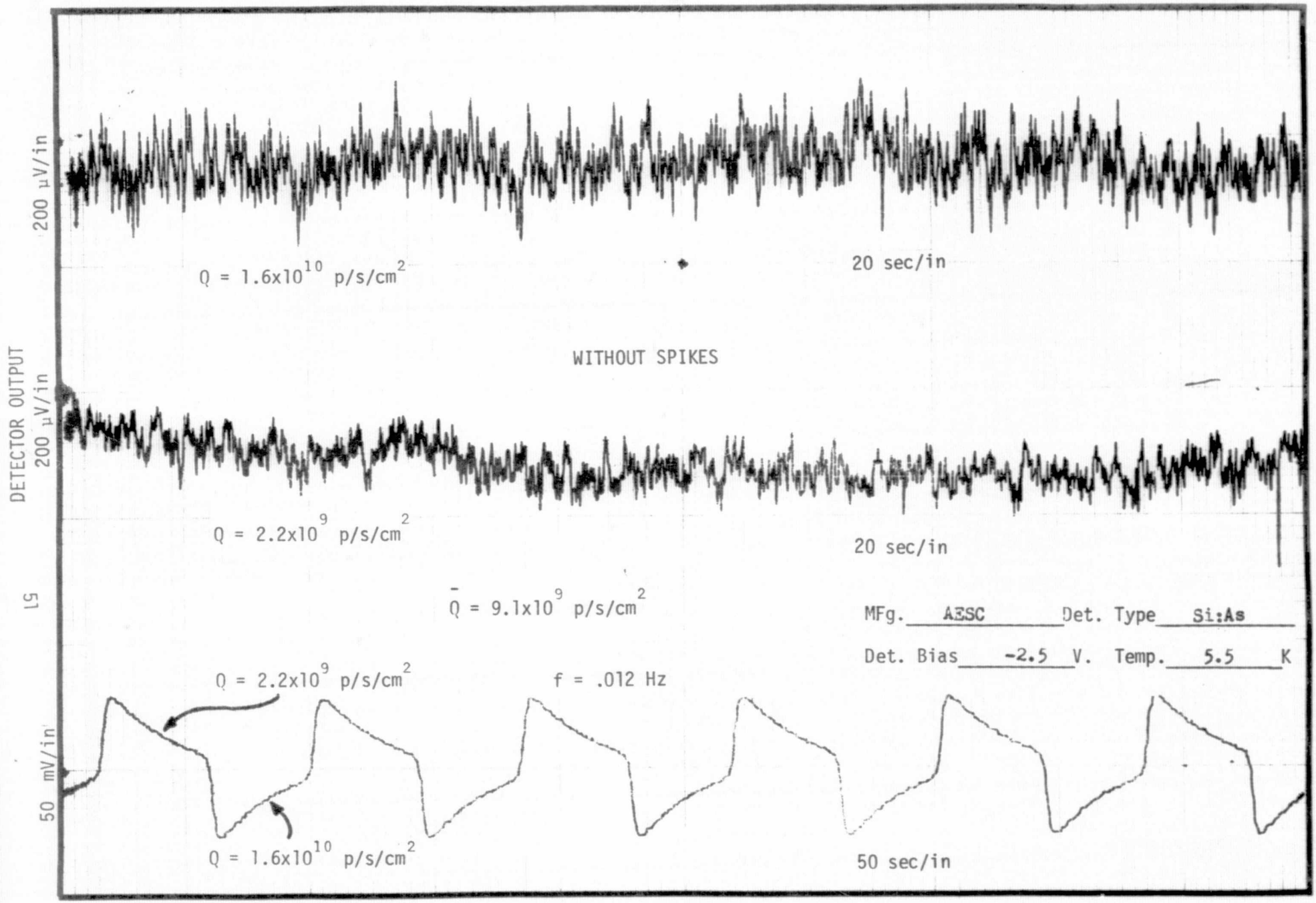
200 μV/in
Q = 1.6x10^10 p/s/cm^2
20 sec/in
WITHOUT SPIKES
DETECTOR OUTPUT
200 μV/in
Q = 2.2x10^9 p/s/cm^2
20 sec/in
Q̄ = 9.1x10^9 p/s/cm^2
MFg. AESC Det. Type Si:As
Det. Bias -2.5 V. Temp. 5.5 K
Q = 2.2x10^9 p/s/cm^2
f = .012 Hz
50 mV/in
Q = 1.6x10^10 p/s/cm^2
50 sec/in
TIME

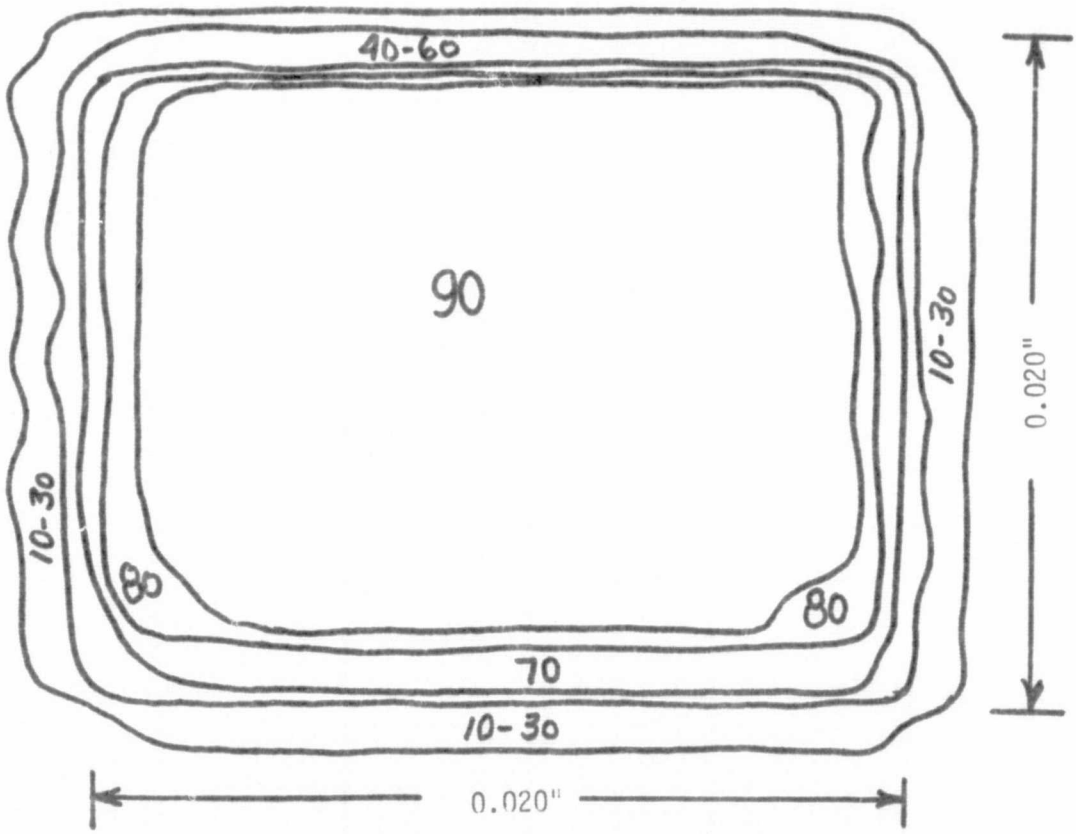

SENSIVITY CONTOUR

Manufacturer AESC Type Si:As

Bias 2.5 V Temp 5.5 K

FREQ 10 Hz Background 10^6 p/s/cm^2

Wavelength 10 microns

5.3 RIC/MSD Si:As. This detector package (NA 002) had a relatively low valued load resistor, about $10^9\Omega$ at 4.5K. This low value limits the magnitude of detector signal at low frequencies. The FET noise was also a bit higher than can be achieved with other available FETs. The combination of low signal and high FET noise results in a NEP which is higher than could be achieved with another combination of load resistor and FET.

Since the current responsivity of this detector was relatively high, it was felt that another set of measurements should be made using a higher valued load resistor. The load was replaced with one of higher value ($\sim 6\times10^{10}\Omega$ at 4.5K) and the tests redone. Both sets of data are shown. The NEP at low frequencies is seen to be more than an order of magnitude lower with the NELC load resistor than with the original one.

The sensitivity contour of this detector appears quite similar to those observed on other bulk detectors having their electric field perpendicular to the incident radiation. The signals seen at the top and bottom of the contour plot are due to radiation striking the vertical sides of the detector.

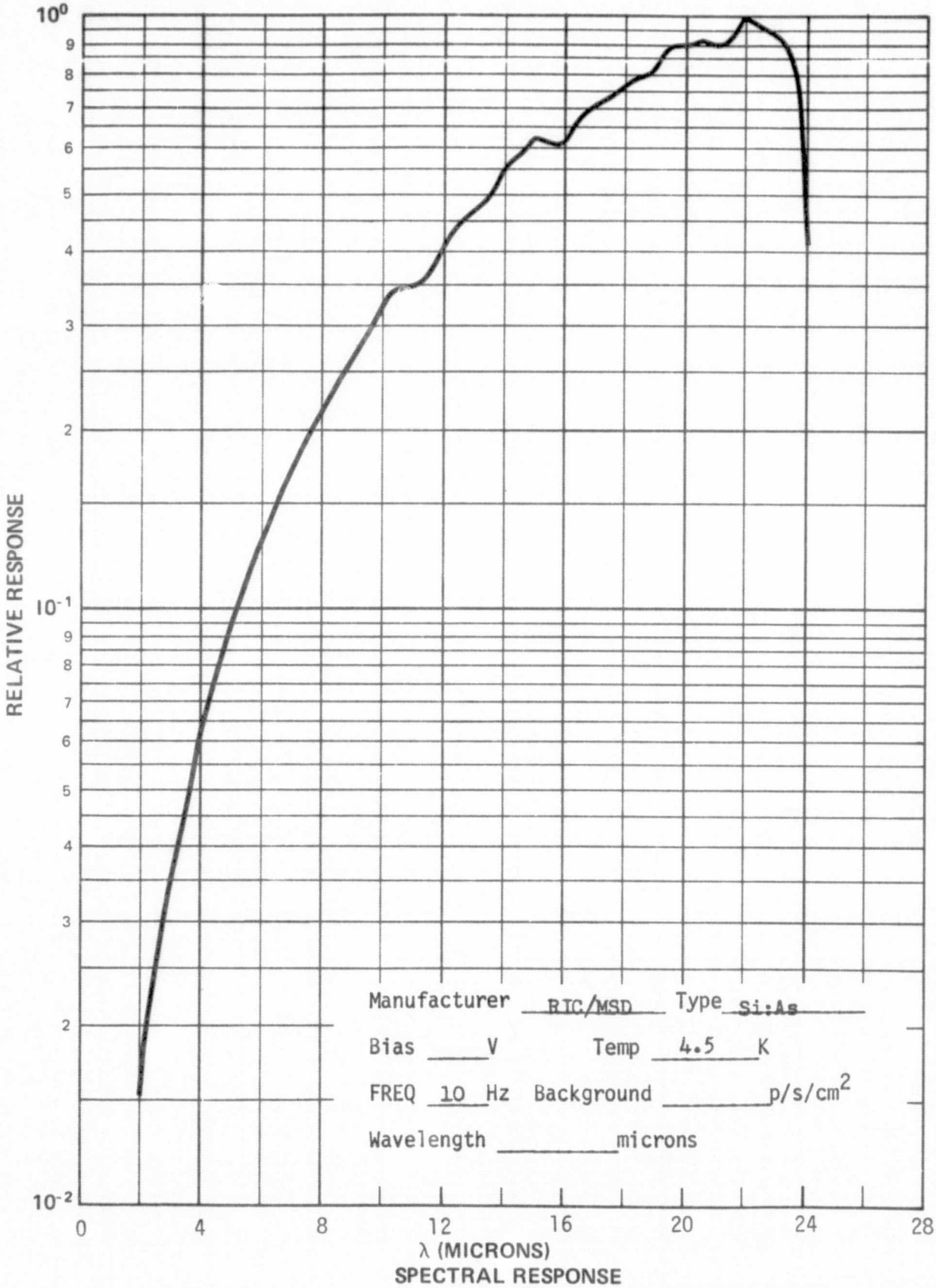

SPECTRAL RESPONSE

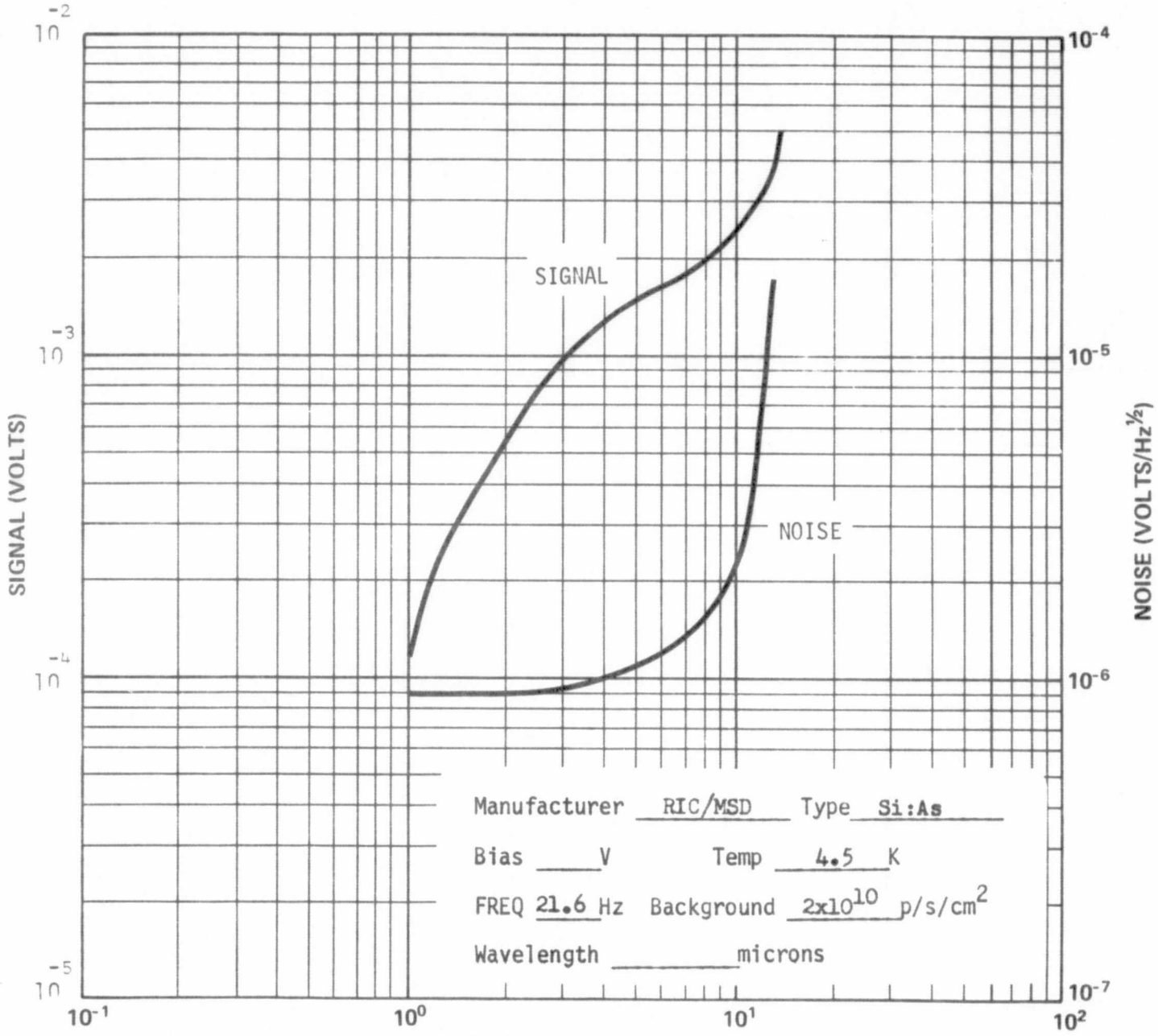

DETERMINATION OF OPTIMUM BIAS

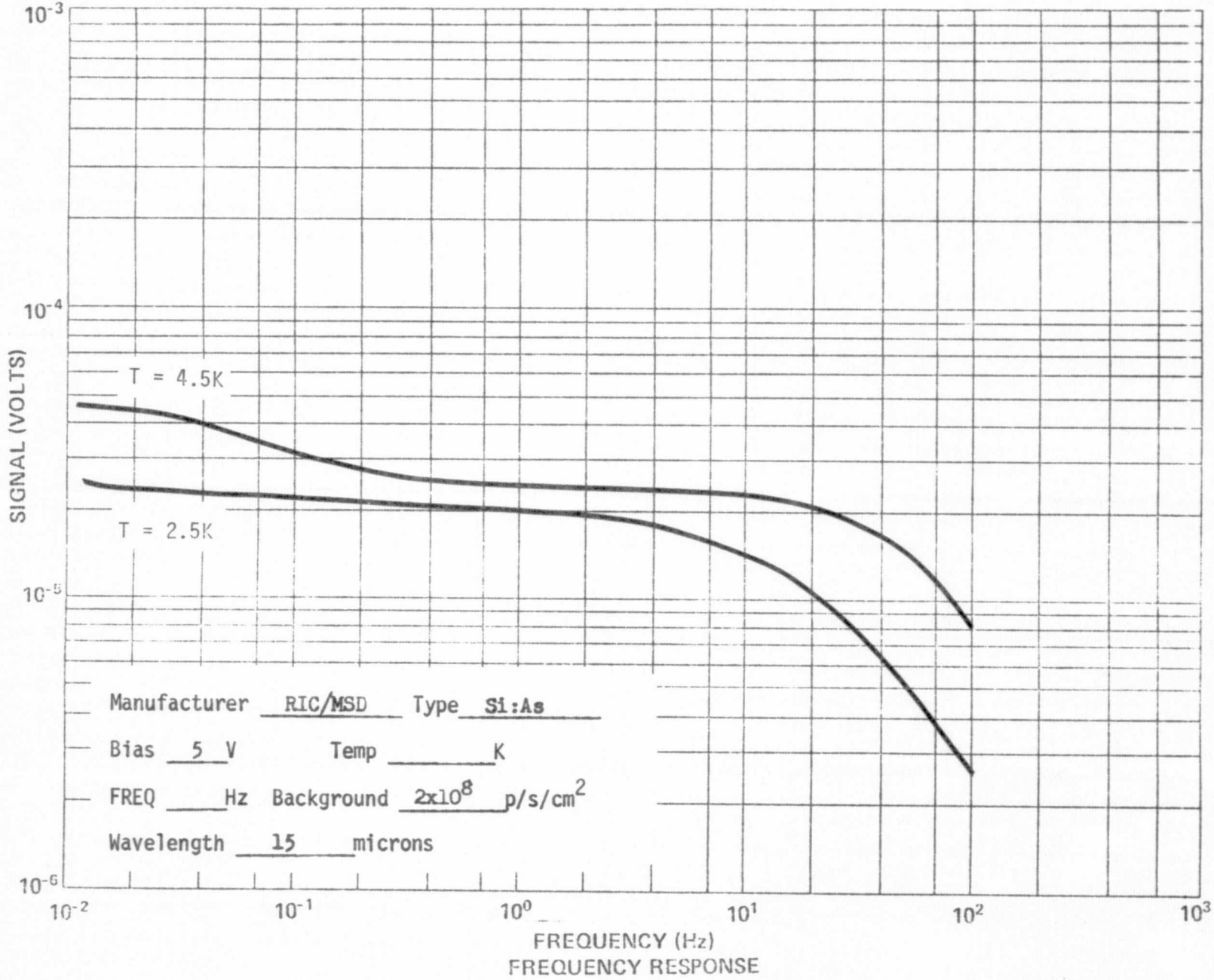

FREQUENCY RESPONSE

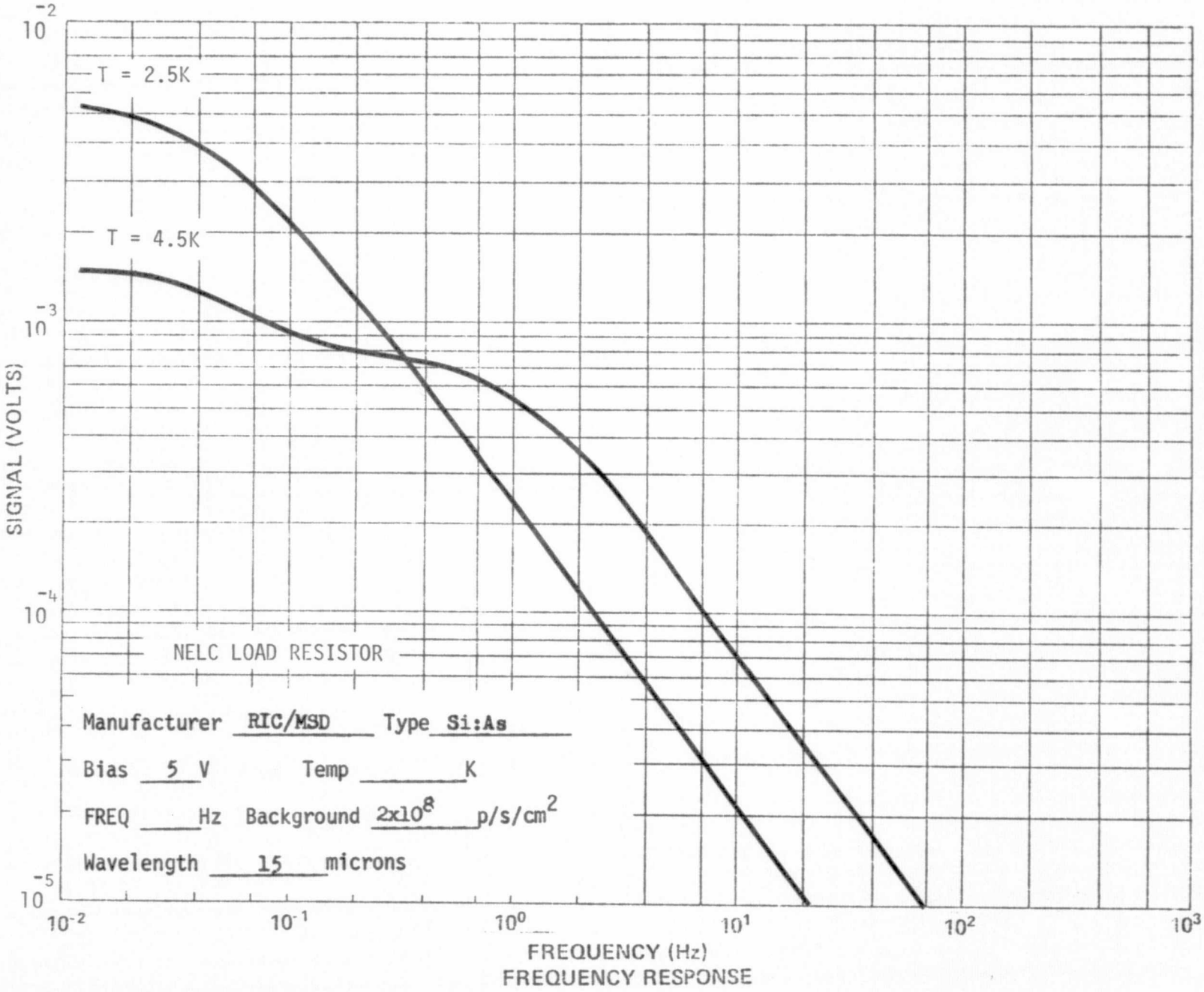
T = 2.5K
T = 4.5K
NELC LOAD RESISTOR
Manufacturer RIC/MSD Type Si:As
Bias 5 V Temp K
FREQ Hz Background 2x10^8 p/s/cm^2
Wavelength 15 microns
SIGNAL (VOLTS)
FREQUENCY (Hz)
FREQUENCY RESPONSE

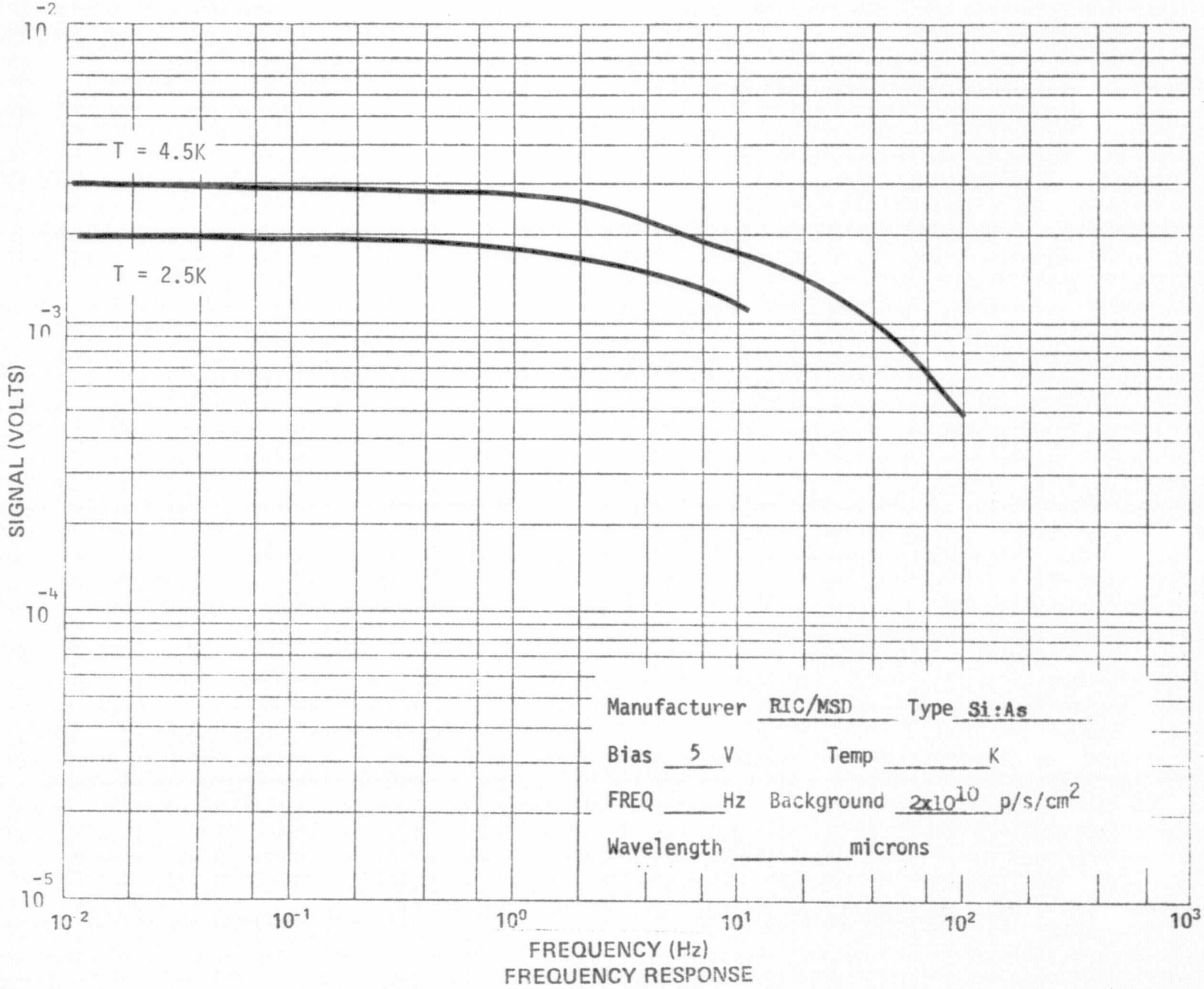

FREQUENCY RESPONSE

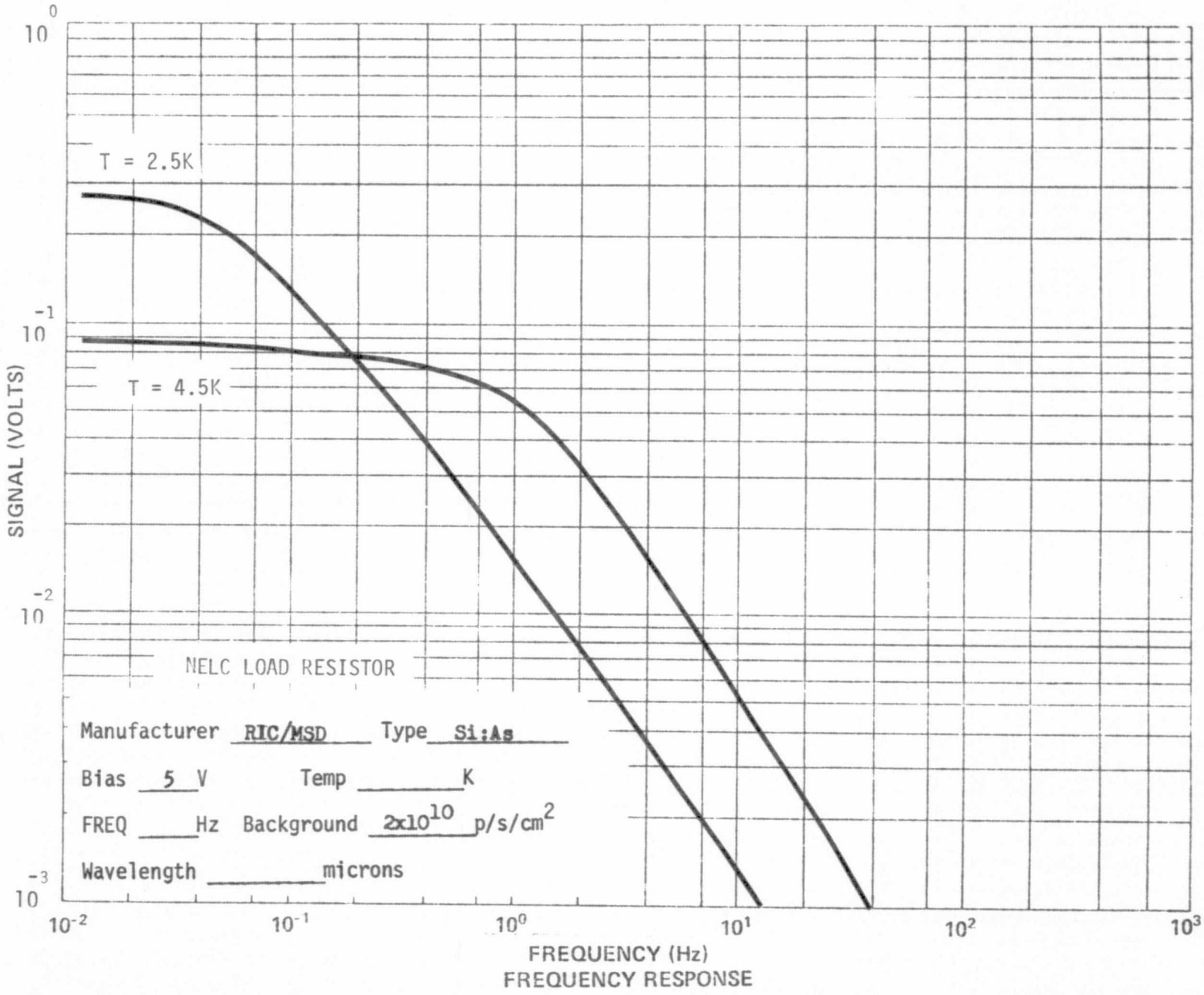

FREQUENCY RESPONSE

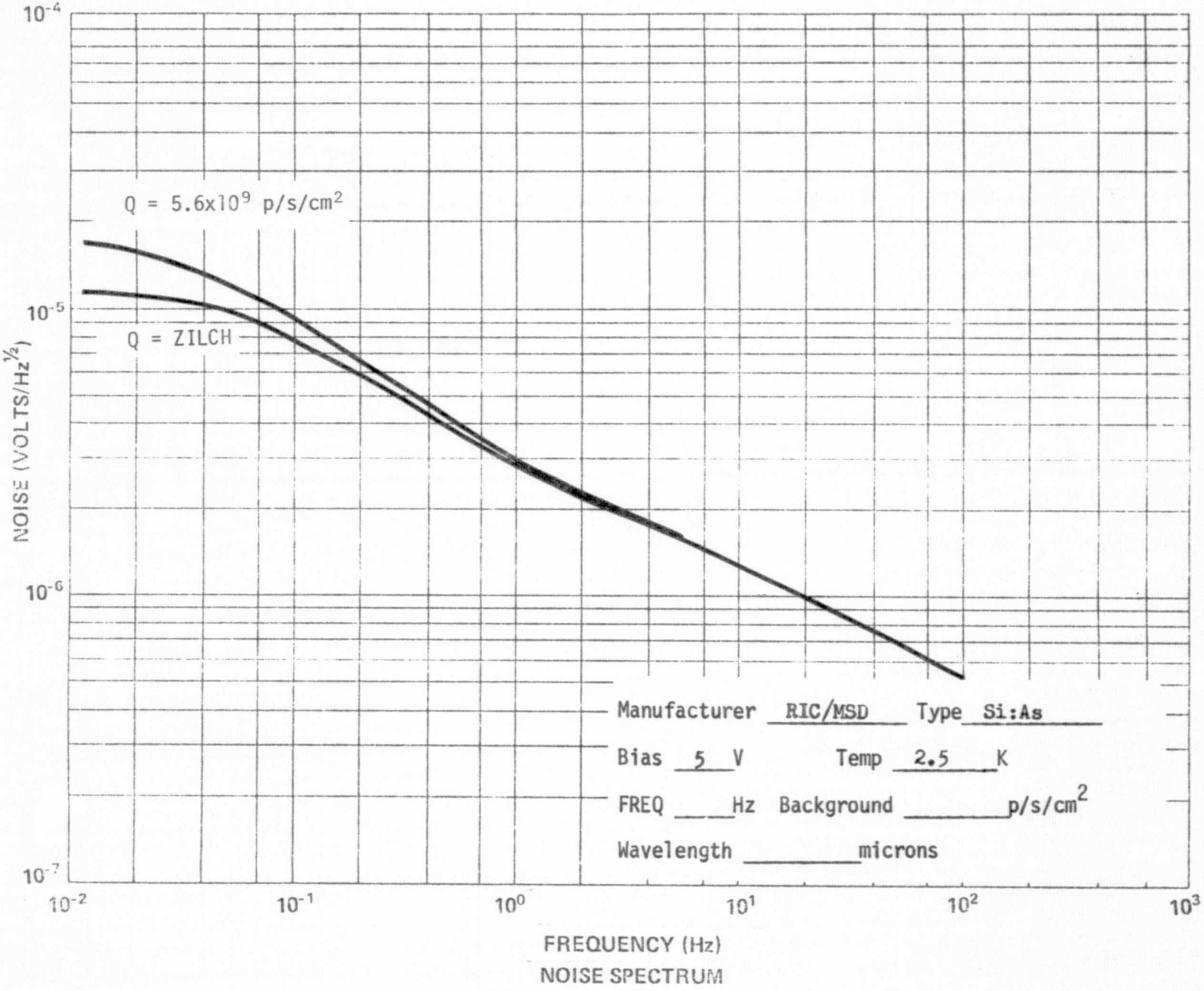

NOISE SPECTRUM

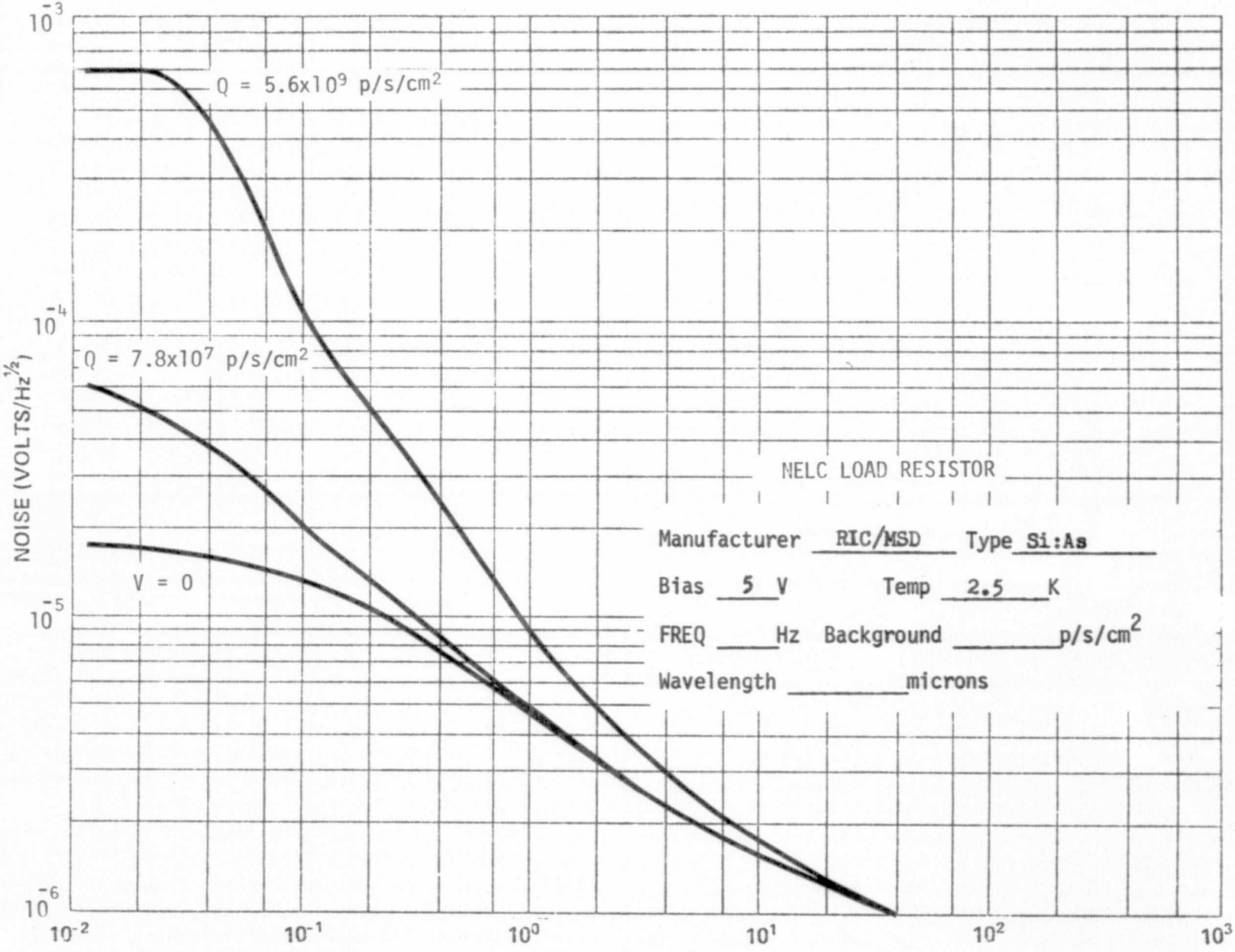

NOISE SPECTRUM

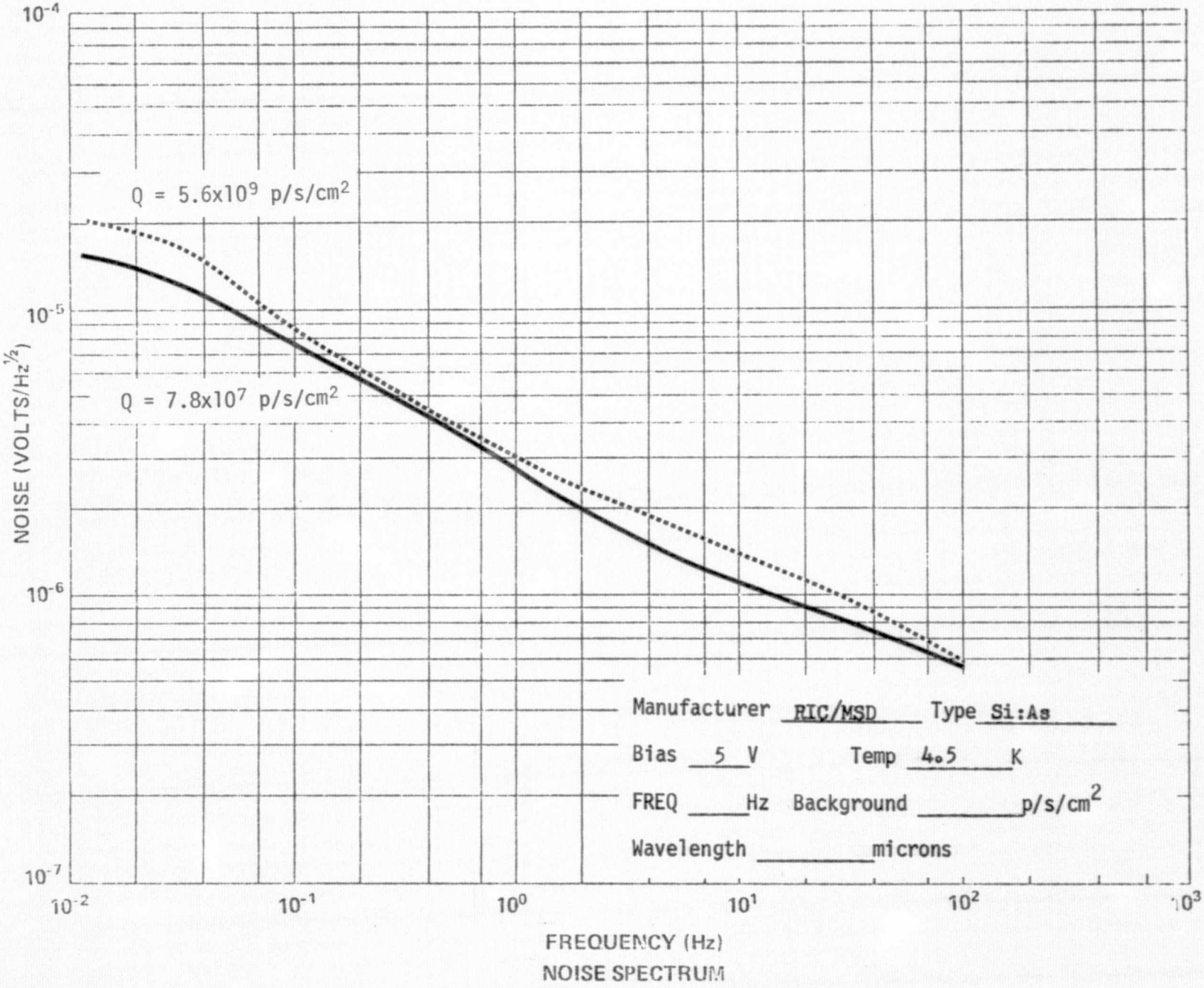

NOISE SPECTRUM

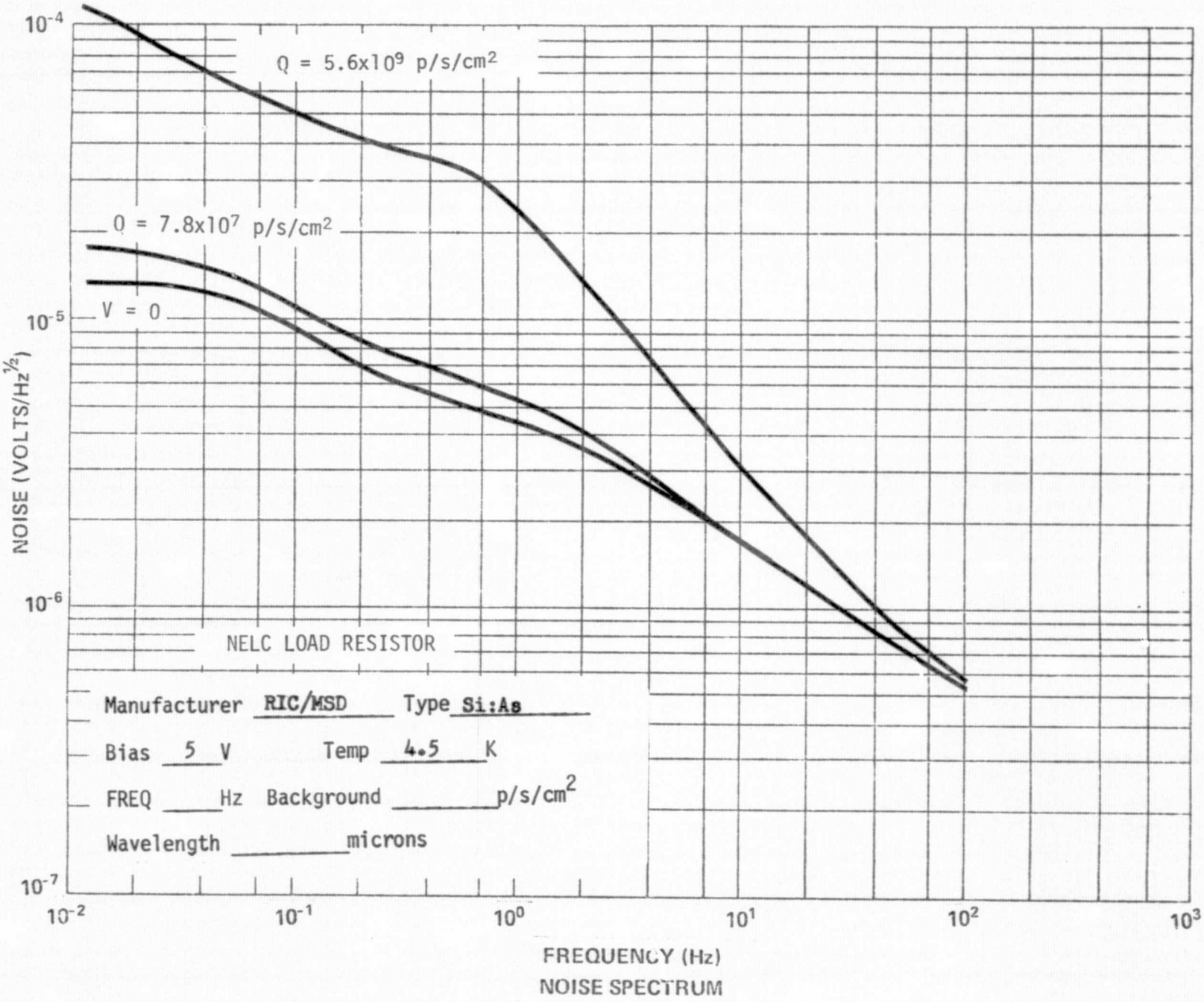

NOISE SPECTRUM

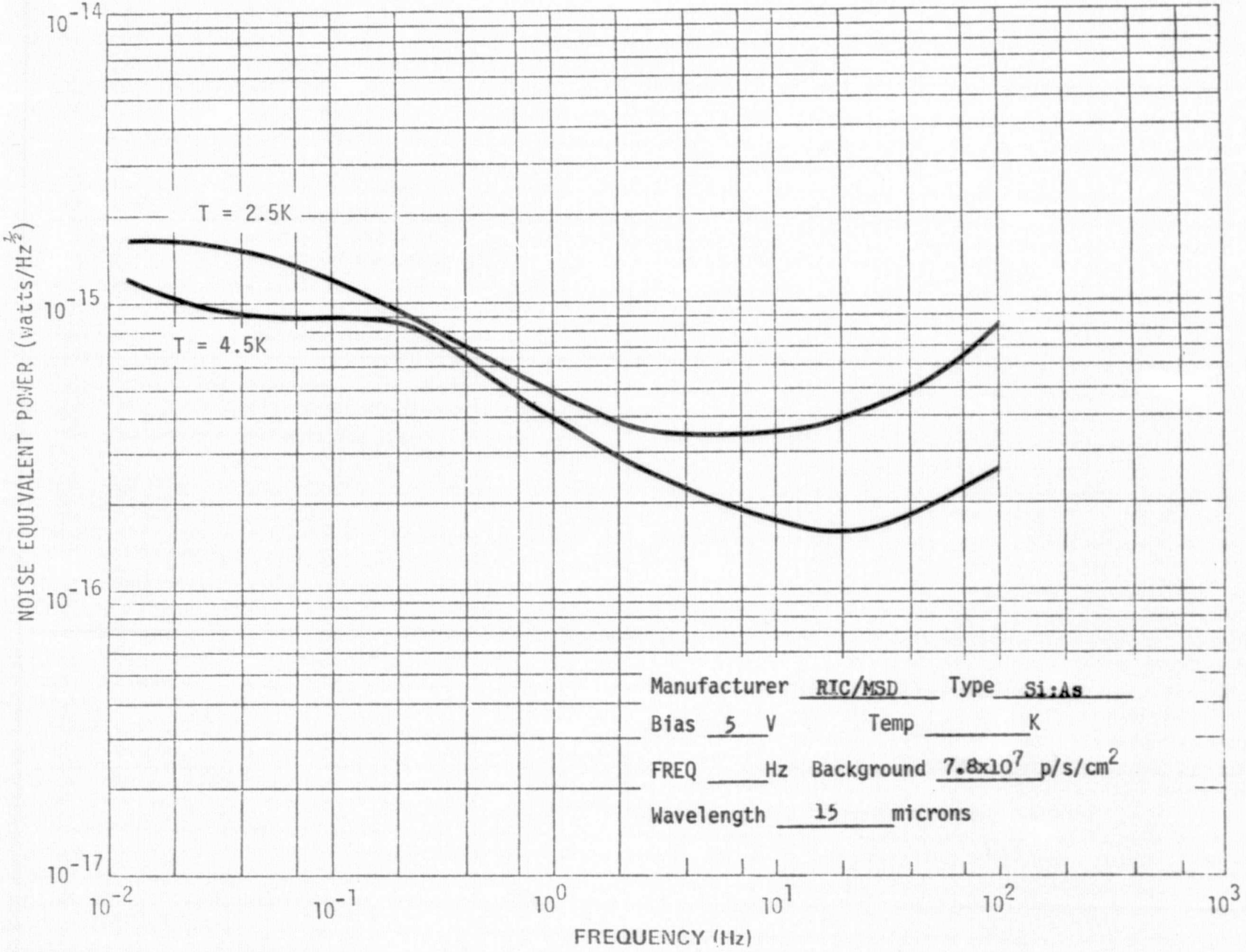
NOISE EQUIVALENT POWER (watts/Hz^½)
10^-14
10^-15
10^-16
10^-17
T = 2.5K
T = 4.5K
Manufacturer RIC/MSD Type Si:As
Bias 5 V Temp ____ K
FREQ ____ Hz Background 7.8x10^7 p/s/cm^2
Wavelength 15 microns
10^-2
10^-1
10^0
10^1
10^2
10^3
FREQUENCY (Hz)

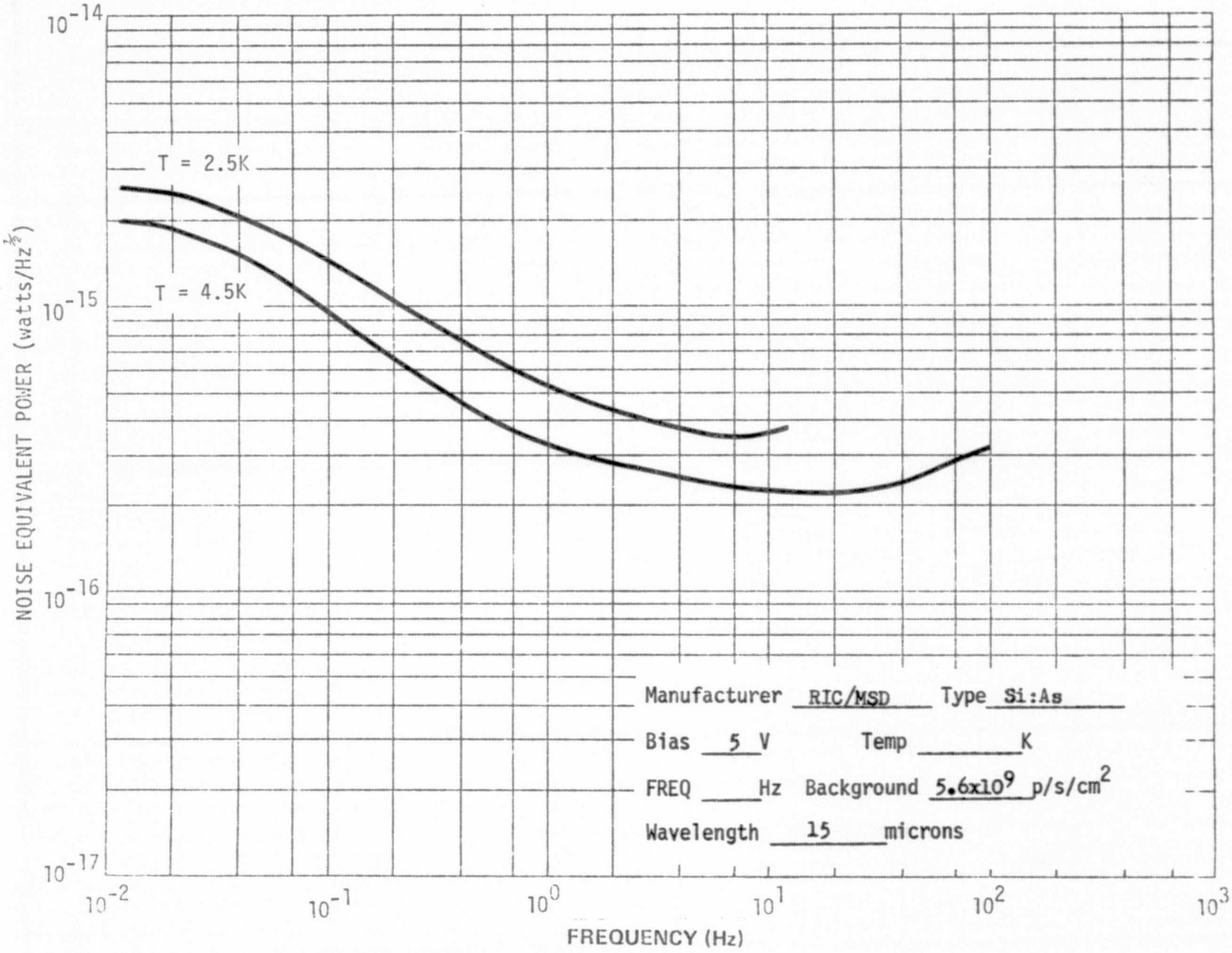
NOISE EQUIVALENT POWER (watts/Hz$^{\frac{1}{2}}$)
10^{-14}
10^{-15}
10^{-16}
10^{-17}
T = 2.5K
T = 4.5K
Manufacturer RIC/MSD Type Si:As
Bias 5 V Temp ____ K
FREQ ____ Hz Background 5.6×10^9 p/s/cm^2
Wavelength 15 microns
10^{-2}
10^{-1}
10^{0}
10^{1}
10^{2}
10^{3}
FREQUENCY (Hz)

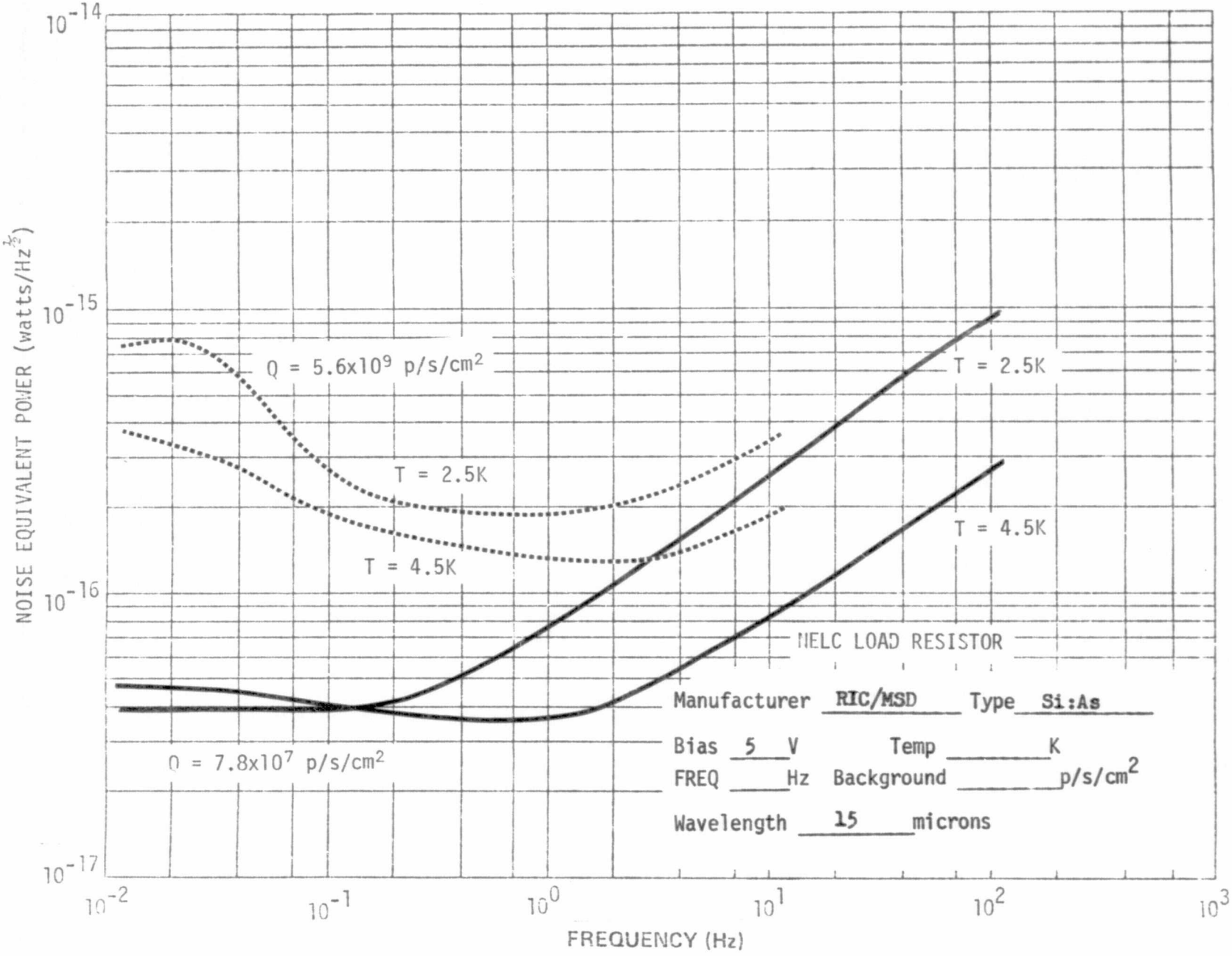
NOISE EQUIVALENT POWER (watts/Hz$^{\frac{1}{2}}$)
10^{-14}
10^{-15}
10^{-16}
10^{-17}
10^{-2}
10^{-1}
10^{0}
10^{1}
10^{2}
10^{3}
FREQUENCY (Hz)
Q = 5.6x10^{9} p/s/cm^{2}
T = 2.5K
T = 4.5K
T = 2.5K
T = 4.5K
Q = 7.8x10^{7} p/s/cm^{2}
NELC LOAD RESISTOR
Manufacturer RIC/MSD Type Si:As
Bias 5 V Temp ____ K
FREQ ____ Hz Background ____ p/s/cm^{2}
Wavelength 15 microns

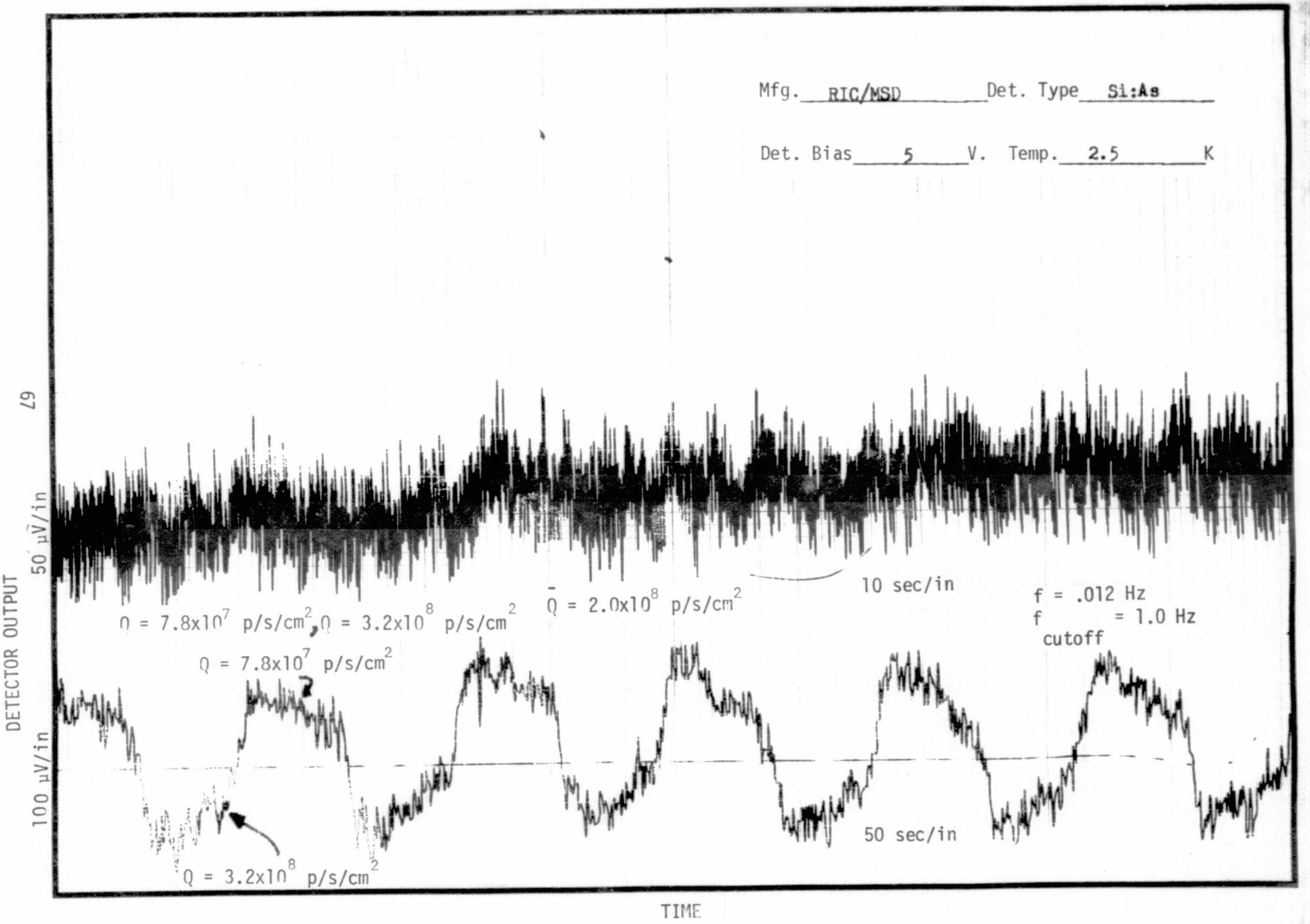
Mfg. RIC/MSD Det. Type Si:As
Det. Bias 5 V. Temp. 2.5 K
67
50 μV/in
DETECTOR OUTPUT
100 μV/in
Q = 7.8x10^7 p/s/cm^2, Q = 3.2x10^8 p/s/cm^2
Q = 2.0x10^8 p/s/cm^2
10 sec/in
f = .012 Hz
f = 1.0 Hz
cutoff
Q = 7.8x10^7 p/s/cm^2
Q = 3.2x10^8 p/s/cm^2
50 sec/in
TIME

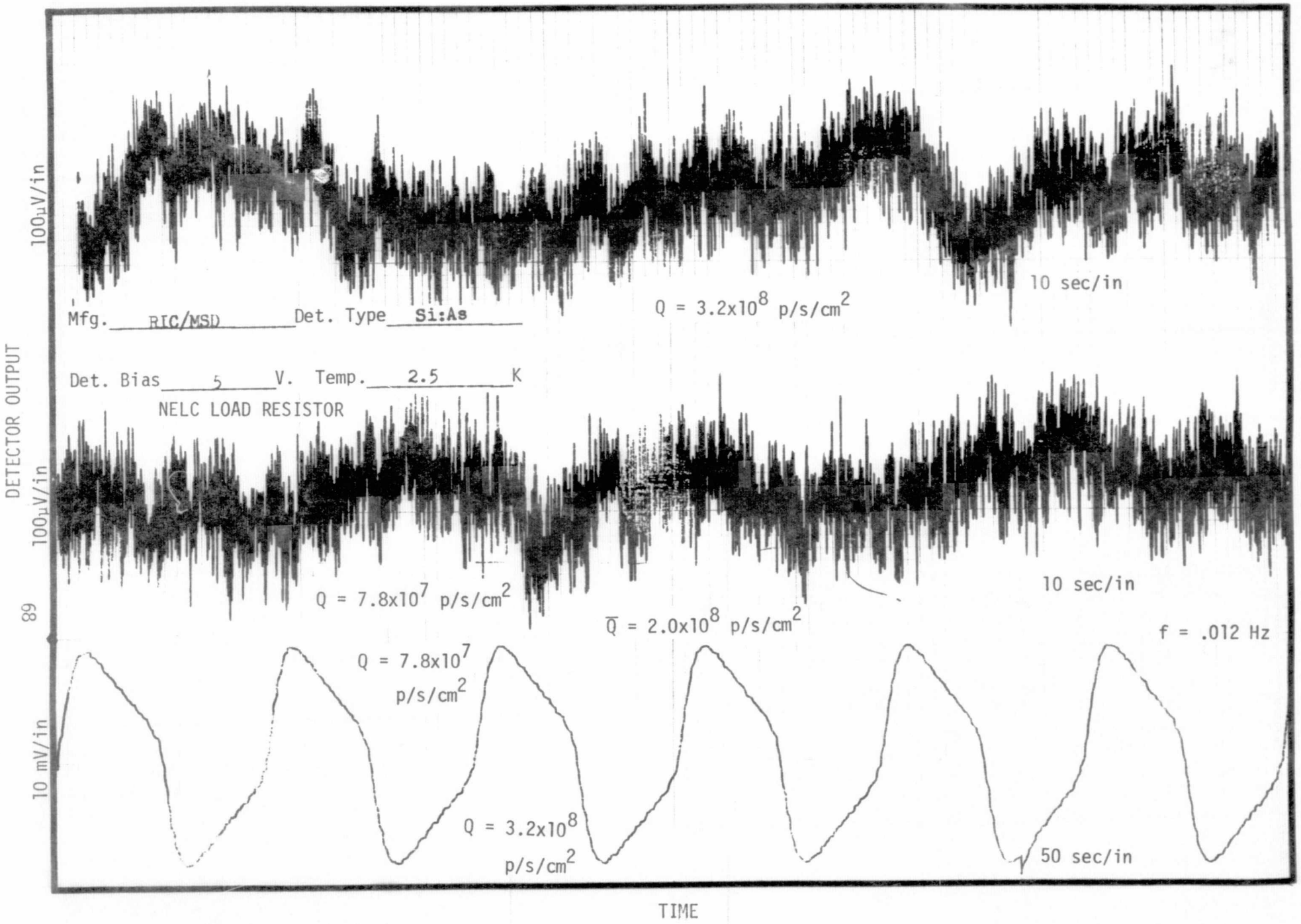
100μV/in
Mfg. RIC/MSD Det. Type Si:As
Det. Bias 5 V. Temp. 2.5 K
NELC LOAD RESISTOR
Q = 3.2x10^8 p/s/cm^2
10 sec/in
DETECTOR OUTPUT
100μV/in
Q = 7.8x10^7 p/s/cm^2
Q̄ = 2.0x10^8 p/s/cm^2
10 sec/in
f = .012 Hz
89
10 mV/in
Q = 7.8x10^7 p/s/cm^2
Q = 3.2x10^8 p/s/cm^2
50 sec/in
TIME

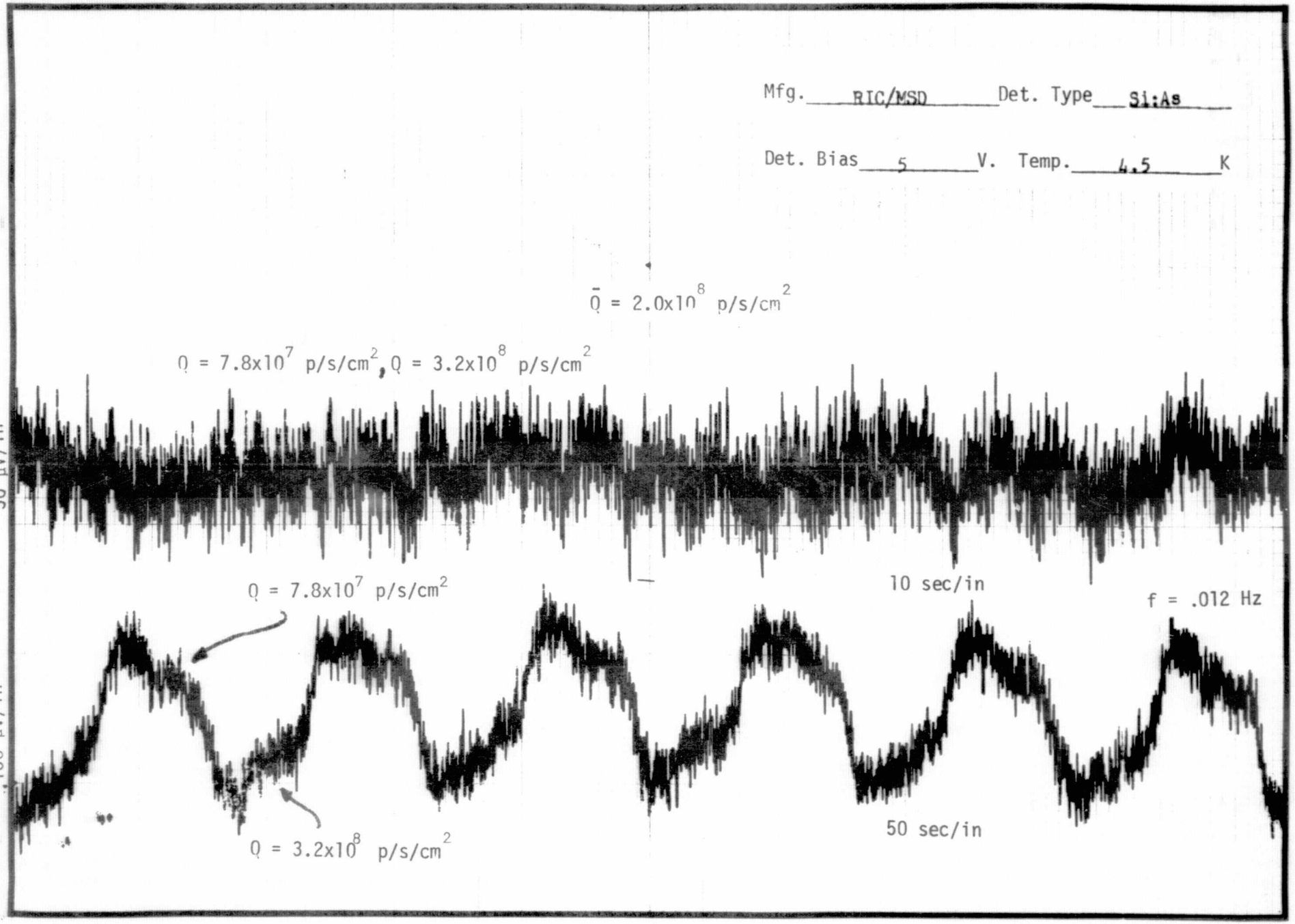
Mfg. RIC/MSD Det. Type Si:As
Det. Bias 5 V. Temp. 4.5 K
$\bar{Q}$ = 2.0x10^8 p/s/cm^2
Q = 7.8x10^7 p/s/cm^2, Q = 3.2x10^8 p/s/cm^2
50 μV/in
10 sec/in
Q = 7.8x10^7 p/s/cm^2
f = .012 Hz
100 μV/in
Q = 3.2x10^8 p/s/cm^2
50 sec/in
DETECTOR OUTPUT
TIME

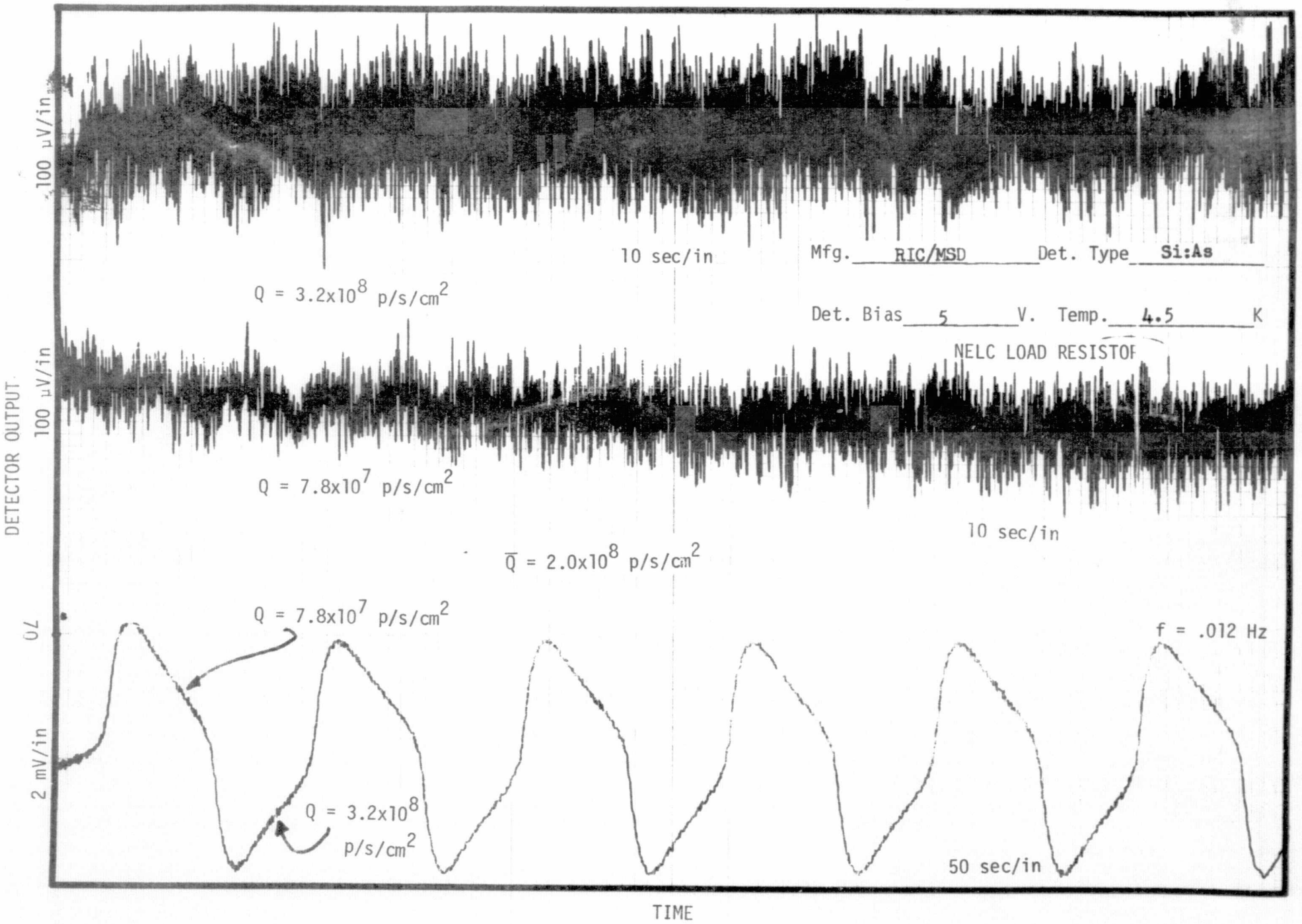
100 μV/in
10 sec/in
Mfg. RIC/MSD Det. Type Si:As
Q = 3.2x10^8 p/s/cm^2
Det. Bias 5 V. Temp. 4.5 K
NELC LOAD RESISTOR
100 μV/in
Q = 7.8x10^7 p/s/cm^2
10 sec/in
Q̄ = 2.0x10^8 p/s/cm^2
DETECTOR OUTPUT
Q = 7.8x10^7 p/s/cm^2
f = .012 Hz
2 mV/in
Q = 3.2x10^8 p/s/cm^2
50 sec/in
TIME

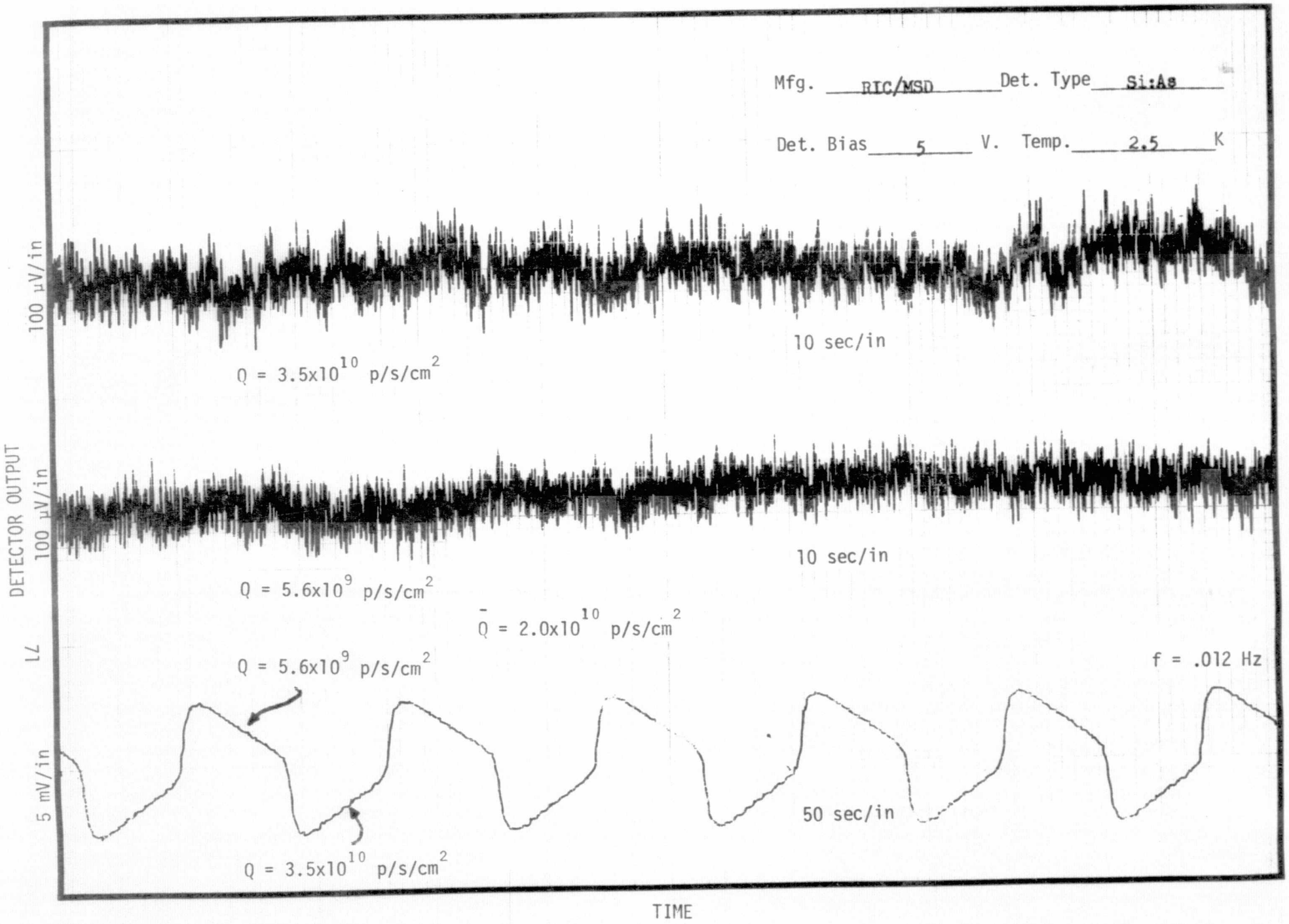
Mfg. RIC/MSD Det. Type Si:As
Det. Bias 5 V. Temp. 2.5 K
100 μV/in
10 sec/in
Q = 3.5x10^10 p/s/cm^2
DETECTOR OUTPUT
100 μV/in
10 sec/in
Q = 5.6x10^9 p/s/cm^2
Q = 2.0x10^10 p/s/cm^2
Q = 5.6x10^9 p/s/cm^2
f = .012 Hz
5 mV/in
50 sec/in
Q = 3.5x10^10 p/s/cm^2
TIME

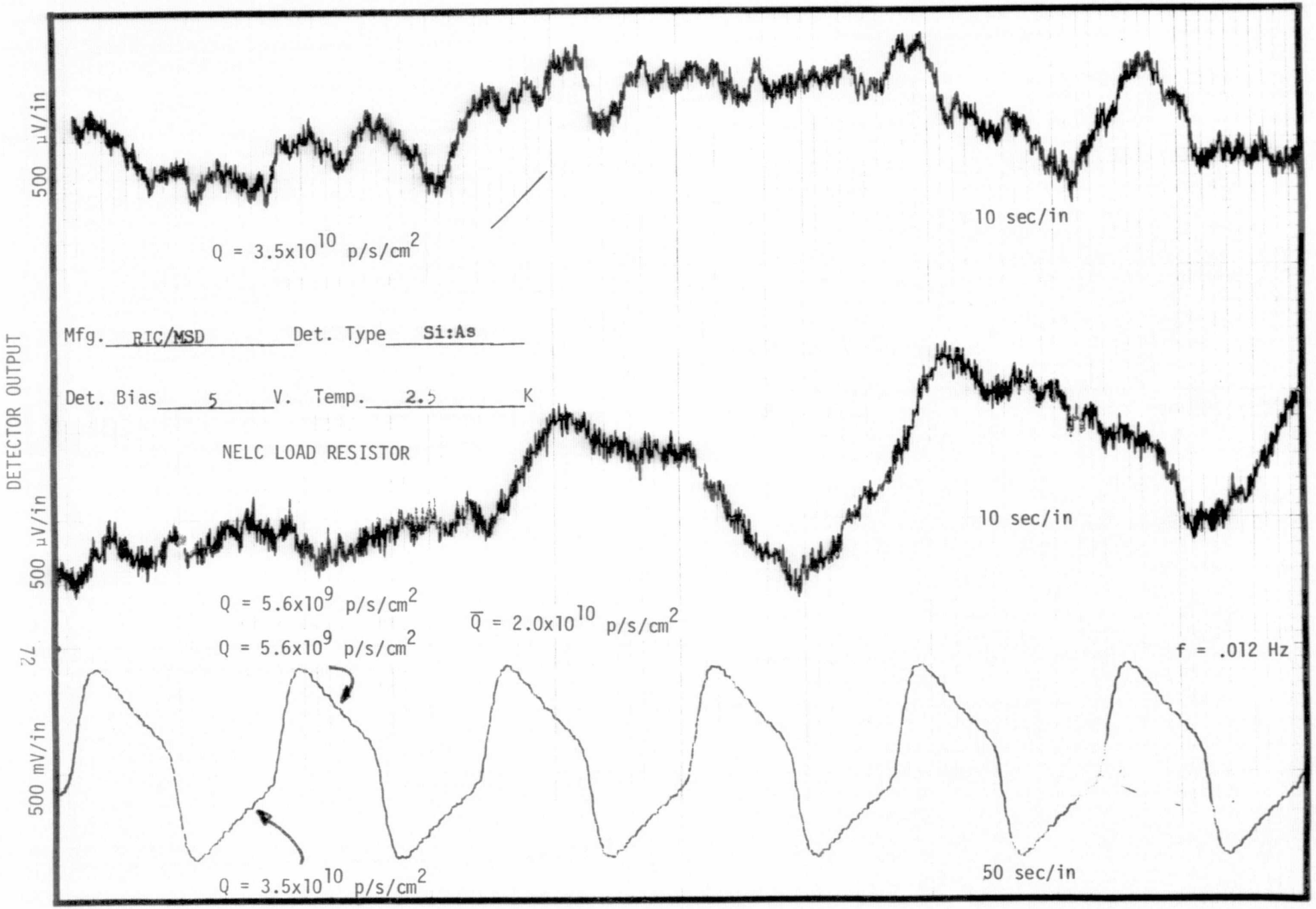
500 µV/in
10 sec/in
Q = 3.5x10^10 p/s/cm^2
Mfg. RIC/MSD Det. Type Si:As
Det. Bias 5 V. Temp. 2.5 K
NELC LOAD RESISTOR
DETECTOR OUTPUT
500 µV/in
10 sec/in
Q = 5.6x10^9 p/s/cm^2
Q = 5.6x10^9 p/s/cm^2
Q = 2.0x10^10 p/s/cm^2
f = .012 Hz
72
500 mV/in
Q = 3.5x10^10 p/s/cm^2
50 sec/in
TIME

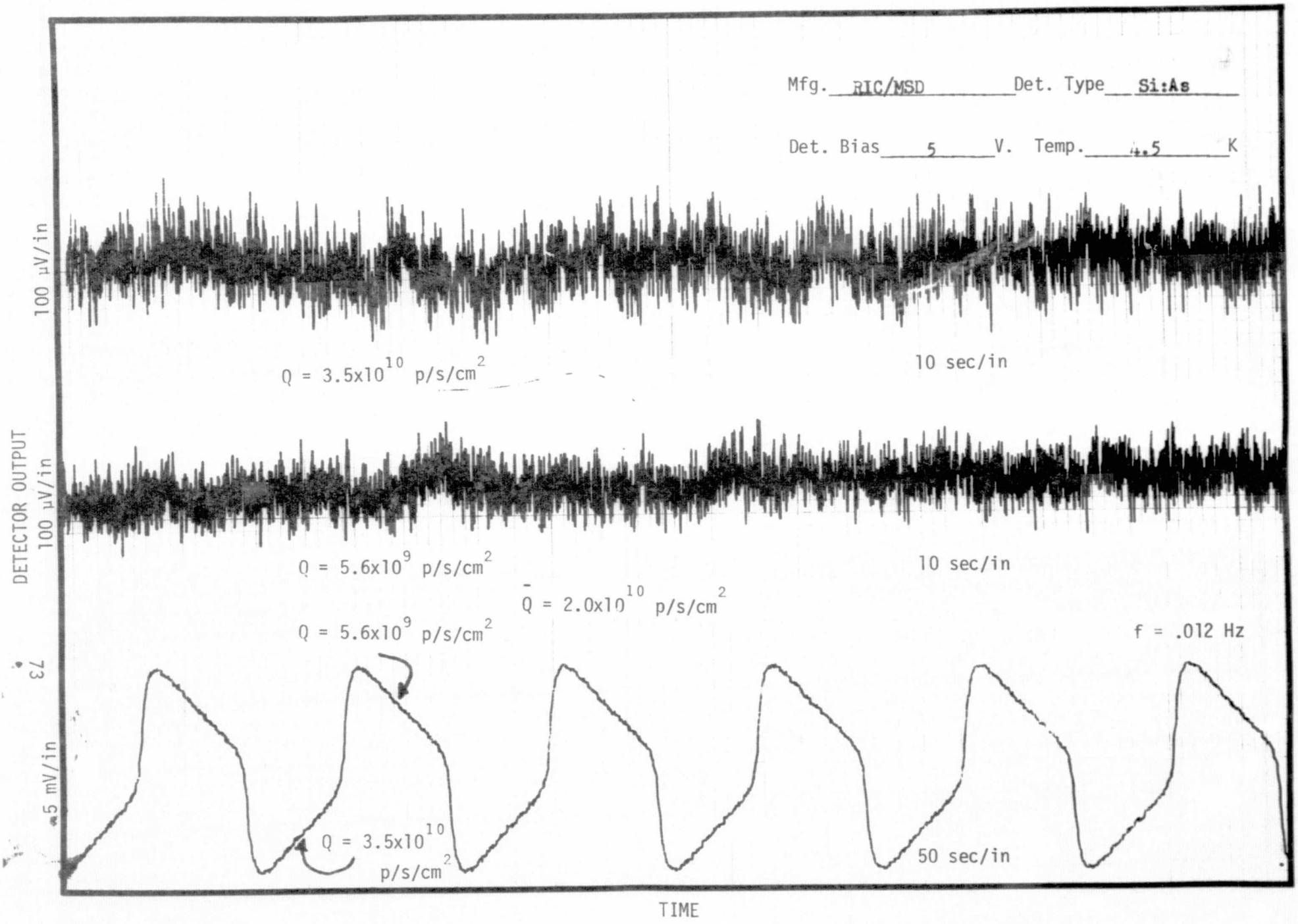
Mfg. RIC/MSD Det. Type Si:As
Det. Bias 5 V. Temp. 4.5 K
DETECTOR OUTPUT
100 μV/in
Q = 3.5x10^10 p/s/cm^2
10 sec/in
100 μV/in
Q = 5.6x10^9 p/s/cm^2
10 sec/in
Q = 2.0x10^10 p/s/cm^2
Q = 5.6x10^9 p/s/cm^2
f = .012 Hz
73
5 mV/in
Q = 3.5x10^10 p/s/cm^2
50 sec/in
TIME

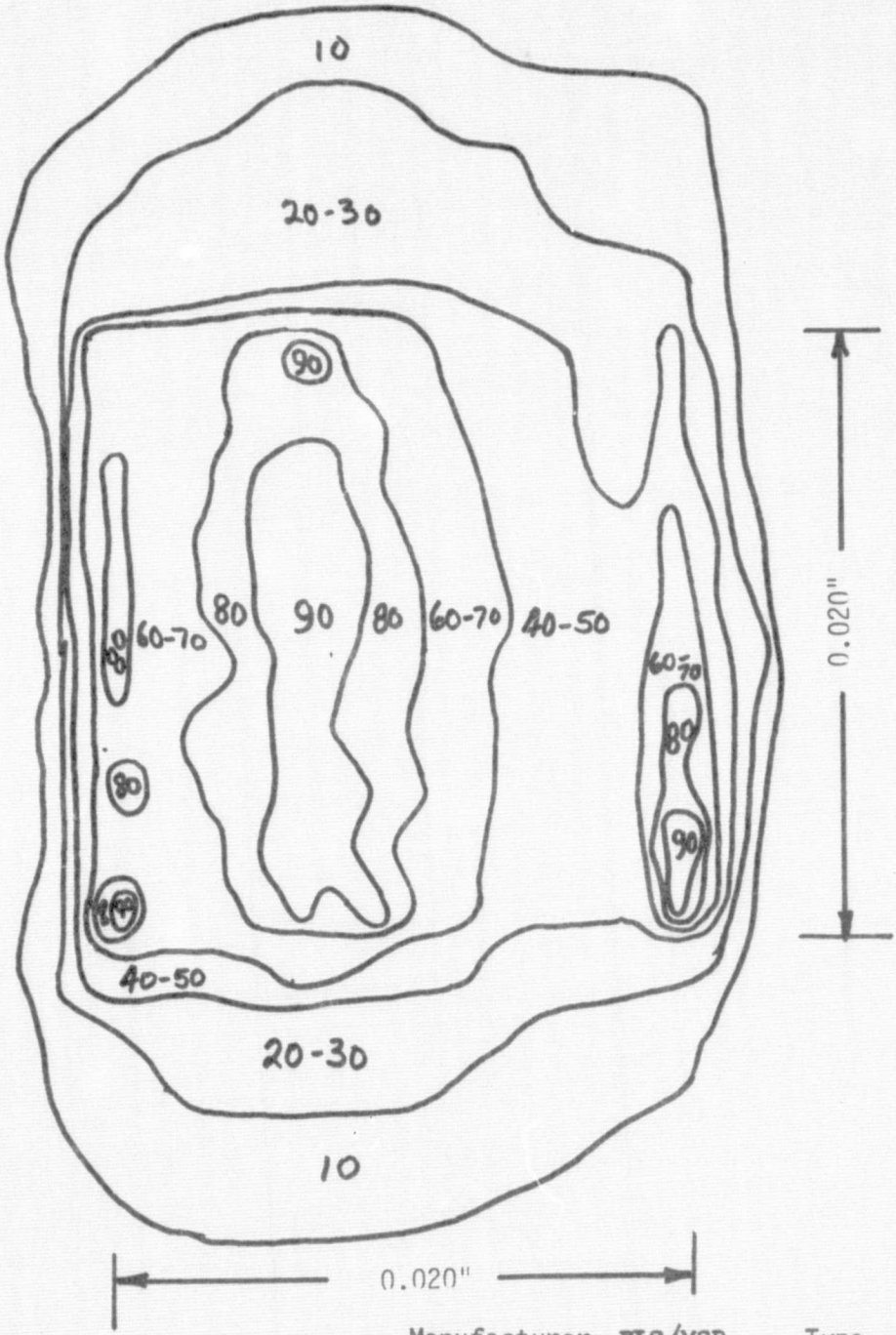

SENSIVITY CONTOUR

Manufacturer RIC/MSD Type Si:As

Bias 5 V Temp 4.5 K

FREQ 10 Hz Background 10^6 p/s/cm^2

Wavelength 10 microns

5.4 SBRC Si:As. A great deal of spiking was observed from this detector (#2), and the spiking rate was higher at the higher background. The spikes contributed significantly to the measured rms noise and therefore effected the determined optimum bias. In fact, the optimum bias was different at the two measurement backgrounds. At the low background, the optimum was 12 volts whereas it was 6 volts at the high background. Data are shown at both biases for the high background case.

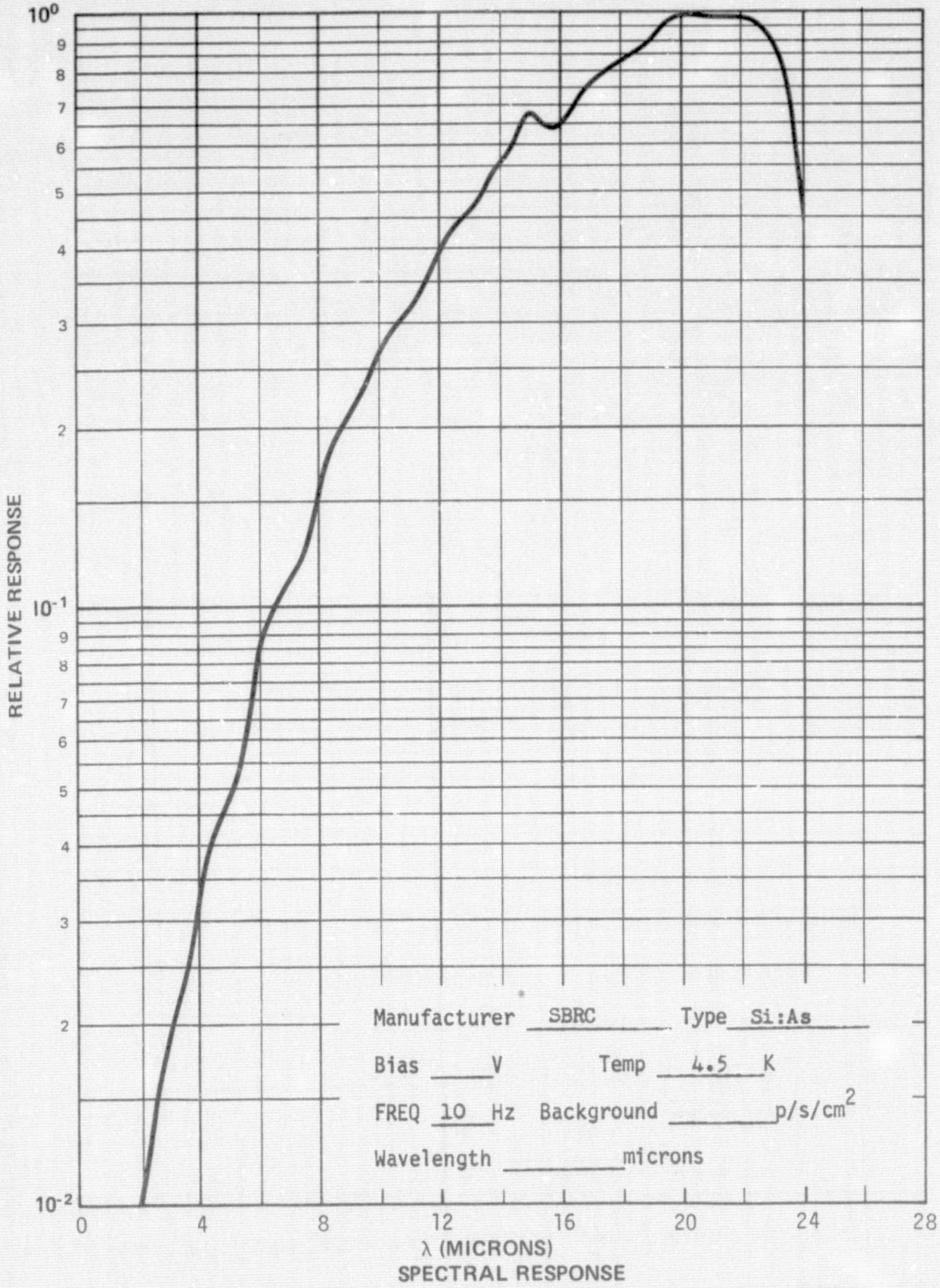

SPECTRAL RESPONSE

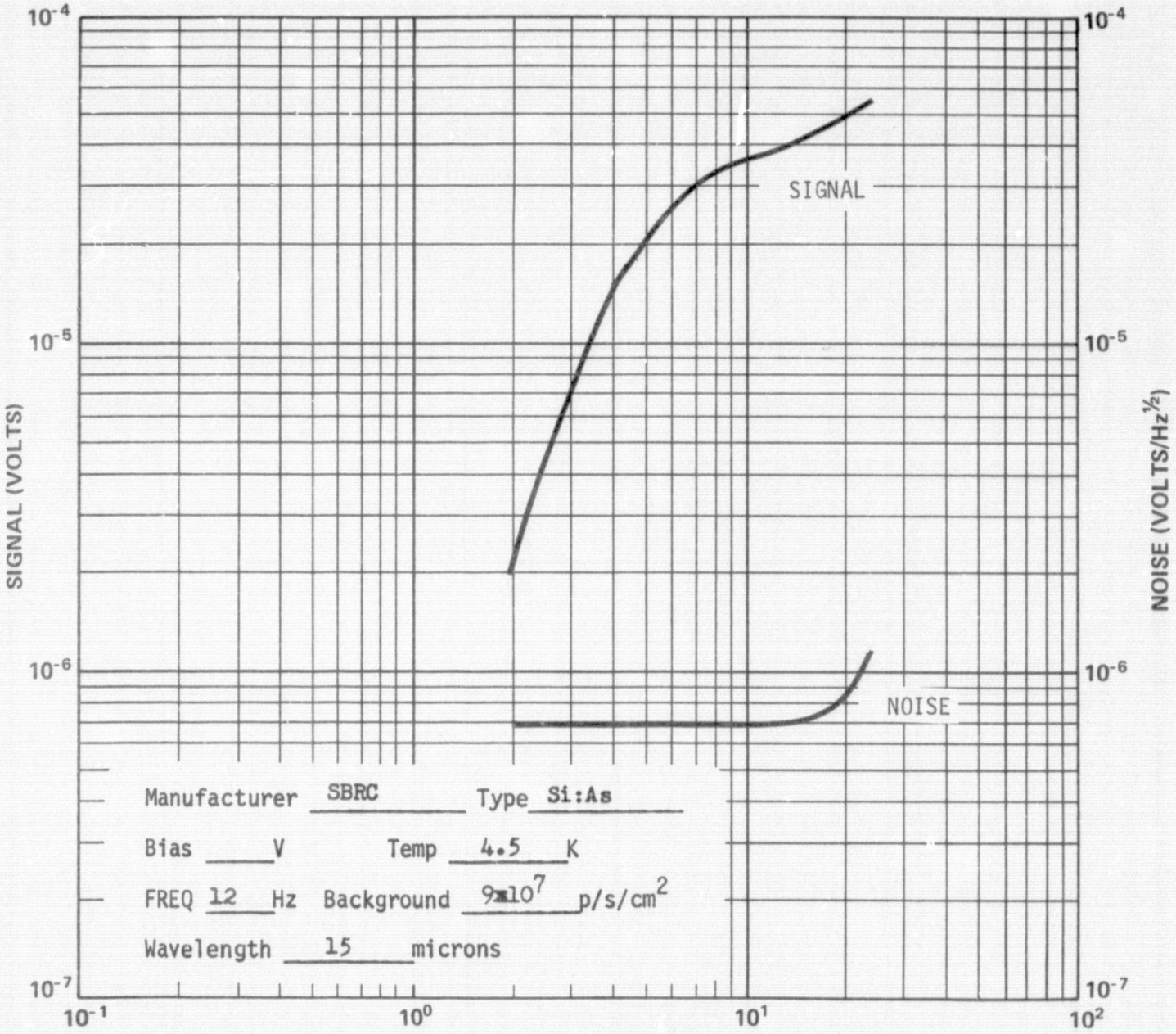

DETERMINATION OF OPTIMUM BIAS

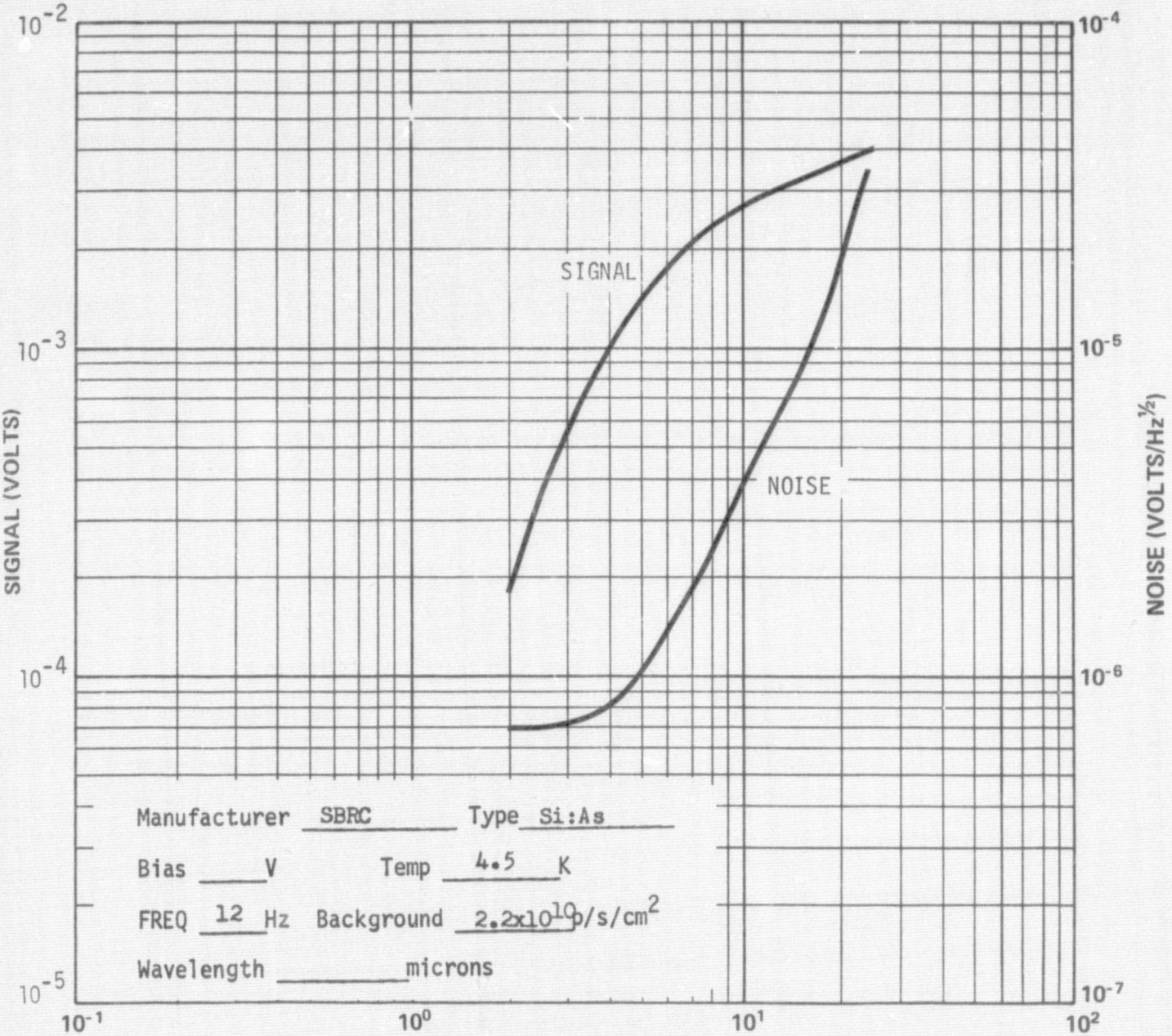

DETECTOR BIAS (VOLTS)
DETERMINATION OF OPTIMUM BIAS

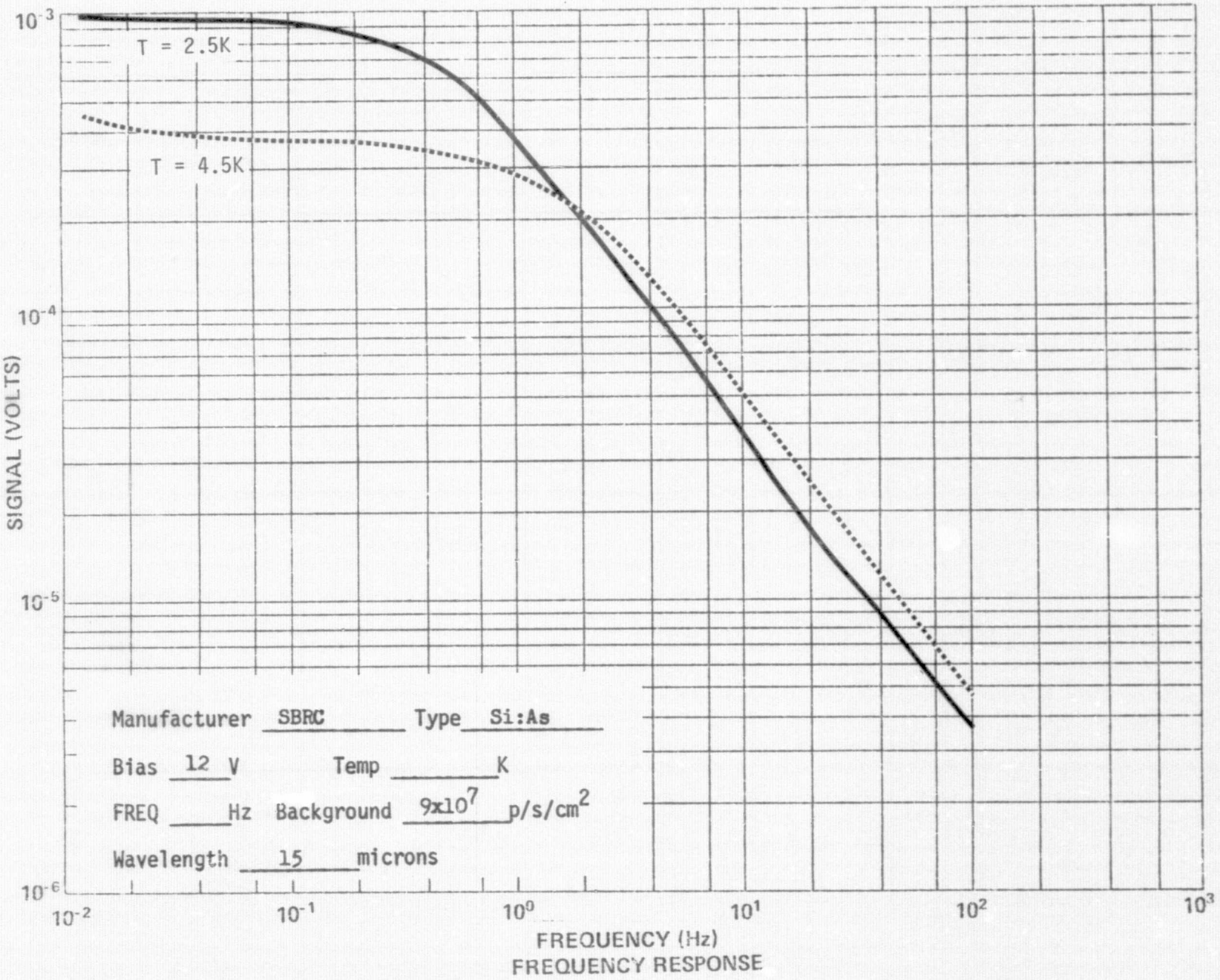

FREQUENCY RESPONSE

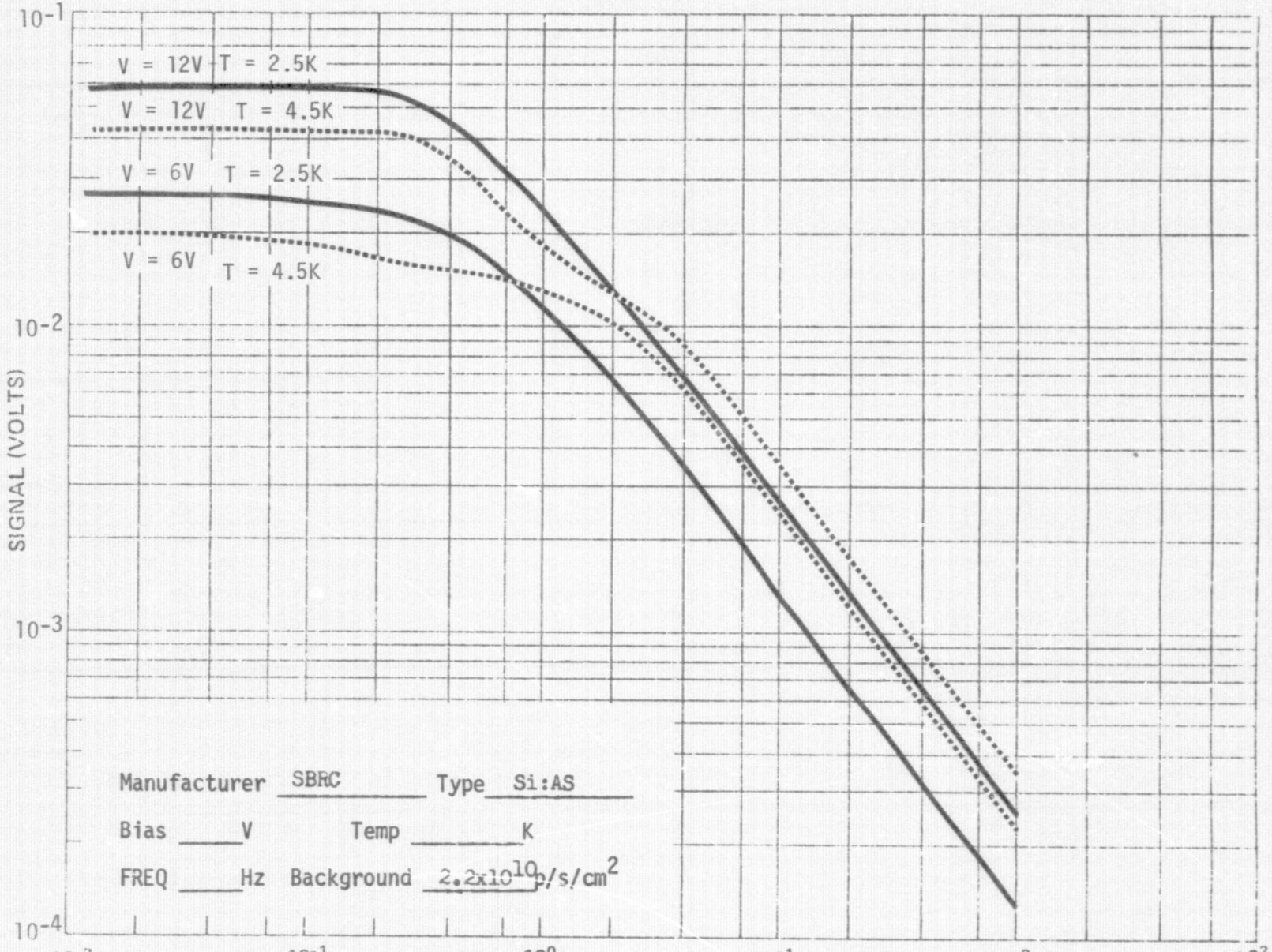

FREQUENCY RESPONSE

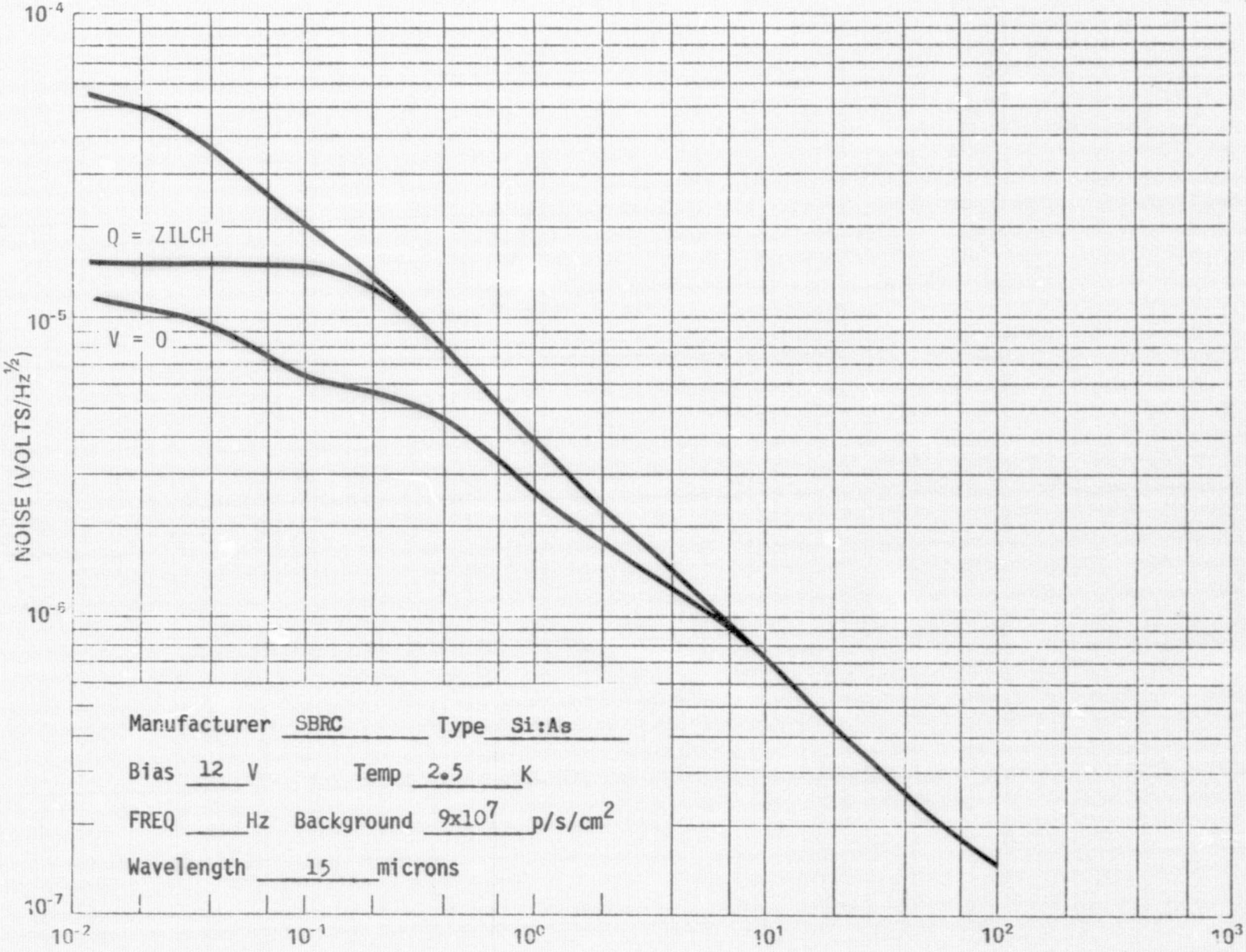

NOISE SPECTRUM

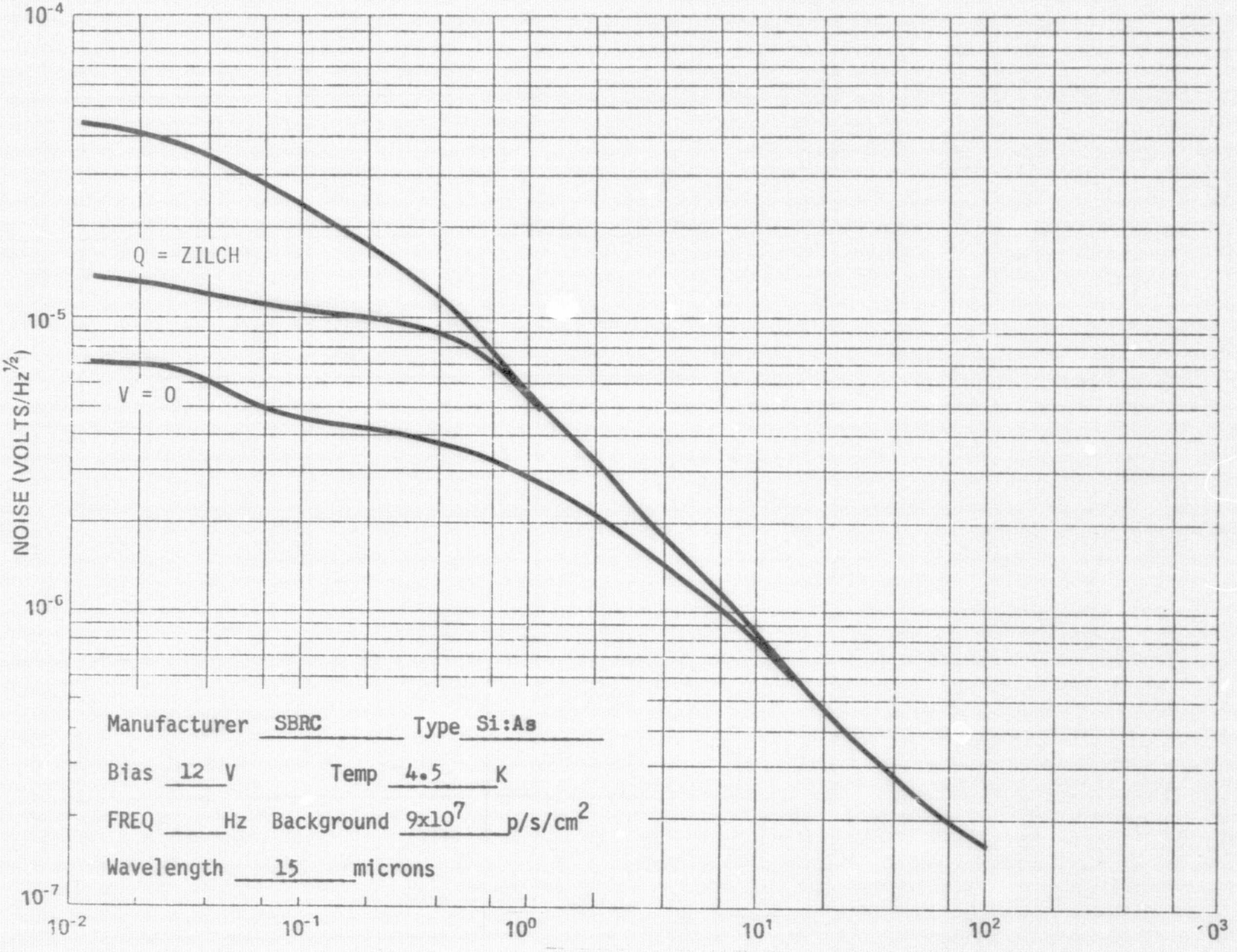

NOISE SPECTRUM

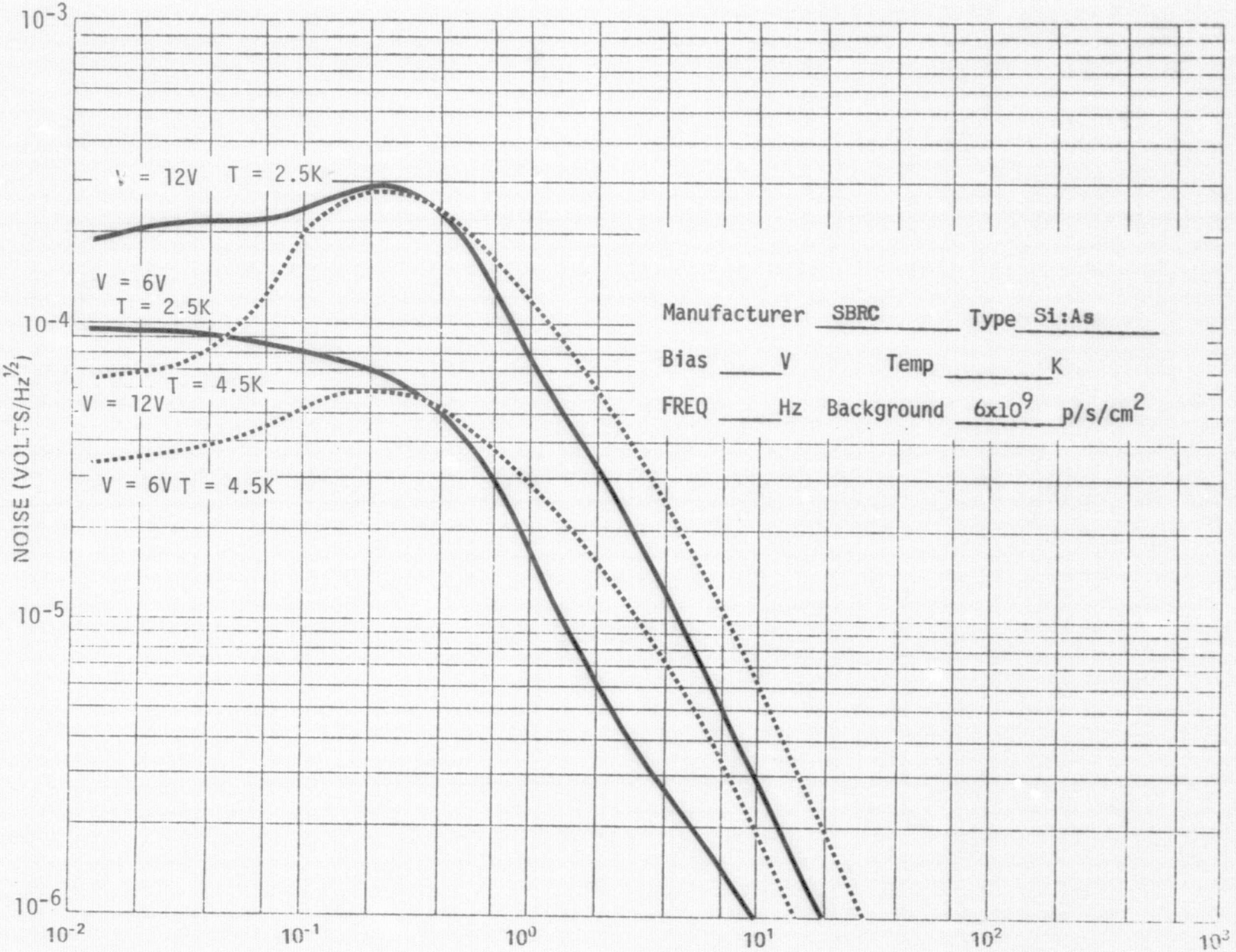

NOISE SPECTRUM

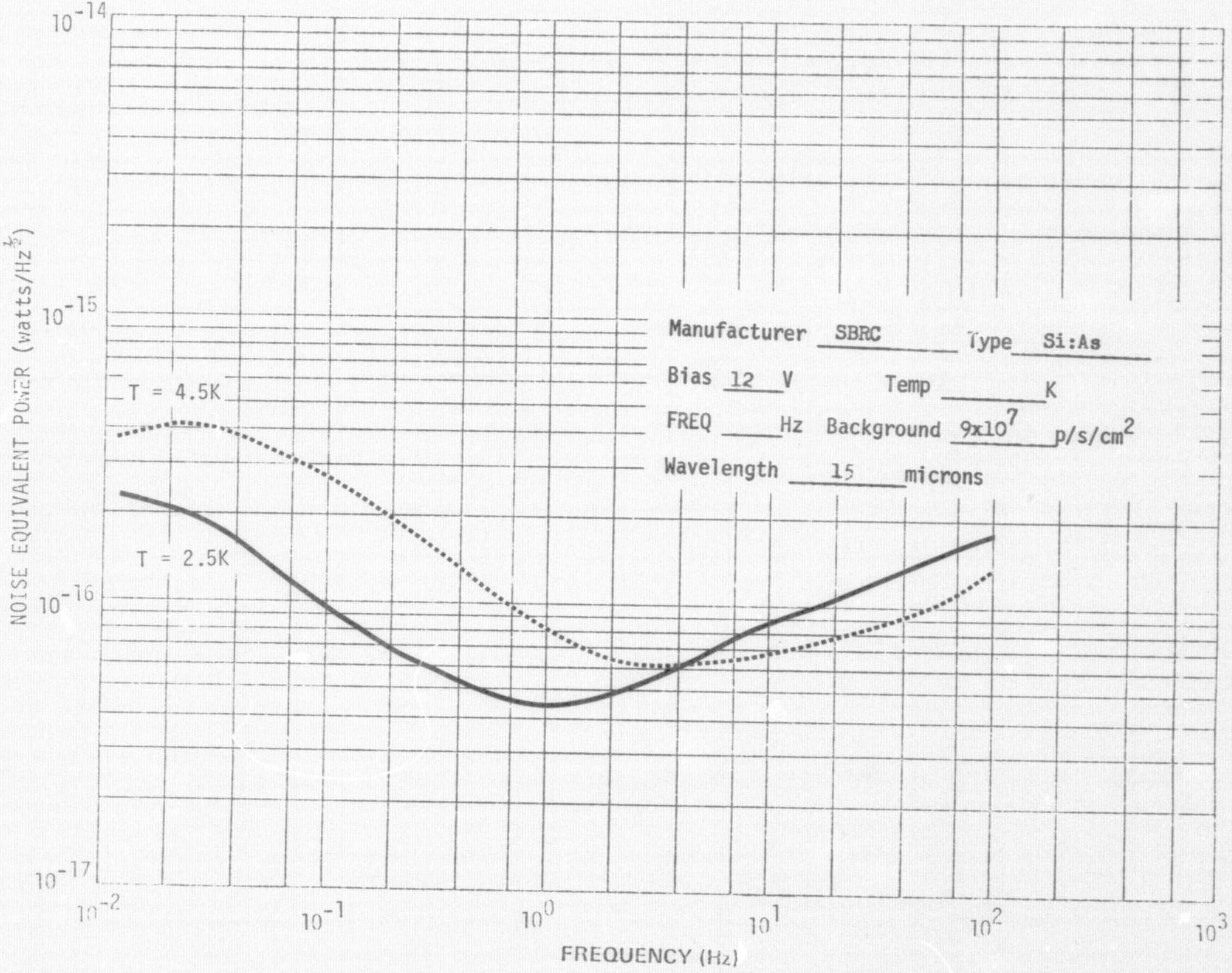
NOISE EQUIVALENT POWER (watts/Hz$^{\frac{1}{2}}$)
10^{-14}
10^{-15}
10^{-16}
10^{-17}
T = 4.5K
T = 2.5K
Manufacturer SBRC Type Si:As
Bias 12 V Temp ____ K
FREQ ____ Hz Background 9x10^7 p/s/cm^2
Wavelength 15 microns
10^{-2}
10^{-1}
10^{0}
10^{1}
10^{2}
10^{3}
FREQUENCY (Hz)

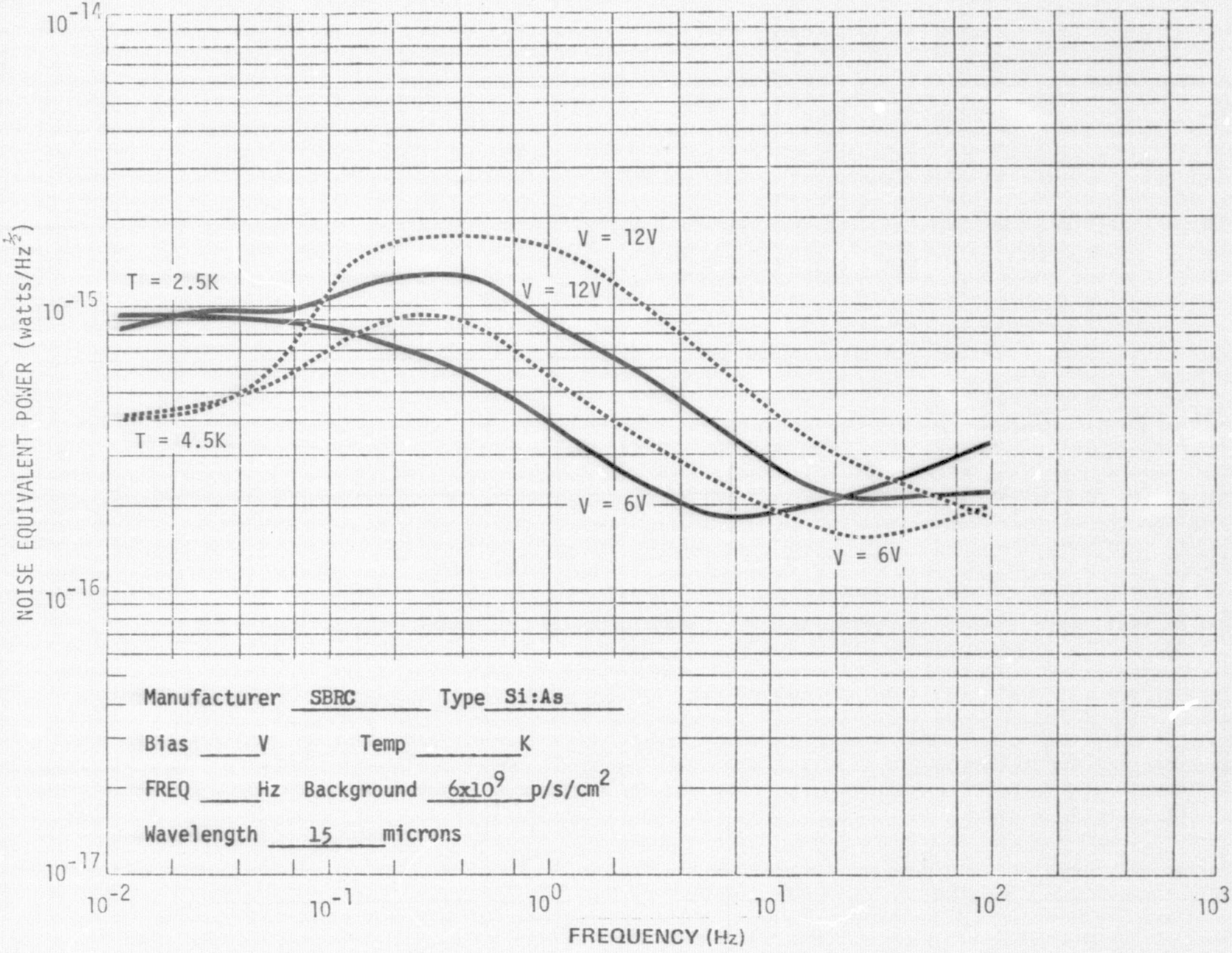
NOISE EQUIVALENT POWER (watts/Hz$^{\frac{1}{2}}$)
10^{-14}
10^{-15}
10^{-16}
10^{-17}
T = 2.5K
T = 4.5K
V = 12V
V = 12V
V = 6V
V = 6V
Manufacturer SBRC Type Si:As
Bias ____V Temp ____K
FREQ ____Hz Background 6x10^9 p/s/cm^2
Wavelength 15 microns
10^{-2}
10^{-1}
10^{0}
10^{1}
10^{2}
10^{3}
FREQUENCY (Hz)

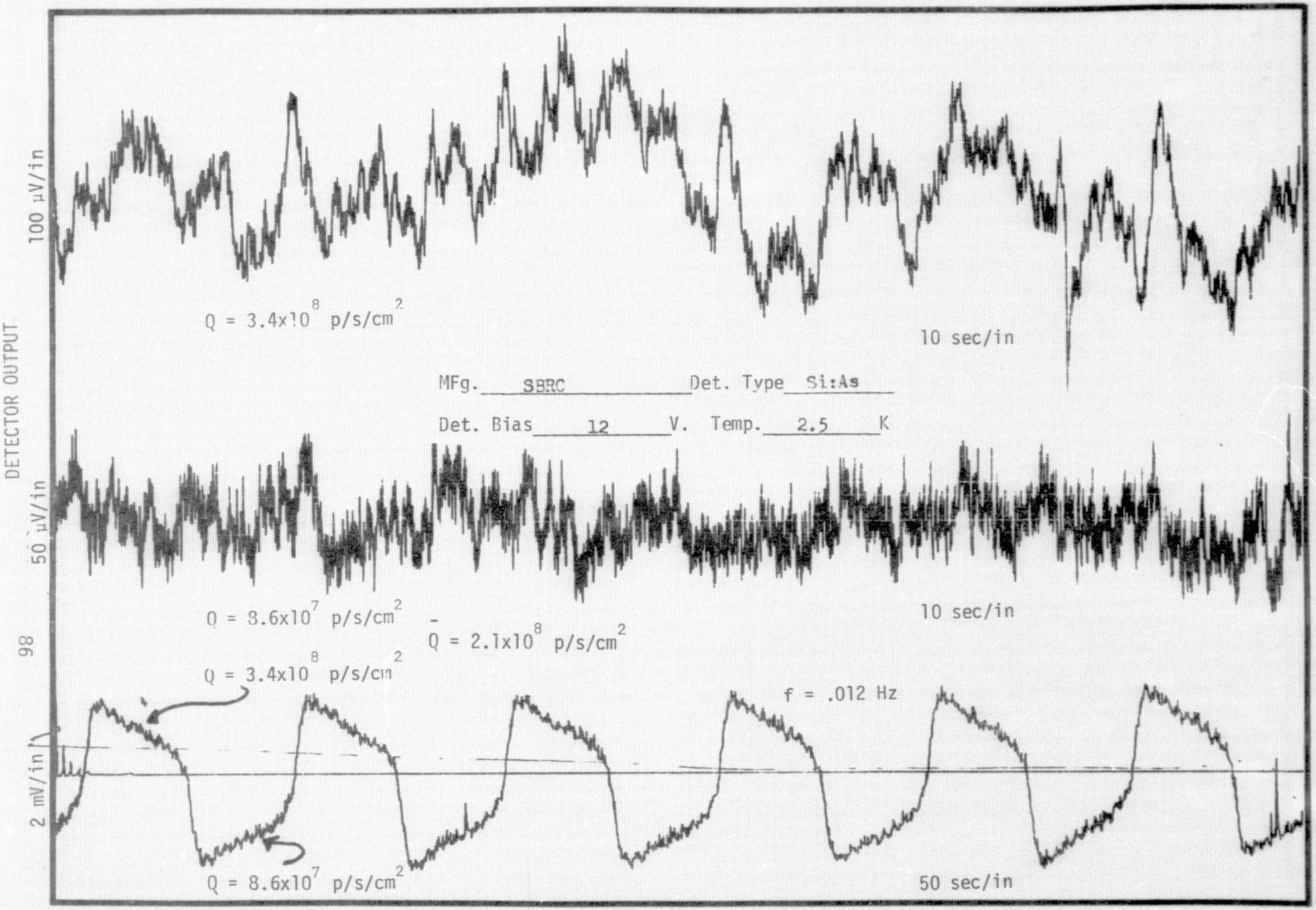
100 µV/in
Q = 3.4x10^8 p/s/cm^2
10 sec/in
MFg. SBRC Det. Type Si:As
Det. Bias 12 V. Temp. 2.5 K
50 µV/in
Q = 8.6x10^7 p/s/cm^2
Q = 2.1x10^8 p/s/cm^2
10 sec/in
Q = 3.4x10^8 p/s/cm^2
f = .012 Hz
2 mV/in
Q = 8.6x10^7 p/s/cm^2
50 sec/in
DETECTOR OUTPUT
TIME

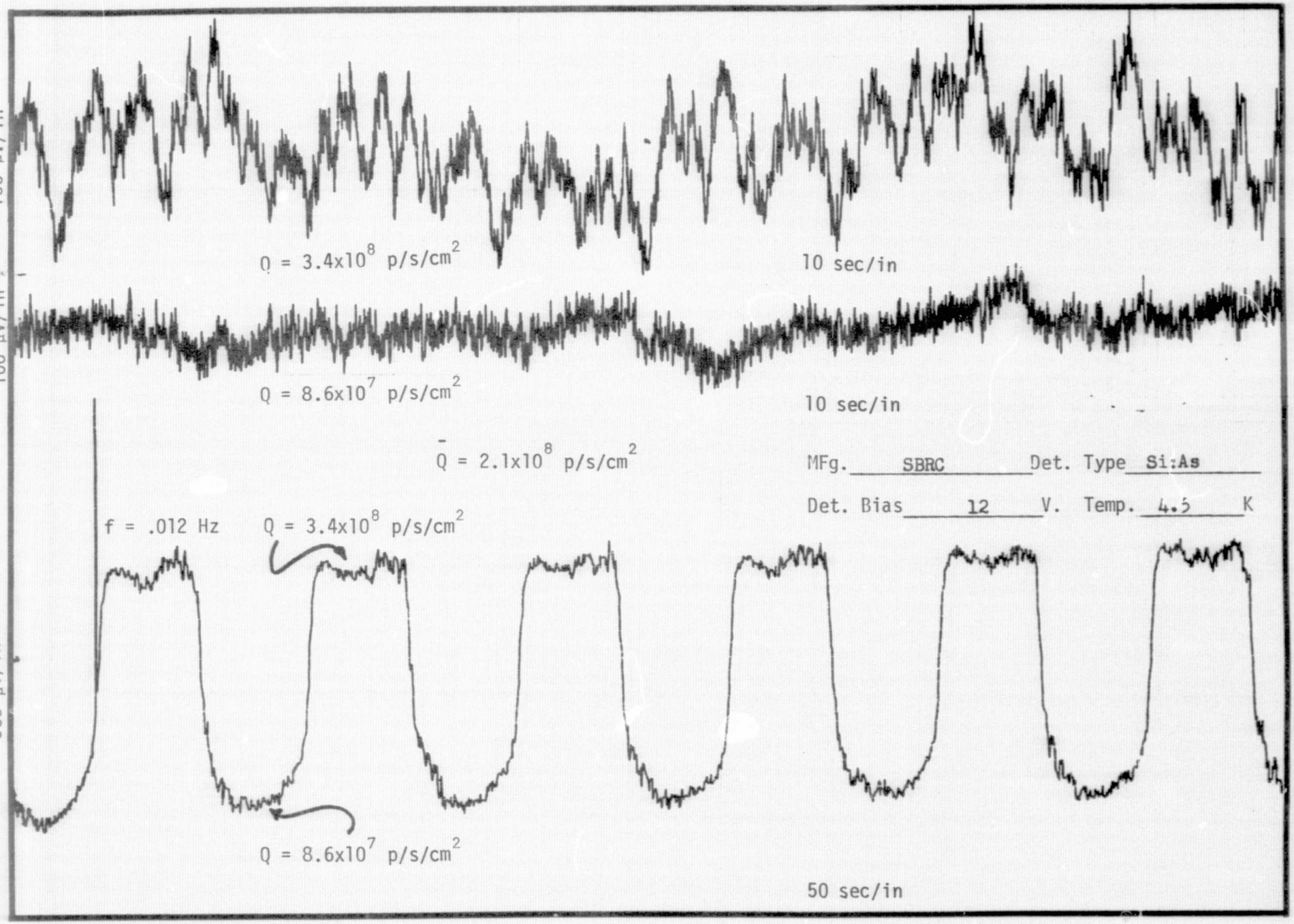
100 μV/in
Q = 3.4x10^8 p/s/cm^2
10 sec/in
100 μV/in
Q = 8.6x10^7 p/s/cm^2
10 sec/in
Q = 2.1x10^8 p/s/cm^2
MFg. SBRC Det. Type Si:As
Det. Bias 12 V. Temp. 4.5 K
f = .012 Hz
Q = 3.4x10^8 p/s/cm^2
500 μV/in
Q = 8.6x10^7 p/s/cm^2
50 sec/in
DETECTOR OUTPUT
TIME

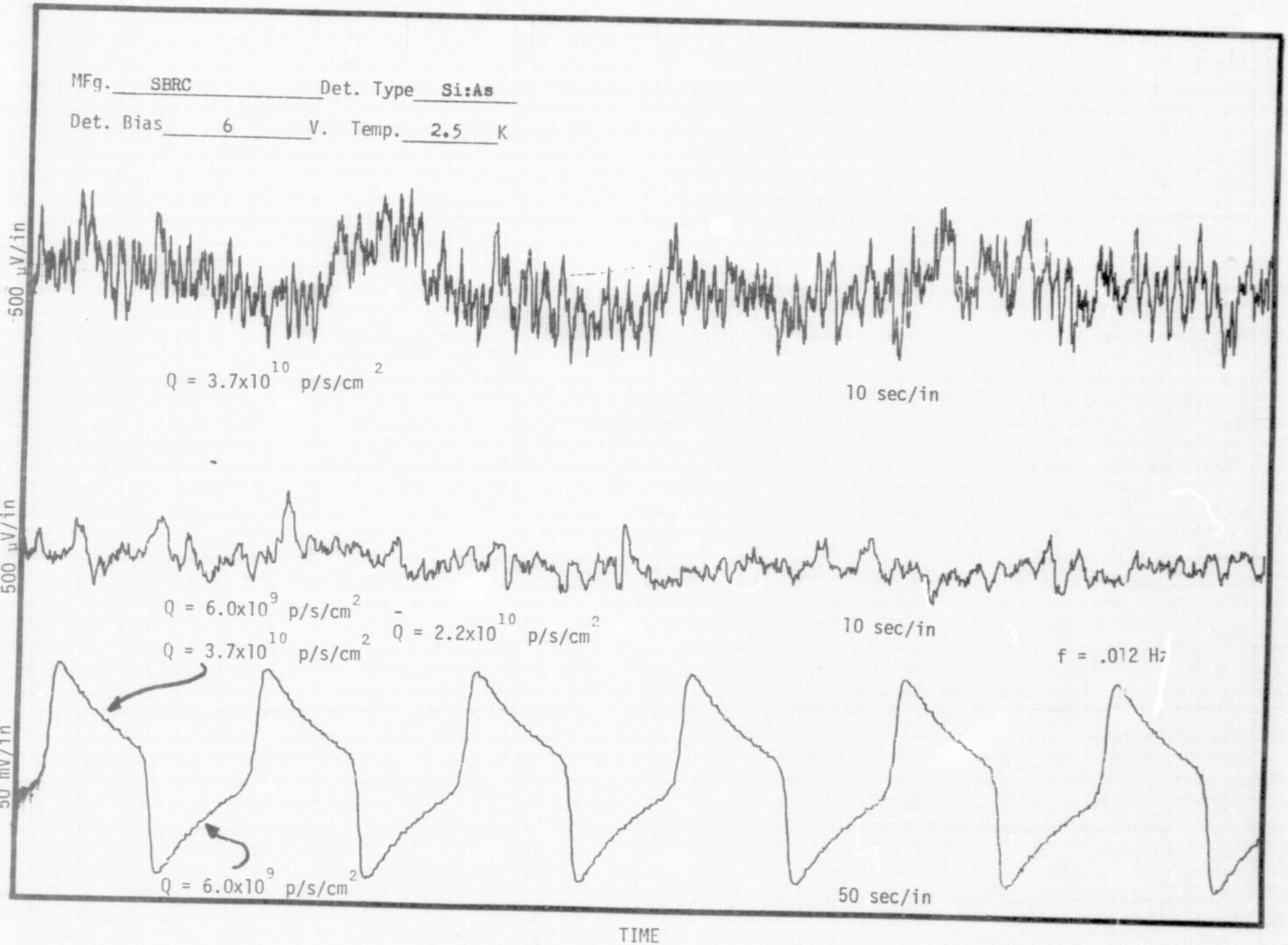
MFg. SBRC Det. Type Si:As
Det. Bias 6 V. Temp. 2.5 K
500 μV/in
Q = 3.7x10^10 p/s/cm^2
10 sec/in
DETECTOR OUTPUT
500 μV/in
Q = 6.0x10^9 p/s/cm^2 - Q = 2.2x10^10 p/s/cm^2
10 sec/in
Q = 3.7x10^10 p/s/cm^2
f = .012 Hz
50 mV/in
Q = 6.0x10^9 p/s/cm^2
50 sec/in
TIME

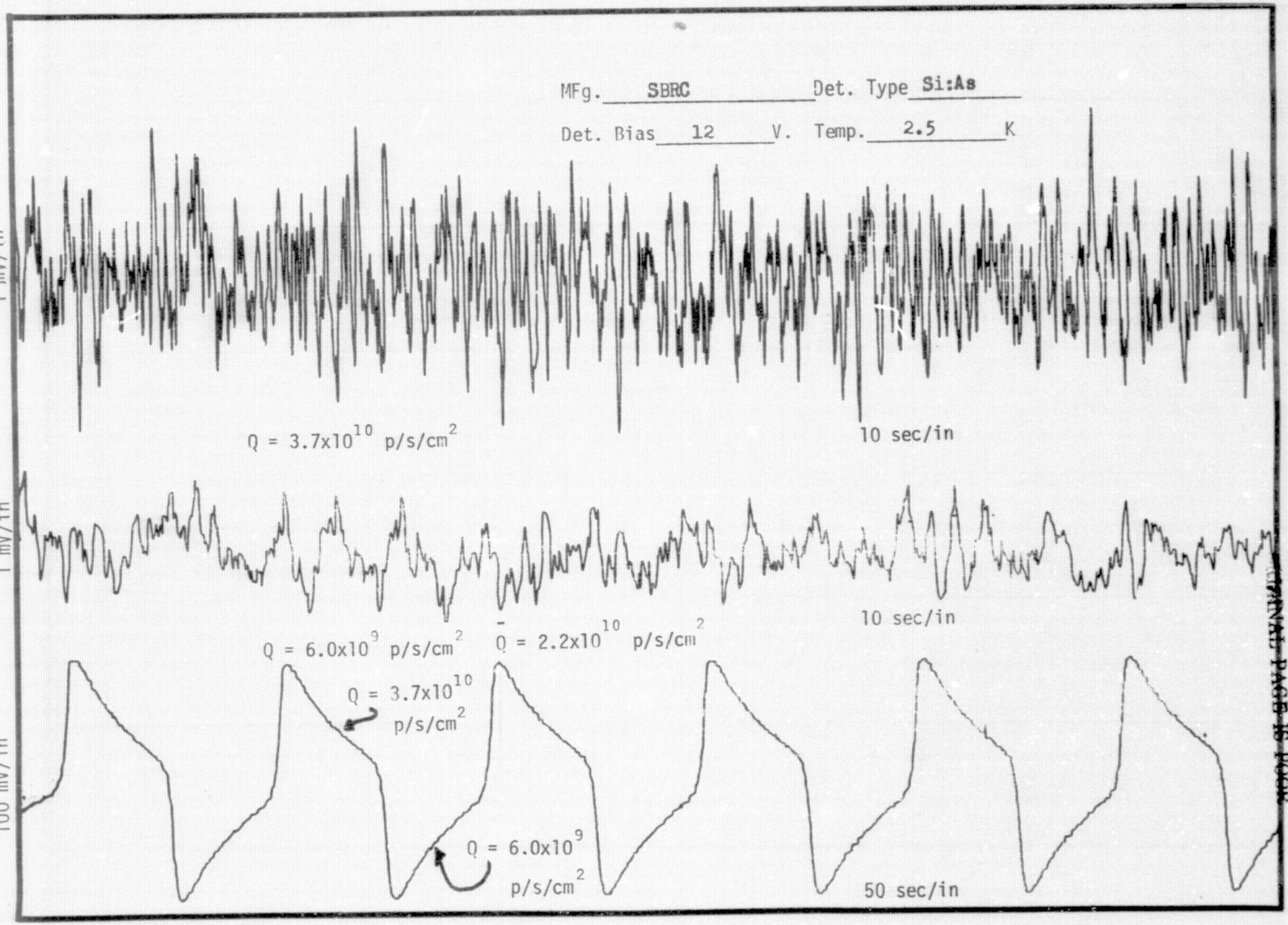

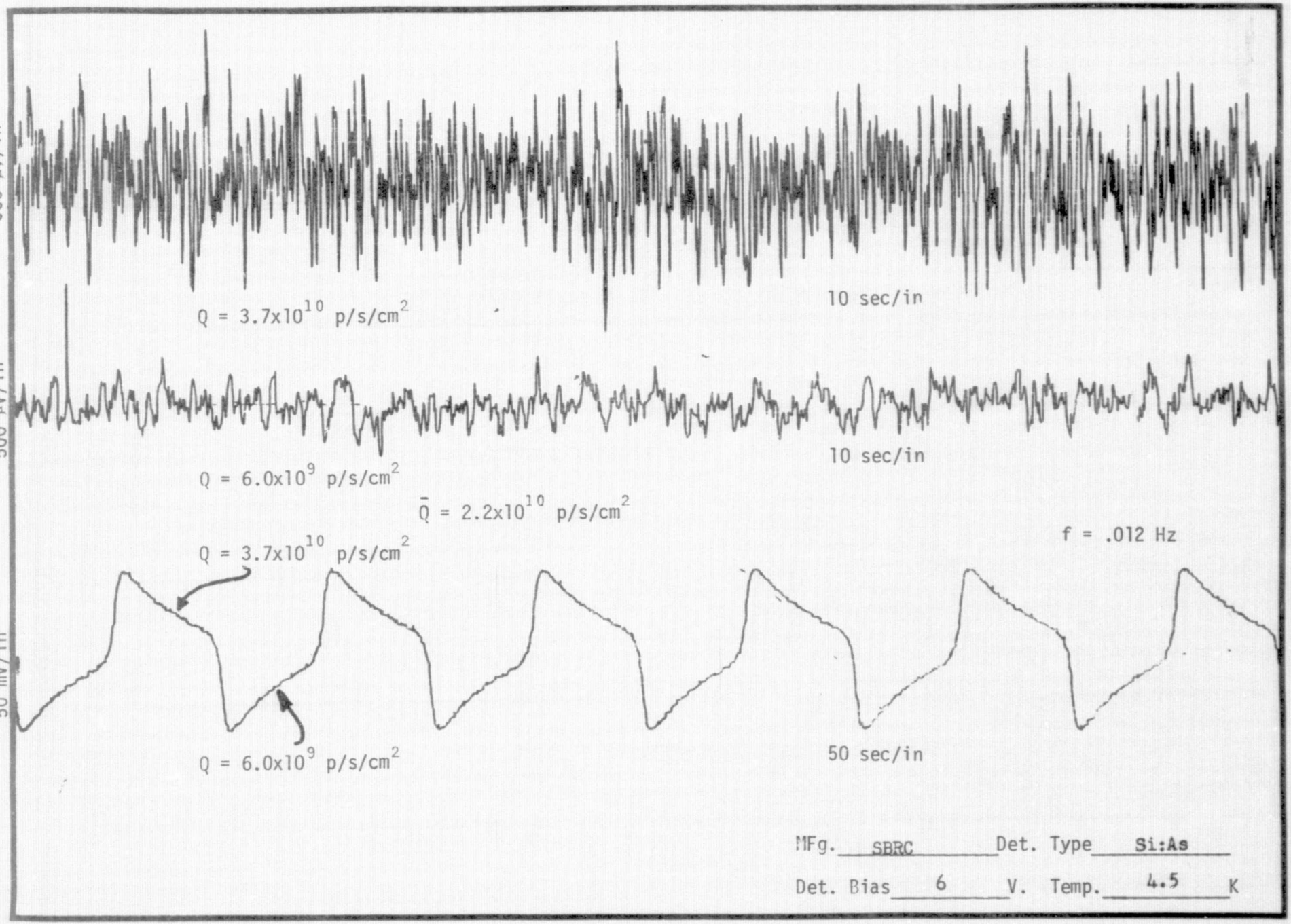
DETECTOR OUTPUT
500 μV/in
Q = 3.7x10^10 p/s/cm^2
10 sec/in
500 μV/in
Q = 6.0x10^9 p/s/cm^2
10 sec/in
Q̄ = 2.2x10^10 p/s/cm^2
Q = 3.7x10^10 p/s/cm^2
f = .012 Hz
50 mV/in
Q = 6.0x10^9 p/s/cm^2
50 sec/in
MFg. SBRC Det. Type Si:As
Det. Bias 6 V. Temp. 4.5 K
TIME

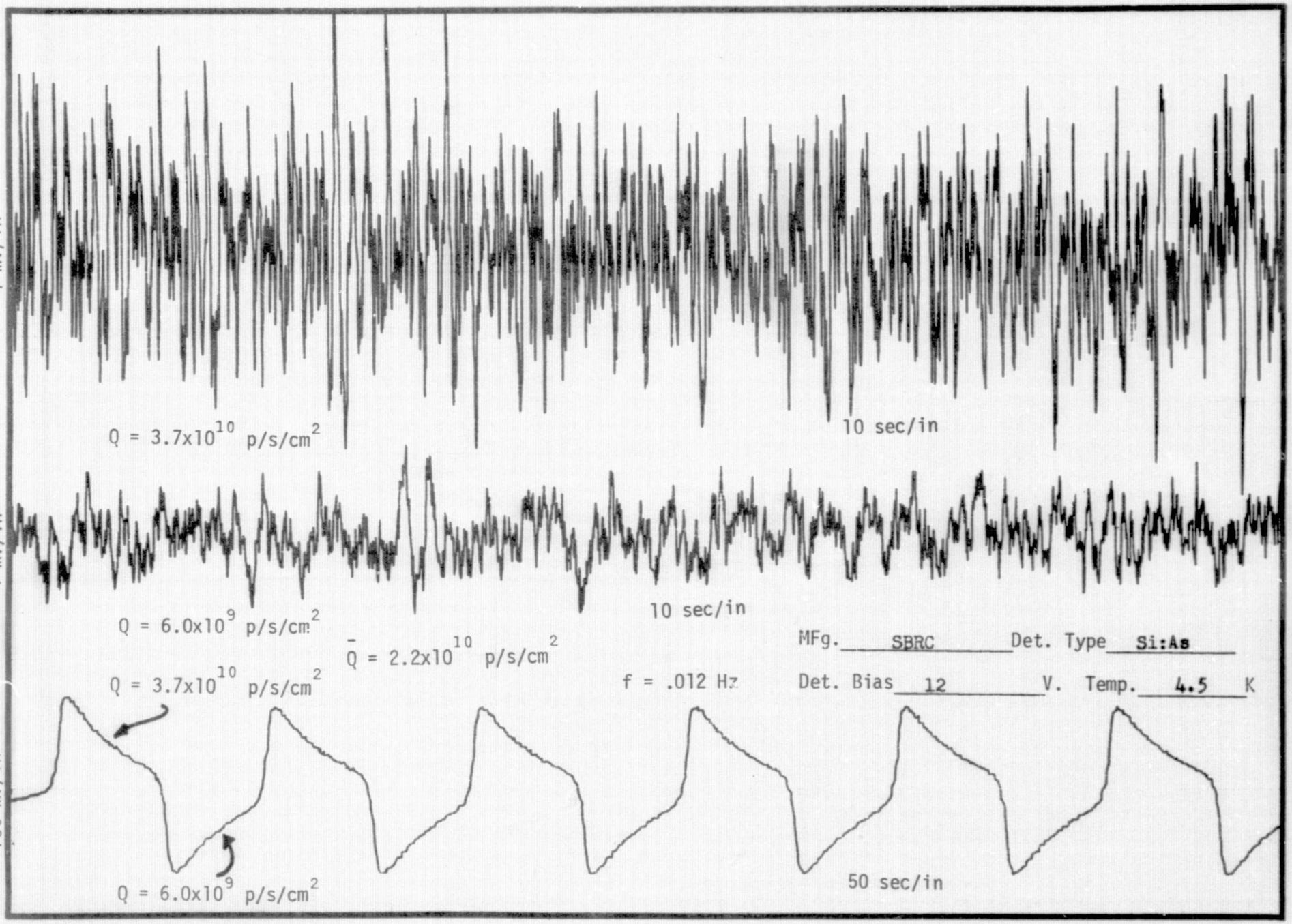
1 mV/in
Q = 3.7x10^10 p/s/cm^2
10 sec/in
1 mV/in
Q = 6.0x10^9 p/s/cm^2
Q = 2.2x10^10 p/s/cm^2
10 sec/in
MFg. SBRC Det. Type Si:As
Q = 3.7x10^10 p/s/cm^2
f = .012 Hz
Det. Bias 12 V. Temp. 4.5 K
100 mV/in
Q = 6.0x10^9 p/s/cm^2
50 sec/in
DETECTOR OUTPUT
TIME

5.5 RIC/MSD Si:Sb. This detector package (NA 005) also had a relatively low valued load resistor (about $10^9\Omega$ at 4.5K). This load value limits the detector signal at low frequencies. Also the FET noise was a bit higher than can be obtained with other FETs. The combination of low load and high FET noise together with the relatively low current responsivity (at 15μ) result in a relatively high NEP, particularly at low frequencies. The poor signal-to-noise ratio made the measurement of frequency response at low backgrounds somewhat difficult.

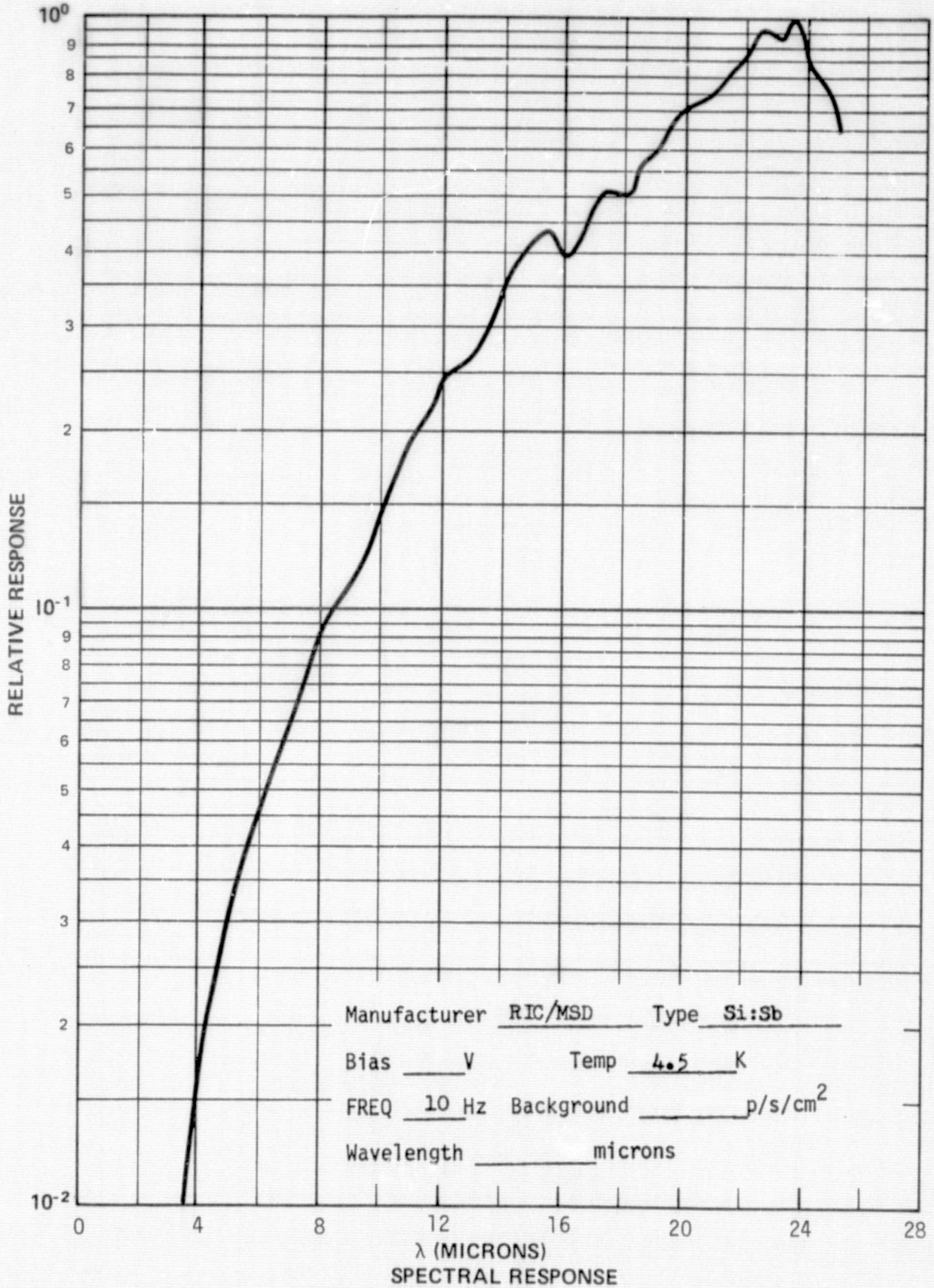

SPECTRAL RESPONSE

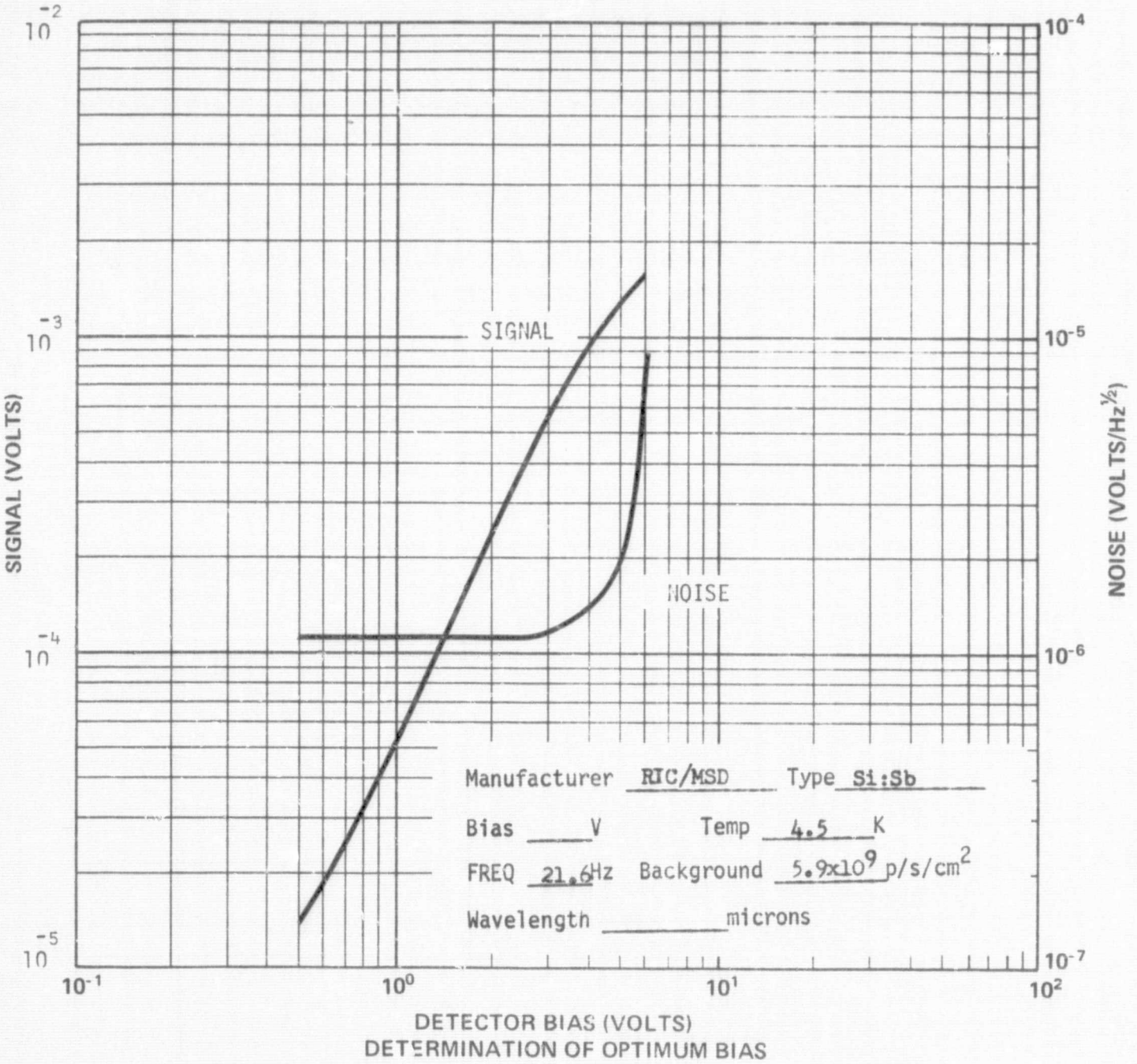

DETERMINATION OF OPTIMUM BIAS

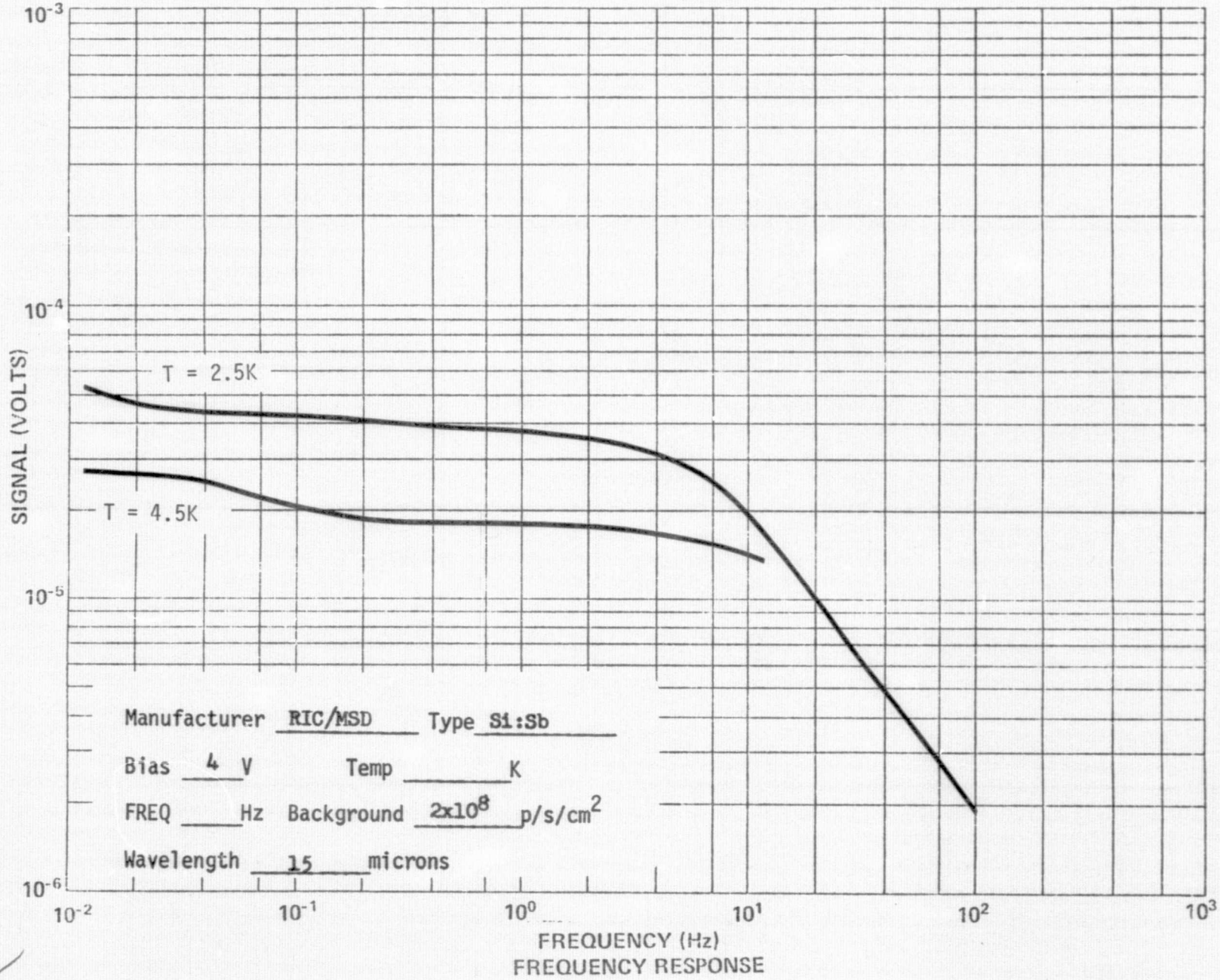

FREQUENCY RESPONSE

C-2

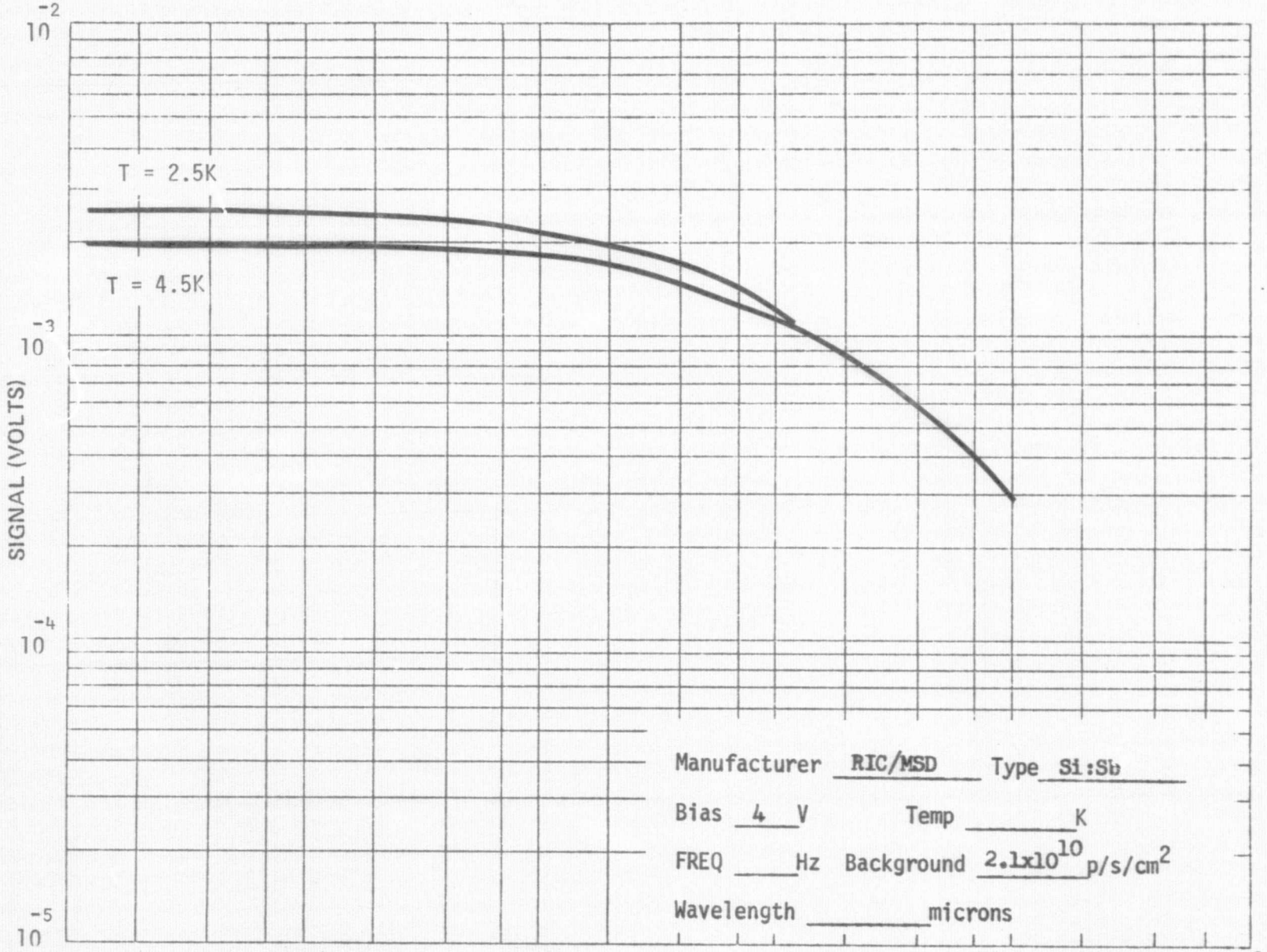

FREQUENCY RESPONSE

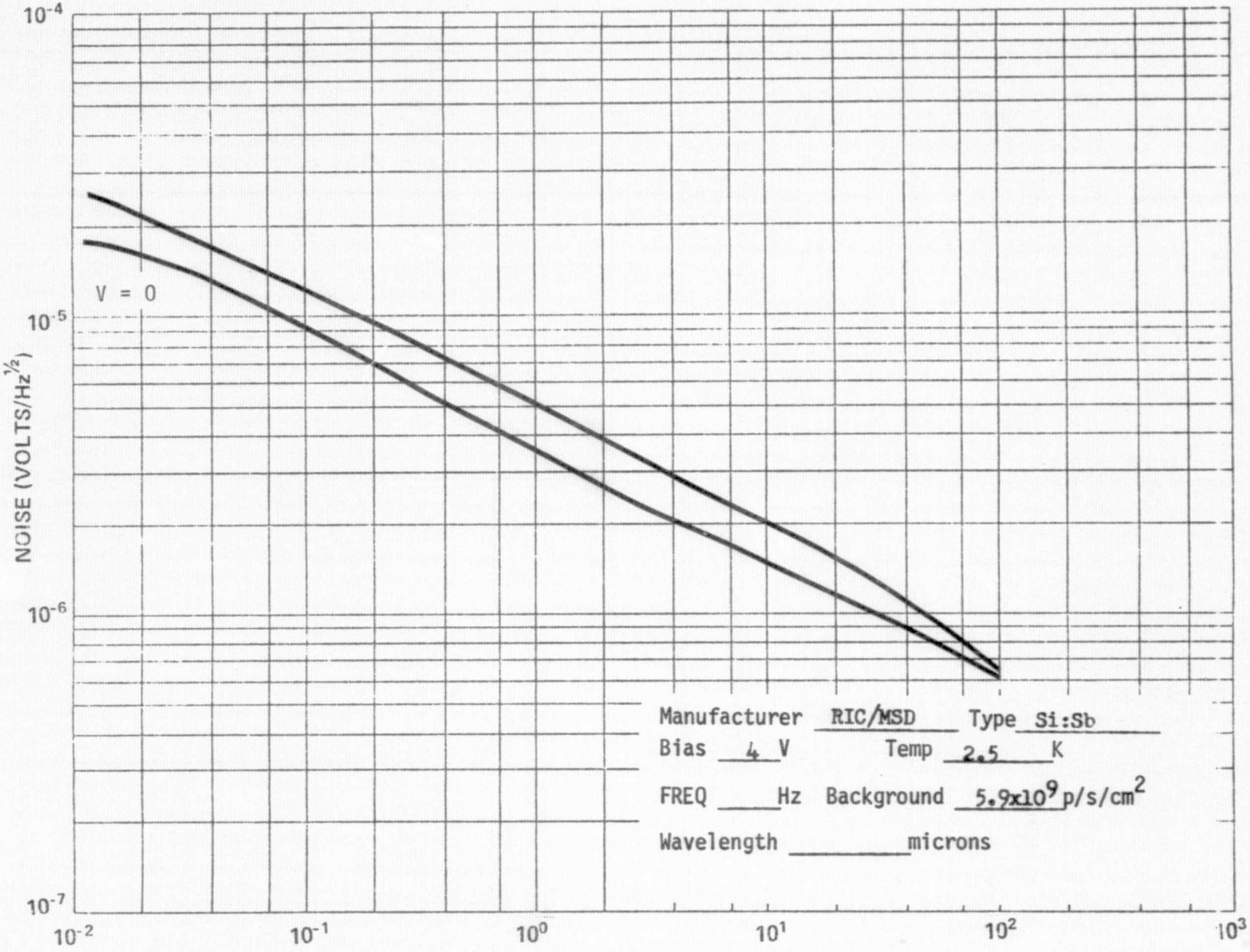

NOISE SPECTRUM

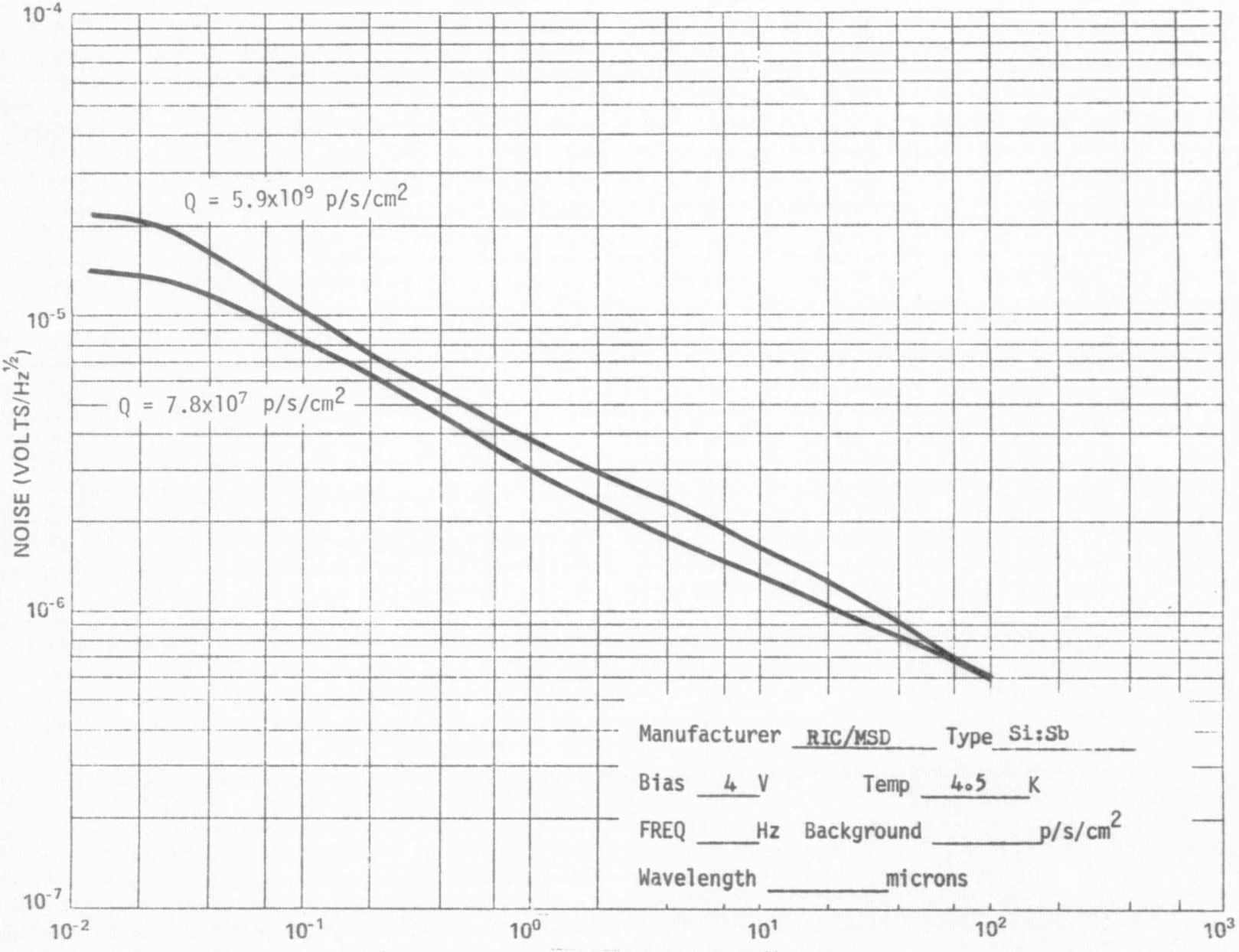

NOISE SPECTRUM

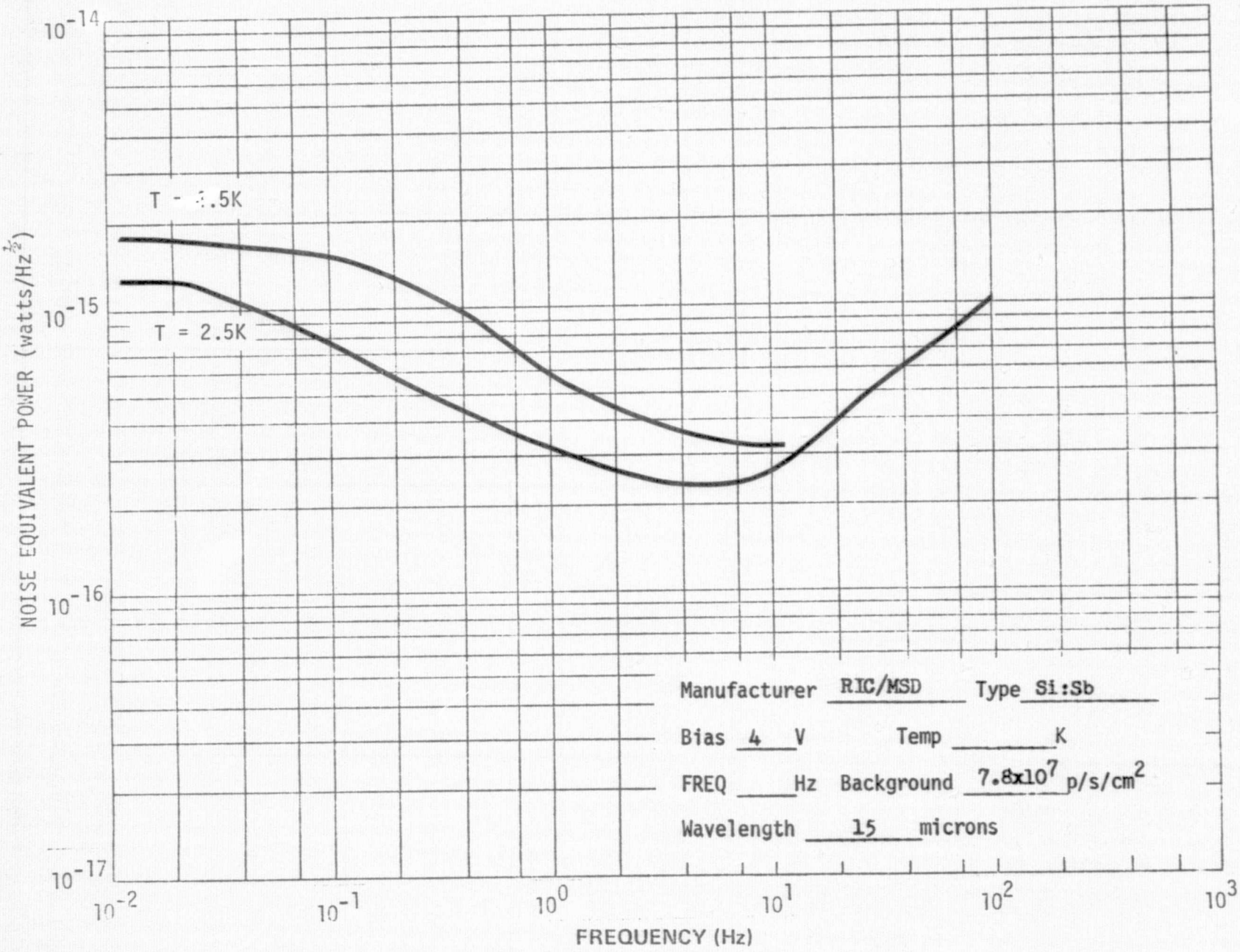
NOISE EQUIVALENT POWER (watts/Hz^½)
10^-14
10^-15
10^-16
10^-17
T = 4.5K
T = 2.5K
Manufacturer RIC/MSD Type Si:Sb
Bias 4 V Temp K
FREQ Hz Background 7.8x10^7 p/s/cm^2
Wavelength 15 microns
10^-2
10^-1
10^0
10^1
10^2
10^3
FREQUENCY (Hz)

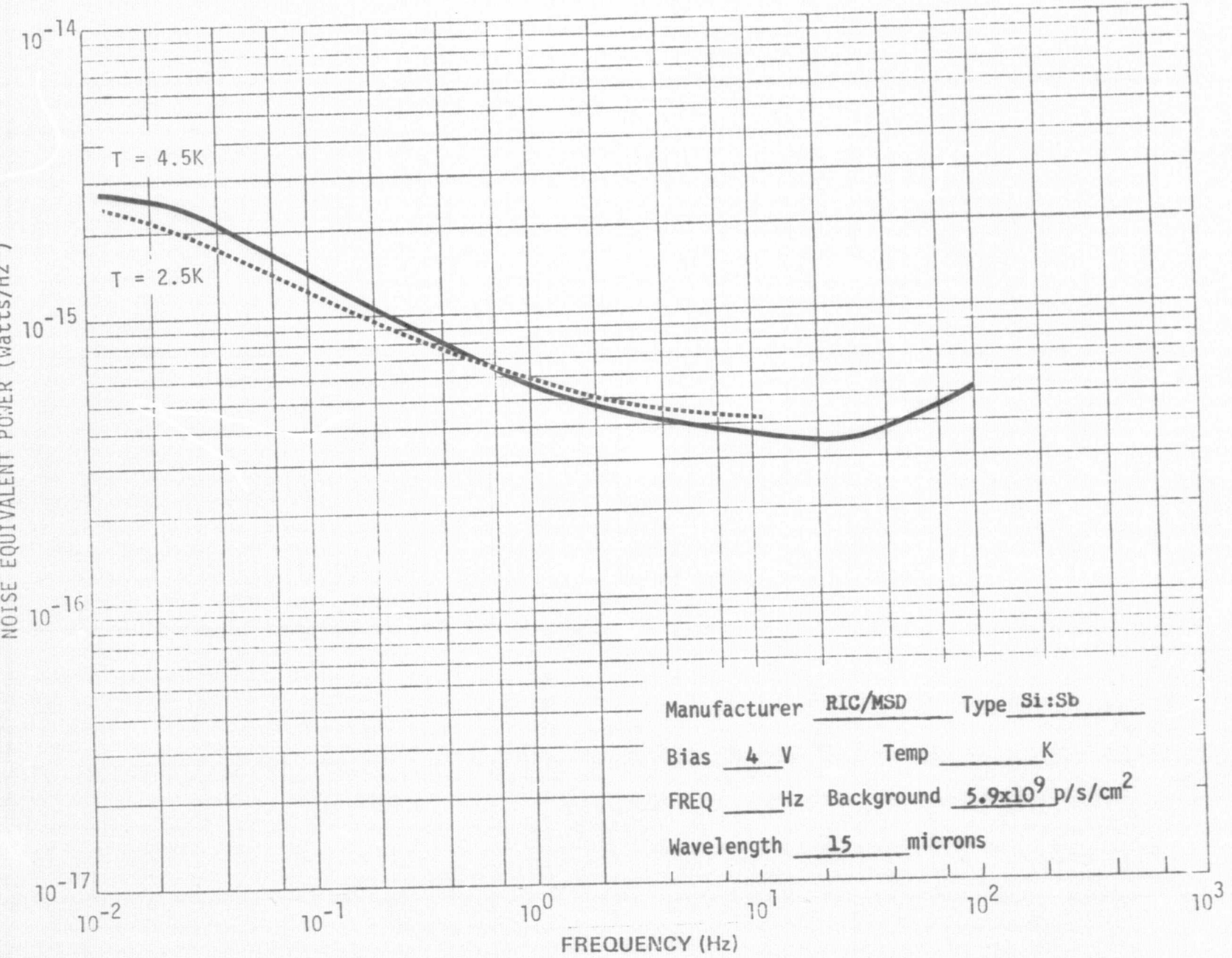
10^{-14}
10^{-15}
10^{-16}
10^{-17}
T = 4.5K
T = 2.5K
NOISE EQUIVALENT POWER (watts/Hz$^{\frac{1}{2}}$)
10^{-2}
10^{-1}
10^{0}
10^{1}
10^{2}
10^{3}
FREQUENCY (Hz)
Manufacturer RIC/MSD Type Si:Sb
Bias 4 V Temp ____K
FREQ ____Hz Background 5.9x10^{9} p/s/cm^{2}
Wavelength 15 microns

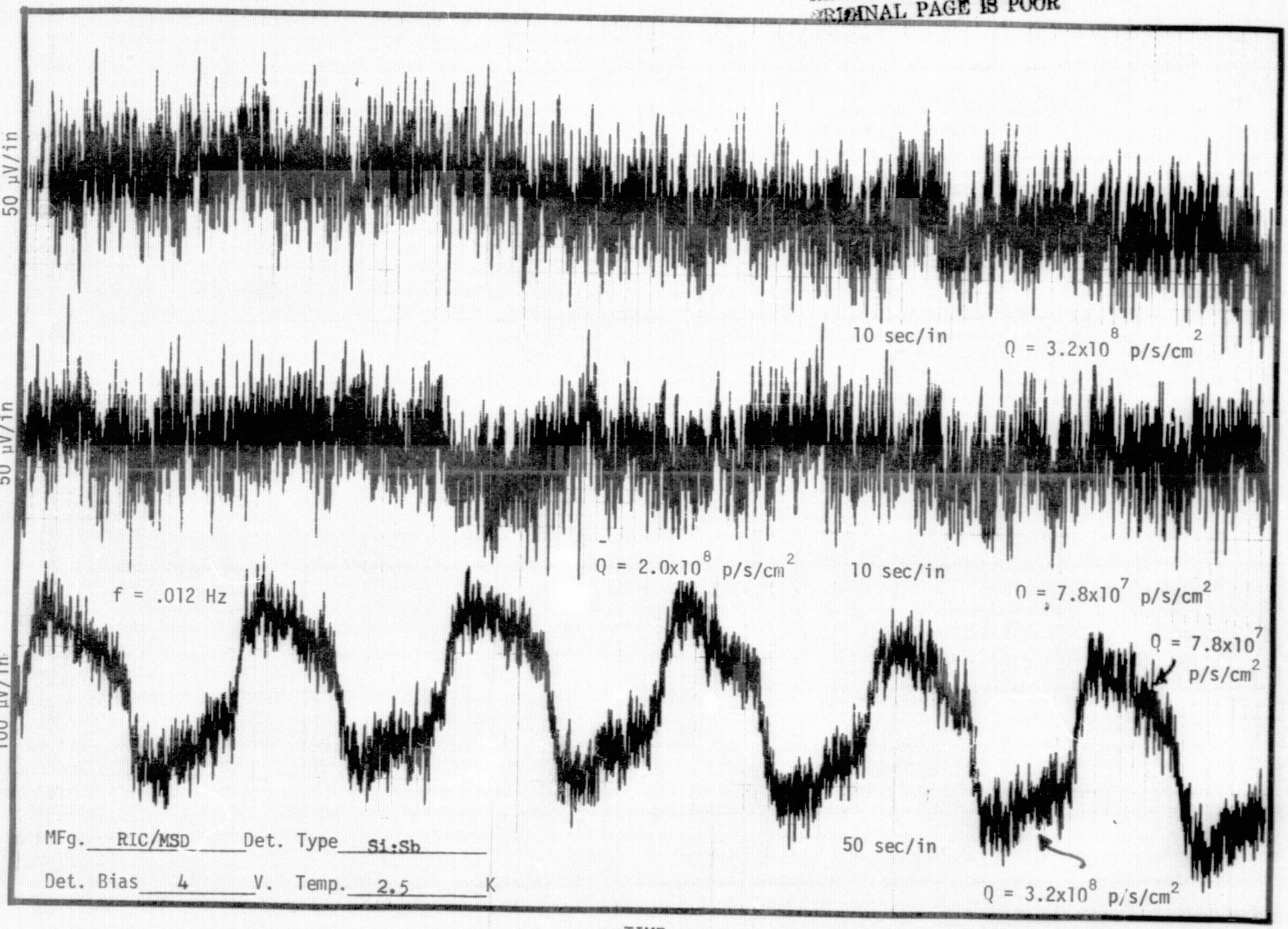

DETECTOR OUTPUT

TIME

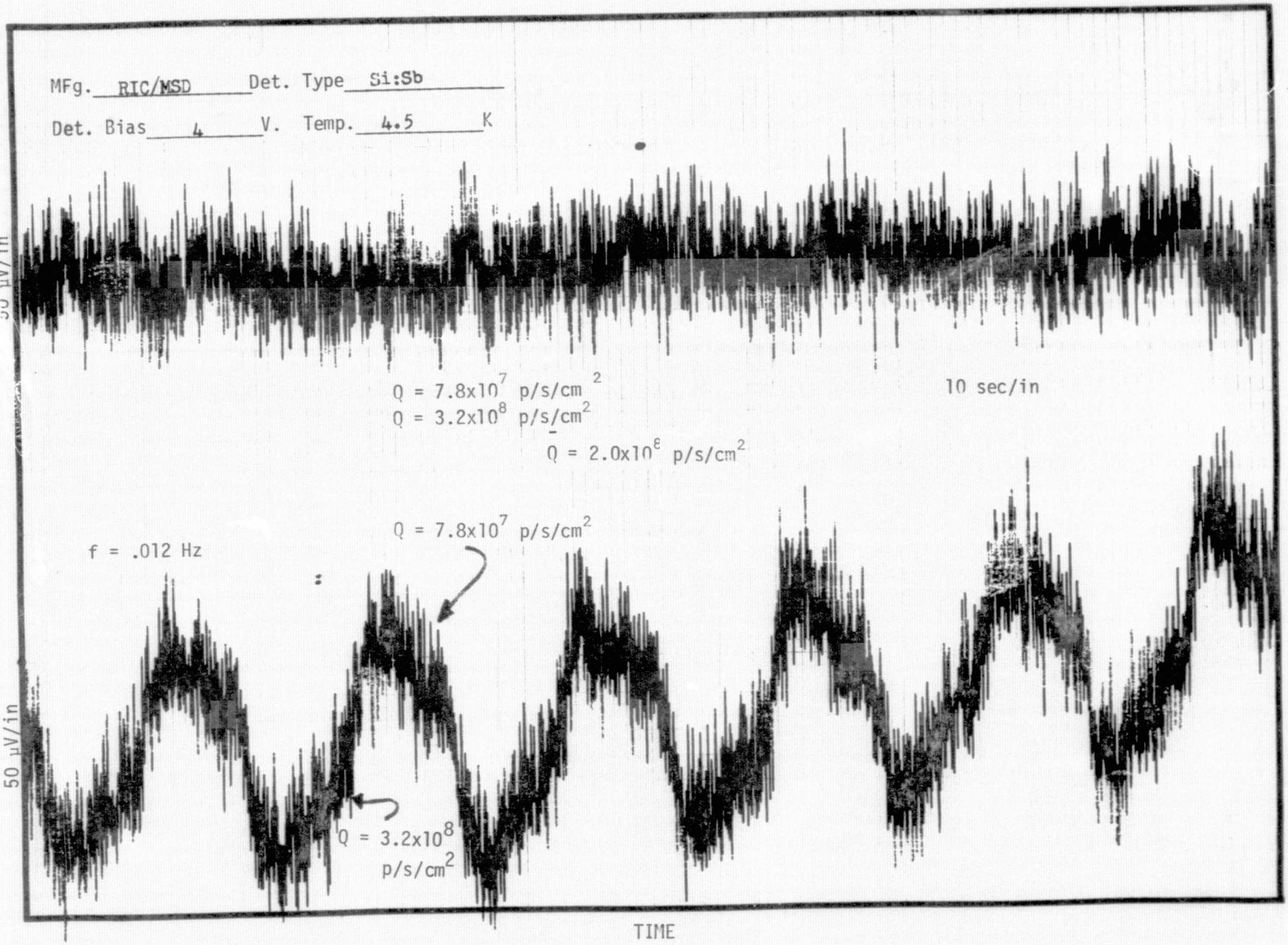
MFg. RIC/MSD Det. Type Si:Sb
Det. Bias 4 V. Temp. 4.5 K
50 μV/in
Q = 7.8x10^7 p/s/cm^2
Q = 3.2x10^8 p/s/cm^2
10 sec/in
Q = 2.0x10^8 p/s/cm^2
DETECTOR OUTPUT
Q = 7.8x10^7 p/s/cm^2
f = .012 Hz
50 μV/in
Q = 3.2x10^8 p/s/cm^2
TIME

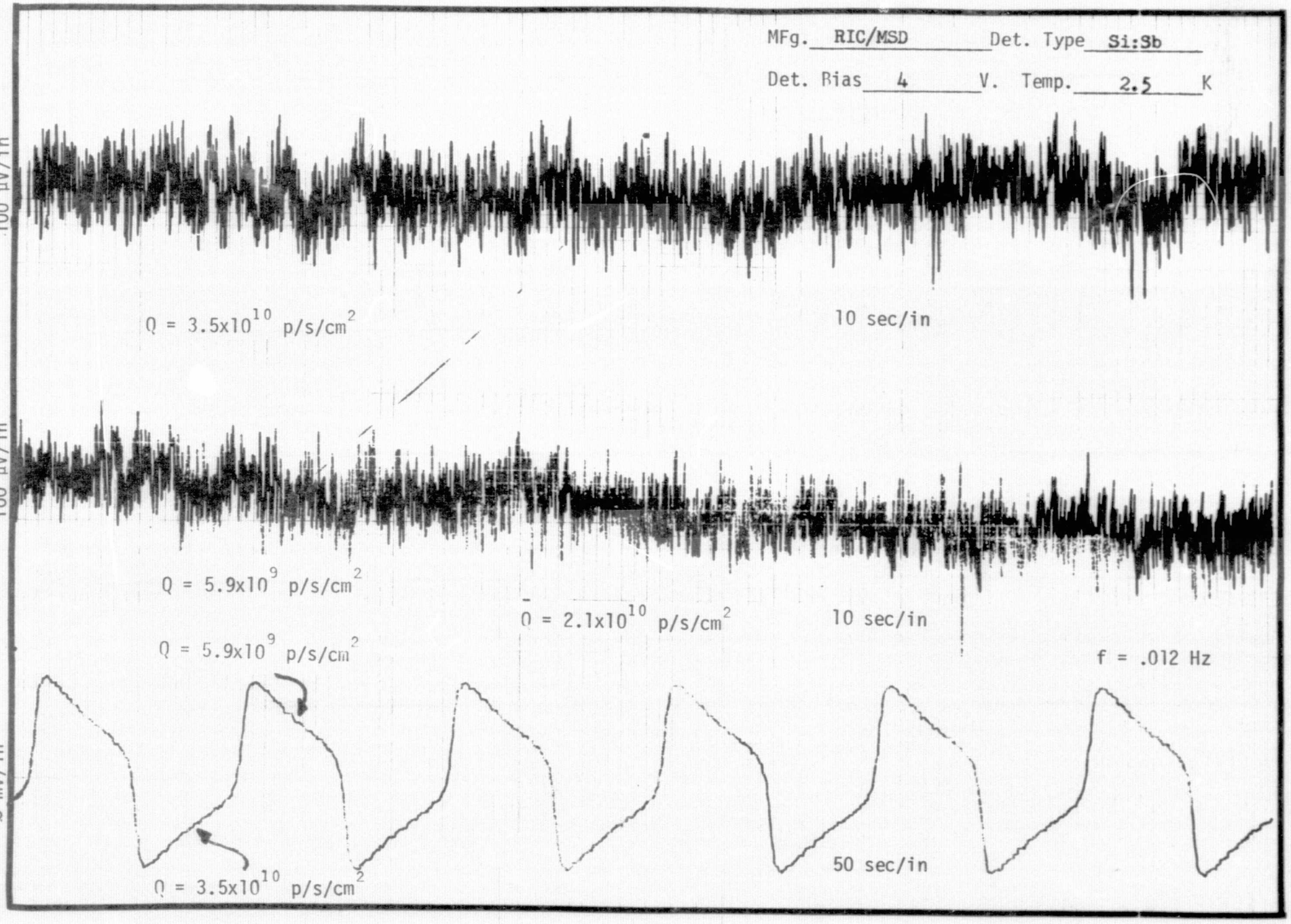
MFg. RIC/MSD Det. Type Si:Sb
Det. Bias 4 V. Temp. 2.5 K
100 μV/in
Q = 3.5x10^10 p/s/cm^2
10 sec/in
DETECTOR OUTPUT
100 μV/in
Q = 5.9x10^9 p/s/cm^2
Q = 2.1x10^10 p/s/cm^2
10 sec/in
EOL
Q = 5.9x10^9 p/s/cm^2
f = .012 Hz
5 mV/in
Q = 3.5x10^10 p/s/cm^2
50 sec/in
TIME

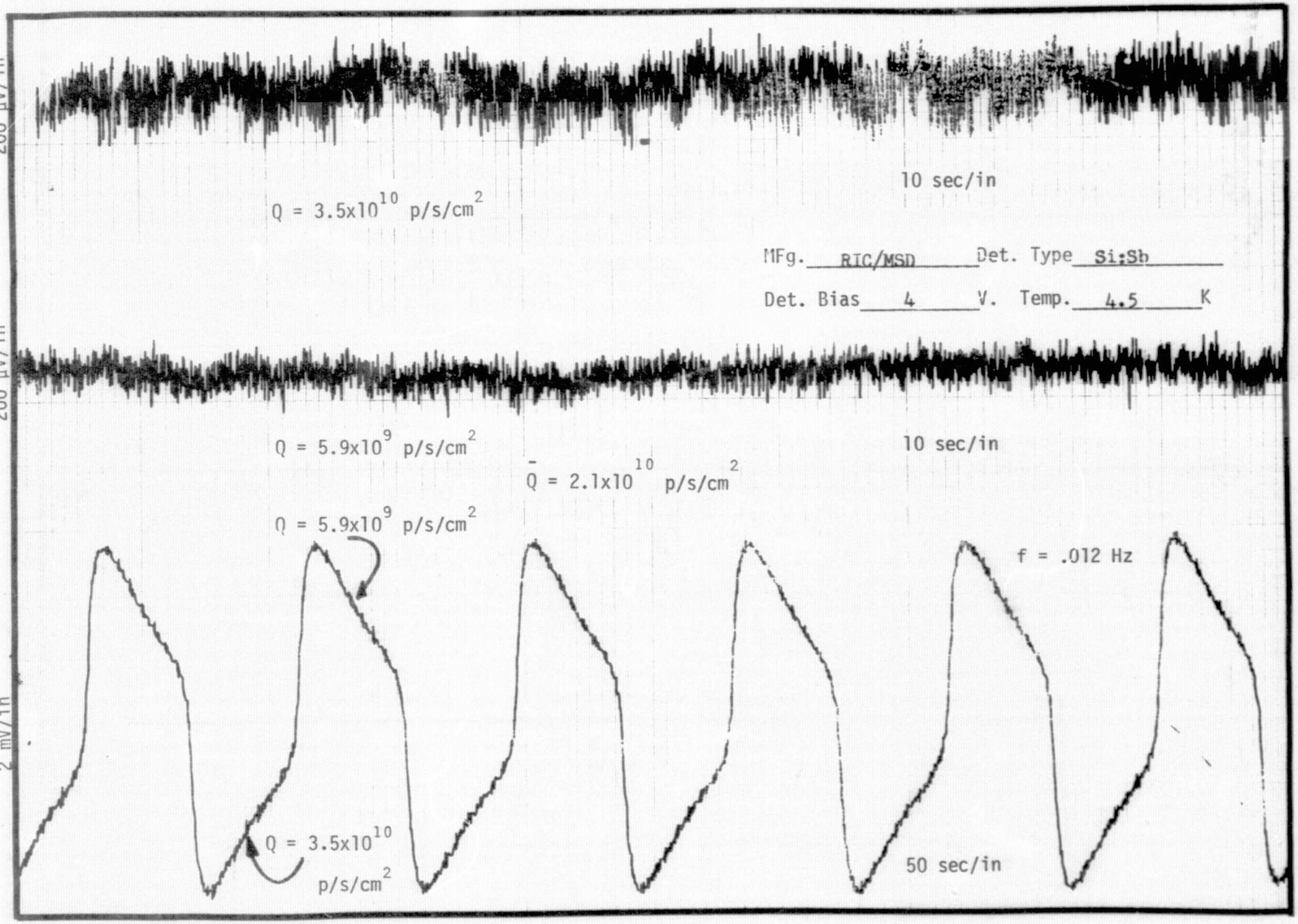
200 μV/in
10 sec/in
Q = 3.5x10^10 p/s/cm^2
MFg. RIC/MSD Det. Type Si:Sb
Det. Bias 4 V. Temp. 4.5 K
200 μV/in
Q = 5.9x10^9 p/s/cm^2
10 sec/in
Q = 2.1x10^10 p/s/cm^2
Q = 5.9x10^9 p/s/cm^2
f = .012 Hz
DETECTOR OUTPUT
10^4
2 mV/in
Q = 3.5x10^10 p/s/cm^2
50 sec/in
TIME

5.6 RIC/MSD Si:P. This detector package (NA 007) also had a low valued load resistor (about $10^9\Omega$ at 4.5K). This low value limits the detector signal at low frequencies. Again the FET noise was somewhat higher than normal. The combination of low load and high FET noise together with low detector responsivity result in a relatively high NEP. This high NEP denied the measurement of frequency response at the low background. A frequency response was, however, calculated from a low background signal measured at 12 Hz and the shape of the frequency response at high background. These calculated frequency responses were used to obtain the low background NEP data.

A significant amount of spiking was observed in the output of this detector at the high background.

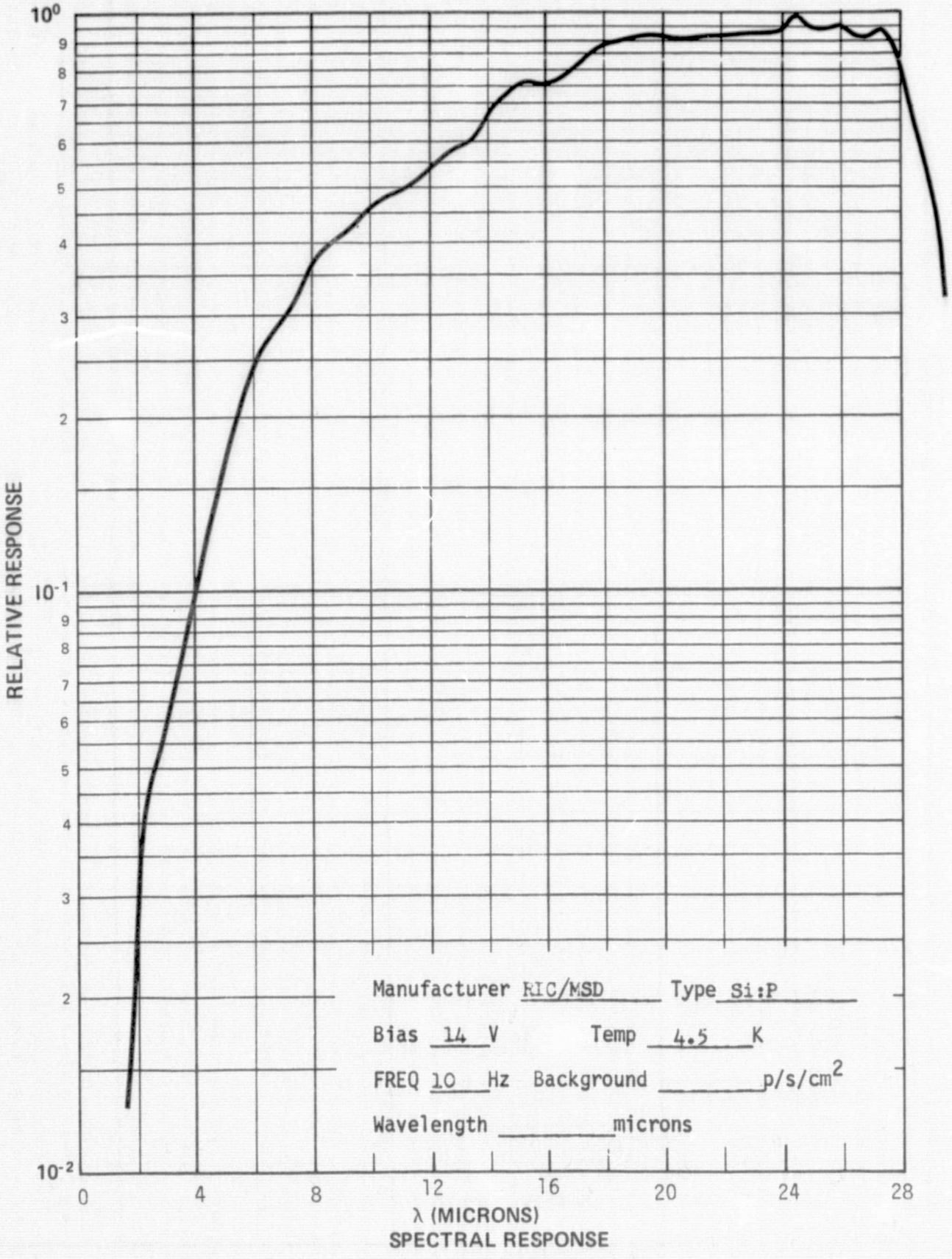

SPECTRAL RESPONSE

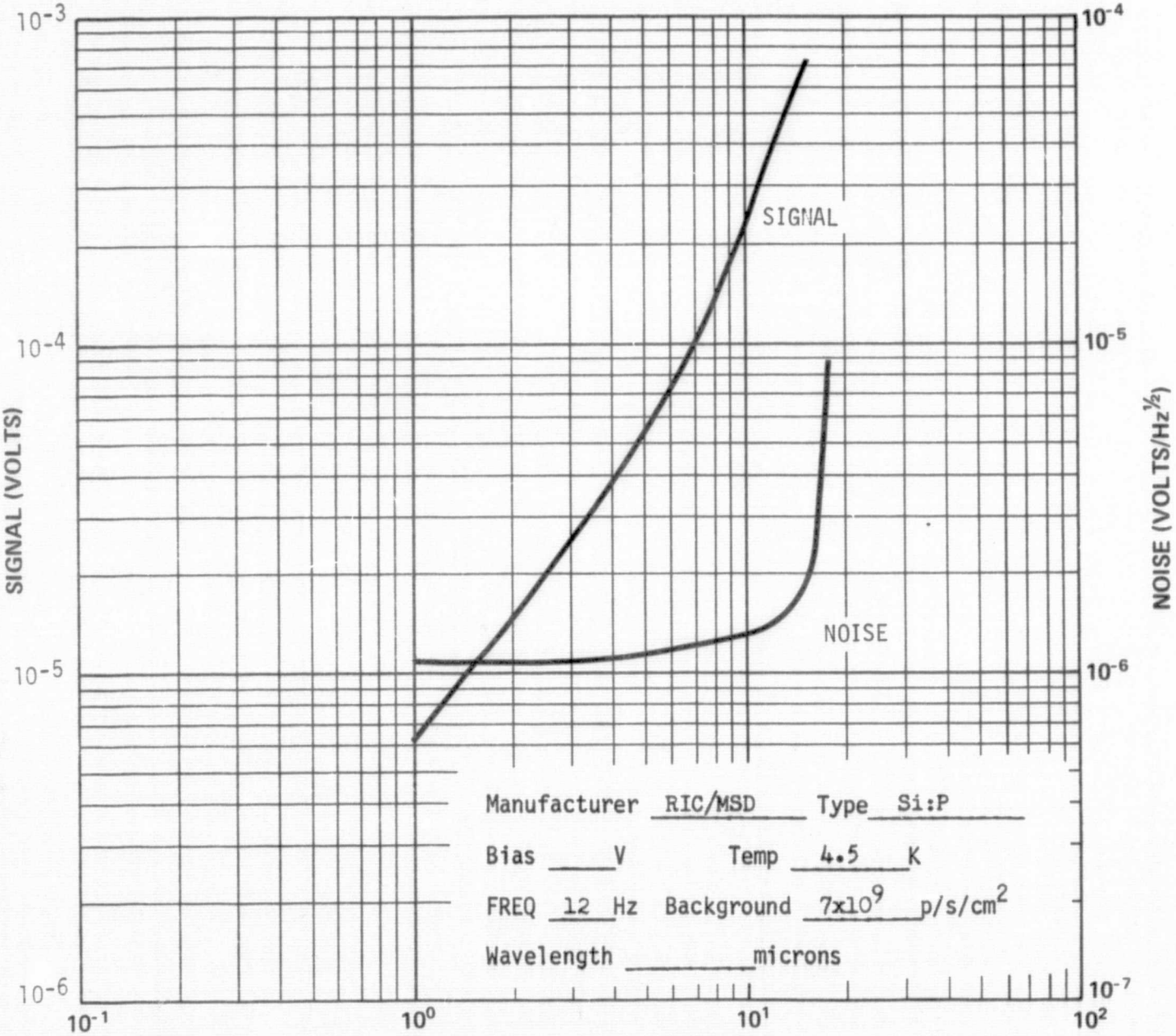

DETECTOR BIAS (VOLTS)
DETERMINATION OF OPTIMUM BIAS

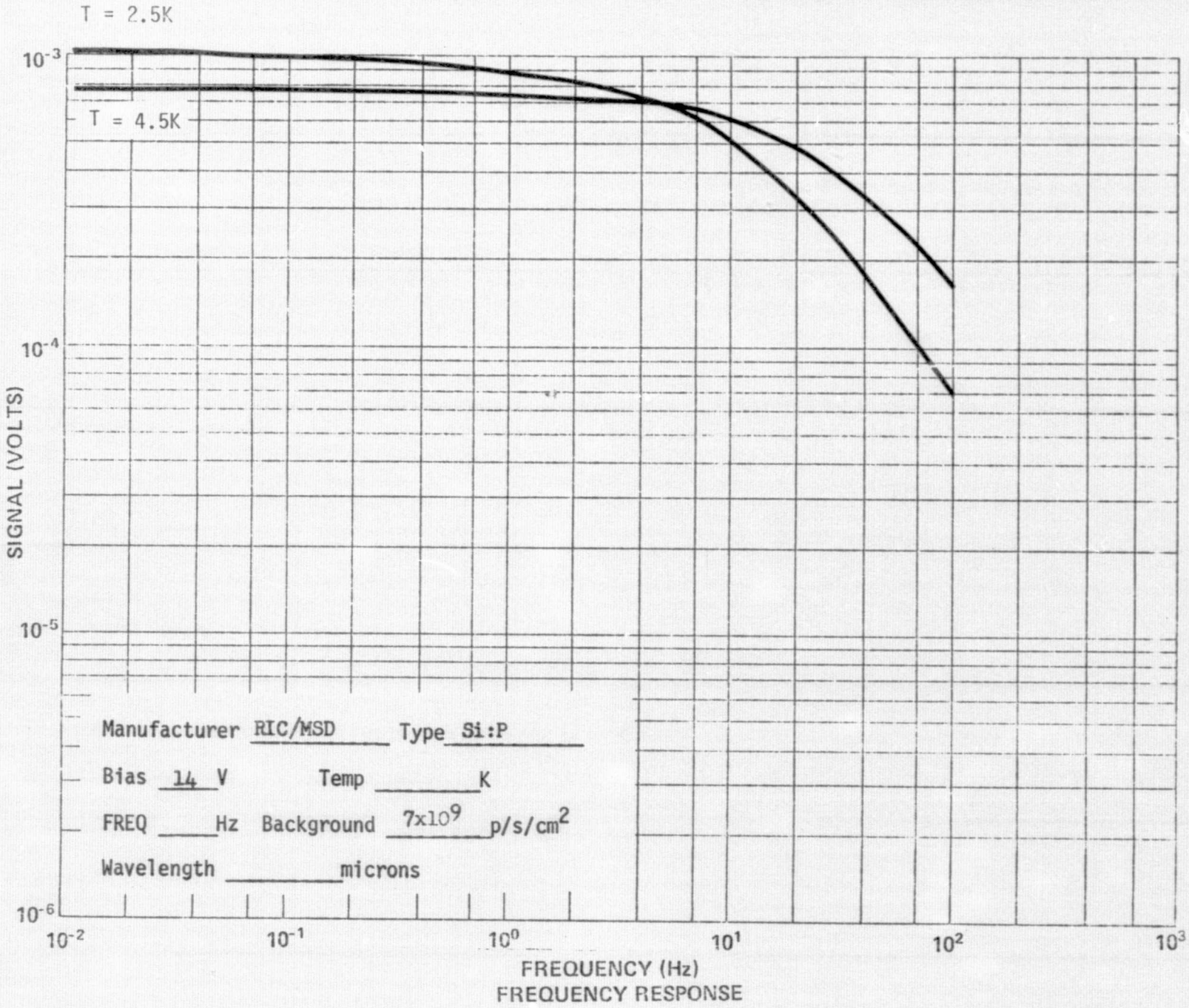

FREQUENCY RESPONSE

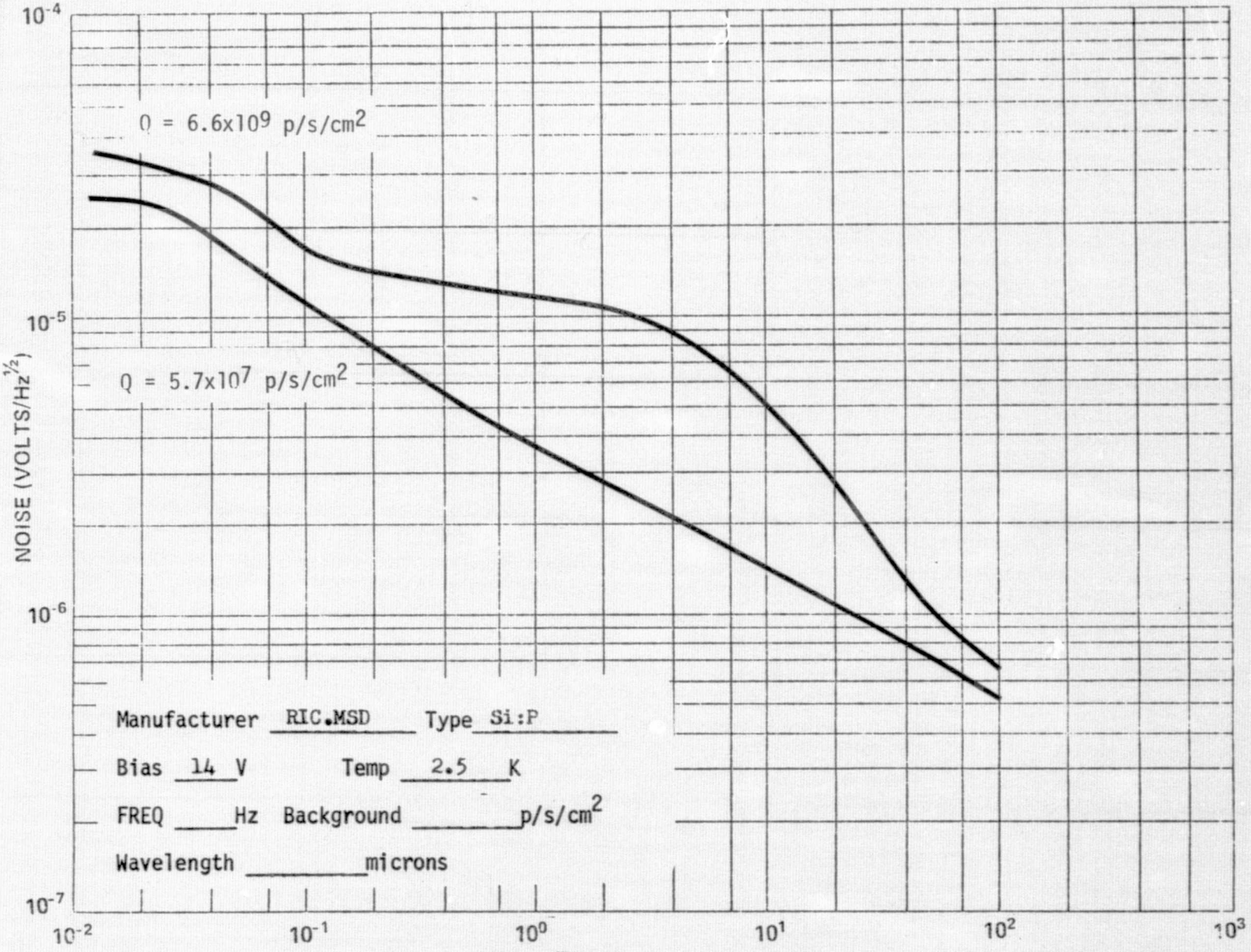

NOISE SPECTRUM

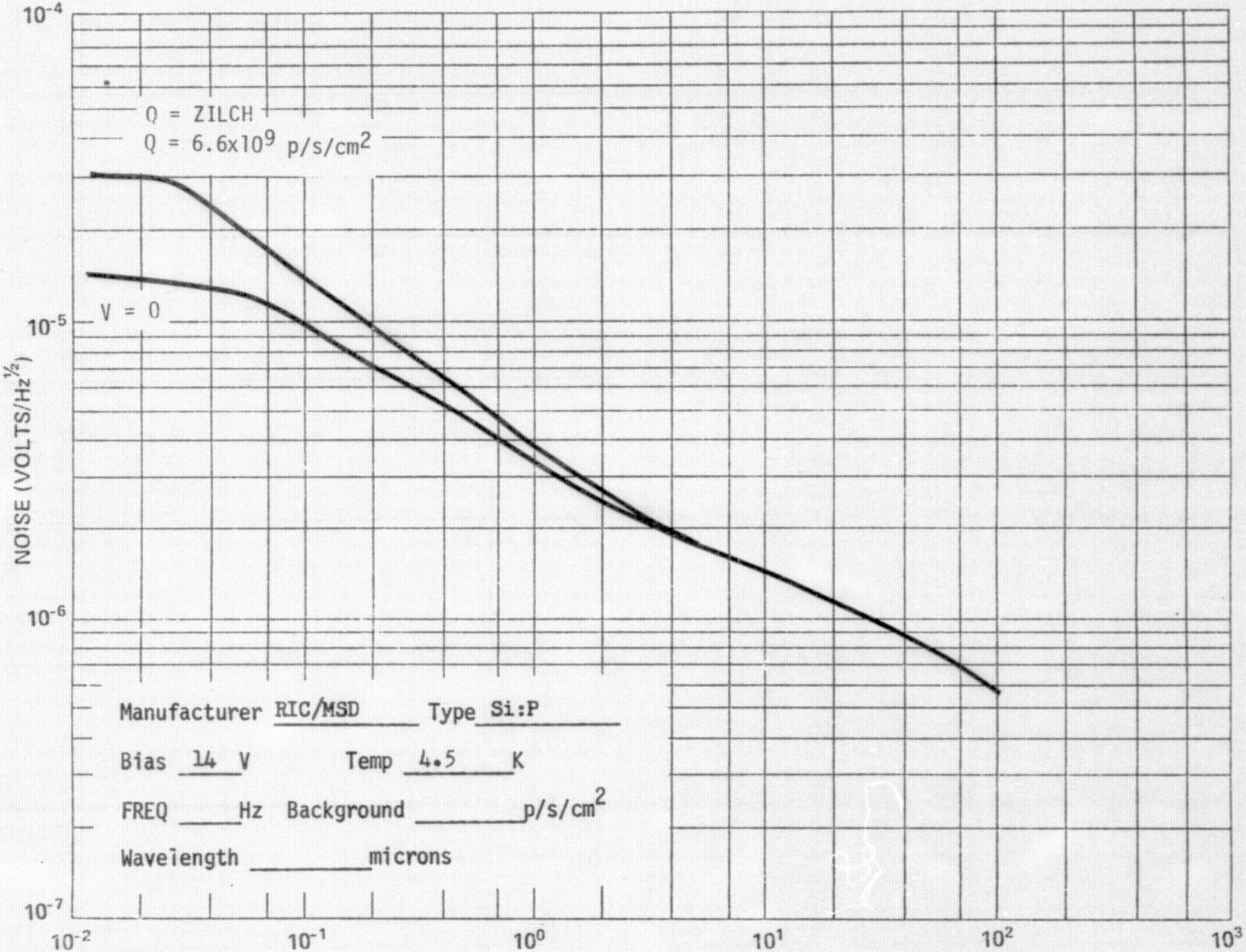

NOISE SPECTRUM

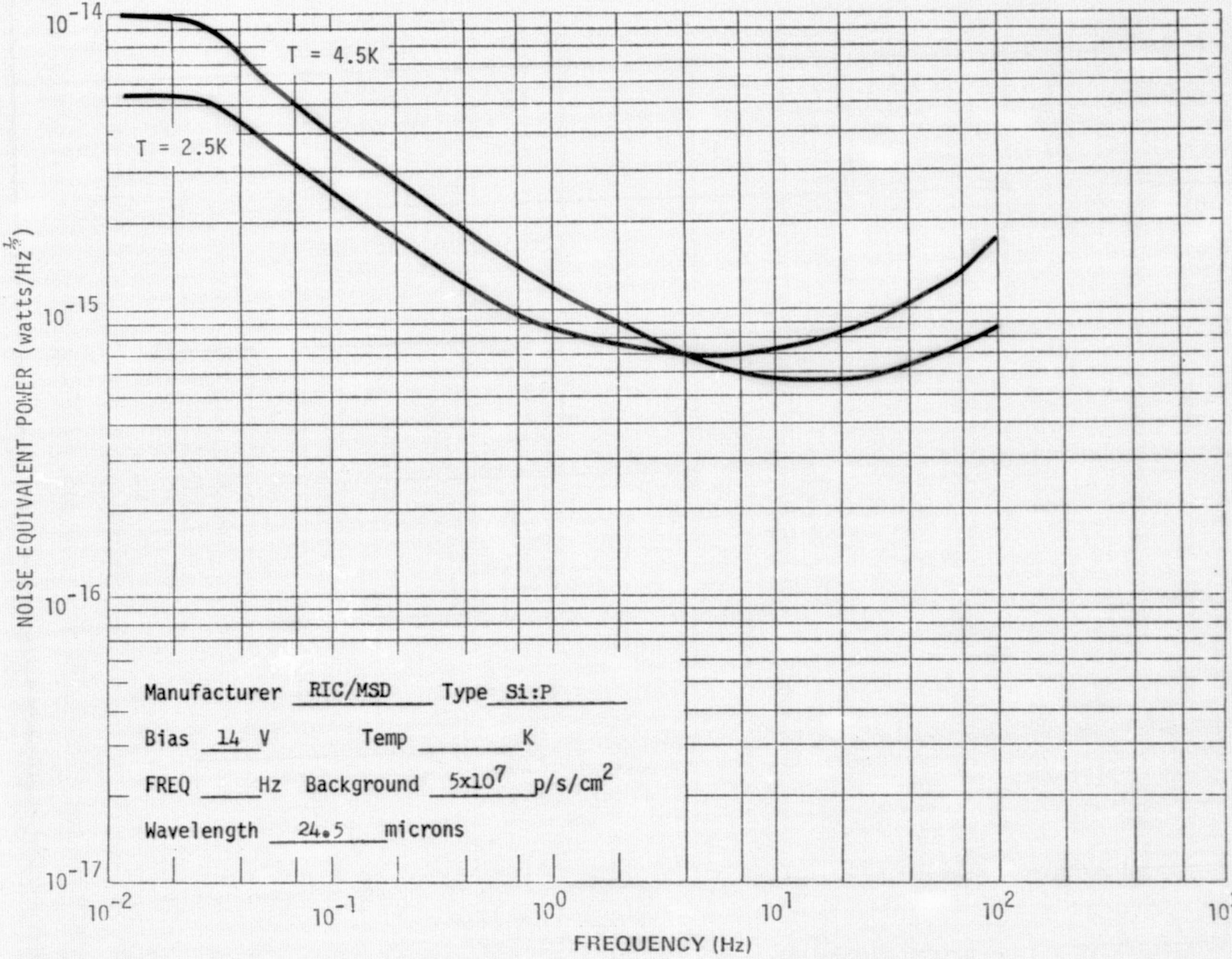
T = 4.5K
T = 2.5K
NOISE EQUIVALENT POWER (watts/Hz^½)
10^-14
10^-15
10^-16
10^-17
10^-2
10^-1
10^0
10^1
10^2
10^3
FREQUENCY (Hz)
Manufacturer RIC/MSD Type Si:P
Bias 14 V Temp ____ K
FREQ ____ Hz Background 5x10^7 p/s/cm^2
Wavelength 24.5 microns

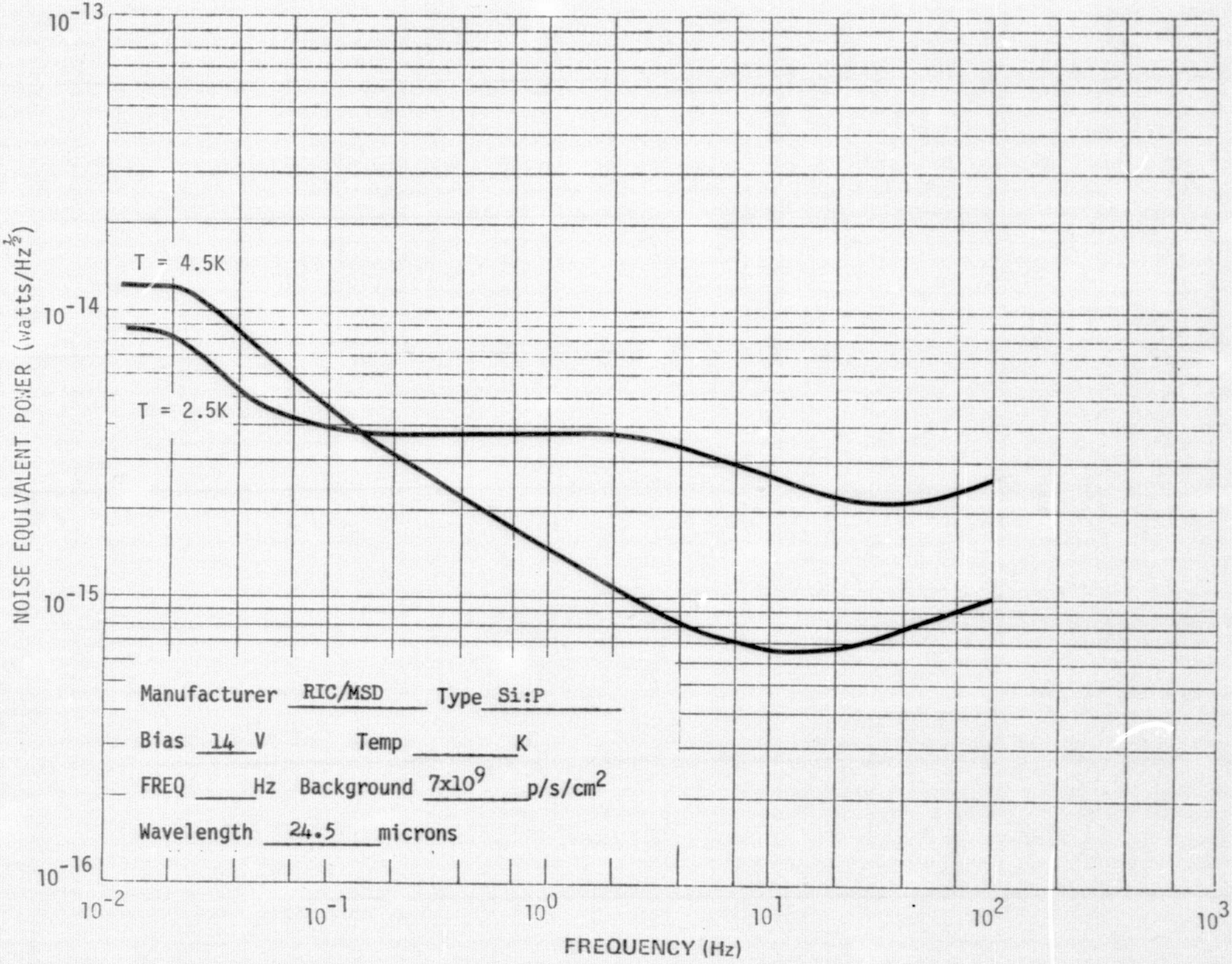
NOISE EQUIVALENT POWER (watts/Hz^½)
10^-13
10^-14
10^-15
10^-16
T = 4.5K
T = 2.5K
Manufacturer RIC/MSD Type Si:P
Bias 14 V Temp ____ K
FREQ ____ Hz Background 7x10^9 p/s/cm^2
Wavelength 24.5 microns
10^-2
10^-1
10^0
10^1
10^2
10^3
FREQUENCY (Hz)

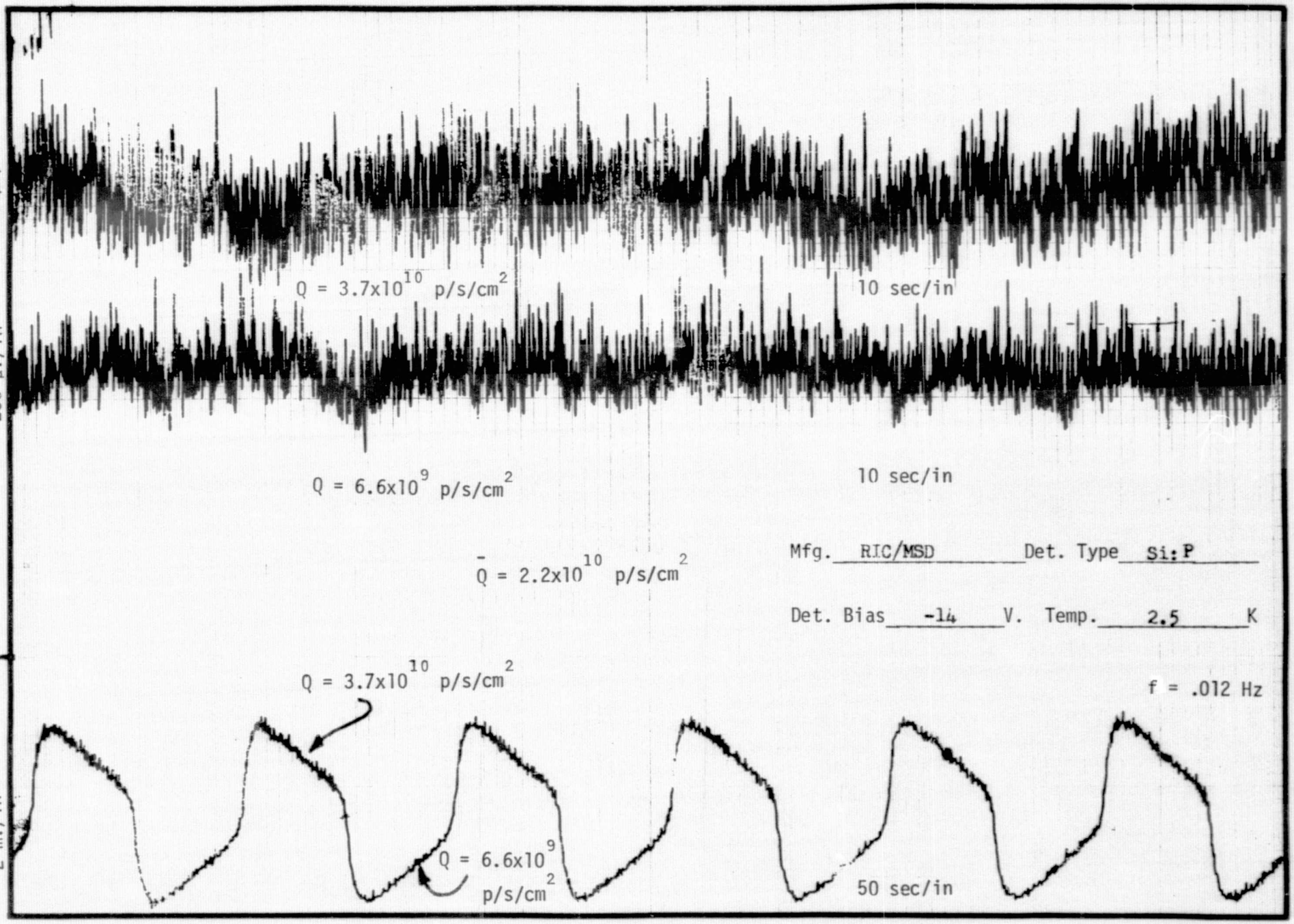
200 μV/in
Q = 3.7x10^10 p/s/cm^2
10 sec/in
200 μV/in
Q = 6.6x10^9 p/s/cm^2
10 sec/in
DETECTOR OUTPUT
Q = 2.2x10^10 p/s/cm^2
Mfg. RIC/MSD Det. Type Si:P
Det. Bias -14 V. Temp. 2.5 K
ε11
Q = 3.7x10^10 p/s/cm^2
f = .012 Hz
2 mV/in
Q = 6.6x10^9 p/s/cm^2
50 sec/in
TIME

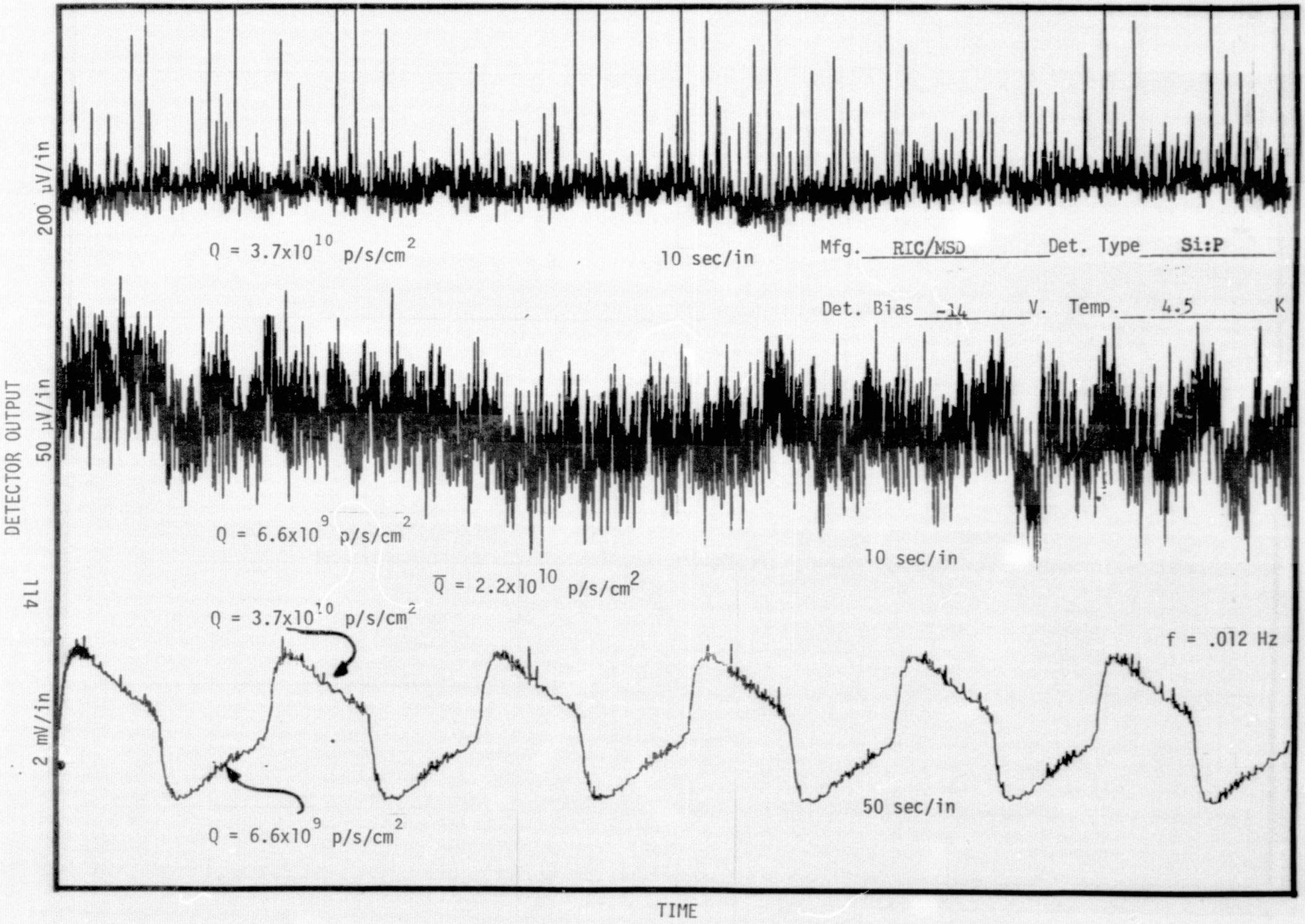
200 μV/in
Q = 3.7x10^10 p/s/cm^2
10 sec/in
Mfg. RIC/MSD
Det. Type Si:P
Det. Bias -14 V.
Temp. 4.5 K
DETECTOR OUTPUT
50 μV/in
Q = 6.6x10^9 p/s/cm^2
10 sec/in
Q = 2.2x10^10 p/s/cm^2
Q = 3.7x10^10 p/s/cm^2
f = .012 Hz
2 mV/in
50 sec/in
Q = 6.6x10^9 p/s/cm^2
TIME

5.7 SBRC Si:P. This detector (#1) exhibited a significant amount of spiking at the high background and these spikes contributed significantly to the rms noise spectra.

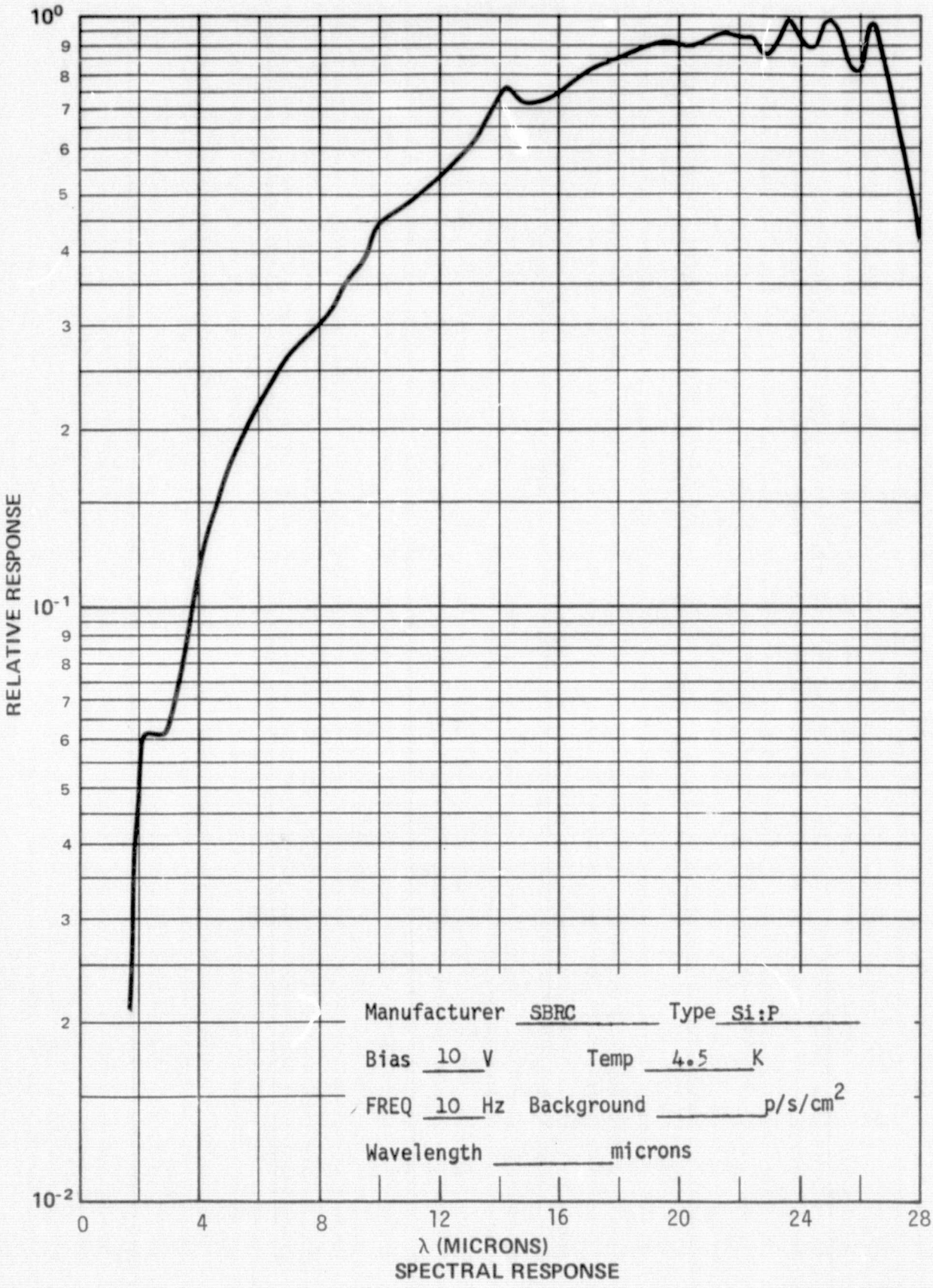

SPECTRAL RESPONSE

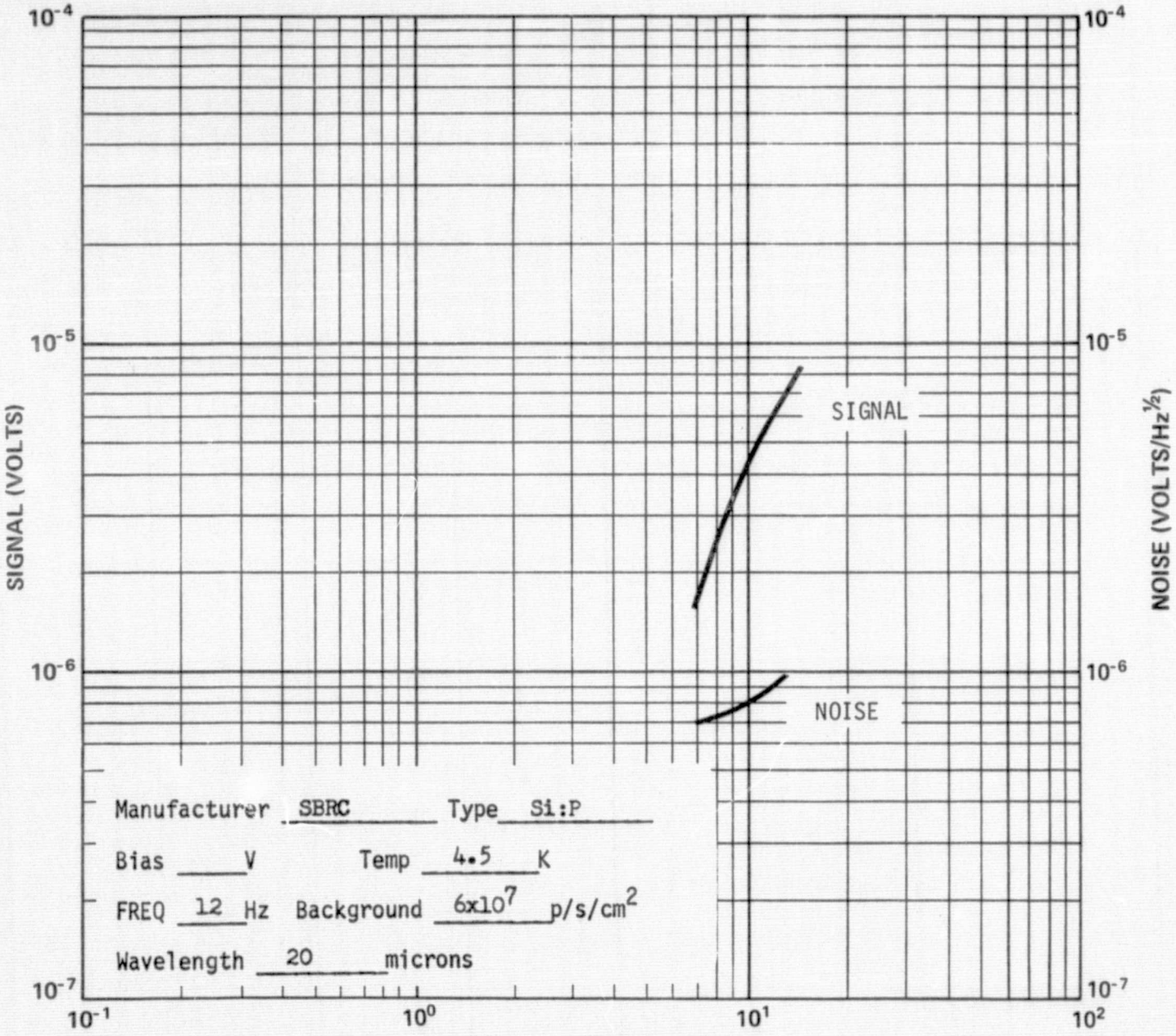

DETERMINATION OF OPTIMUM BIAS

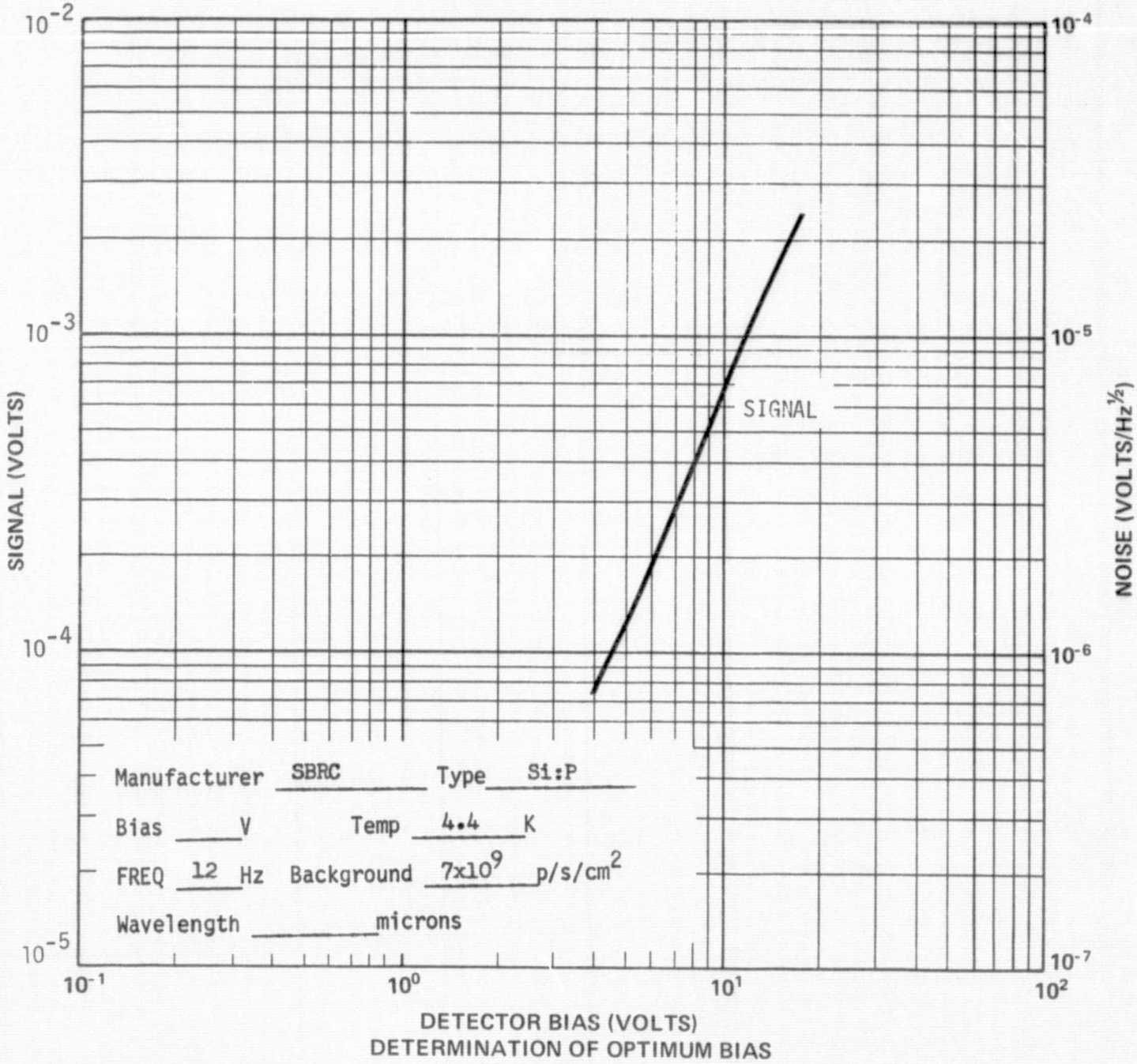

DETERMINATION OF OPTIMUM BIAS

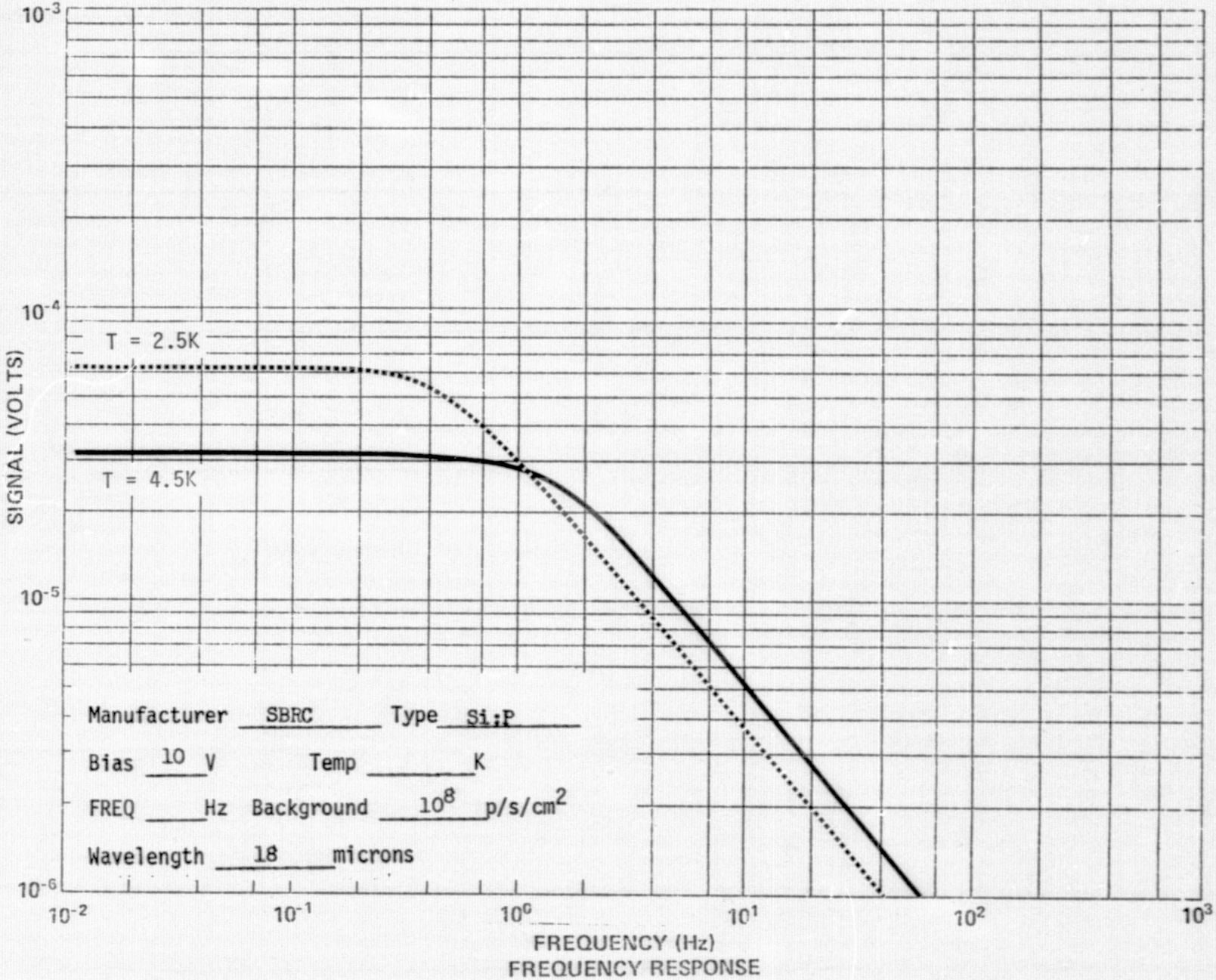

FREQUENCY RESPONSE

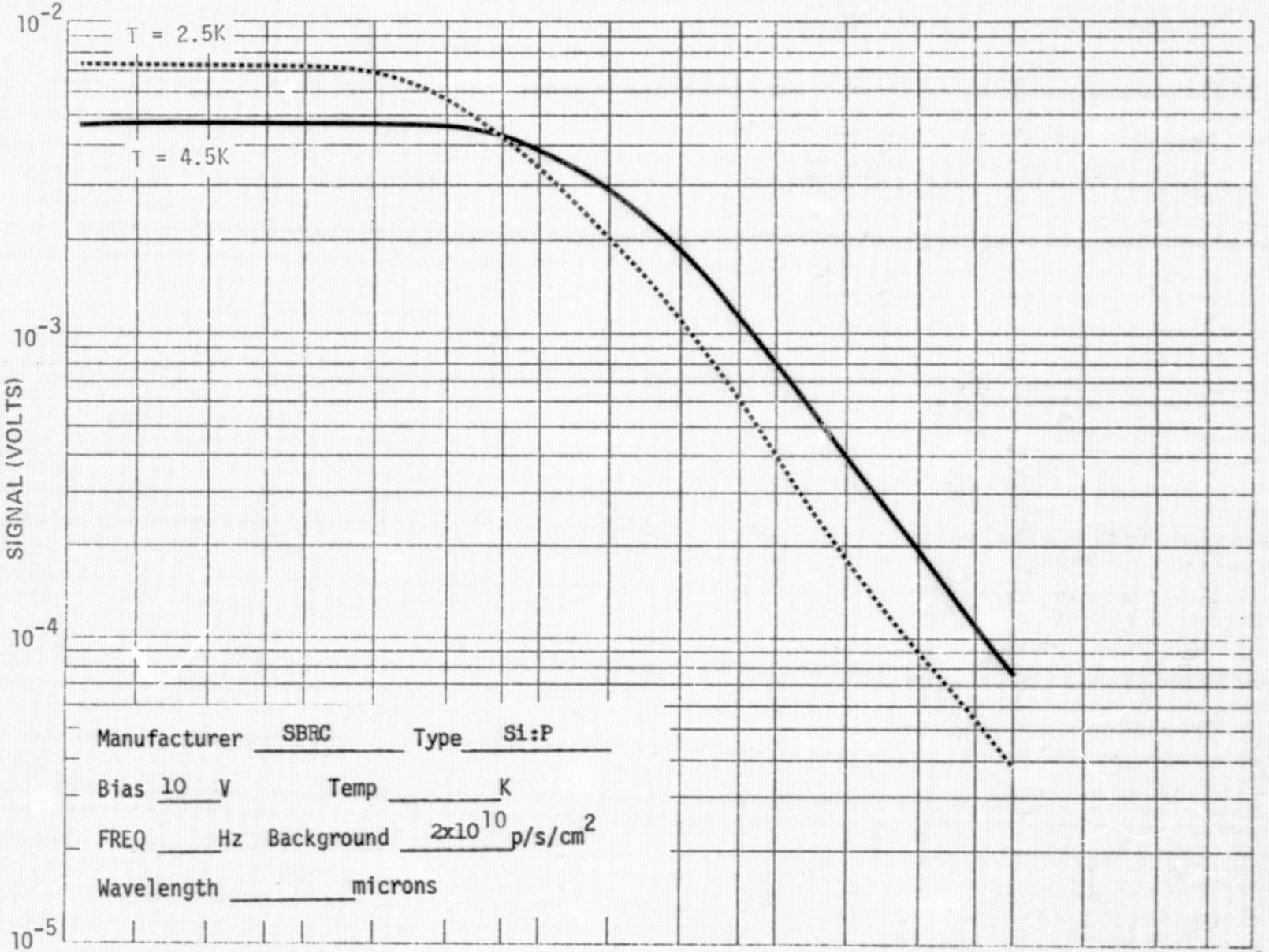

FREQUENCY RESPONSE

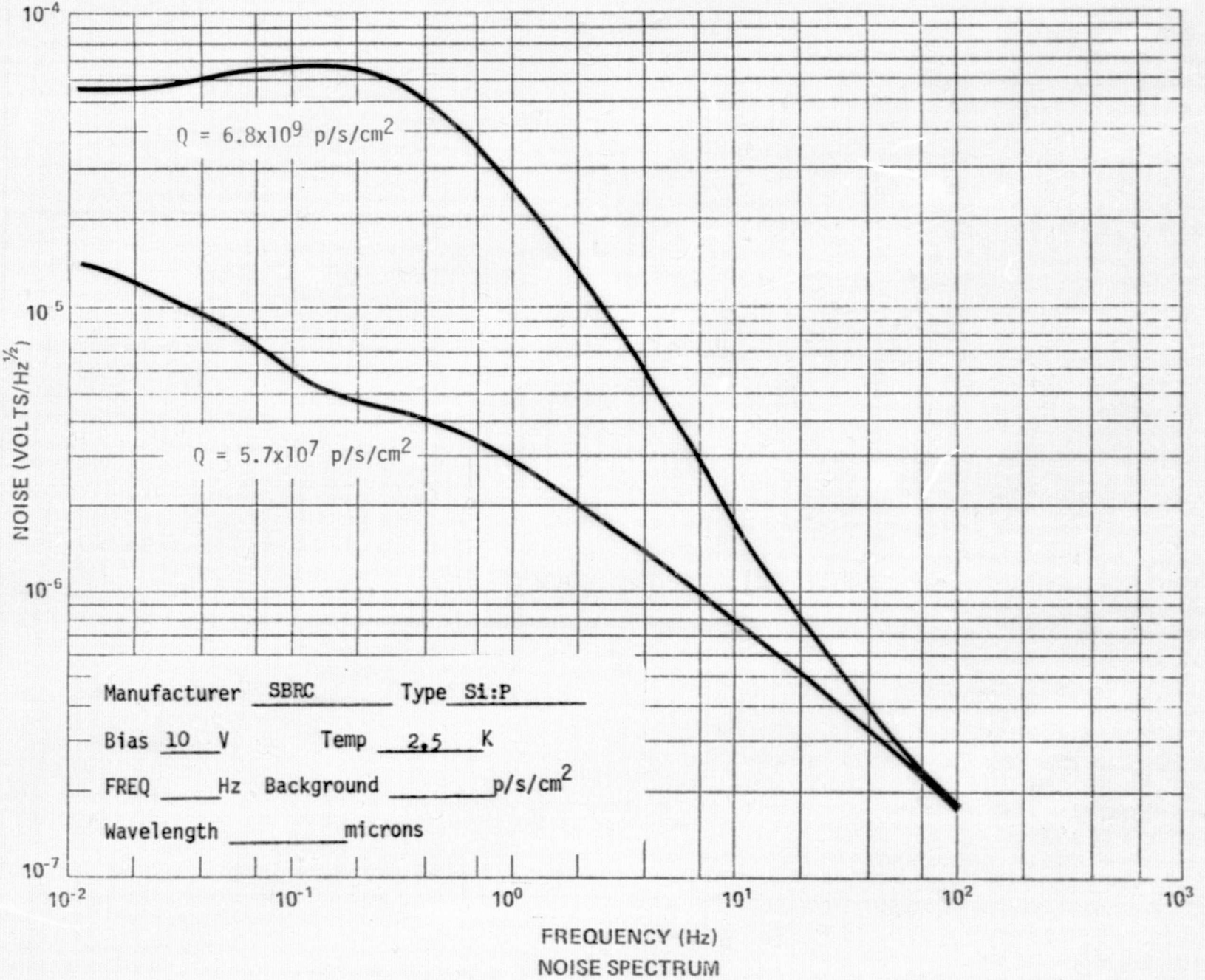

NOISE SPECTRUM

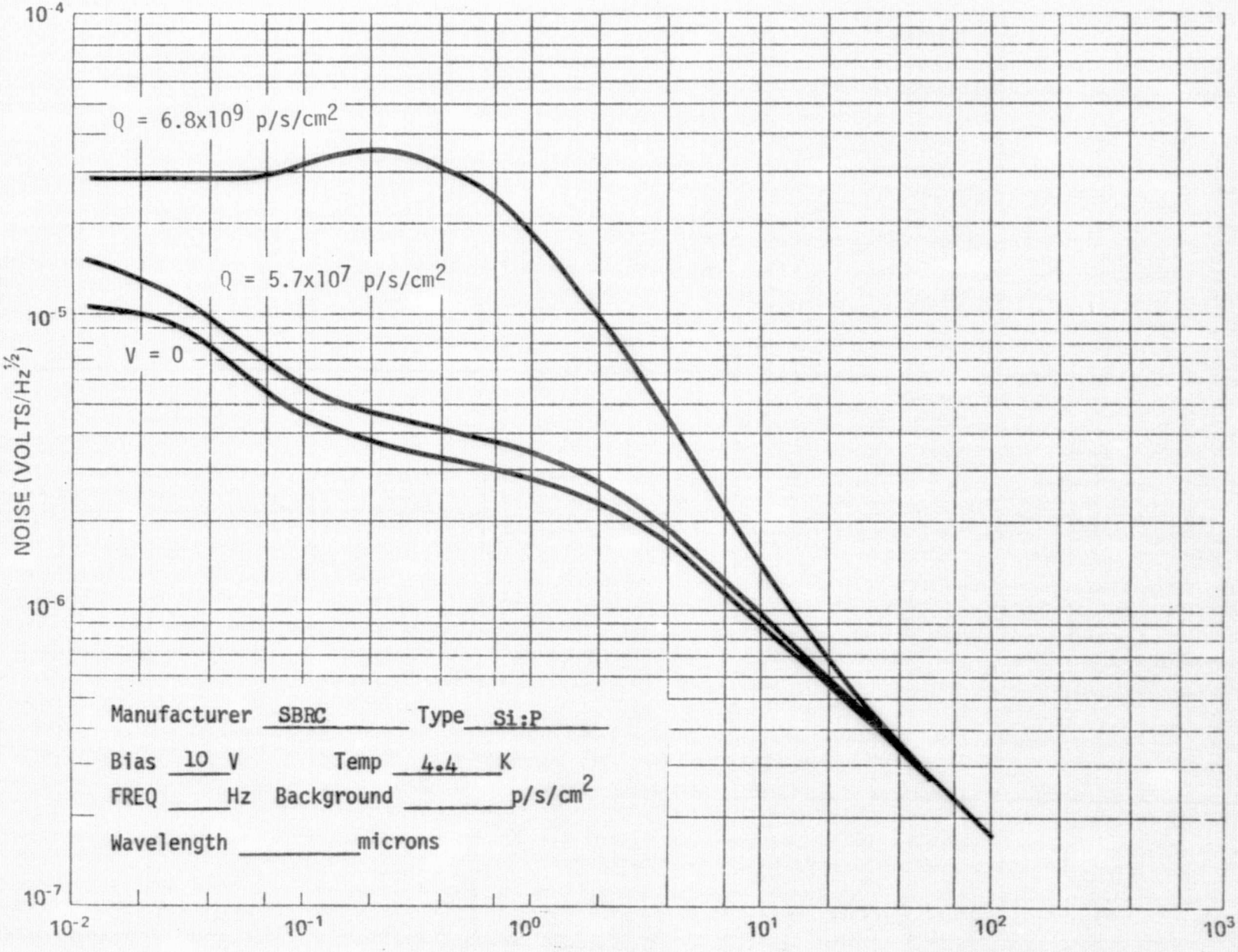

NOISE SPECTRUM

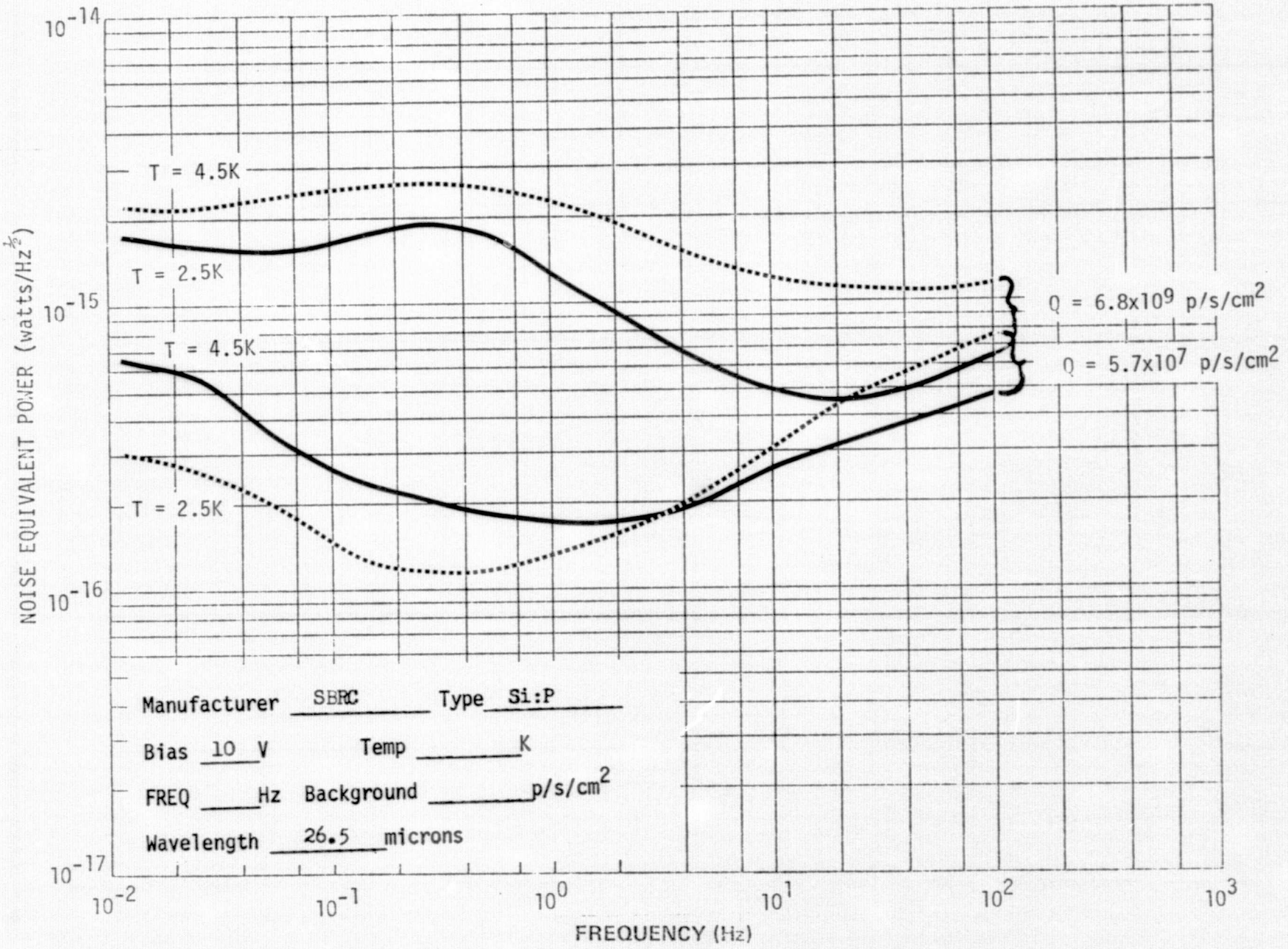
NOISE EQUIVALENT POWER (watts/Hz$^{\frac{1}{2}}$)
10^{-14}
10^{-15}
10^{-16}
10^{-17}
T = 4.5K
T = 2.5K
T = 4.5K
T = 2.5K
Q = 6.8×10^9 p/s/cm^2
Q = 5.7×10^7 p/s/cm^2
Manufacturer SBRC Type Si:P
Bias 10 V Temp ____K
FREQ ____Hz Background ____p/s/cm^2
Wavelength 26.5 microns
10^{-2}
10^{-1}
10^0
10^1
10^2
10^3
FREQUENCY (Hz)

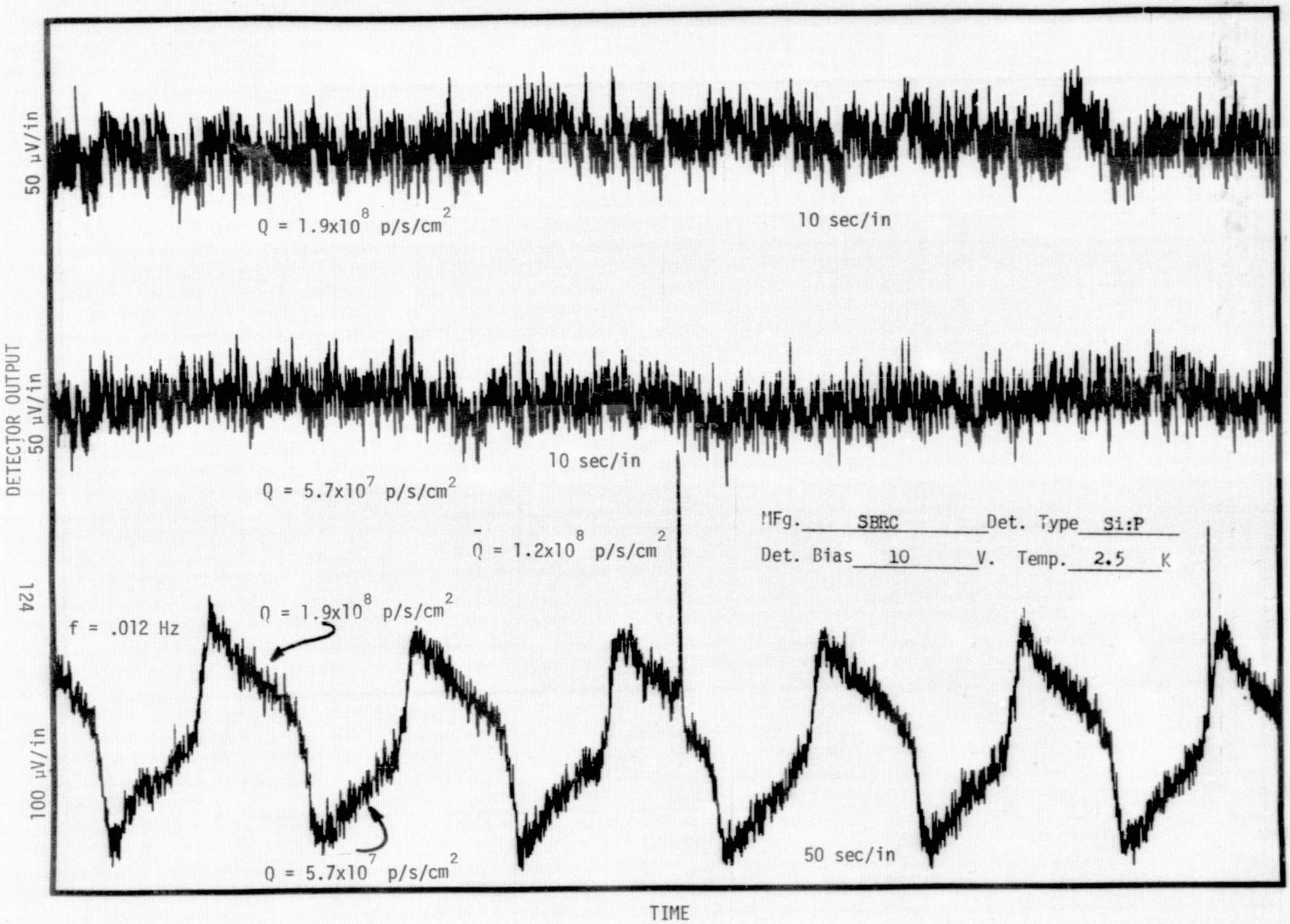
50 μV/in
Q = 1.9x10^8 p/s/cm^2
10 sec/in
DETECTOR OUTPUT
50 μV/in
10 sec/in
Q = 5.7x10^7 p/s/cm^2
Q = 1.2x10^8 p/s/cm^2
MFg. SBRC Det. Type Si:P
Det. Bias 10 V. Temp. 2.5 K
124
f = .012 Hz
Q = 1.9x10^8 p/s/cm^2
100 μV/in
Q = 5.7x10^7 p/s/cm^2
50 sec/in
TIME

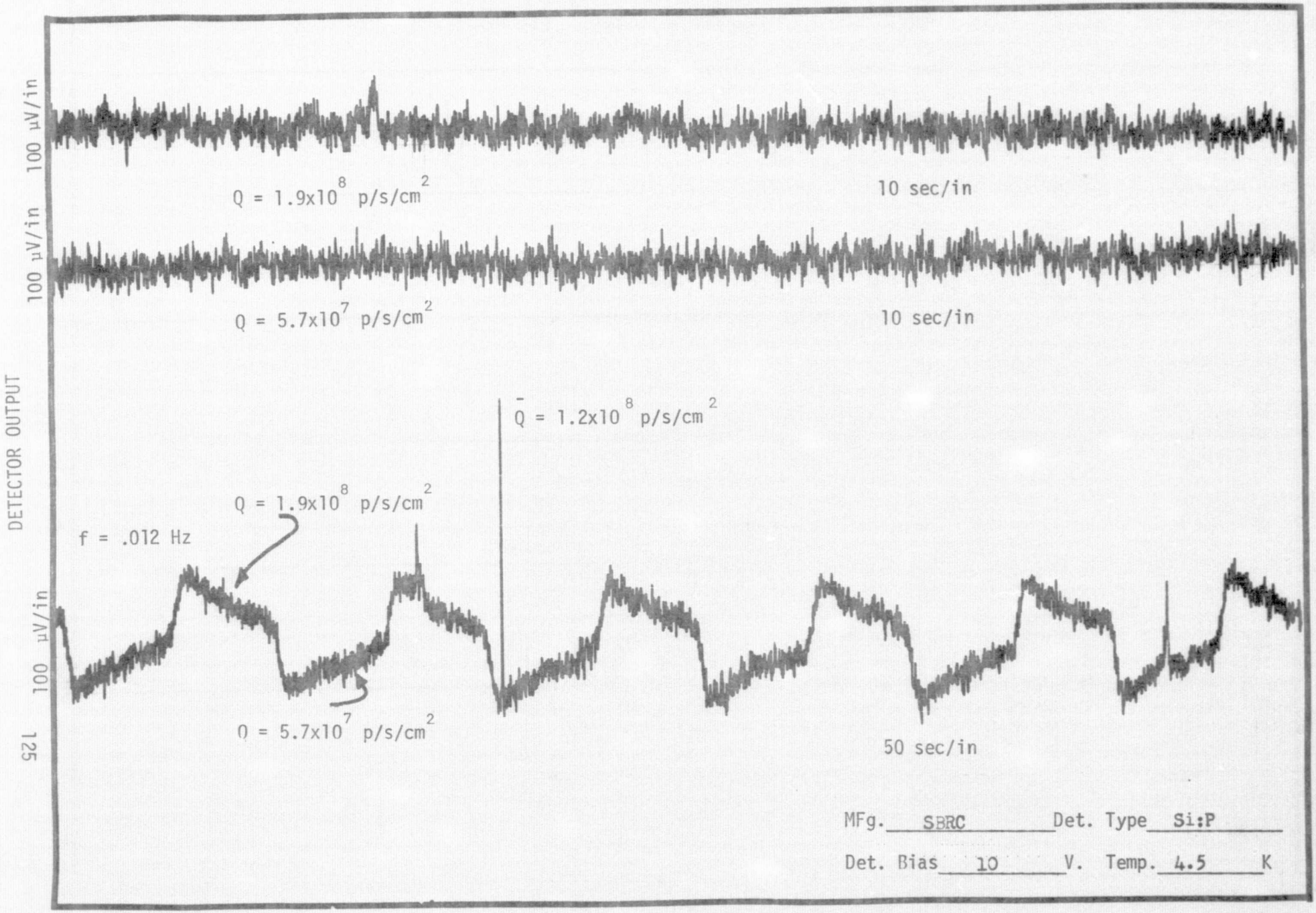
100 μV/in
Q = 1.9x10^8 p/s/cm^2
10 sec/in
100 μV/in
Q = 5.7x10^7 p/s/cm^2
10 sec/in
DETECTOR OUTPUT
Q̄ = 1.2x10^8 p/s/cm^2
Q = 1.9x10^8 p/s/cm^2
f = .012 Hz
100 μV/in
Q = 5.7x10^7 p/s/cm^2
50 sec/in
MFg. SBRC Det. Type Si:P
Det. Bias 10 V. Temp. 4.5 K
TIME

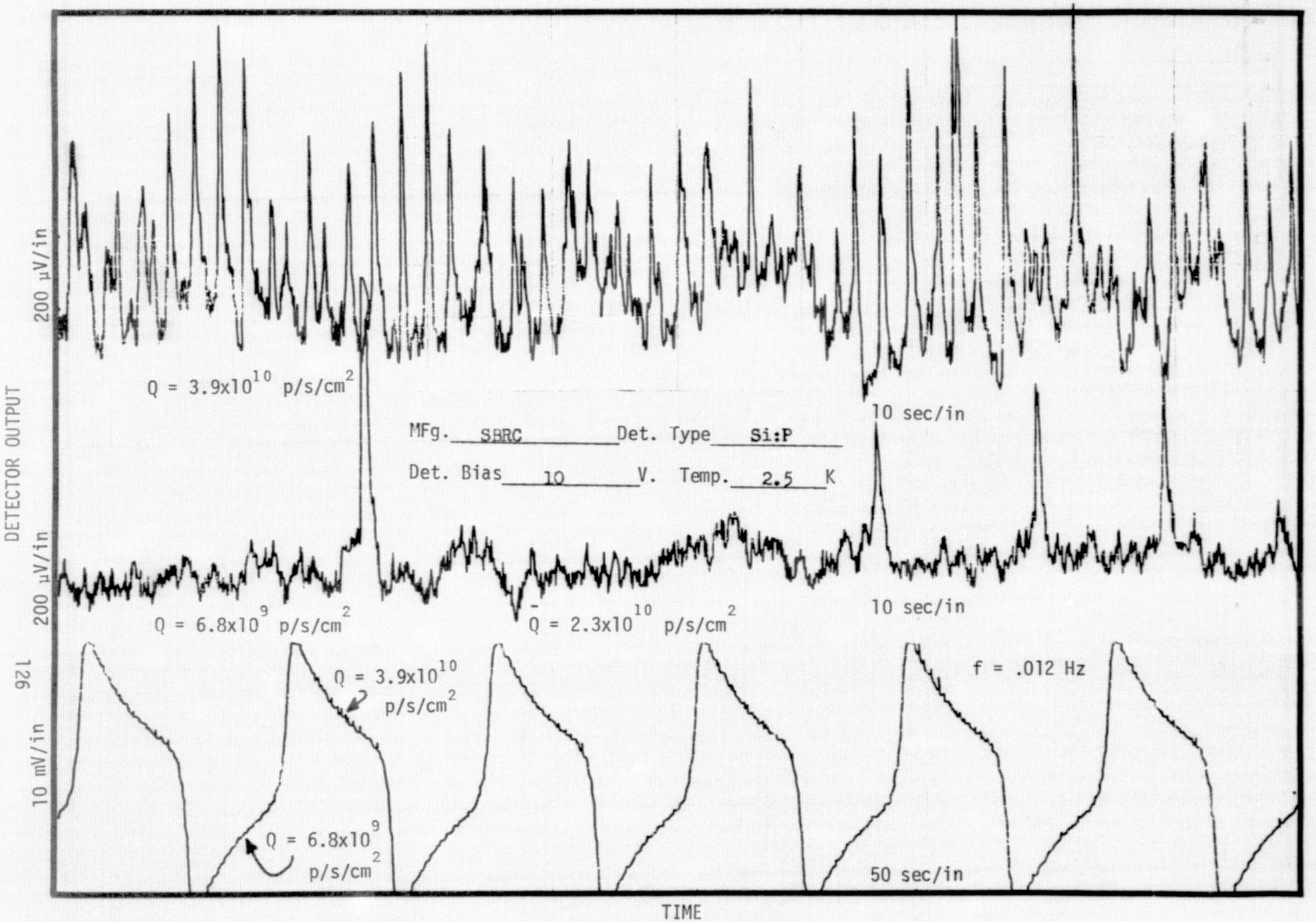
DETECTOR OUTPUT
200 μV/in
Q = 3.9x10^10 p/s/cm^2
10 sec/in
MFg. SBRC Det. Type Si:P
Det. Bias 10 V. Temp. 2.5 K
200 μV/in
Q = 6.8x10^9 p/s/cm^2
Q = 2.3x10^10 p/s/cm^2
10 sec/in
926
10 mV/in
Q = 3.9x10^10 p/s/cm^2
f = .012 Hz
Q = 6.8x10^9 p/s/cm^2
50 sec/in
TIME

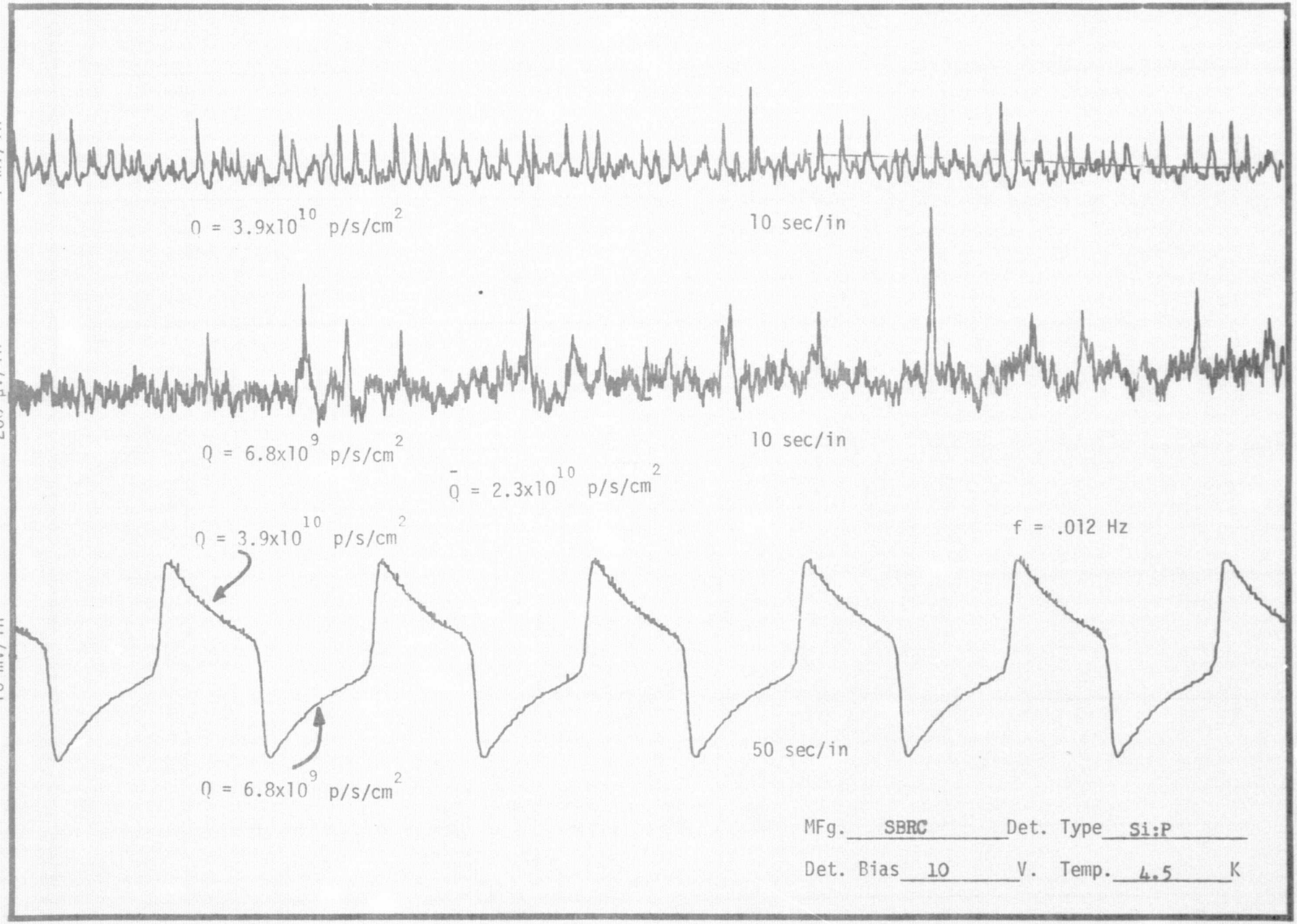
1 mV/in
Q = 3.9x10^10 p/s/cm^2
10 sec/in
200 μV/in
Q = 6.8x10^9 p/s/cm^2
10 sec/in
Q = 2.3x10^10 p/s/cm^2
Q = 3.9x10^10 p/s/cm^2
f = .012 Hz
10 mV/in
50 sec/in
Q = 6.8x10^9 p/s/cm^2
MFg. SBRC Det. Type Si:P
Det. Bias 10 V. Temp. 4.5 K
DETECTOR OUTPUT
TIME

6.0 CONCLUSIONS

A large volume of data has been presented on the performance of four types of doped-silicon detectors. Tests have been performed in operating environments similar to those expected for the IRAS sensor. Some general conclusions can be drawn from the data concerning the use of these types of detectors in the IRAS program.

Perhaps the most important conclusion to be drawn from the data concerns the operation of these detectors/FETs at low temperatures (2.5K) and low frequencies (0.01 Hz). Prior to these measurements no data was available for detectors of these types under these conditions. It appears that no significant problems exist which are peculiar to either low temperature or low frequency operation.

From the system point-of-view, there are two concepts related to detector/FET performance which are important: radiometric precision and minimum noise equivalent power (NEP). Some observations concerning these concepts are presented below.

6.1 Noise Equivalent Power. In order to minimize the NEP, one would like to maximize the detector signal and minimize the noise. As was discussed in section 4.3, the low frequency output signal depends on detector responsivity and load resistance, and on detector responsivity and input capacitance at high frequencies. In order to obtain a large output signal, one should maximize detector responsivity and load resistance, and minimize the input capacitance.

The total noise is made up of three noise sources:

(1) detector noise;

(2) load resistor Johnson noise; and

(3) FET noise.

Detector noise varies with load resistance and input capacitance in exactly the same way as does the signal. This means that in a situation where the detector noise is the dominant noise source, the NEP would be independent of the load resistance and input capacitance. However, in the usual situation, the FET noise is the dominant noise source except at low frequencies where the load resistor Johnson noise may dominate. One would like to have a FET with the lowest noise and input capacity in any case.

At low frequencies, the detector signal and noise vary linearly with the load resistance value whereas the Johnson noise of the load resistance varies as the square root of the resistance. The optimum value of load resistor is thus achieved by picking a value of load so so that the detector noise, at low frequencies, is greater than the Johnson noise at the lowest background expected. Note that the input time constant ($\tau = R_L C_i$) increases linearly with the load resistance, and at extremely low backgrounds (high R_L), the low frequency region ($\omega R_L C_i << 1$) may not lie within a frequency range of interest. In this case the FET noise becomes the limiting noise for all frequencies.

Another detector characteristic which may affect system NEP is the spontaneous spiking rate. Most of the detectors discussed in this report exhibited significant spiking and the rate of spikes appears to

be a function of background flux, operating temperature, and detector bias. These spikes are characterized temporarily as having a rapid rise and a slow decay limited by the system bandwidth. For these measurements the bandwidth was limited by the input time constant, $\tau = R_L C_i$.

The bandwidth may be increased (and decay time shortened) by using the load resistor as the feedback element of a transimpedance amplifier. The bandwidth of such an amplifier is usually limited by the time constant of the feedback resistor and its associated parasitic capacitance. Unfortunately, this associated capacitance is usually not a lumped parallel one, but rather contains distributed components. This distributed capacitance results in a decay which is not characterized by a single time constant. Also, it should be pointed out that no data exist on the low frequency noise characteristics of transimpedance amplifiers.

A better solution to the spiking problem would obviously be to eliminate them. To-date, however, no manufacturer has been able to relate spiking rate to any controllable detector parameter. However, based on the observations made for the AESC Si:As detector, some investigations seem to be in order concerning the relationship between mechanical stress and spiking rate.

6.2 Radiometric Precision. If the detector output signal is used as a measure of the incident irradiance, the relationship between the two at any anticipated operating condition must be known. As was discussed in section 6.1, the output signal is seen to be a function of

operating temperature at a fixed irradiance level through both the detector responsivity and the value of load resistance. The responsivity (at low modulation frequencies) of most detectors is a function of irradiance level because of dielectric relaxation. There is also another nonlinear effect which occurs at high signal values related to the fact that most cryogenic load resistors are non-ohmic (resistance is a function of applied voltage).

Another detector characteristic which may limit the precision of a radiometric measurement relates to any nonuniformity in the spatial sensitivity of the detector. That is, if the blur circle does not completely fill a detector which is nonuniform, the output signal will depend on which part of the detector is illuminated. Detectors with "good" transparent electrodes seem to minimize these effects.

6.3 Comments. By their nature, survey measurements such as these seldom resolve all of the detector problems relating to a sensor system. This difficulty has been addressed in the past by means of a small "sample" array. A sample array is built early in the sensor program. It contains a few detector elements which are similar to the detector used in the system focal plane array (i.e., same material, size, construction, etc.). The performance of the sample array is then measured under conditions that more closely duplicate the sensor system.

The FETs used with most of the detectors reported here are considerably poorer than state-of-the-art.

The spontaneous noise spike phenomena is not understood. The spike rate appears to be dependent upon background, operating temperature and bias field. However, very little quantitative data exists.

Several nonlinear effects have been observed in extrinsic detectors that are related to the spatial distribution of the incident radiation on the detector surface. Again, little quantitative data is available and the effects are not understood.[6]

It should be pointed out that responsivities listed in Table II are little more than estimates of the detector responsivities. For detectors of the same type, the range in the given responsivities is not much more than expected from experimental errors and/or errors in assumptions (i.e., input capacitance, "active area," etc.). All of the data for each detector should be considered when attempting to evaluate the detector in terms of the mission requirements of the IRAS sensor.

FOOTNOTES:

1. "Low Background Spectral D* Apparatus," NELC/TR 1940, 30 Aug 1974.
2. "Survey of Anomalous Behaviors Observed in Semiconductor Infrared Detectors," M. Warren *et al*, McDonnell-Douglas Astronautics Co., July 1974 (classified document).
3. "Sourcebook of Extrinsic Detector Irregularities," Vols. 1 and 2, Ballistic Missile Defense Advanced Technology Center, January 1976 (classified document).
4. "Hardened Detectors/Circuits Study," Vol. I, Aerojet Electrosystems Co., 6 October 1976. (classified document)
5. "Minutes of the Conference on Extrinsic Detector Behavior," Ballistic Missile Defense Advanced Technology Center, March 1976, (classified document).
6. "Characteristics of Detectors Having Partially Illuminated Sensitive Areas," C. Sayre *et al*, IRIS Specialty Group on Infrared Detectors, 1976 (classified document).